Technische Universität Braunschweig

Systems biological investigation of aerobic and anaerobic aromatic catabolism in the bacterium *Aromatoleum aromaticum* EbN1

Von der Fakultät für Lebenswissenschaften

der Technischen Universität Carolo Wilhelmina zu Braunschweig

zur Erlangung des Grades einer

Doktorin der Naturwissenschaften

(Dr. rer. nat.)

genehmigte

D i s s e r t a t i o n

von Britta Katrin Müller
aus Solingen

1. Referent: **Prof. Dr. Dietmar Schomburg**
2. Referent: Prof. Dr. Ralf Rabus
3. Referent: apl. Professor Dr. Michael Hust
eingereicht am: 07.03.2016
mündliche Prüfung (Disputation) am: 22.06.2016

Druckjahr 2016

Vorveröffentlichungen der Dissertation

Teilergebnisse aus dieser Arbeit wurden mit Genehmigung der Fakultät für Lebenswissenschaften, vertreten durch den Mentor der Arbeit, in folgenden Beiträgen vorab veröffentlicht:

Publikationen

Wolf, J., Stark, H., Kruse, K., Albersmeier, A., Pham, T.K., Müller, B. K., Meyer B., Albaum, S., Kouril, T., Schmidt-Hohagen, K., Kalinowski, J., Wright, P. C., Siebers, B., Schomburg, D. (2016) Hot systems biology reveals a new L-fucose degradation pathway in Sulfolobus solfataricus, Molecular Microbiology, *under review*

Tagungsbeiträge

Müller, B. K., Wittenberg, T., Schmidt-Hohagen, K., Schomburg, D. (2013) Development of a General Method for the HPLC/MS-based Analysis of Coenzyme A Derivatives and Cofactors from Cell Extracts. 9th Annual International Conference of the Metabolomics Society; Glasgow, England

Müller, B. K. (2014) Covering a blind spot of GC-MS: A robust HPLC method for analyzing CoA intermediates from diverse microorganisms. Trends in Metabolomics - Analytics and Applications, DECHEMA; Frankfurt, Germany

Table of Contents

Abbreviations

Abbreviation	**Explanation**
ABC transporter	ATP-binding cassette transporter
APCI	atmospheric pressure chemical ionization
ATP	adenosine-triphosphate
BCA	bicinchoninic acid
CDW	cell dry weight
CoA	coenzyme A
EC	enzyme commission number
e.g.	Latin: *exempli gratia*, for example
EI	electron ionization (formerly known as electron impact)
ESI	electrospray ionization
et al.	Latin: *et alii*, and others
GC	gas chromatography
HPLC	high performance liquide chromatography
HPP	3-(4-hydroxyphenyl)propanoate
HZI	Helmholtz Zentrum für Infektionsforschung, Braunschweig
ICBM	Institut für Chemie und Biologie des Meeres, Oldenburg
m/z	mass to charge ratio
MPI	Max-Planck-Institut für Marine Mikrobiologie, Bremen
MS	mass spectrometry
MS/MS	two-stage mass spectrometry
MSTFA	N-methyl-N-(trimethylsilyl)-trifluoro-acetamide
NAD^+/NADH	nicotinamide adenine dinucleotide (*oxidised/reduced*)
$NADP^+$/NADPH	nicotinamide adenine dinucleotide phosphate (*oxidised/reduced*)
OD_{660nm}	optical density, measured at 660 nm
PHB	poly-(R)-3-hydroxybutanoate
rcf	relative centrifugal force
RI	retention index
SPE	solid phase Extraction
TCA	tricarboxylic acid cycle, also known as citrate cycle
TMS	trimethylsilyl
TOF	time of flight (mass spectrometry)
v/v	volume per volume

Abbreviation	Explanation
w/v	weight per volume
μ	specific growth rate

Furthermore, units were abbreviated according to the international unit system (SI, Systéme international d'unités), except for molar concentrations (mol/l), which were abbreviated with the capital letter M. Chemical elements were abbreviated by their symbols of the periodic table of elements.

Summary

Aromatic compounds are widely distributed in the environment, where their remineralization plays a crucial role in the global carbon cycle. Since various natural habitats exhibit low oxygen availability, the anaerobic and micro-aerobic biodegradation of these compounds by bacteria is of ecological importance. *Aromatoleum aromaticum* EbN1 represents one of the best-characterized model organisms for the catabolism of aromatic substrates under limited oxygen conditions. However, some degradation pathways are based on enzyme function predictions alone and a comprehensive characterization of the aromatic metabolism is still wanting.

In this thesis, the catabolism of four aromatic substrates by *A. aromaticum* EbN1 under oxic and anoxic growth conditions was investigated by comprehensive metabolomic studies, complemented by collaborative transcriptomic and proteomic analyses.

Application of CoA-ester analysis showed the anaerobic degradation of 3-hydroxybenzoate to proceed via 3-hydroxybenzoyl-CoA and yield 4-oxopimeloyl-CoA as intermediate. The subsequent pathway was found to proceed via 3-hydroxypimeloyl-CoA, analogous to the lower anaerobic benzoyl-CoA degradation pathway. The data from this work additionally contradicts the previously predicted dehydroxylation of 4-hydroxybenzoyl-CoA during 3-(4-hydroxyphenyl)propanoate (HPP) degradation via the annotated 4-hydroxybenzoyl-CoA reductase. Instead, benzoyl-CoA reductase could be involved, revealing new aspects of anaerobic radical-mediated reduction.

An unexpected cellular adaption to anaerobic benzoate degradation was the accumulation of putative osmolytes, correlating with high concentrations of intracellular benzoate. Neither the biosynthesis of the osmolytes nor a role in the cell response to potentially toxic intracellular benzoate concentrations was previously anticipated. These findings could be of interest, regarding the biotechnological production of glucosides and the implications on enhanced chemical resistance during bioremediation.

Over all, this thesis provides a systems biological view on the catabolic network of aromatic degradation, revealing several aspects of adaption to the environmental niche of aromatic degradation in aqueous sediments. Furthermore, new details on specific degradation pathways were gained and a first observation of osmolyte accumulation during anaerobic benzoate degradation was reported.

Zusammenfassung

Aromatische Verbindungen sind in unserer Umwelt weit verbreitet und ihre Mineralisierung ist Teil des globalen Kohlenstoffkreislaufes. Da zahlreiche natürliche Lebensräume nur über eingeschränkten Sauerstoffeintrag verfügen, ist der anaerobe Aromatenabbau durch Bakterien ökologisch besonders relevant. *Aromatoleum aromaticum* EbN1 ist der am besten charakterisierte Modellorganismus für die Verstoffwechselung von Aromaten unter Sauerstofflimitierung. Allerdings basieren viele der für den Organismus beschriebene Abbauwege ausschließlich auf funktionellen Enzymvorhersagen, während direkte metabolische Untersuchungen noch fehlen.

Im Rahmen dieser Arbeit wurde der aerobe und anaerobe Abbau von vier aromatischen Substraten in *A. aromaticum* EbN1 untersucht. Es wurden umfassende Metabolomanalysen mit kollaborativ gewonnen Transkriptom- und Proteomdaten kombiniert um ein systembiologisches Gesamtbild zu erhalten.

Der anaerobe Abbau von 3-hydroxybenzoate über 3-hydroxybenzoyl-CoA und 4-oxopimeloyl-CoA konnte durch die Verwendung einer neuen Analysemethode für CoA-Ester erstmals auf Metabolomebene gezeigt werden. Der weitere Abbau findet über 3-hydroxypimeloyl-CoA, analog zum unteren Teil des anaeroben Benzoyl-CoA Weges, statt. Außerdem widersprechen die Ergebnisse der vorhergesagten Dehydroxylierung von 4-hydroxybenzoyl-CoA durch die 4-hydroxybenzoyl-CoA reductase während des aeroben und anaeroben HPP-Abbaus. Statt dessen könnte die Benzoyl-CoA reductase beteiligt sein, was neue Einsichten in die radikalische anaerobe Reduktion ermöglichen würde.

Bemerkenswert war die Ansammlung von mutmaßlichen Osmolyten, die während des anaeroben Benzoatabbau mit einer hohen intrazellulären Benzoatkonzentration korrelierte. Weder die Biosynthese der Substanzen, noch ihre Rolle in der Zellantwort auf Biozide war bisher bekannt. Diese Ergebnisse können zukünftig relevant sein für die biotechnologische Produktion von Glucosiden und Anwendungen zur Bioremediation.

Insgesamt wurde in dieser Arbeit ein erster systembiologischer Blick auf das Netzwerk der aromatischen Abbauwege gezeigt, die Anpassung an den Aromatenabbau in Sedimenten beschrieben und neue Erkenntnisse zu einzelnen Abbauwegen gewonnen. Außerdem wurde erstmals die Akkumulation von Osmolyten während dem anaeroben Benzoatabbaus beschrieben.

1 Introduction

Aromatic compounds represent the second largest group of hydrocarbons in the ecosphere and play a crucial role in the global carbon cycle (for reviews see (Fuchs *et al.*, 2011; Vranova *et al.*, 2013)). The bio-degradation by fungi and bacteria in aerobic and anaerobic habitats plays a crucial role not only in re-mineralization of biopolymers, but also in the removal of man-made chemical or mineral-oil-based pollution. Bacteria from the family *Rhodocyclaceae* play an important role in the degradation of aromatic compounds under denitrifying conditions. The first bacterium of this family, of which the genome was fully sequenced, was *Aromatoleum aromaticum* EbN1 (Rabus *et al.*, 2005). With its broad metabolic capabilities, well established aerobic and anaerobic cultivation procedures and numerous proteomic studies on the aromatic degradation processes, *A. aromaticum* EbN1 is a representative and well studied model organism for aromatic degradation (Rabus *et al.*, 2014).

1.1 Background

1.1.1 Biodegradation of aromatic compounds

Aromatic compounds are characterized by a chemically stable aromatic ring structure. These compounds are highly abundant in nature and comprise a wide variety of biological functions. For example, aromatic compounds are the building blocks of the structural plant polymer lignin; the three aromatic amino acids phenylalanine, tyrosine, and tryptophane occure in all living organisms; and a large and diverse group of plant secondary metabolites as well as animal hormones contain aromatic structures. Human activities, including petrochemical processing, application of biocidal products and various forms of waste disposal, release further aromatic compounds into the environment (Vranova *et al.*, 2013).

While possessing broad capabilities of biosynthesis, most plants and animals are only capable of degrading a very limited range of aromatic compounds, including the aromatic amino acids. Degradation of lignin from wood to humus is a very slow process, facilitated by aerobic fungi and aerobic and anaerobic bacteria (Mäkelä *et al.*, 2014).

The aerobic degradation of aromatic compounds has been studied extensively on the example of benzoate. Mono- and dioxygenases play a key role in the aerobic dearomatization pathway of bacteria and fungi (Díaz *et al.*, 2013). The involved reactions require molecular oxygen as co-substrate and often produce free reactive oxygen species as byproducts. Under anoxic growth conditions, different catalytic strategies have to be employed to overcome the resonance energy of aromatic structures. However, despite the initial high energy requirement of dearomatization, aromatic substrates are usually rewarding, high energy substrates to promote microbial growth (Cao *et al.*, 2009).

A large variety of ecosystems is characterized by a restricted oxygen availability. Examples of anaerobic habitats are sediments, the lower digestive systems of all animals and soil layers with restricted drainage. First evidence of the complete decomposition of aromatic substrates under anoxic growth conditions by sewage sludge was gathered in 1934 (Tarvin and Buswell, 1934). The anaerobic degradation of benzoate by the photoheterotrophic bacterium *Rhodopseudomonas palustris* was found to proceed via reduction of the aromatic ring rather than oxidation processes (Dutton and Evans, 1968). Furthermore, anaerobic benzoate degradation in *R. palustris* was found to be dependent on substrate activation by thioesterification with coenzyme A (CoA) and energy consumption in the form of ATP hydrolysis (Dutton and Evans, 1970; Whittle *et al.*, 1976). Similar reductive dearomatization of benzoyl-CoA was shown to occur in the denitrifying betaproteobacterium *Thauera aromatica*, where more detailed studies of the benzoyl-CoA reductase were conducted (Anders *et al.*, 1995; Boll and Fuchs, 1995; Koch and Fuchs, 1992).

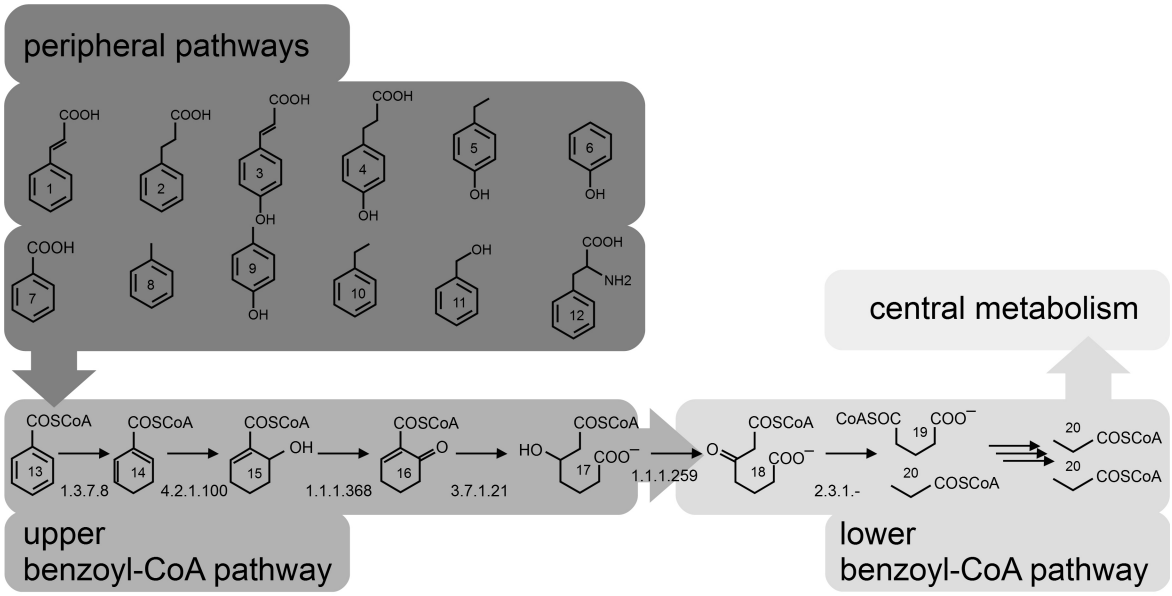

Figure 1: Overview of the anaerobic benzoyl-CoA degradation pathway with peripheral pathways, upper and lower degradation pathway and connection to the central metabolism via acetyl-CoA
Examples for substrates metabolized through the anaerobic benzoyl-CoA degradation pathway: (1) cinnamate, (2) hydrocinnamate, (3) p-coumarate, (4) 3-(4-hydroxyphenyl)propanoate, (5) 4-ethylphenol, (6) phenol, (7) benzoate, (8) toluene, (9) p-cresol, (10) ethylbenzene, (11) benzylalcohol, (12) phenylalanine; CoA-esters from the upper benzoyl-CoA degradation pwathway: (13) benzoyl-CoA, (14) cyclohexa-1,5-dienecarbonyl-CoA, (15) 6-hydroxycyclohex-1-enecarbonyl-CoA, (16) 6-ketoxycyclo hex-1-ene-1-carboxyl-CoA, (17) 3-hydroxypimelyl-CoA; Selected intermediates of the lower benzoyl-CoA degradation pathway: (18) 3-ketopimelyl-CoA, (19) glutaryl-CoA, (20) acetyl-CoA

This mechanism of anaerobic benzoyl-CoA reduction and the subsequent degradation to acetyl-CoA by β-oxidation reaction sequences, represents a central metabolic pathway in most bacteria during anaerobic aromatic degradation. Diverse aromatic substrates are channeled into this central pathway. Aromatic acids are converted to their respective CoA-esters by specific CoA-ligases and converted to benzoyl-CoA. Examples for substrates being metabolized anaerobically via benzoyl-CoA are 2-aminobenzoate (Altenschmidt *et al.*, 1991), 4-chlorobenzoate (Löffler *et al.*, 1992) or phenylacetate (Martínez-Blanco *et al.*, 1990). Phenolic or anthranilic compounds can be carboxylated to allow for CoA-thioesterification and subsequent removal of functional groups to generate benzoyl-CoA. (reviewed in (Boll *et al.*, 2014; Heider and Fuchs, 1997)). Furthermore, different strategies for the anaerobic oxidation of various alkyl side chains from aromatic compounds exist and lead to benzoate or benzoyl-CoA, to be channeled into the central benzoyl-CoA pathway (Boll *et al.*, 2014). The benzoyl-CoA degradation pathway can be divided into an

upper pathway, which includes the reductive dearomatization and hydrolytic ring opening of benzoyl-CoA, and a lower pathway, which is a modified β-oxidation process. Finally, the produced acetyl-CoA can be channeled into the citric acid cycle or biosynthetic routes of the central metabolism (Figure 1).

The aerobic degradation of benzoate and other aromatic compounds via mono- and dioxygenases has been studied for a long time. However, an alternative mode of aerobic benzoate degradation, which like the anaerobic pathway relies on CoA-bound intermediates, was discovered in *Azoarcus evansii* (Altenschmidt *et al.*, 1993; Anders *et al.*, 1995). This appears to be the preferred pathway in micro-aerobic and facultatively anaerobic bacteria (Fuchs *et al.*, 2011).

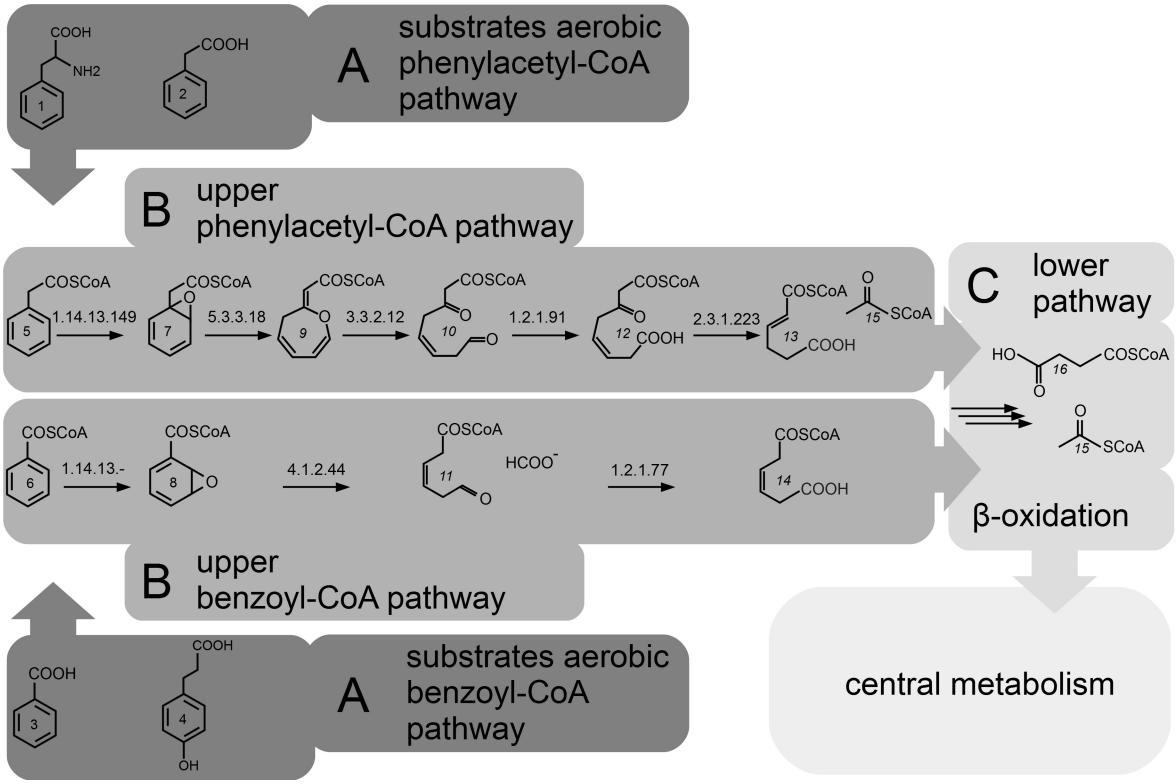

Figure 2: Epoxy-CoA pathways of aerobic benzoyl-CoA and phenylacetyl-CoA degradation
Examples for substrates channeled into these pathways are (1) phenylalanine, (2) phenylacetate, (3) benzoate, (4) 3-(4-hydroxyphenyl)propanoate; CoA ester intermediates of the pathways are (5) phenylacetyl-CoA, (6) benzoyl-CoA, (7) 2-(1,2-epoxy-1,2-dihydrophenyl)acetyl-CoA, (8) 2,3-epoxybenzoyl-CoA, (9) 2-oxepin-2(3H)-ylideneacetyl-CoA, (10) 3-oxo-5,6-dehydrosuberyl-CoA semialdehyde, (11) 3,4-didehydroadipyl-CoA semialdehyde, (12) 3-oxo-5,6-dehydrosuberyl-CoA, (13) 2,3-didehydroadipyl-CoA, (14) 3,4-didehydroadipyl-CoA and (15) acetyl-CoA; Products of the subsequent β-oxidation are (16) succinyl-CoA and (15) acetyl-CoA, which are channeled into the central metabolism

This pathway of aerobic aromatic degradation combines the activation of intermediates by CoA-thioesterification with the attack of molecular oxygen to form epoxy-CoA intermediates (Rather *et al.*, 2010). The starting metabolite of this pathway is either benzoyl-CoA or phenylacetyl-CoA, for both of which specific sets of enzymes are necessary (Ismail and Gescher, 2012). Parallels and differences of the aerobic phenylacetyl-CoA pathway and the aerobic benzoyl-CoA pathway are displayed in figure 2.

Like the anaerobic benzoyl-CoA pathway, the aerobic aromatic degradation via epoxy-CoAs can be divided into three parts: A) The various peripheral pathways, which convert different substrates into a few central metabolites; B) the two upper pathways, which include dearomatization and ring cleavage in parallel reactions for benzoyl-CoA and phenylacetyl-CoA; and C) a combined lower pathway, which joins the two parallel upper pathways into one β-oxidation reaction sequence, producing metabolites of the central metabolism.

As mentioned above, CoA-ester epoxydation presents a strategy for aerobic aromatic degradation under low or fluctuating oxygen availability. The most common strategy in aerobic bacteria with no restrictions in oxygen availability is to use mono- or di-oxygenases to transform various aromatic substrates into the corresponding catecholic compounds (catechol, protocatechuate, gentisate). In these compounds, the aromatic nature of the ring is weakened by the presence of two hydroxy groups in the ring. Thus the compound is susceptible to *ortho* or *meta* cleavage by dioxygenases (reviewed in (Fuchs *et al.*, 2011)). An example of a pathway with dioxygenase mediated ring cleavage of a catecholic intermediate is the gentisate pathway of aerobic 3-hydroxybenzoate degradation. The pathway has been studied in *Klebsiella pneumoniae* M5a1 and *Salmonella enterica* ssp. I ser. Typhimurium (Goetz and Harmuth, 1992; Jones and Cooper, 1990). This degradation pathway can be divided into two parts: I) various substrates are transformed into the central intermediate gentisate; II) gentisate is oxidized to maleylpyruvate, isomerized and cleaved into fumarate and pyruvate, which can be fed into central metabolism. Examples for substrates that can be metabolized via this pathway are 3-hydroxybenzoate, salicylate and cresoles (Rabus *et al.*, 2014).

1.1.2 Aromatoleum aromaticum *EbN1*

Aromatoleum aromaticum EbN1, officially: *Azoarcus* sp. EbN1, is a gram-negative betaproteobacterium, first described in 1995 (Rabus and Widdel, 1995). The organism was isolated from mud samples from the Weser river in Bremen (Germany) due to the capability to anaerobically degrade ethylbenzene. Since the bacterium lacks genes for N2 fixation and symbiotic plant interaction, which are typical for *Azoarcus* species, classification as a new genus has been proposed (Rabus *et al.*, 2005).The species name *Aromatoleum aromaticum* is already widely used in scientific publications (Boll *et al.*, 2014; Hille *et al.*, 2014; Muhr *et al.*, 2015; Philipp and Schink, 2012).

A. aromaticum EbN1 was the first bacterium described to anaerobically degrade ethylbenzene along with seven other aromatic substrates and the genome was sequenced (Rabus *et al.*, 2005; Rabus and Widdel, 1995). Today, *A. aromaticum* EbN1 is one of the best-studied model organisms for anaerobic aromatic degradation in dentirifying bacteria. Proteomic and genomic studies served to create a catabolic network for anaerobic degradation of 24 aromatic compounds with 85 predicted enzymes, of which 65 could be identified (Rabus *et al.*, 2014; Trautwein *et al.*, 2012b; Wöhlbrand *et al.*, 2007). This catabolic network is unique in the investigation of aromatic degradation and represents a first step towards a systems biological analysis, advancing from the examination of isolated reactions and pathways.

1.1.3 Systems biology

Systems biology is the systematic integration and combination of multiple high throughput data sets and computational modeling to generate a comprehensive view of the total system (Figure 3). The integrated data typically include genomics and other omics data sets, which describe the various levels of the cellular processes under investigation. In this study, systems biology is applied to investigate the bacterium *A. aromaticum* EbN1 under different growth conditions. For a review on systems biology and integrated methods, see (Zhang *et al.*, 2010).

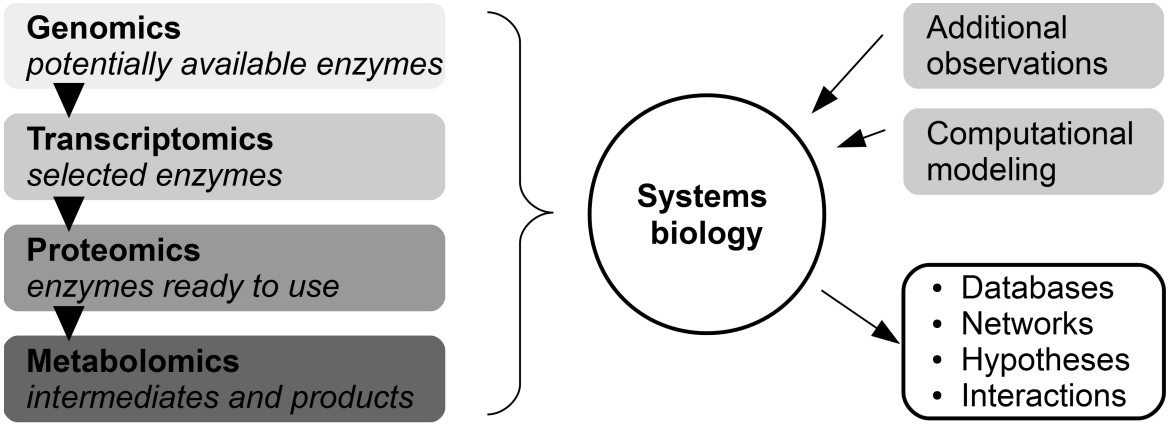

Figure 3: Systems biology integrates various levels of cellular processes of a biological system. Instead of focusing on single reactions, it is the science of integrating comprehensive data from all available omics approaches to investigate the interactions and regulation within a complex network.

The first level of systems biological data sets is the genome, which is investigated by using genomics and encodes all enzymes possibly available in a specific organism. It represents the potentially available tools, a cell could apply to adapt to different growth conditions. The uniformity of the DNA units and the over all static character of the genome facilitate genomic analysis (For a review see (Conesa and Mortazavi, 2014).

The next level of cellular response is transcription, which is analyzed by transcriptomics, where the abundances of mRNAs from different genes are measured. These are influenced by transcriptional regulation as well as by post-transcriptional regulation, depending on the necessity for growth and maintenance under the respective growth conditions. Transcriptomic adaption to environmental changes occurs within minutes to hours and represents the selection of the enzymatic tools from the genomic toolkit. Transcriptomics at systems biological level is usually conducted with microarray technology or RNA seq technology (Sorek and Cossart, 2010).

The third stage in the omics-cascade is the proteome, which is analyzed by proteomics. The measured protein levels are the result of post trancriptional regulation, as well as the regulation of protein stability. Proteomics is the first level of -omics analysis where different fractions of analytes need to be analyzed by different methods. For proteomic studies, extraction methods for specific groups of proteins are usually combined with a separation technique, such as gel electrophoresis or column chromatography, coupled to a detection method like MALDI-TOF or ESI-TOF for peptide identification (For reviews see (Bantscheff *et al.*, 2012; Wöhlbrand *et al.*, 2013)).

The final omics level is metabolomics, which aims to characterize the metabolite pools in a cell (Kell, 2004). These pools are the result of enzyme activity and transport processes. The resulting metabolom data represents the most complex level of omics data, including multiple levels of regulation responses between environmental trigger and the observed phenotype. Metabolomics, as applied in this thesis, is described in the following sections *1.1.4* and *1.1.5* in greater detail. The majority of metabolomic analyses is conducted using mass spectrometric analysis in combination with various separation techniques (Dettmer *et al.*, 2007).

Systems biology aims to integrate experimental data from all available omics analyses of the system under investigation. Complementing the omics experiments, computational modeling is often used to predict or analyze the entire cascade of cellular responses in the system. Furthermore, additional information on the phenotype, growth or respiration rates, excretion of substances or other experimental results can be integrated to optimize predictive or descriptive power of a systems biological approach and the computational model. Thus, an important aspect of systems biology is the data storage and information management of the large data sets generated by the omics methods.

1.1.4 Metabolomics

Metabolites represent the end-product of cellular biochemistry, e.g. the products and intermediates of enzyme catalyzed reactions and transport processes. Metabolomics aim to provide qualitative and quantitative information on the metabolites present under a specific experimental condition. In contrast to other analytes, metabolites do not share a uniform biochemical character but represent a diverse mixture of compounds with varying chemical properties like polarity, acidity, molecular weight, volatility and reactivity. A review on some of the different methodical developments to face the diversity of metabolites is given in (Mashego *et al.*, 2006) and (Issaq *et al.*, 2009).

One approach to simplify the complex metabolomic analysis is metabolic fingerprinting, where metabolic profiles are generated from samples and compared across experimental setups, without identification of every metabolite (Dettmer *et al.*, 2007; Fiehn, 2002). Methods in metabolomics are also restricted by the applied analytical methods and their specificity for a certain group of chemically similar substances. To

combine different methods or apply quantitative analysis, it is necessary to identify metabolites, compare synthetic chemical standards and/or isotopically labeled standards. By combining four different analytical methods, 95% of the 694 metabolite predicted to occur in *E. coli* during aerobic growth with glucose were detected (Werf *et al.*, 2007). However, this study also makes note of an other problem in metabolomics: only little more than 50% of the predicted metabolites were available as chemical standards. This rate can be expected to be much higher when investigating more exotic processes than aerobic glucose metabolism.

1.1.5 Methods in metabolomics

As described above, no single method is sufficient to analyze the whole metabolome qualitatively and quantitatively as would be required in the strictest definition of the term metabolomics. Instead, different methods focus on quantitative or qualitative analysis of specific groups of metabolites. By combining different methods, a more comprehensive measurement of the metabolome is possible.

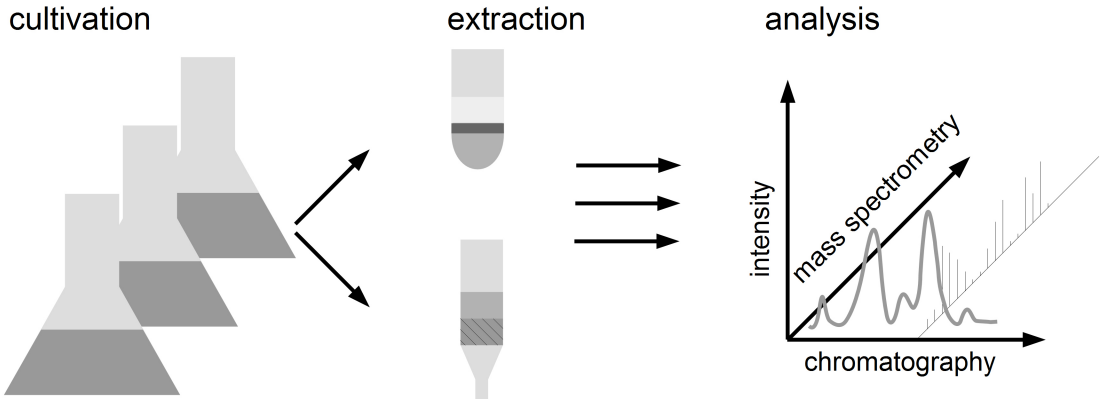

Figure 4: Multiplication of analytical dimensions when different cultivation conditions, extraction and analysis methods are combined
To analyze a comprehensive fraction of the metabolome, combination of lateral extraction and analytical methods is necessary. This leads to a large set of multidimensional data, from which metabolites need to be identified before data sets can be combined for interpretation.

Typically, methods for metabolomic analysis comprise of optimized procedures for sample preparation (harvest and extraction), analyte separation (chromatography) and analyte detection (mass spectrometry) (Figure 4). The methods relevant for this thesis are described below.

1.1.5.1 Sample preparation

Sample preparation aims to concentrate, clean and preserve the analytes of interest for any specific analytical method. Thus, sample harvest needs to remove extracellular compounds that could bias measurement of intracellular metabolites and at the same time needs to ensure sample integrity by eliminating post-harvest enzymatic activity or analyte decay. Depending on the applied analytical method, extraction methods are applied to further clean up the sample, eliminate matrix influences and concentrate analytes of interest.

Sample harvesting:

A harvest method needs to be as quick, quantitative and reproducible as possible and should include measures to quench enzymatic activity. For an overview of sampling strategies for metabolomics see (Mashego *et al.*, 2006; van Gulik, 2010)

Centrifugation allows to separate cells from various volumes of medium. Furthermore, the surrounding temperature and gas-phase composition inside the centrifugation container can be controlled and the centrifugational force applied may be adapted to the cell's robustness and their sedimentation behavior. However, centrifugation is generally less rapid than filtration and the cells are exposed to considerable physical forces, such as pressure, acceleration and shearing force. Centrifugation times usually increase with larger sample volumes.

Quenching is the rapid stopping of enzymatic activity in a sample to preserve the current state of the metabolome. A common practice is quenching with cold methanol and buffer solution. However, this method can lead to significant loss of metabolites through unspecific leakage (Bolten *et al.*, 2007). Additionally, the mixing of culture broth with substantial amounts of cold organic solvent poses an expensive and laborious work flow with greatly increased volumes during centrifugation and large amounts of organic waste. Shock freezing in liquid nitrogen is another common technique to stop metabolic activity but can only be applied after separating the cells from the medium.

Extraction methods:

All extraction methods aim to make the analytes of interest accessible to the applied analytical method. For this purpose bacterial cells need to be disrupted and compounds that would interfere with the analysis need to be removed from the sample.

Disruption of cells can be achieved for example by freez-dry cycles, enzymatic lysis, heat, ultra sonification or grinding. The disruption method, as well as accompanying factors like temperature or solvent have to be adapted according to specific durability of the cell envelopes and of the analytes of interest.

Theoretically, the cell extracts are ready for analysis after disruption of the cells, if the applied solvent is compatible with the following analytical method. However, most commonly additional steps of sample cleanup are necessary to remove cell debris, eliminate interfering or bulk metabolites, to replace the solvent or reduce the sample size. These measures include the centrifugational elimination of cell debris or phenol/chloroform extraction to remove protein from the samples. Solid phase extraction (SPE) offers various options to selectively clean up basic or acidic compounds or to select compounds by relative size or polarity. A variety of commercially available solid phase columns, which are compatible with several washing and elution protocols allow to extract very specific groups of compounds and even produce several fractions, if necessary.

The main advantages of phenol/chloroform extraction are the simple work flow and the relatively low material expenses, as all solvents are mixed in one tube and separated by centrifugation. The only selectivity of this extraction method is the removal of unpolar compounds, which is often not complete if only one step of extraction is applied. Thus, a complex and representative mixture of polar metabolites remains for metabolic profiling with e.g. GC-MS. However, the complexity of the mixture, bulk metabolites and residues from the medium like phosphate and salts can interfere with derivatization and measurement (see *1.1.5.4 Analysis of small polar metabolites via GC-MS*). In contrast to that, the sample, wash buffer and elution buffer have to be added sequentially onto a prepared column for SPE. Flow of solvents needs to be facilitated by pressure or suction and, depending on the sample matrix and column setup, large cell debris has to be removed from the sample beforehand. However, SPE is highly specific for groups of metabolites and allows for very thorough sample clean up, thus largely eliminating matrix effects during HPLC-MS.

1.1.5.2 Chromatography

Chromatography is a means of separating compounds according to their physico-chemical properties by harnessing the differences in distribution between a stationary and a mobile phase. The stationary phase can be planar, as in thin layer or paper chromatography or in form of a column, as in HPLC or GC. The mobile phase can be any kind of liquid solvent or a gas, that is directed across the surface of the solid phase. The analytes to be separated are dissoved in the mobile phase. When encountering the solid phase, specific interactions of the analytes with the solid phase result in slowing down the analytes according to their physico-chemical properties. These interactions can be very diverse: adhesion and adsorption as well as polar or ionic interactions.

Liquid chromatography:

Liquid chromatography (LC) usually indicates a chromatography method with a liquid mobile phase and a column of stationary phase with various materials. HPLC columns are typically packed with small porous particles, leading to increased surfaces. These surfaces are chemically bonded with functional groups that provide specific physico-chemical properties. Based on these properties numerous HPLC separation modes can be distinguished. Some examples are: Normal phase chromatography (polar stationary phase and non-polar mobile phase), Reversed phase and Hydrophopic interaction Chromatography. While the stationary phase is typically fixed throughout an experiment, the mobile phase can either be applied with constant composition (isocratic) or with a changing composition over the time of analysis by varying the aqueous/organic ratio (gradient) (For a reviwe on HPLC in metabolomics see (Allwood and Goodacre, 2010)).

Gas chromatography:

Gas chromatography (GC) applies a carrier gas as mobile phase, which is directed through a capillary with inside coating as stationary phase. The choices of mobile and stationary phase are generally more restricted in GC than in HPLC. Typical carrier gases are helium, nitrogen, argon, hydrogen or air. Stationary phases are typically modified polysiloxanes (silicone). In addition to the separation by retention on the column, a valuable additional separation step is the sequential heating of the sample, providing a pre-separation of the analytes according to their evaporation temperature. Retention is specific

for every compound and chromatography parameters are less variable than in LC. Thus, it is possible to convert the retention time into a retention index, which allows for higher comparability of retention across analyses and laboratories. A commonly applied retention index is based on the retention time relative to the retention of n-alkanes, converting the retention time in relative alkane length (Kováts, 1958).

A crucial property for metabolites to be analyzed with GC, is their volatility. Highly volatile compounds can be analyzed directly from the head-space of enclosed sample containers. Less volatile compounds can be evaporated by heating, if they are thermo-stable. Additionally, a broad range of polar metabolites can be converted into more volatile derivatives by sylation reactions. Common reagents for the derivatization are MSTFA (N-methyl-N-(trimethylsilyl)-trifluoro-acetamide) or BSTFA (N,O-bis(trimethyl-silyl)-trifluoro-acetamide) which result in slightly different volatility (Halket *et al.*, 2005). MSTFA, which was used in this study, replaces the reactive hydrogen atom of hydroxy-groups, carboxylates, amines, amides and thiols with a trimethyl-silano group, thus reducing polarity. In addition to that, methoximation of carbonyl groups can be applied to lock sugars in the open ring formation and reduce the number of resulting signals. Drawbacks of the derivatization reactions are the occurrence of byproducts, incomplete derivatization and other artifacts.

1.1.5.3 Mass spectrometry

Mass spectrometry analyzes molecules or molecule-fragments according to their molecular weight and abundance. The analytes have to be ionized and mobile before they are accelerated in an electromagnetic field for analysis of the mass to charge ratio.

Ionization:

An important aspect of mass spectrometry is the ionization of the analytes. In case of liquid chromatography, the analytes also have to be separated from the eluent. The ionization methods used in this work are described below.

Electron ionization (EI) can be applied to gaseous analytes. The analytes are guided through a beam of ions, leading to fragmentation and ionization. Thus EI is termed a “hard” ionization technique, in contrast to techniques that produce intact molecular ions without fragmentation. EI fragmentation is highly specific and reproducible, facilitating the

compilation of EI-spectra data bases (Kelleher *et al.*, 1999; Kind *et al.*, 2009; Kopka *et al.*, 2005). Additionally, the specific fragmentation can help to identify unknown metabolites, albeit additional methods usually need to be applied (Fiehn *et al.*, 2000b).

Electro spray ionization (ESI) is the most common method to couple LC and mass spectrometry. The stream of eluent is nebulized while the nebulizer needle at the same time conveys an electrical charge to the droplets. A stream of heated dry-gas serves to evaporate the solvent from the droplets. An electrical field funnels the charged molecules into the mass spectrometer. This method produces mostly intact molecular ions with a positive or negative charge. However, ionization strongly depends on the character of the analyte, some of which are hardly ionizable or only susceptible to positive or negative charge. Larger molecules can receive multiple charges, resulting in the detection of different ions and reducing sensitivity. The resulting mass spectra typically allow to determine the molecular mass and, if mass resolution is high enough, the calculation of the elemental composition.

Atmospheric pressure chemical ionization (APCI) applies ionization through a corona discharge needle directly to the gas stream from GC. The electrons from the corona needle initiate series of ion reactions between analyte molecules and molecules from the surrounding air (Carroll *et al.*, 1974). APCI produces mainly molecular ions with one or more charges. The molecular ions from APCI can serve to determine molecular mass and elemental composition for identification of unknown metabolites (Strehmel *et al.*, 2013).

Mass spectrometer:

After ionization, the various analyte ions have to be separated according to their mass to charge ratio (m/z) and quantified. This step can be conducted by different technical solutions: Quadrupol mass spectrometer generate an oscillating electromagnetic field between four parallel electrodes. The strength and amplitude of this field allows only for ions of a certain m/z to traverse the electrodes in a stable trajectory. A detector registers the impacts of ions with the specific m/z as intensity. In this way, a range of mass to charge ratios is scanned one after the other across a defined range. The same principle applies in hexapol mass spectrometers. The Advantage of these spectrometers lies in their robustness and sensitivity while the mass resolution is usually restricted.

Time of flight (TOF) mass spectrometers separate ions by acceleration through a fixed

electromagnetic potential. The traveling speed in a high vacuum depends solely on the m/z and can be measured over a specific distance. The detector registers the ion impacts as intensity with a chronological separation according to the mass to charge ratio. TOF mass spectrometers can provide high mass resolution but tend to be less sensitive and robust than quadrupol mass spectrometers.

Other instruments use the deflection or trapping of ions in magnetic fields to measure the mass to charge ratio.

1.1.5.4 Analysis of small polar metabolites via GC-MS

Small metabolites constitute a large part of the primary metabolism, including organic acids, amino acids, phosphorylated compounds and sugars. The most commonly used method for profiling small polar metabolites is GC-MS. Coupling of gas chromatography to mass spectrometry was first described in 1969 to analyze carbohydrates (DeJongh *et al.*, 1969). The technique evolved and was applicable for diagnostic metabolic profiling from urine samples in 1988 (Jellum *et al.*, 1988). Since then, GC-MS advanced to a robust and versatile method applicable to metabolic profiling from tissue, plants and microorganisms as shown by the identification of half of 326 putative metabolites from plant samples (Fiehn *et al.*, 2000a). The application of retention time indices and EI-MS to generate reproducible fragmentation spectra allowed for the construction of several data bases for metabolite identification.

However, GC-MS is restricted to termostabile not to large metabolites that are either volatile or can form sufficiently volatile derivatives. Further restrictions are posed by the applied extraction method, which defines the range of polarity or volatility.

1.1.5.5 Analysis of CoA-esters via HPLC-MS

One class of metabolites that is particularly important to the investigation of anaerobic aromatic degradation, are coenzyme A esters. As described in section *1.1.1 Biodegradation of aromatic compounds*, thioesterification of aromatic acids is prerequisite for aromatic degradation under anoxic or microoxic conditions.

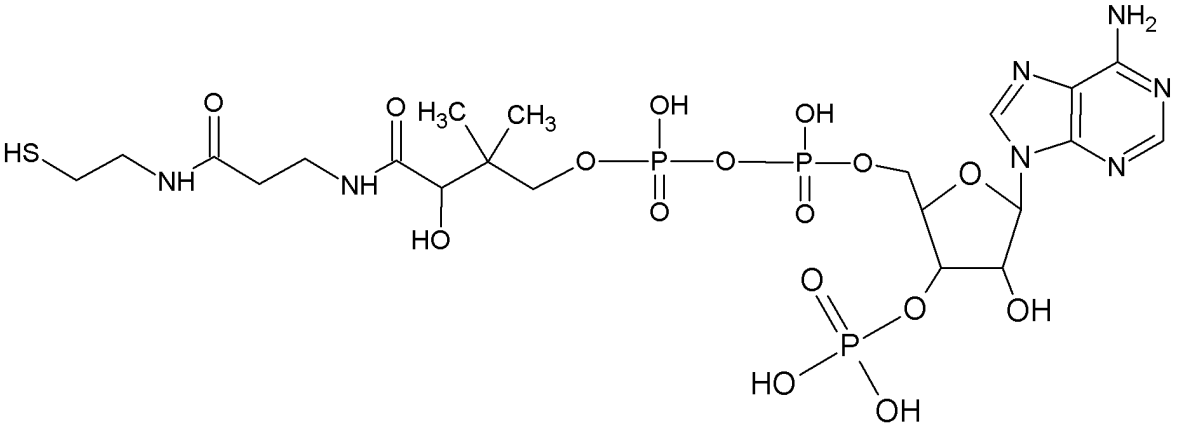

Figure 5: Chemical structure of coenzyme A

Coenzyme A is a relatively large metabolite (767.535 Da) with several polar functional groups groups (Figure 5). The high molecular weight, in combination with the chemically and enzymatically susceptible thiol- and phosphate-bonds render analysis of CoA-esters a complicated process. Moreover, the structure of the attached substrate also influences the chemical stability of the molecule significantly (Kolkmann and Leistner, 1987). This low chemical stability reflects in the low recovery rates reported for diverse extraction methods (40% for maolonyl-CoA (Reszko *et al.*, 2001), and 5% to 75% for malonyl-CoA from different rat tissues with different liquid or solid phase methods (Minkler *et al.*, 2006; Onorato *et al.*, 2010). An additional challenge for analysis of biological CoA-esters is the limited availability of synthetic standards. Especially when investigating degradation pathways and processes beyond the central metabolism, no synthetic standards are commercially available to identify the detected compounds by direct comparison.

Analysis of CoA-esters is mostly conducted by application of a liquid or solid phase extraction method and various versions of liquid chromatography coupled to mass spectrometry (Armando *et al.*, 2012; Gilibili *et al.*, 2011; Magnes *et al.*, 2008; Onorato *et al.*, 2010; Peyraud *et al.*, 2009; Yang *et al.*, 2010).

1.2 Motivation and Objectives

In most studies of bacterial aromatic degradation, metabolomic analyses were restricted to single methods or targeted analyses of very few substances of interest (Gall *et al.*, 2013). To elucidate details of degradation pathways, mostly products of enzyme assays were analyzed, rather than the whole metabolism (Rather *et al.*, 2010; Teufel *et al.*, 2010). So far, analysis of aromatic degradation pathways is focused on single enzymes or pathways, active under one growth condition. To date, no studies addressing the bacterial aromatic degradation on a broader metabolomic level, much less on a systems biological level, are published.

However, bacterial degradation processes are not isolated enzymatic reaction chains but networks of peripheral and central pathways, influencing the whole cellular system from gene transcription to cell physiology. Thus, a systems biological analysis of different aerobic and anaerobic aromatic degradation processes will provide new insight beyond the previously described pathways. This could lead the way to a deeper understanding of restrictions in degradation capacities and the cellular context of these processes. A first attempt in this direction was the construction of a network of aromatic degradation pathways from *A. aromaticum* EbN1 on a proteomic level, without transcriptomics or metabolomics data (Rabus *et al.*, 2014; Wöhlbrand *et al.*, 2007).

This thesis aims to provide an analysis of the aerobic and anaerobic aromatic metabolism of *A. aromaticum* EbN1 in a comprehensive systems biological approach. For this purpose, the following objectives were met:

Firstly, since CoA-esters play a crucial role in anaerobic and micro-aerobic aromatic degradation pathways, a method for the analysis of CoA-esters from bacterial cell extracts had to be implemented and optimized. This method served to complement the analysis of small polar metabolites via GC-MS. Furthermore, additional small polar metabolites from the GC-MS measurements had to be identified. The resulting HPLC-MS/MS method and information on the identification of CoA-esters, as well as small polar metabolites are presented in section *3.1 Identification of metabolites*.

Secondly, to depict the complex network of degradation pathways and their potential interaction, a representative set of aromatic substrates was selected and analyzed under comparable growth conditions. Metabolomics data were collected from *A. aromaticum* EbN1 cells, grown aerobically and anaerobically in the presence of four aromatic substrates (benzoate, 3-hydroxybenzoate, 3-(4-hydroxyphenyl)propanoate and phenylacetate) and one non-aromatic reference (acetate). Additionally, the biomass composition under all ten growth conditions was determined and quantified. An overview of the data is presented in chapters *3.2.1 General results* and *3.2.5 Physiological effects3.2.1* ans *3.2.5*.

Thirdly, to provide a systems biological view beyond single omics perspective, the metabolomic data were integrated with transcriptomic and proteomic data, generated by the cooperation partners. Subsequently, the responses of the central metabolism and other significant metabolic changes, were analyzed. These results are presented and discussed in chapter *3.2 Comparison of the different growth scenarios*.

Lastly, the combined systems biological data were analyzed in the context of the different aromatic degradation pathways. A special focus was placed on the comprehensive reconstruction of pathways previously postulated based on enzyme function predictions and differential protein expression. Furthermore, the systems biological data served to elucidate unclear aspects of specific pathways (e.g. aerobic HPP degradation and anaerobic 3-hydroxybenzoate degradation). The degradation pathways with all related systems biological data are presented and discussed in chapter *3.3 Degradation pathways*.

2 Material and methods

All experiments were conducted in cooperation with with the research group of Prof. Ralf Rabus (Institute for Chemistry and Biology of the Marine Environment (ICBM) of the Carl von Ossietzky Universität Oldenburg, Department of General and Molecular Microbiology), namely in collaboration with Dr. Kathleen Trautwein. Additional cultivations for transcriptomic analysis were conducted at the Max-Planck-Institut für Marine Mikrobiologie, Bremen (MPI). All cultivations of *Aromatoleum aromaticum* EbN1 for the systems biological experiments, including sampling for every analysis, were simultaneously conducted for every growth condition. Kathleen Trautwein and coworkers conducted the quantitative physiological studies for the systems biology approach. Proteomic analysis was conducted by Lars Wöhlbrand (ICBM). Transcriptomic analysis and data processing of *A. aromaticum* was performed by Dr. Robert Geffers (Research Group Genome Analytics at the Helmholtz center for infection research, Campus Braunschweig).

All samples for determination of the biomass composition, GC-MS and HPLC-MS metabolomic analysis were prepared by myself during excursions to Oldenburg, where the cultivations took place.

2.1 Organism and cultivations

All media were prepared in Oldenburg by the research group of Prof. Ralf Rabus as described previously (Rabus and Widdel, 1995; Widdel and Bak, 1992). Cultivation and cell harvest was then conducted corporately in the ICBM and MPI laboratories, before transporting metabolomic, transcriptomic and biomass composition samples to Braunschweig.

Anaerobic cultivation was carried out in 500 ml flat bottom flasks with 400 ml anoxic, phosphate buffered minimal medium and sealed with oxygen-impermeable butyl rubber stoppers at 28°C. The headspace space was filled with sterile, oxygen free N_2:CO_2 (9:1) atmosphere. Aerobic cultivation was carried out in 1 l screw-cap glass bottles with 400 ml oxic, phosphate buffered medium and 600 ml head space with sterile air. The bottles were

sealed with screw cabs and butyl rubber septa and incubated at 28°C at 120 rpm on a rotary shaker.

Basic mineral medium for anaerobic cultivation (1 l), sterilized by autoclaving

KH_2PO_4	1.12 g
K_2HPO_4	5.60 g
NH_4Cl	0.80 g
Na_2SO_4	0.23 g
NaCl	1.00 g

All compounds were dissolved in 1 liter of water, the pH was adjusted to 7.2 and then sterilized by autoclaving for 25 min at 121°C. For anaerobization, the gasphase was replaced with an oxygen free N_2:CO_2 (9:1) atmosphere during the cooling after autoclaving. After cooling down, the following solutions were added aseptically, ascorbate was only added to anaerobic cultures.

Composition of final growth medium as described by (Rabus and Widdel, 1995)

basic mineral medium (see above)	1 l
salt concentrate: $MgCl_2$ (6 H_2O) 324 g/l, $CaCl_2$ (2 H_2O) 29.4 g/l	1 ml
trace element solution (see below)	1 ml
selenate/tungstate solution: NaOH 0.4 g/l, Na_2SeO_3 (5 H_2O) 6 mg/l, Na_2WO_4 (2 H_2O) 8 mg/l	1 ml
vitamin B12 solution: cyanocobalamine 0.5 g/l	1 ml
vitamin solution (see below)	1 ml
$NaHCO_3$ 84 g/l	30 ml
acsorbate (1M) (anoxic medium only)	4 ml

All vitamin and trace element solutions were filter-sterilized (nitrocellulose, pore size 0.2 µm) and stored at 4°C in the dark, before addition to the medium.

Before inoculation, all media were supplied with substrate and nitrate (only anaerobic) from sterile stock solutions. Table 1 summarized the applied concentrations, as well as the measured initial concentrations of substrates and nitrate.

Trace element solution (1 l), sterilized by autoclaving

NaEDTA	5.2 g
$FeSO_4$ (7 H_2O)	2100 mg
H_3BO_3	30 mg
MnCl (4 H_2O)	100 mg
$CoCl_2$ (6 H_2O)	190 mg
$NiCl_2$ (6 H_2O)	24 mg
$CuCl_2$ (7 H_2O)	2 mg
$ZnSO_4$ (7 H_2O)	144 mg
Na_2MoO_4 (2 H_2O)	36 mg

Vitamine solution in 10 mM sodium phosphate buffer, pH 7.1 (100 ml) sterilized by filtration

4-aminobenzois acid	4 m
d(+)-biotin	1 mg
nicotinic acid	10 mg
calcium D(+)-panthotenate	5 mg
pyridoxine dihydrochloride	15 mg

Table 1: Initial concentrations of substrates and nitrate

Column "calc" indicates the intended concentrations of substrate and nitrate in mM, column "measured" represents the mean concentration measured by HPLC-analysis at the beginning of the experiment, SD indicates the standard deviation across all cultures.

condition	calc	measured	calc	measured
Ace-O2	8	8 ± 0.13	0	–
Ace-NO3	8	8.02 ± 0.06	7	5.86 ± 0.10
Ben-O2	2	1.79 ± 0.06	0	–
Ben-NO3	4	3.68 ± 0.30	7	5.94 ± 0.26
Hbe-O2	2	2.01 ± 0.01	0	–
Hbe-NO3	4	3.64 ± 0.04	7	6.25 ± 0.06
HPP-O2	4	3.99 ± 0.14	0	–
HPP-NO3	2	1.91 ± 0.01	7	6.48 ± 0.18
Phe-O2	2	1.92 ± 0.004	0	–
Phe-NO3	4	3.37 ± 0.01	10	10 ± 0.03

2.2 Analysis of small polar metabolites using GC-EI-MS and GC-APCI-MS

2.2.1 Harvesting of cell material

Bacterial cells were grown to an optical density of 0.3 (660 nm) in 400 ml oxic or anoxic medium as described in *2.1 Organism and cultivations*. Upon harvest, the whole culture was transferred into 500 ml centrifugation beakers and centrifuged for 15 min at 4°C and 17000 rcf. The supernatant was decanted and replaced by 200 ml 0.9% NaCl washing solution. After suspending the cells by vigorous shaking, they were separated from the washing solution by centrifugation for 15 min at 4°C and 17000 rcf. The cells were dispersed in 2 ml methanol-ribitol solution (15 µl/ml of a 0.2 mg/ml aqueous ribitol solution) by pipetting on ice. The resulting cell suspension was split and transferred into two precellys tubes with 600 mg glass beads each (70-110 µm, Kuhmichel). Samples were frozen in liquid nitrogen and transported on dry ice. In Braunschweig, the samples were stored at -80°C until extraction of the metabolites.

For anaerobic samples, transferring the culture into centrifugal beakers as well as replacing the supernatant with NaCl washing solution was carried out under a constant flow of nitrogen as described by (Hungate, 1969). For these experiments, the washing solution was made anoxic by replacing the gasphase inside the bottle with nitrogen after autoclaving but before cooling. In this manner, oxygen impact was limited to the brief period between decanting the washing solution and quenching the metabolism with ice cold methanol.

For every set of samples, blank controls were generated by filling 1 ml methanol-ribitol solution into a precellys tube with 600 mg glass bead. The extraction blanks were then treated exactly like the cell samples.

2.2.2 Metabolite extraction

Samples were thawed on ice before homogenization at -10°C with 3 cycles at a speed of 6800 rpm for 30 seconds with breaks of 30 seconds, using Precellys24 homogenizator (Peqlab). 400 µl aqua bides were then added to the sample, followed by mixing for 2 min

at 2000 rpm (MixMate, Eppendorf). 250 µl chloroform was added subsequently and mixed again for 2 min at 2000 rpm before centrifugation for phase separation at 10000 rpm and 4°C for 10 min. In case of incomplete phase separation, samples were stored at -20°C for 30 minutes before repeating centrifugation.

The polar phase was then transferred to new 2 ml reaction tubes and dried at 14°C under vacuum. Samples were stored at -20°C until derivatization.

2.2.3 Derivatization and GC-MS measurement

Derivatization:

For every GC-MS analysis, a chemical derivatization was employed. In the first step, 40 µl pyridine with 20 mg/ml methoxiamine hydrochloride was added and incubated for 90 min at 30°C under constant agitation (1000 rpm) (Thermomixer comfort, Eppendorf). Secondly, 60 µl MSTFA was added, mixed by vortexing and incubated at 37°C for 30 minutes followed by 120 min at 25°C for complete derivatization under constant agitation.

For analysis of PHB extracts, automated derivatization was used, employing a MPS 2 XL autosampler coupled to the Leco Pegasus 4d GC × GC TOF MS system.

GC-EI-MS analysis:

Three different GC-MS set-ups were used for different samples. Originally, intracellular metabolome samples were optimized for measurement with the DSQ II GC-MS. This method was successfully applied to the anaerobic samples of all substrates. Backup measurements of the samples were diluted 1:15 in MSTFA and measured using the Jeol JMS-T100GC system, but showed very low analytical coverage. Due to technical issues, the aerobic samples had to be analyzed using only Jeol JMS-T100GC system, in this case the samples were measured splitless.

All exometabolome samples were analyzed in one batch, using DSQ II GC-MS. PHB extracts were analyzed with the Leco Pegasus 4d GC × GC TOF MS applying one-dimensional GC and a splitless method with automated derivatization. Technical specifications of the three GC-EI-MS systems are listed below.

(1) Leco

MPS 2 XL autosampler (Gerstel)

7890 Agilent GC (Agilent Technologies)

Leco Pegasus 4D mass spectrometer (Leco Instruments)

(2) Jeol

MPS 2 Twister autosampler (Gerstel)

6890N Agilent GC (Agilent Technologies)

Accu TOF GC JMS-T100GC (JEOL GmbH)

(3) DSQ II

Autosampler 3000 (Thermo Fisher Scientific)

Thermo GC Ultra (Thermo Fisher Scientific)

DSQII (Thermo Fisher Scientific)

GC-APCI-MS

Additional measurements of single samples were conducted with the Bruker micrOTOF-QII MS (vendor software micrOTOFcontrol 3.0) coupled to a GC (CTC) and equipped with a GC PAL autosampler, a PTV injector (CTC) and a 71 × 1 mm baffled CIS 4 glass liner (Gerstel). These measurements served to gain addition information on unknown compounds. The vendor software Hystar 3.2 was used to control GC and MS and the mass spectrometer was calibrated according to the manufacturer with an APCI/APPI Calibrant Solution (Fluka). The following parameters were applied: Injection of 1 µl derivatized sample with a split mode of 1:10 to 1:50, adapted to the sample concentration. Settings for the mass spectrometer are given in supplementary table 1.

2.2.4 Data Analysis

GC-EI-MS analysis:

Raw data was exported in NetCDF format from the specific software of the GC-EI-MS instruments. NetCDF files and the in-house library were then imported for processing into the *Metabolite Detetcor* software (Hiller *et al.*, 2009), which was further developed by

Christian Nieke until 2013 (Version2.2N-2013-01-15). The software converted NetCDF data into *.bin format for peak detection. An alkane mix measurement was part of every measurement sequence and served to generate retention indices from the retention time (Kováts, 1958), in additon to that, *Metabolite Detector* performed a correction of over all retention time according to the retention of the internal standard ribitol. The alkane-mix contained 0.5 g/l of the following substances: Decan ($C_{10}H_{22}$), Dodecan ($C_{12}H_{26}$), Pentadecan ($C_{15}H_{32}$), Nonadecan ($C_{19}H_{10}$), Docosan ($C_{22}H_{46}$), Octacosan ($C_{28}H_{58}$), Dotriacontan ($C_{32}H_{66}$) and Hexatriacontan ($C_{36}H_{74}$) in cyclohexane. Identification of the detected peaks was accomplished by comparison of retention indices and mass spectra with the in-house library (BIBC, TU Braunschweig). For relative quantification of metabolites, specific fragment ions were used, so called quantification ions (QI), which were either preset in the library or manually curated.

For analysis of the experiments, batches with different settings were analyzed in *Metabolite Detector* to account for especially small or large peaks. After integration of the different batch results, missing signals were curated manually and integrated if possible. For signals that were not present in all samples a limit of detection was estimated as 90% of the lowest measured peak area. Known artifacts like phtalate, polysiloxanes or column residuals were removed from the analysis manually. The analyzed extraction blanks served to further eliminate non-biological signals and the relative peak areas were then normalized to the exact biomass in every sample. After these steps, the resulting peak areas were normalized to the internal standard ribitol, before recursive central normalization was applied to account for varying sample concentrations. Central normalization is a modified form of median normalization, where the median is calculated across a reduced set of metabolites, excluding those with very high impact on over all deviation. The schematic procedure of central normalization towards a reference sample is illustrated in supplement 2. For this procedure, an automated R-script was developed in the course of this work (supplement 3).

The normalized relative peak areas of derivatives of the same metabolite were then summed by application of the in-house software tool *itool* and the related data base of metabolite derivatives (BIBC, TU Braunschweig).

GC-APCI-MS

Data obtained from GC-APCI-MS measurement was analyzed in the vendor software *DataAnalysis* 4.0. For peak deconvolution, the implemented *Dissect*-algorithm was applied, which combines all mass signal with a maximum at the same retention time into one mass spectra for the peak. Assignment of the compounds across GC-EI-MS and GC-APCI-MS was done manually by comparison of the relative retention times and comparison of the fragmentation spectra.

Since APCI is a "soft" ionization technique, typically the highest mass ion represents the intact molecular ion plus a proton. This allowed to calculate the possible elemental formula of the molecule via the implemented tool *SmartFormula3D* based on the accurate mass and the isotopic pattern. The following restrictions were applied to elemental formula calculation: $n_C \geq 3\ n_{Si}$, $2\ n_N + n_O + n_S \geq n_{Si}$, n_P min $3\ n_O$ (n: number of; C, N, O, P and Si: elements), mass tolerance: 10 ppm, limit mSigma: 40. The results were checked manually against metabolite data bases and verifiedwith synthetic standard substances, if possible.

2.3 Analysis of coenzyme A derivatives using LC-MS

2.3.1 Harvesting of cell material

Samples were cultivated and harvested as described for GC-MS analysis (*2.2.1 Harvesting of cell material*) with the following changes: The washing step was omitted and the samples were suspended in 2 ml methanol-biochanin A (10µl/ml of an aqueous 0.02 mg/ml biochanin A stock solution) instead of methanol-ribitol solution.

2.3.2 Metabolite extraction

Samples were thawed on ice before homogenization at -10°C with 3 cycles at a speed of 6800 rpm for 30 seconds with breaks of 30 seconds, using Precellys24 homogenizator (Peqlab). Cell lysate and glass beads were transferred into 15 ml falcons with 10 ml ice cold 25 mM ammonium acetate (pH 6) to dilute the organic solvent. After centrifugation for 5 min at 4°C and 10000 rcf, the supernatant without glass beads and cell debris, was used for solid phase extraction.

The solid phase extraction columns (Strata XAW, Phenomenex) were conditioned before extraction by sequential application of 1 ml methanol, 1 ml methanol/water/ formic acid (50:45:5 $^{v}/_{v}$) and 1 ml water. The supernatant from the diluted cell lysates was applied to the SPE-columns with a suction of 900-700 mbar and passed the coulmn in ca. 5 minutes. The columns were then rinsed with 1 ml 25 mM ammonium acetate (pH 6) and 1 ml methanol sequentially. Before elution of the analytes, the SPE column was dried for 5 min with an air flow at 700 mbar suction. Analytes were eluted from the column by application of 1 ml methanol with 0.5% dissolved ammonia in two steps of 500µl. The samples were then dried at 14°C under vacuum and stored at -20°C until measurement.

2.3.3 LC-MS/MS measurement

The dried cell extracts were resuspended in 200 µl sample buffer (25 mM ammonium formate, pH 3.5 and 2% methanol), of which 50 µl were injected for analysis with the Dionex Ultimate 3000 system. The analysis was performed with a C_{18} *Gemini* column with 150 mm length, 2 mm diameter, 3µm particle size and 110 Å pore size (Phenomenex). Eluent A was 50 mM ammonium formate in water, pH 8.1 and eluent B was pure methanol. The flow rate was constant 0.22 ml/min at 35°C column oven temperature. A stepwise gradient was applied: 0-1 min 5% B, 1-19 min increase to 30% B, 19-26 min increase to 95% B, 26-30 min 95% B. Reaquilibration of the column after every measurement was accomplished in a separate gradient. At the beginning of every measurement 20 µl sodium formate cluster for mass calibration (see below) were injected into the mass spectrometer automatically. The mass spectrometer (Bruker MicroTOF QII) was operated in ESI+ mode with 3 Hz data acquisition and automated MS/MS acquisition. Mass range was set to 90-1178 m/z with an end plate offset of -500 V, capillary voltage of 4500 V, 1.2 bar nebulizer pressure, 8 l/min dry gas and 200°C dry temperature.

Sodium formate cluster for mass calibration (10 ml):

aqua bidest	4.95 ml
2-propanol (HPLC grade)	4.95 ml
formic acid (HPLC grade)	10 µl
NaOH 1 mol/l	100 µl

2.3.4 Data Analysis

The raw data mass spectra were recalibrated to the sodium formate cluster, injected prior to every measurement, and exported as MZXML files using DataAnalysis 4.0 automation scripting (Bruker). Peak detection and alignment was then conducted with R package XCMS version 1.38.0 (Benton *et al.*, 2010; Smith *et al.*, 2006; Tautenhahn *et al.*, 2008) using the R script developed in the course of this work (supplement 4). The relevant parameters for peak detection are given in table 2, all parameters are included in the script.

Table 2: Parameters applied during peak detection with R XCMS

parameter	value	explanation
method	"centWave"	algorithm applied for peak detection
mz_min	340	lower bound of m/z values
mz_max	950	upper bound of m/z values
ppm	15	mass accuracy within one peak
peakwidth	c(6,30)	peak with in seconds, in this case 6 to 30 seconds
snthresh	1	signal-to-noise threshold
prefilter	c(1,200)	exclusion of signals that show not at least one scan with an intensity of 200 or greater
mzdiff	0.2	Difference of masses necessary to distinguis two overlapping peaks
scanrange	c(700, 5000)	Range of scans to be included in the peak detection

Peak alignment was done in three recursive steps using the commands *group* and *retcor* from the XCMS package. The successively stricter parameters are included in the script. Finally, the command *fillPeaks* was used to fill missing peaks with the integrated baseline value as limit of detection.

From the resulting peak table, signals for CoA-esters were identified by comparison of retention time and accurate masses. The first comparison was conducted automatically with the R script (supplement 5), which was developed in the course of this work. Afterward, the results were manually checked for occurrence of the single charged molecular ion and typical MS/MS patterns. All relative peak areas are the peak areas of the doubly charged molecular ions, which are more abundant under the applied HPLC-MS settings.

2.4 Determination of biomass composition

2.4.1 Quantification of protein content

Extraction:

Samples for protein quantification were harvested from 2 ml culture broth by centrifugation (10 min, 4°C, 14000 rcf) and resupended in 1 ml 0.9% NaCl solution for washing. The cells were separated by a second centrifugation (10 min, 4°C, 14000 rcf), frozen in liquid nitrogen and transported to Braunschweig on dry ice, were they were stored at -80°C until extraction.

The pellets were resuspended in 150 µl lysis buffer (0.5 M NaOH and 2% SDS) and incubated for 30 min at 80°C in an ultrasonic bath. Cell debris was removed by centrifugation at 10000 rcf and 20°C for 5 min, the clear supernatant was transferred into a new eppendorf cup and stored until measurement at -20°C.

Bicinchoninic acid assay (Sigma Aldrich):

20 µl of the clear supernatant were diluted with 80 µl water for measurement with the bicinchoninic acid (BCA) assay. 25 µl of the diluted sample were mixed with 200 µl BCA working solution (4% Copper(II) sulfate pentahydrate solution and bicinchoninic acid solution, 1:50) in a transparent, flat bottom, 96 well plate for analysis. Simultaneously with the sample triplicates, standards for calibration were measured in the same 96 well plate with duplicates of bovine serum albumin in lysis buffer (0, 100, 200, 400, 800 und 1000 µg/ml), which were treated and diluted exactly like the samples. The plates were incubated for 30 min at 37°C and agitation in the Infinite M200 NanoQuant (Tecan), where then the absorption at 562 nm was measured. Protein concentrations were calculated from the absorption and the linear calibration standards.

RC DC™ Protein Assay (Bio-Rad):

This method was applied to some samples to verify the extremely high protein concentrations detected during phenylalanine degradation. This protocol includes precipitation of the protein and removal of all compounds that could interfere with protein quantification. The same protein extracts were used, as for the BCA assay and bovine

serum albumin calibration samples (200, 300, 400, 500, 800 µg/ml) were prepared from a 1 g/ml stock solution in lysis buffer. The samples were diluted 1:2 in lysis buffer to accommodate the calibration range. 25 µl of the diluted samples or undiluted standards were mixed with 125 µl RC reagent I, vortexed and incubated for 1 min at room temperature. 125 µl RC reagent II were added, vortexed and cooled on ice. The samples were then centrifuged for 5 minutes at room temperature and 13000 rcf to precipitate the protein. The supernatant was removed and the protein pellet was dissolved in 125 µl reagent A' (reagent A and reagent S, 50:1) and incubated at room temperature for 30 minutes.

Absorption at 750 nm was measured using Infinite M200 NanoQuant (Tecan). The linear calibration samples served to calculate the protein concentration in the samples.

2.4.2 Quantification of DNA

Cells for DNA quantification were harvested from 10 ml culture broth by centrifugation (30 min, 4°C, 4000 rcf) in a 15 ml falcon tube. The pellets were then resuspended in 1 ml 0.9% NaCl-solution and transferred to 2-ml eppendort reaction cups for a second centrifugation (10 min, 4°C, 14000 rcf). The samples were frozen in liquid nitrogen, transported to Braunschweig on dry ice and stored at -80°C until extraction.

DNA was extracted using the extraction kit “Genomic DNA from tissue” NucleoSpin® Tissue (Macherey-Nagel), according to the manufacturers protocol for bacteria.

Photometric quantification of the DNA was conducted with the Infinite M200 NanoQuant (Tecan).

2.4.3 Quantification of RNA

Cells from 2 ml culture broth were harvested by centrifugation at 4°C and 14000 rcf for 10 minutes. The pellets were resuspended in 1 ml 0.9% NaCl solution and centrifuged again (4°C, 14000 rcf, 10 min) to remove residues from the medium. The samples were then frozen in liquid nitrogen, transported to Braunschweig on dry ice and stored at -80°C until extraction.

RNA was extracted using the RNA isolation kit NucleoSpin® RNA (Macherey-Nagel)

according to the vendors protocol for RNA extraction from up to 10^9 bacterial cells. The cell pellet was resuspended in 100 µl TE buffer (10 mM Tris-HCl, 1 mM EDTA, pH 8) with 2 mg/ml lysozyme and incubated for 1 h at 37°C in an ultrasonic bath. 350 µl buffer RA1 and 3.5 µl β-mercaptoethanol were added and mixed by vortexing. Samples were then filtered through the pink NucleoSpin® Filters to reduce viscosity. 350 µl 70% ethanol ($^{v}/_{v}$) were added to the lysate and mixed thoroughly before application of the sample to the NucleoSpin RNA column (centrifugation at room temperature, 11000 rcf for 30 seconds). The columns were then rinsed with 350 µl membrane desalting buffer and centrifuged for 1 minute at 11000 rcf. DNA was degraded on column with 10 µl rDNAse stock solution in 90 µl DNAse reaction buffer for 15 minutes at room temperature. The column was then rinsed with 200 µl buffer RAW2, 600 µl buffer RA3 and 250 µl buffer RA3, sequentially. RNA was then eluted in two steps with 30 µl RNAse free water, each.

Photometric quantification of the RNA was conducted with the Infinite M200 NanoQuant (Tecan).

2.4.4 Quantification of PHB

Samples for PHB quantification were harvested from 10 ml culture broth by centrifugation (30 min, 4°C, 4000 rcf). The supernatant was decanted and the samples were frozen in liquid nitrogen, before transportation to Braunschweig on dry ice. Samples were stored at -80°C until extraction.

The cell pellet was resuspended in 1 ml 2 M NaOH and incubated for 1 hour at 95°C. After cooling on ice for 2 minutes, 1 ml 2 M HCl was added for neutralization and mixed by vortexing. Cell debris was removed by centrifugation (5 min, 13000 rcf, room temperature) and the supernatant was transferred into a fresh eppendorf cup. 2.5 µl lysate were dried under vacuum over night for GC-MS analysis. Derivatization of the sample was conducted as described in section *2.2.3 Derivatization and GC-MS measurement*. 1 µl of the derivatization mix was applied for splitless measurement with the Leco Pegasus 4d GC × GC TOF MS. With every measurement, calibration samples were generated from a PHB-stock solution (0.2 mg/ml) with final amounts of 1, 2, 4, 6, 8 and 10 ng/ µl derivatization mix. Hydrolyzed PHB was detected as 3-hydroxybutanoic acid (Butanoic_acid,_3-hydroxy-_(2TMS)_1163.2) and the concentration was calculated from the relative peak

area with the linear calibration measurements. Calibration samples were measured in triplicates and the biologic samples were measured in biological triplicates with technical duplicates.

2.4.5 Quantification of Lipids

Lipids were quantified by methyl-tert-butyl ether extraction and gravimetric quantification as described by (Matyash *et al.*, 2008). Cells from 200 ml culture broth were harvested by centrifugation at 17700 rcf and 4°C for 15 minutes. The cell pellet was resuspended in 1.5 ml methanol, transferred into 15 ml falcon tubes and frozen in liquid nitrogen. The samples were transported to Braunschweig on dry ice and stored at -80°C until extraction.

Cells were lysed in an ultrasonic bath at 70°C for 15 minutes. Lipides were extracted with 5 ml methyl-tert-butyl ether for 1 h at room temperature under constant agitation. 1.25 ml water were added, mixed by vortexting and incubated for 10 more minutes at room temperature under constant agitation. The phases were separated by centrifugation for 10 mit at 1000 rcf at room temperature and the upper, organic phase was transferred into a new falcon tube. The aqueous phase was extracted a second time with 1.29 ml methyl-tert-butyl ether and 0.387 ml methanol for 1 h under constant agitation at room temperature. Before phase separation, 0.323 ml water were added, vortexed and incubated for 10 min at room temperature and constant agitation. Phases were separated by centrifugation at room temperature for 10 min at 1000 rcf and the upper, organic phase was pooled with the organic phase from the first extraction step.

The organic extract was then stepwise evaporated in a previously dried and weighted glass vial, which was then dried completely over night at vacuum. The extracted lipid fraction was quantified from the weight difference of the vials.

2.4.6 Quantification of ATP

Samples for ATP quantification were generated by rapidly freezing 1 ml of culture broth in an eppendorf cup in liquid nitrogen.

Quantification of ATP was conducted with the BacTiter-Glo™ Microbial Cell Viability

Assay (Promega). The samples were diluted in water 1:2 before mixing 50 µl diluted sample with 50 µl BacTiter-Glo™ buffer in an opaque-walled 96-well-plate. The luminescence was measure with the Infinite M200 NanoQuant (Tecan). All samples were analyzed in biological triplicates with technical dublicates. A calibration series was measured with 300 nM, 150 nM, 75 nM, 37.5 nM, 18.75 nM and 0 nM ATP.

2.5 Computational methods

2.5.1 Statistical data analysis and visualization

Cluster analysis of metabolic profiles

For this analysis, the relative peak areas of all metabolites without any additional transformation or normalization severed as input for R, using the *gplot* package, version 2.16.0 (Warnes *et al.*, 2015). For the non-detected peaks, "NA" was used instead of the respective limits of detection. Correlation between the different metabolic profiles were calculated as Pearson's correlation coefficients, using all pairwise complete observations in case of missing values. Cluster analysis was conducted using euclidean distances and Ward's minimum variance method (Ward, 1963).

Cluster analysis of transcript and protein profiles

For this analysis, the ratio of every expression value and mascot score to the respective statistical average was calculated and transformed to the base 2 logarithm. Missing protein mascot scores were replaced with 1 to allow for the calculation of ratios and logarithms. This data set was then submitted to row-wise clustering with Manhattan distances and Ward's minimum variance method (Ward, 1963), using R *gplots* package (Warnes *et al.*, 2015).

2.5.2 Interpretation of genomic data

Interpretation of the systems biology data in this study was based on the genome annotation of *A. aromaticum* EbN1in EnzymeDetector (Quester and Schomburg, 2011). This Annotation was manually compared with the original genome annotation (Rabus,

2005; Rabus *et al.*, 2005) for ambiguous results.

Additional analyses of single genes and searches for new enzymes were conducted in the course of this work using the Basic Logical Alignment Tool (BLAST) provided on the NCBI website (http://blast.ncbi.nlm.nih.gov/Blast.cgi) on protein sequences with the *blastp* algorithm and standard settings.

2.5.3 Interpretation of transcriptomic data

Transcriptomic analyses were conducted by the team of Robert Geffers (HZI) using RNA-seq technology with an average of $3*10^7$ reads per sample. The data was provided as Rockhopper output with expression levels calculated from the mean values of three replicates after normalization, alignment and assembly (McClure *et al.*, 2013; Tjaden, 2015). During the raw data analysis, no cutoff value was applied to reduce noise. However, an estimated value of 50 for the raw data counts was suggested based on experience from other projects. Application of this suggestion led to the inclusion of all expression values larger than 1 into the scaling and interpretation of the transcriptomic data sets.

2.5.4 Interpretation of protein shotgun data mascot scores

Proteomics data were provided by the cooperation partners (Lars Wöhlbrand, ICBM) as list of locus tags with mascot scores for the protein identification within each experimental condition. These mascot scores are derived from biological triplicates and represent mean values. Only proteins with a mascot score larger than 50 were reported.

Mascot scoring is a probability value, describing the chance for a false positive identification of a peptide (Perkins *et al.*, 1999). This probability is represented as negative logarithm to achieve comprehensible data. For a protein mascot score, all ion mascot scores that match to a peptide from that protein are summed up, if they are above the minimal threshold (Matrix Science Inc, 2015). Previous studies showed that differential protein expression of a ration of 1:5 can be reliably detected by using probability based identification scores of the protein (Allet *et al.*, 2004). All in all, the protein mascot scores presented here should reflect changes in specific protein abundance between different growth conditions at least on a relative scale. This is further supported by a proteomics study in *Dinoroseobacter shibae*, where protein mascot scores and exponentially modified

protein abundance indices of the same protein analysis were compared and showed consistent tendencies (Laass *et al.*, 2014).

2.5.5 Interpretation of systems biology data

For visualization of the different data types within the data tables of every pathway, the relative peak areas of metabolomic HPLC-MS and GC-MS analysis, gene expression levels and the protein mascot scores were taken into account. Since the data scales differ, color coding of percentiles within every data set was applied (Figure 6).

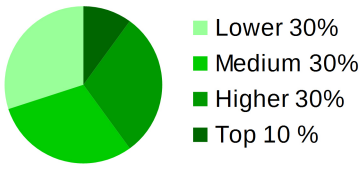

Figure 6: Color coding of systems biology data according to percentiles
The color scheme was applied in all tables including different systems biology data for integrated visualization

3 Results and Discussion

3.1 Identification of metabolites

3.1.1 Analysis of CoA-esters

Coenzyme A (CoA) activated metabolites play an important role in several central metabolic pathways like the citric acid cycle, the fatty acid biosynthesis or the metabolism of some amino acids. Moreover, CoA-activation is employed in anaerobic and aerobic aromatic degradation pathways to allow for ATP-dependent reductive dearomatization as an alternative to dearomatization by monooxigenases. Thus, the implementation of the analytical means to investigate CoA-intermediates was prerequisite to this study.

In the course of this work, a comprehensive method for analysis of CoA-esters was established. The method comprises of an optimized solid phase extraction, an adapted High Performance Liquid Chromatography separation with two-stage mass spectrometric detection and an automated peak detection and identification pipeline. Additionally, a data base with compound information, retention times and accurate masses for CoA-esters with and without synthetic standards was compiled.

As extraction method, a protocol with mechanical cell lysis at -10°C and anion exchange solid phase extraction (SPE) was established. Based on a standard protocol for extraction of weak acids, provided by the SPE-column vendor (Phenomenex), the extraction protocol was optimized to minimize CoA-ester degradation. The method parameters are described in detail in *2.3.2 Metabolite extraction*. Recovery rates of CoA-ester standards by the method were determined at an early stage of method development (supplement 6). The only CoA-ester which showed substantial losses during extraction was acetoacetyl-CoA. This metabolite is most likely prone to degradation, as the β-keto group facilitates hydrolytic or thiolytic cleavage of the molecule. A similar tendency to degradation can be expected of all CoA-esters with keto-groups at the β-carbon atom.

The HPLC method implemented here was previously described by (Peyraud *et al.*, 2009). The method was modified to achieve a better resolution of isomers and to include the medium chain fatty acid CoA-esters, hexanoyl-CoA and decanoyl-CoA. The final

method parameters are described in *2.3.3 LC-MS/MS measurement*. For metabolite detection, a positive-mode MS/MS standard method, provided by the mass spectrometer manufacturer (Bruker), was optimized for detection of CoA-esters and reduction of in-source fragmentation.

For the identification of CoA-esters from the HPLC-MS data, a reference data base was compiled in the course of this work. The data base includes 20 CoA-esters that were purchased as synthetic standards. CoA-esters for which no synthetic standard was available were identified by molecular formula calculation from the accurate mass and isotopic pattern, analysis of the characteristic isomerization pattern and interpretation of the MS/MS mass spectra. To distinguish isomers, data from different projects and organisms were compared to ascertain the identity of specific isomers from the biological context. A list of all CoA-esters detected in this study and the parameters applied for identification are presented in supplement 7 and supplement 8. A full data processing pipeline was implemented in the course of this work, using R scripting and R package XCMS (Smith *et al.*, 2006) (*2.3.4 Data Analysis*).

3.1.2 Analysis of unknown metabolites via GC-MS

Of the 112 small polar metabolites detected via GC-MS analysis, 27 metabolites were reproducibly detected in metabolomic samples, but could not be identified using the mass spectra library. An overview of the compounds is given in supplement 9.
Most compounds were only present at low abundance and did not contribute to the specificity of the metabolic profiles in a significant way. Four compounds however, were detected in high amounts and subjected to further analysis regarding the GC-EI-MS mass spectra and, when possible, the GC-APCI-MS mass spectra. Interpretation of the mass spectra was based on the principles and fragmentation patterns suggested in literature (Fiehn *et al.*, 2000b; Strehmel *et al.*, 2013). This resulted in a verified identification of two compounds and a tentative identification of two other compounds. All other compounds showed low mean abundances and were not analyzed further.

Unknown-ebn1-13

The compound was detected in very high amounts in cells degrading benzoate anaerobically (Figure 7A). Lower signals were detected in all samples, except during aerobic benzoate degradation. The GC-EI mass spectrum revealed a possible molecular ion with *m/z* 363 and a M-CH_3-fragment ion with *m/z* 348. Furthermore, the spectrum indicated an amino-acid structure and the possible presence of two carboxylic acid groups, very similar to the spectrum of aspartate-3TMS (Figure 7B). The substance eluted very close to glutamate-3TMS at a retention index of 1613.48.

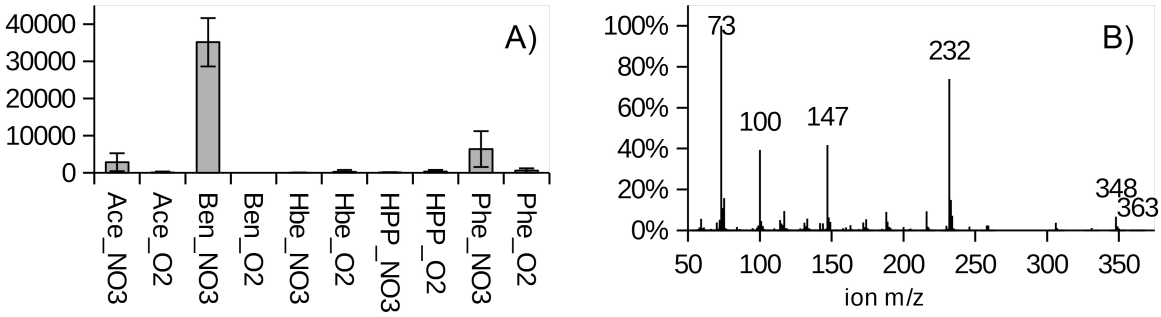

Figure 7: Unknown-ebn1-13
The compound was identified as iso-glutamate-3TMS by comparison with a synthetic standard A) relative peak areas B) GC-EI-MS mass spectrum

GC-APCI measurement confirmed the molecular ion and suggested $C_{14}H_{33}NO_4Si_3$ as elemental formula with a mass error of 3.9 ppm. Unfortunately, the peak was overloaded, which resulted in weak mSigma values for the iostopic pattern. However, Database research using METLIN: Metabolite Search (https://metlin.scripps.edu/index.php) suggested iso-glutamate as a possible compound, which correlated well with the observed retention close to glutamate-3TMS. Measurement of the synthetic standard resulted several signals, with one derivative having a retention time and mass spectra identical to the unknown-ebn1-13, which was thereby identified as iso-glutamate-3TMS (3-aminopentanedioic acid).

Unknown-ebn1-02

The metabolite eluted shortly before glutamate-2TMS and displayed an EI spectrum with some fragments similar to aspartate-2TMS. These observations resemble some of the aspects observed in unknown-ebn1-13, which was identified as iso-glutamate-3TMS.

Indeed, measurement of the synthetic iso-glutamate standard gave rise to an additional derivative signal with a retention time and characteristic mass spectrum matching that of unknown-ebn1-02. Thus, unknown-ebn1-02 was identified as iso-glutamate-2TMS.

Unknown-ebn1-21

This compound was detected with high abundances during anaerobic benzoate degradation (Figure 8A). The compound is identical to a compound previously detected in *Yersinia pseudotuberculosis* (Unknown#1878.81-ypy-mse_031) and in *Pseudomonas putida* (Unknown#1882.25-ppu-cja_009). The mass spectrum showed a putative molecular ion of 420 *m/z*, from which a CH_3-group can be subtracted to form the fragment ion at 405 *m/z* (Figure 8B). Furthermore, the spectrum indicated an amino acid structure and some structural resemblance to asparagine-4TMS. GC-APCI-MS measurement showed a peak with the mass of the M+H ion and similar retention time, for which an elemental formula was calculated: C17H44N2O2Si4 (mSigma 29.8 and 0.7 ppm mass error). This elemental composition is identical to ornithine-4TMS but the retention time differed by 60 retention time units. Thus, unknown-ebn1-21 is possibly the 4TMS derivative of an isomer to ornithine. The only isomer to ornithine (METLIN database, https://metlin.scripps.edu/index.php) was 2,4-diaminopentanoate, which could not be purchased as synthetic standard. Thus, identification of unknown-ebn1-21 as 2,4-diaminopentanoate remains tentative.

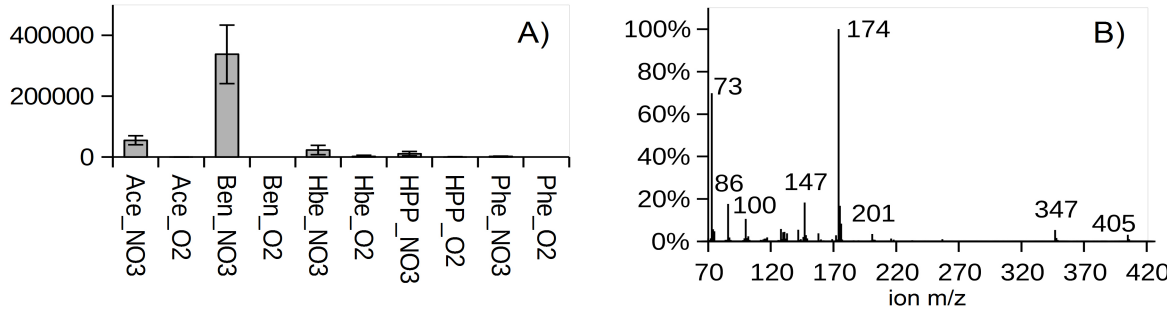

Figure 8: Unknown-ebn1-21
tentatively identified as 2,4-diaminopentanoate; A) relative abundances of the metabolite; B) GC-EI-MS mass spectrum of the compound

unknown-ebn1-19

This compound was detected in all, but the aerobic phenylalanine degrading cells (Figure 9A). It was previously detected in samples of *Phaeobacter inhibens* under nitrogen limitation and included in the library as Unknown#1594.3-pin-mhe_030. The GC-EI-MS mass spectrum indicated a dicarboxylic acid structure with two TMS groups in the derivative (Figure 9B). GC-APCI-MS measurement and elemental formula calculation gave the best results for the formular of (R)-3-((R)-3-hydroxybutanoyloxy)butanoate-2TMS+H ($C_{14}H_{31}O_5Si_2$) with an mSigma value for the isotopic pattern of 3.8 and mass error of 0.4 ppm. These values lie well within the published values for confident elemental formular calculations (Strehmel *et al.*, 2013). The metabolite is not available as synthetic standard. An experiment with alkaline lysis of PHB for short time intervals and at lower temperature only resulted in detection of the monomeric 3-hydroxybutanoate in rising concentrations. Thus, the identification of unknown-ebn1-19 as (R)-3-((R)-3-hydroxybutanoyloxy)- butanoate remains tentative.

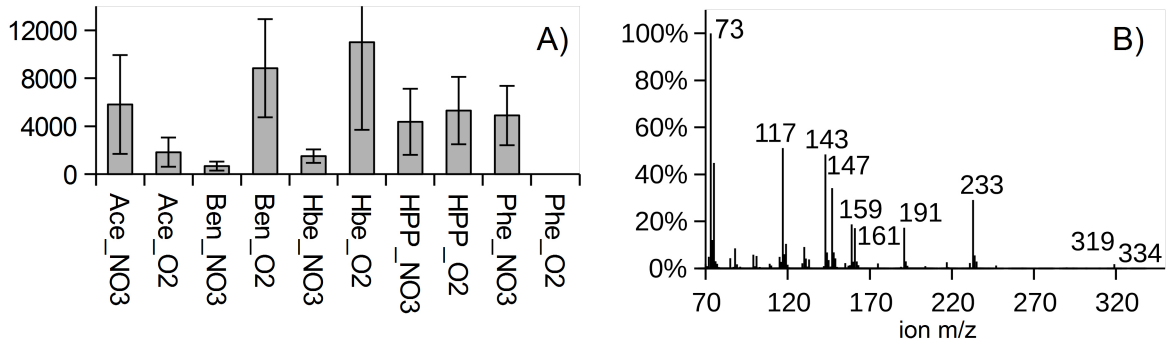

Figure 9: Unknown-ebn1-19
tentatively identified as (R)-3-((R)-3-Hydroxybutanoyloxy)butanoate; A) relative peak areas of the compound in the systemsbiology experiments; B) GC-EI-MS mass spectrum of the compound

3.2 Comparison of the different growth scenarios

3.2.1 General results

3.2.1.1 Systems biology project layout

The scope of this work was to present a comprehensive metabolomic survey of the aromatic degradation pathways in *Aromatoleum aromaticum* EbN1. Transcriptomic and proteomic analyses served to complement the metabolomic data and helped to explain details of ambiguous pathways. Additionally, this project provides a database of systems biology data, which can be the basis for further investigation with bioinformatic and data mining tools in the future.

The investigated substrates were benzoate, phenylalanine, 3-(4-hydroxyphenyl)-propanoate (HPP) and 3-hydroxybenzoate, while acetate served as a non-aromatic reference substrate. Degradation of all substrates was studied both under oxygen (aerobic) and nitrate (anaerobic) respiration. All cultivations were conducted in 400 ml shaking-flask cultures with minimal medium and analyzed during the exponential growth phase.

Cultures for metabolomic, proteomic and transcriptomic samples were inocculated from the same pre-culture and harvested simultaneously at the laboratories of MPI Bremen and ICBM Oldenburg. Metabolomics samples and samples for determination of biomass composition were harvested as part of this work during several excursions to Oldenburg. Extraction and analysis of metabolites, exo-metabolome analysis via GC-MS and analysis of biomass composition were conducted at the TU Braunschweig as part of this thesis. Proteomic analyses were conducted by Lars Wöhlbrand (ICBM Oldenburg) and transcriptomic analysis was conducted by Robert Geffers (HZI Braunschweig). Growth parameters, substrate consumption rates and physiological observations were determined by Kathleen Trautwein (MPI Bremen) and Daniela Thieß (MPI Bremen). Data integration and further processing was performed as part of this work.

3.2.1.2 Extracellular metabolites

Analysis of extracellular metabolites from culture supernatant revealed excretion of 4-hydroxybenzoate during aerobic HPP degradation. To further investigate the excretion of

4-hydroxybenzoate, the substance concentration, along with HPP concentration and optical density of the bacterial culture were measured by Kathleen Trautwein (MPI) and are presented in *3.3.3 Aerobic and anaerobic HPP degradation*. Apart from that, only the substrates benzoate and 3-hydroxybenzoate were detected extracellularly with GC-MS along with media compounds like phosphate. A quantitative analysis of all substrates was performed in Oldenburg and is presented in *3.2.5 Physiological effects*. Exometabolom results are summarized in supplement 10.

3.2.1.3 Intracellular metabolites

Intracellular metabolome analysis comprised of GC-MS analysis of the small polar metabolites and LC-MS/MS analysis of CoA-esters. All in all, 190 different metabolites were detected in cell extracts of *A. aromaticum* EbN1 (table 3).

Table 3: Overview of intracellular metabolites with different carbon sources and electron acceptors LC-MS/MS: high performance liquid chromatography-mass spectromety analysis of CoA-intermediates, GC-MS: gas chromatography-mass spectrometry analysis of small polar intracellular metabolites

Growth conditions		**LC-MS/MS**	**GC-MS**	
Substrate	Electron acceptor	identified	detected	identified
acetate	nitrate	35	75	63
acetate	oxygen	27	74	55
benzoate	nitrate	49	81	66
benzoate	oxygen	35	62	47
3-hydroxybenzoate	nitrate	55	78	62
3-hydroxybenzoate	oxygen	33	75	58
3-(4-hydroxyphenyl) propanoate	nitrate	55	72	58
3-(4-hydroxyphenyl) propanoate	oxygen	50	83	63
L-phenylalanine	nitrate	59	70	58
L-phenylalanine	oxygen	47	72	56
Total		**78**	**112**	**85**

Of the detected metabolites, 16 were specific for a single growth condition and could not be detected in other samples. 21 metabolites were observed in two different growth conditions, of which 5 metabolites were specific for degradation of one substrate under aerobic and anaerobic respiration. 87 metabolites were either increased or decreased by factor > 5 or < 0.2, relative to the median relative peak area, in at least one growth condition. The reasons for this high metabolic variety are the dramatic differences in growth conditions, entailing distinct changes in physiology, which are described in *3.2.5 Physiological effects*. A full list of all detected metabolites with relative peak areas is presented in supplement 11.

Only 11 metabolites presented fold-changes < 2 and > 0.5 for all growth conditions and were detected in at least half of the samples in this study. Of these constant metabolites the sugars glucose and fructose need to be synthesized via gluconeogenesis from acetyl-CoA during all growth conditions. Acetyl-CoA and succinyl-CoA, along with free coenzyme A and it's derivative, CoA-disulfide, also showed unwavering and high intracellular concentrations. This is in accordance with the necessity to keep a defined pool of these metabolites available for central metabolism and to respond to metabolic fluctuation. Lastly, two amino acids, glycine and methionine, were detected at constant levels throughout all growth condition.

Distinct metabolic profiles were detected for every growth condition. The most relevant global aspects are discussed here. Metabolites that are relevant for specific degradation pathways are discussed in the context of these pathways in the respective sections below.

Five out of the ten observed growth conditions induce catabolic pathways via benzoyl-CoA as main degradation route. Pearson correlation of the metabolic profiles reflects this differentiation in hierarchical clustering (Figure 10). In this analysis, the relative peak areas of all metabolites served to calculate correlation of the metabolic profiles. Thus, the results are dominated by the influence of metabolites with high relative peak areas.

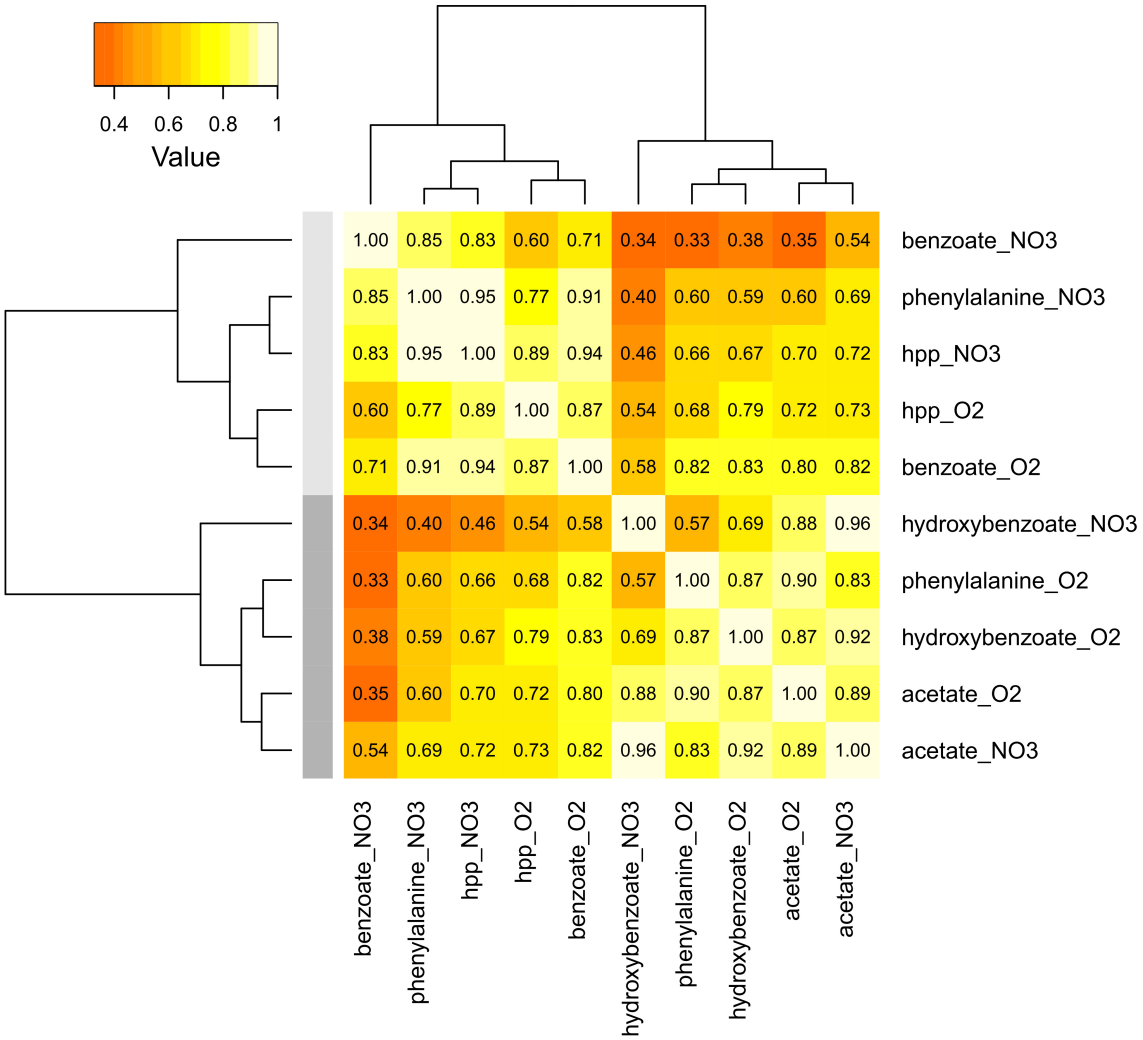

Figure 10: Overview of metabolite profile correlations, showing main clustering according to the role of benzoyl-CoA in aerobic and anaerobic degradation pathways
Correlations between growth conditions were calculated from mean relative peak areas of all metabolites, excluding non detected metabolite; Pearson correlation coefficients were calculated using all complete pairs of observations on each pair of conditions; Hierarchical clustering was conducted using euclidean distances and Ward's minimum variance method; appended _NO3 indicates anaerobic denitrification and _O2 aerobic respiration

The first group of the cluster analysis comprises of aerobic and anaerobic benzoate and HPP degradation as well as anaerobic phenylalanine degradation. All five pathways proceed via benzoyl-CoA as intermediate. The high correlation coefficients between anaerobic phenylalanine and HPP degradation (0.95) reflects the usage of the same central anaerobic benzoyl-CoA degradation pathway. Likewise, aerobic benzoyl-CoA and HPP degradation, which is degraded via the aerobic benzoyl-CoA degradation pathway, show a high correlation of 0.87.

Anaerobic benzoate degradation shows the greatest distance to the other scenarios employing benzoyl-CoA. An important metabolic feature under this growth condition was the production of large amounts of compatible solutes. Details on compatible solutes and other potential stress responses on the proteomic and transcriptomic level are described in *3.2.4 Metabolic stress responses*.

The second group of the cluster analysis comprises of the anaerobic acetate and hydroxybenzoate metabolism as well as the aerobic acetate, hydroxybenzoate and phenylalanine metabolism. None of these are degraded via benzoyl-CoA, as is also evident from the benzoyl-CoA levels presented in figure 11. Within this group, no strong clustering into oxic and anoxic conditions or into CoA-mediated and other pathways is apparent. Aerobic 3-hydroxybenzoate degradation shows the greatest diversity within the second group but shows high correlation with anaerobic acetate degradation.

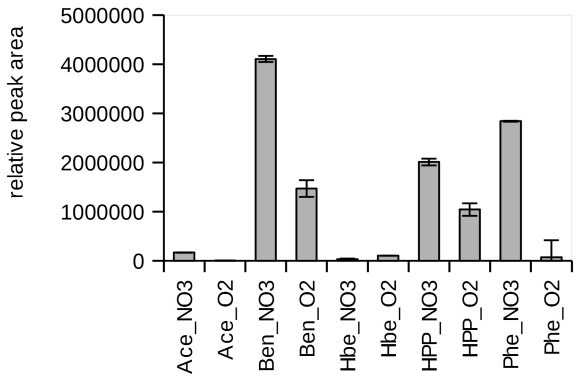

Figure 11: Benzoyl-CoA: relative peak areas with standard deviation of biological and technical replicates; Substrates are indicated as following: Ace = acetate, Ben = benzoate, Hbe = 3-hydroxybenzoate, HPP = 3-(4-hydroxyphenyl)propanoate,Phe = phenylalanine, appended _NO3 indicates anaerobic denitrification and _O2 aerobic respiration

In contrast to the correlation analysis of non-transformed relative peak areas, correlation analysis of the metabolic profiles after logarithmic transformation reduced the influence of the more abundant metabolites (supplement 12). In this case, the growth conditions are again divided into two groups, but these are characterized by aerobic and anaerobic respiration.

Specific metabolites

To further investigate metabolic responses under the different growth conditions beyond the discussed detailed pathways, specifically elevated metabolites are discussed. The metabolites were selected based on their fold-change relative to the median, with a cutoff of 10 fold upregulation compared to the median. Metabolites with only low abundances

(within the lower 30% of method signal intensities) were excluded. The full list contained 48 metabolites, beside the metabolites already discussed in their specific pathways (supplement 13 and supplement 14). Of these, 14 metabolites were not identifiable with the applied GC-MS mass spectra library and are discussed in detail in section *3.1.1* . One compound (alpha-glucosylglycerol) is a known osmolyte and is discussed in chapter *3.2.4 Metabolic stress responses*. Another five metabolites represented fatty acids or metabolites from fatty acid metabolism, which could originate from the cell membrane. Five potential metabolites are most likely artifacts from metabolite extraction and derivatization. The remaining 23 metabolites can be divided into two groups: 14 metabolites represent putative byproducts of the CoA-mediated aromatic degradation pathways (table 4) and nine metabolites showed specific upregulation without any obvious connection to the degradation pathways (table 5).

Of the specifically elevated metabolites, 14 CoA-esters of partially unclear isomeric nature are most likely byproducts of the various CoA-mediated aromatic degradation pathways. These byproducts could either originate from error-prone enzymatic reactions or they could result from decay of particularly sensitive intermediates during sample processing. This theory is supported by the finding, that none of the CoA-esters showed a maximum fold-change during acetate degradation or aerobic 3-hydroxybenzoate degradation. These are the only growth conditions, where the substrate is not degraded via CoA-esters. As explained in *3.1.1 Analysis of CoA-esters*, metabolite identification based on the calculation of the molecular formula was complicated for most of the CoA-esters with low abundances, this is especially true for the here presented putative byproducts. In the following, only CoA-esters with good evidence of correct elemental formula assignment (**) will be discussed.

2-Ketocyclohexane-1-carboxyl-CoA is an intermediate of the *Rhodopseudomonas* pathway of anaerobic benzoate degradation (see *3.3.2.1 Rhodopseudomonas pathway*) and an accurate mass signal was detected elevated during anaerobic 3-hydroxybenzoate degradation. The isomer 6-hydroxycyclohex-1-enecarbonyl-CoA is an intermediate of the main anaerobic degradation pathway of benzoate. The recorded signal could constitute a further isomer with a keto- or hydroxy-group at the third carbon atom as result of reduction of 3-hydroxybenzoyl-CoA. In any case, no such intermediate was ever postulated to participate in anaerobic degradation of 3-hydroxybenzoate.

Table 4: Putative byproducts of the CoA-mediated aromatic degradation pathways with minimum fold-changes > 10

Fold-changes were calculated against the median of the mean relative peak are, including the estimated detection limit for non detected metabolites; Metabolites with over all low abundance were excluded; Column R indicates the reliability of identification of CoA-esters, as described in chapter 3.1.1: 0 = no strong evidence, * = weak evidence (weak elemental formula, small peak), ** = good evidence, *** = very good evidence; light blue indicates fold-changes < 0.1, medium blue indicates fold-changes between 10 and 0.1, dark blue indicates fold-changes > 10, Substrates are indicated as following: Ace = acetate, Ben = benzoate, Hbe = 3-hydroxybenzoate, HPP = 3-(4-hydroxyphenyl)propanoate,Phe = phenylalanine; with NO_3 indicating anaerobic denitrification and O_2 aerobic respiration

Metabolite	R	Ace NO_3	Ace O_2	Ben NO_3	Ben O_2	Hbe NO_3	Hbe O_2	HPP NO_3	HPP O_2	Phe NO_3	Phe O_2
2,5-dioxo-cyclohex-1-carbonyl-CoA_1	0	NA	NA	NA	NA	NA	NA	NA	NA	NA	37.7
3-oxoadipyl-CoA	0	NA	NA	NA	NA	338.2	NA	NA	7.2	NA	NA
4-hydroxyphenylacetyl-CoA	*	NA	NA	NA	NA	NA	NA	NA	NA	45.5	NA
phenoxyacetyl-CoA	*	NA	NA	NA	NA	NA	NA	NA	NA	31.6	NA
2-ketocyclohexane-1-carboxyl-CoA	**	NA	NA	NA	NA	1586	6.8	1.6	NA	1.3	4.2
geranoyl-CoA	0	NA	NA	NA	NA	69.1	NA	26.0	25.4	NA	NA
3-ketopimelyl-CoA	0	NA	NA	NA	NA	NA	NA	NA	4.2	NA	271.5
4-hydroxybenzoylacetyl-CoA	0	NA	NA	NA	NA	20.7	NA	NA	NA	NA	NA
2,3-didehydro-pimeloyl-CoA_3	**	NA	NA	5.6	53.9	NA	NA	0.9	19.9	1.1	1.6
2,6-dihydroxycyclohexane-1-carboxyl-CoA	*	NA	NA	21.9	NA	70.2	NA	7.4	NA	NA	NA
pimeloyl-CoA_1	**	NA	0.4	5.2	NA	1.9	NA	1.5	NA	20.0	0.5
5-methyl-3-oxo-4-hexenoyl-CoA	*	NA	NA	NA	NA	242.1	1.9	NA	NA	NA	NA
2-hydroxycyclohexane-carbonyl-CoA	**	NA	NA	NA	NA	116.1	NA	NA	NA	NA	NA
2-hydroxycyclohexane-1-carboxyl-CoA	*	NA	NA	64.4	NA	2.8	NA	97.8	NA	6.1	NA

2,3-Didehydro-pimeloyl-CoA is an intermediate of anaerobic benzoate degradation via the *Rhodopseudomonas* pathway (see *3.3.2.1*) and was detected specifically elevated during aerobic benzoate degradation. The metabolite plays no known role in aerobic

benzoate degradation and neither does any isomer of the substance. Hypothetically, this substance could be formed during aerobic benzoate degradation, if the hydrolytic ring opening of the epoxy-intermediate would proceed without cleaving off formate. Pimeloyl-CoA is also an intermediate of the *Rhodopseudomonas* pathway of anaerobic benzoate degradation and was detected in all samples grown anaerobically with aromatic substrates, as well as during aerobic degradation of acetate and phenylalanine (see *3.3.2.1*). 2-Hydroxy-cyclohexanecarbonyl-CoA is another intermediate of the *Rhodopseudomonas* pathway of anaerobic benzoate degradation. The observed signal could also be an isomer with the hydroxy-group at the third carbon atom, originating from 3-hydroxybenzoate.

Table 5: Selected metabolites, other than putative byproducts of aromatic degradation pathways, with minimum fold-changes > 10

Fold-changes were calculated against the median of the mean relative peak are, including the estimated detection limit for non detected metabolites; Metabolites with over all low abundance were excluded; Column R indicates the reliability of identification of CoA-esters, as described in chapter 3.1.1: 0 = no strong evidence, * = weak evidence (weak elemental formula, small peak), ** = good evidence, *** = very good evidence; light blue indicates fold-changes < 0.1, medium blue indicates fold-changes between 10 and 0.1, dark blue indicates fold-changes > 10, Substrates are indicated as following: Ace = acetate, Ben = benzoate, Hbe = 3-hydroxybenzoate, HPP = 3-(4-hydroxyphenyl)propanoate,Phe = phenylalanine; with NO_3 indicating anaerobic denitrification and O_2 aerobic respiration

Metabolite	R	Ace NO_3	Ace O_2	Ben NO_3	Ben O_2	Hbe NO_3	Hbe O_2	HPP NO_3	HPP O_2	Phe NO_3	Phe O_2
glucose-6-phosphate		3.1	0.3	17.0	NA	3.4	0.0	3.3	1.6	0.2	0.4
glyceraldehyde		37.2	NA	300.8	NA	113.9	NA	102.9	NA	NA	NA
2-isopropylmalic acid		NA	NA	NA	NA	466.5	NA	NA	NA	NA	NA
2-isocaprenoyl-CoA	*	NA	NA	NA	NA	NA	NA	2.0	14.1	NA	NA
beta-Alanine		NA	NA	1.4	NA	NA	10.1	5.3	49.9	0.6	154.5
3-phenyllactate		NA	NA	NA	NA	NA	NA	734.9	NA	181.9	NA
thymine		NA	8.2	0.1	10.7	NA	4.8	NA	1.9	0.1	5.3
lysine		9.9	NA	14.7	NA	NA	2.8	NA	2.0	NA	13.7
glycylglycine		195.8	NA	337.9	NA	131.3	NA	60.1	2.0	NA	NA

The nine metabolites summarized in table 5 could be connected to different metabolic systems. Glucose-6-phosphate and glyceraldehyde (probably formed from glyceraldehyde-3-phosphate during sample preparation) were highly elevated during anaerobic benzoate

degradation. This indicates an active gluconeogenesis under this condition. Most likely, the elevated glucose production serves as precursor for the biosynthesis of α-glucosylglycerol, which accumulated to high levels during anaerobic benzoate degradation (see *3.2.4 Metabolic stress responses*). 2-Isopropylmalic acid is an intermediate of leucine metabolism and was detected in high concentrations during anaerobic 3-hydroxybenzoate degradation. However, leucine was not detected under this growth condition. 2-isocaprenoyl-CoA was detected specifically during HPP degradation, with higher signals during aerobic growth. The metabolite is only known from leucine fermentation in *Clostridium difficile* (Kim *et al.*, 2005). β-Alanine plays a role in panthothenate and coenzyme A biosynthesis. The metabolite was detected during HPP and phenylalanine metabolism as well as during aerobic 3-hydroxybenzoate and anaerobic benzoate degradation, but massively upregulated during aerobic phenylalanine degradation. 3-phenyllactate was detected during anaerobic HPP degradation and, with a lower signal, during anaerobic phenylalanine degradation. This substance can be formed enzymatically from phenylpyruvate but could also be an unspecific byproduct, possibly from hydrolysis of a CoA-ester. The free nucleobase thymine was detected in all aerobic samples but showed the highest fold-change during aerobic benzoate degradation. The detected amount of thymine showed no correlation with either growthrate, DNA or RNA content. The amino acid lysine was detected during anaerobic acetate and benzoate degradation, as well as during aerobic 3-hydroxybenzoate, HPP and phenylalanine degradation. The dipeptide glycylglycine has no known metabolic role and most likely originates from peptide degradation during sample processing. It was detected in most anaerobic samples and elevated during anaerobic benzoate degradation.

Proteomics

Shot-gun proteomic analysis of cells from the different growth conditions resulted in identification of 1020 cytosolic proteins. The provided mascot protein scores are summed peptide probability scores and can be interpreted in a qualitative way, as explained in chapter *2.5.4 Interpretation of protein shotgun data mascot scores*.

Transcriptomics

Transcriptomic analysis of cells from the different growth conditions resulted in Expression counts for 5903 genomic regions. 4646 of these were mapped to annotated genes in *A. aromaticum* EbN1. Of the remaining 1257 RNAs, 775 were shown to constitute antisense RNA to annotated genes.

3.2.1.4 Summary of the general metabolic results

This work constitutes a comprehensive systems biological analysis of aerobic and anaerobic aromatic degradation pathways in *A. aromaticum* EbN1. Metabolic profiles emphasize the role of benzoyl-CoA pathways in the context of aromatic degradation. And the results stress the importance of CoA-ester analysis to complement classical GC-MS based metabolomic analysis.

Beyond the pathway centered analysis of metabolites, untargeted analysis of specifically elevated metabolites revealed a large number of potential by products from CoA-mediated degradation pathways. The relatively large number of CoA-esters with high signal intensities could indicate an over all vagueness of the CoA-mediated aromatic degradation pathways. Other metabolites were linked to coenzyme A biosynthesis or the accumulation of osmolytes.

3.2.2 Central metabolism

A. aromaticum EbN1 possesses all genes necessary for glycolysis and gluconeogenesis, as well as the non-oxidative part of the pentose phosphate pathway. Furthermore, *A. aromaticum* EbN1 is capable of running a complete citric acid cycle for energy generation including the glyoxylate shunt to channel C2-units toward biomass production (Rabus *et al.*, 2005).

3.2.2.1 Citric acid cycle

The citric acid cycle represents a core process of respirational bacterial metabolism and all degradation pathways eventually lead here. Thus, the different growth conditions from the systems biology experiments influence the central metabolism in various ways.

All metabolites, transcripts and proteins involved in the citric acid cycle in *A. aromaticum* EbN1 are presented in figure 12 as a pathway graph with a table of the relative peak areas, expression values and mascot scores.

Sequential metabolic pathway

(1) acetyl-CoA

Acetyl-CoA is a major product of most investigated degradation pathways and marks the central entry point to the citric acid cycle. The metabolite was detected with high levels in all samples, regardless of the degradation pathways.

(2) citrate and (3) isocitrate

Synthesis of citrate from acetyl-CoA and oxaloacetate marks the beginning of the citric acid cycle. Citrate synthase (ebA6687) gene transcript and protein levels were high in all samples.

The reaction product citrate was generally detected in very low concentrations and was below the detection limit in anaerobic samples. Exceptions were the HPP degrading samples, where similar concentrations were found during aerobic and anaerobic respiration. Additionally, citrate levels were elevated during phenylalanine degradation with a maximum during anaerobic growth and low citrate levels during aerobic growth.

The observed anaerobic accumulation of citrate during phenylalanine degradation is not very pronounced and could be explained by a NADH feedback regulation within the citric acid cycle, since NAD^+ regeneration is less effective during denitrification (Michal and Schomburg, 2012). Phenylalanine degradation to phenylacetate generates additional NADH which could lead to further impairment of the citric acid cycle and explain the higher anaerobic accumulation.

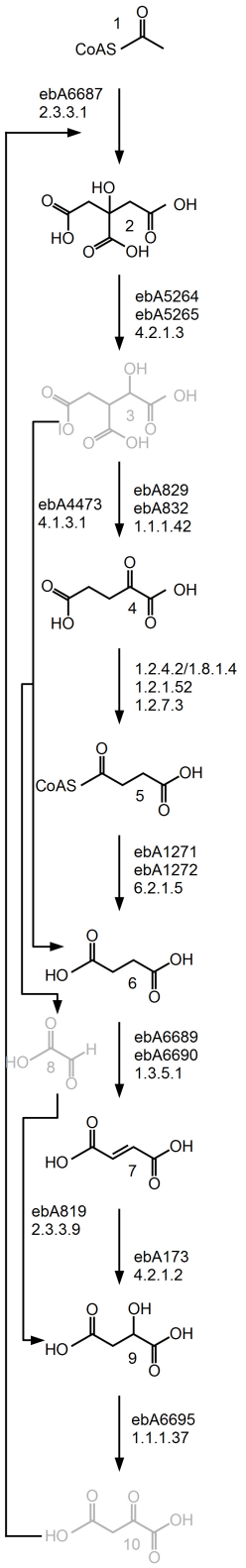

		Ace NO_3	Ace O_2	Ben NO_3	Ben O_2	Hbe NO_3	Hbe O_2	HPP NO_3	HPP O_2	Phe NO_3	Phe O_2
(1) acetyl-CoA		1328592	758914	846490	977224	1139162	1320983	589337	760534	886646	663864
ebA6687	T	3190	2951	2335	1938	1635	2157	2865	1103	2922	2264
	P	1109	1464	1312	1298	974	1025	1202	1340	850	1409
(2) citrate		68	NA	130	NA	190	NA	121	122	801	36
ebA5264	T	36	27	46	32	40	56	37	30	65	37
	P	NA	NA	NA	NA	NA	NA	NA	NA	NA	NA
ebA5265	T	578	271	386	351	146	332	253	128	262	444
	P	2102	3084	1959	2270	1366	1853	1089	1739	1995	2783
(3) isocitrate		NA	NA	NA	NA	NA	NA	NA	NA	NA	NA
ebA829	T	1425	1034	1125	1158	1074	1958	1143	1355	1935	1761
	P	1020	978	1044	812	1022	952	1194	1133	1280	1250
ebA832	T	1368	1217	960	818	574	938	844	561	734	981
	P	1330	2133	1319	1789	850	1339	971	1681	840	1969
(4) 2-oxoglutarate		242	35	92	65	161	142	135	329	NA	46
		2-oxoglutarate dehydrogenase systems									
(5) succinyl-CoA		322845	400537	329498	263021	369126	235378	173528	195625	222840	302463
ebA1271	T	1827	1204	1127	1225	1147	668	1114	765	646	815
	P	795	635	662	605	717	677	609	586	628	574
ebA1272	T	4175	2863	2372	2248	2382	1507	2490	1730	1024	1780
	P	1349	1356	1248	1305	1177	1184	1206	1182	1103	1245
(6) succinate		1072	11031	7665	15259	5636	11023	3102	9022	587	8639
ebA6689	T	1124	906	866	686	506	726	875	419	778	895
	P	558	554	513	555	479	495	453	419	548	598
ebA6690	T	1599	1148	1194	843	720	1031	1080	632	918	1151
	P	1252	1710	1255	1418	926	1142	1222	1193	977	1332
(7) fumarate		417	10042	5704	9032	2176	16778	1139	12477	629	2469
ebA173	T	413	306	225	245	210	264	308	283	64	162
	P	929	1023	781	986	596	700	701	696	310	561
ebA4473	T	3228	2120	2149	1500	722	944	2389	738	1010	1820
	P	1347	1646	1552	1313	1263	1046	1308	1165	1332	1433
(8) glyoxylate		NA	NA	NA	NA	NA	NA	NA	NA	NA	NA
ebA819	T	301	353	1414	196	236	127	574	181	697	283
	P	1675	2026	2064	1353	1723	719	2018	1321	1343	1453
(9) malate		1083	1461	1159	1380	3034	1279	2698	1108	415	312
ebA6695	T	2050	1641	1393	1107	802	1248	1670	922	1007	1468
	P	1285	1276	1241	1162	1138	1137	1187	1166	1219	1325
(10) oxaloacetate		NA	NA	NA	NA	NA	NA	NA	NA	NA	NA

Figure 12: Citric acid cycle of *A. aromaticum* EbN1 with glyoxylate shunt
Growth conditions are abbreviated as substrate and electron acceptor: Ace = acetate, Ben = benzoate, Hbe = 3-hydroxybenzoate, HPP = 3-(4-hydroxyphenyl)propanoate, Phe = phenylalanine, NO_3 = nitrate, O_2 = oxygen; Metabolites are indicated in bold and numbered according to the pathway diagram, genes are identified by locus tag with T indicating expression values of transcription and P indicating mascot scores of proteins;

All Omics data are classified in percentiles and color coded: Gray = below detection limit, light green = lowest 30%, bright green = medium 30%, green = higher 30%, dark green = top 10%, NA = not detected metabolite or protein

Dehydrogenation of citrate to aconitate and hydration to isocitrate are catalyzed by an aconitate hydratase (EC 4.2.1.3). Of the three copies of aconitate hydratase in the genome of *A. aromaticum* EbN1, only ebA5265 (*acnB*) showed transcription and translation under all analyzed growth conditions. The other two genes, ebA5264 (*acnA*) and ebA6773 (*acnA2*), are both annotated as type A aconitases, which are specific for nutritional or oxidative stress in *E. coli* (Cunningham *et al.*, 1997). The applied GC-MS system did not allow to distinguish between citrate and isocitrate, because of the similar retention times and mass spectra. Additionally, isocitrate is usually below the detection limit. Intermediate aconitate was also not detectable, since it is not usually released from the enzyme in between reactions.

(4) 2-oxoglutarate

Decarboxylation of isocitrate to 2-oxoglutarate is catalyzed by NAD^+ or $NADP^+$ dependent enzymes. Two genes, ebA829 and ebA832, are annotated as isocitrate dehydrogenases, next to each other on the chromosome of *A. aromaticum* EbN1. Both genes appeared to be co-transcribed and translated to produce similar protein mascot scores. Protein levels of ebA832 were slightly elevated in aerobic samples, while ebA829 showed near identical scores under both respiratory conditions for every substrate. Both genes are annotated as $NADP^+$ dependent isocitrate dehydrogenases, but ebA829 shows the highest similarity (73.43%) to an *E. coli* gene while ebA832 shows 64.99% identity to an *Azotobacter vinelandii* gene. The existence of the two different isoenzymes could play a role in the regulation of isocitrate levels and thus activity of the glyoxylate shunt.

The product, 2-oxoglutarate, was detected in small amounts in most samples. It was elevated during anaerobic acetate and aerobic HPP degradation, but below the detection limit during anaerobic phenylalanine degradation. 2-Oxoglutarate is a co-substrate of the aromatic-amino-acid transaminase, which was translated during phenylalanine degradation to phenylacetate (*3.3.4.1 Aerobic and anaerobic degradation of phenylalanine to phenylacetate*). This could explain the reduced levels of 2-oxoglutarate during phenylalanine degradation.

(5) succinyl-CoA

The second decarboxylation in the citric acid cycle of 2-oxoglutarae to succinyl-CoA can be facilitated by different 2-oxoglutarate dehydrogenase systems. Three putative 2-oxoglutarate dehydrogenase systems or parts of such systems are annotated in the chromosome of *A. aromaticum* EbN1 and showed RNA transcription and protein translation under different growth conditions (Figure 13).

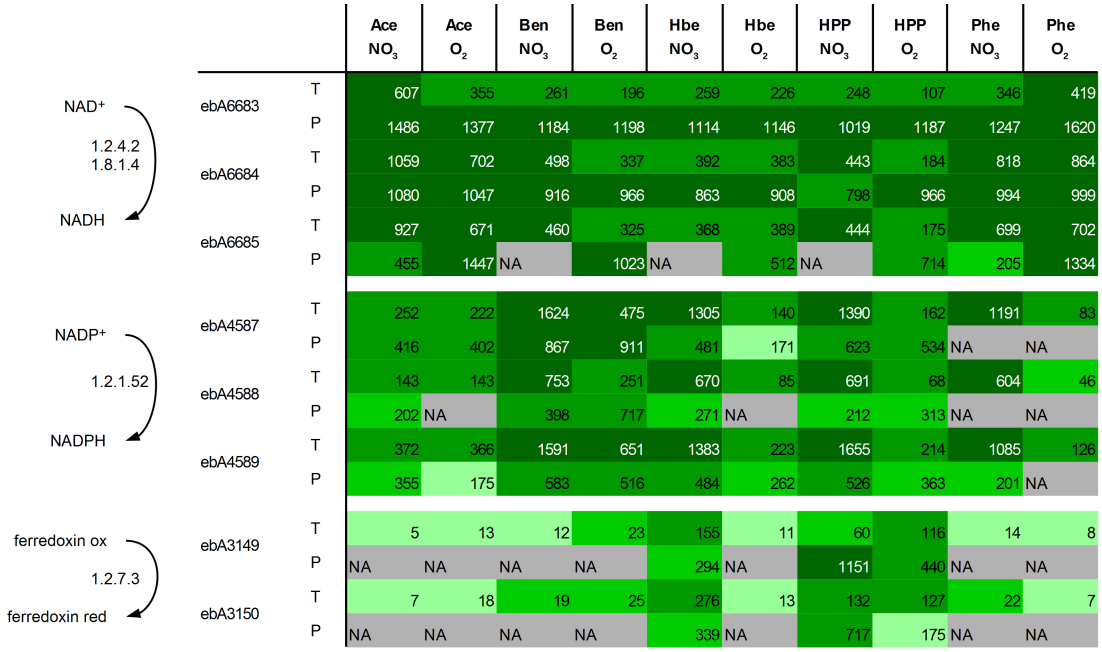

Figure 13: 2-oxoglutarate dehydrogenase systems in *A. aromatoleum* EbN1 with different reduction agent preferences
Growth conditions are abbreviated as substrate and electron acceptor: Ace = acetate, Ben = benzoate, Hbe = 3-hydroxybenzoate, HPP = 3-(4-hydroxyphenyl)propanoate, Phe = phenylalanine, NO_3 = nitrate, O_2 = oxygen; Genes are identified by locus tag with T indicating expression values of transcription and P indicating mascot scores of proteins; All Omics data are classified in percentiles and color coded: Gray = below detection limit, light green = lowest 30%, bright green = medium 30%, green = higher 30%, dark green = top 10%, NA = not detected protein

A NADH producing 2-oxoglutarate dehydrogenase is encoded by ebA6683, ebA6684 and ebA6685 (EC 1.2.4.2 and EC 1.8.1.4). Transcription was generally high in all samples and additionally elevated during aerobic and anaerobic acetate and phenylalanine degradation. Two subunits, ebA6683 and ebA6684 showed high protein mascot scores in all samples, while protein ebA6685 was not detectable in anaerobic benzoate, 3-hydroxybenzoate and HPP degrading samples. Protein mascot scores of the last subunit were generally reduced during anaerobic growth.

A 2-oxoglutarate:$NADP^+$ oxidoreductase system (EC 1.2.1.52) is encoded by ebA4587, ebA4589 and ebA4588. Transcription of all subunits was high in all samples but additionally elevated during anaerobic degradation of all aromatic substrates. Protein scores were elevated during aerobic and anaerobic benzoate degradation while one or more subunits were below detection limit during aerobic and anaerobic phenylalanine degradation, as well as during aerobic 3-hydroxybenzoate and acetate degradation.

A ferredoxin reducing 2-oxoglutarate synthase (EC 1.2.7.3) is encoded by ebA3149 and ebA3150. Transcription of these genes was very low in most samples but elevated during aerobic benzoate and HPP degradation and during anaerobic 3-hydroxybenzoate and HPP degradation. The proteins were only detectable during HPP degradation and anaerobic 3-hydroxybenzoate degradation, with reduced protein mascot scores during aerobic HPP degradation.

Regulation of the different enzyme systems reflects the varying needs for special types of reduction equivalents. The NADH-producing 2-oxoglutarate dehydrogenase was upregulated in aerobic samples to provide NADH for the efficient respiratory chain. During anaerobic benzoyl-CoA degradation on the other hand, the NADPH-producing 2-oxoglutarate synthase was upregulated, since NADPH is necessary for reductive dearomatization of benzoyl-CoA. Apparently, phenylalanine degradation lead to downregulation of the NADPH-producing enzyme, even though the anaerobic pathway includes NADPH-dependent dearomatization of benzoyl-CoA. Lastly, the 2-oxoglutarate:ferredoxin oxidoreductase is specifically upregulated during HPP degradation and could provide the reduction equivalents for the side chain degradation. A similar NADPH dependent regulation has previously been described for *Azoarcus evansii* and was hypothezised for *A. aromaticum* EbN1 based on genetic evidence (Ebenau-Jehle *et al.*, 2003; Rabus *et al.*, 2005).

The product succinyl-CoA was detected in all samples in high concentrations. Even though aerobic HPP, benzoate and phenylalanine degradation produce succinyl-CoA as final products, no response in the metabolite levels was apparent. This reflects the strict regulation of this part of the citric acid cycle to provide constant levels of central metabolites.

The rest of the citric acid cycle showed no substrate specific variations. Only a mild accumulation of succinate (6) correlated with aerobic growth with every substrate. Fumarate (7) was elevated during aerobic 3-hydroxybenzoate degradation, since it is a final product of the gentisate pathway (see *3.3.5.1 Aerobic 3-hydroxybenzoate degradation pathway*).

glyoxylate shunt

Enzymes and metabolites that are involved in the glyoxylate bypass of the citric acid cycle are included in figure 12 in the lower part of the table. Isocitrate lyase (ebA4473) showed uniform protein levels under all growth conditions, as did malate synthase (ebA819). The only exception was a mild down regulation of the malate synthase protein levels during aerobic 3-hydroxybenzoate degradation. This down regulation is in accordance with expectations, because aerobic 3-hydroxybenzoate degradation directly yields fumarate.

Regulation of the glyoxylate shunt was found to occur via reversible enzyme inhibition of isocitrate dehydrogenase to allow for a greater flux through the isocitrate lyase in *E. coli* (Holms, 1987). Even though neither isocitrate nor glyoxylate could be measured in this study, the lack of observable regulation on translational or transcriptional level supports a similar mode of regulation in *A. aromaticum* EbN1.

3.2.2.2 Pyruvate decarboxylation and anaplerotic reactions

Pyruvate is a key intermediate at the central junction of the citric acid cycle and gluconeogenesis and the starting point of several anabolic pathways. Its main catabolic and anaplerotic reactions are presented in figure 14. Pyruvate was detected in all samples, except during anaerobic phenylalanine degradation.

Pyruvate dehydrogenase subunits, ebA133, ebA135 and ebA136, showed a uniform medium transcription, which was only elevated in aerobic 3-hydroxybenzoate degrading cells. All three subunit proteins were detected in samples aerobically degrading aromatic substrates. Highest levels of pyruvate dehydrogenase subunit transcripts and proteins were detected during aerobic 3-hydroxybenzoate degradation. This is in accordance with expectations, since aerobic 3-hydroxybenzoate degradation via the gentisate pathway generates pyruvate as final product. Additionally, the pyruvate dehydrogenase complex

appears to be present in all aerobic samples except during acetate degradation. The enzyme complex is strictly regulated by its products (Reed and Cox, 1970), which could explain the downregulation in the presence of acetate, where the entire carbon flux is directed through acetyl-CoA.

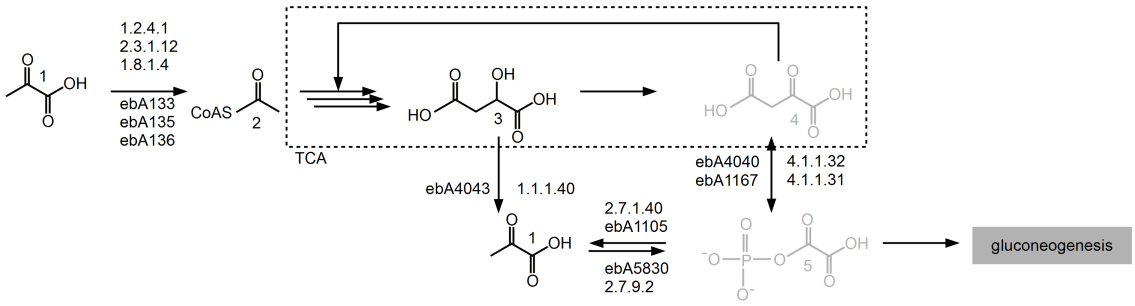

		Ace NO_3	Ace O_2	Ben NO_3	Ben O_2	Hbe NO_3	Hbe O_2	HPP NO_3	HPP O_2	Phe NO_3	Phe O_2
(1) pyruvate		499	933	1908	462	1720	1823	694	1085	NA	684
ebA133	T	140	133	124	207	403	620	186	150	291	213
	P	NA	NA	NA	535	NA	963	NA	446	NA	713
ebA135	T	40	55	30	63	96	217	66	55	101	81
	P	NA	323	348	579	NA	876	413	558	255	806
ebA136	T	51	84	39	81	105	371	108	91	156	122
	P	NA	134	143	715	152	1110	487	481	399	565
(2) acetyl-CoA		1328592	758914	846490	977224	1139162	1320983	589337	760534	886646	663864
(3) malate		1083	1461	1159	1380	3034	1279	2698	1108	415	312
ebA4043	T	88	98	89	100	62	84	62	59	57	84
	P	182	810	397	765	NA	243	176	743	193	764
(4) oxaloacetate		NA	NA	NA	NA	NA	NA	NA	NA	NA	NA
ebA4040	T	1043	784	671	643	457	674	596	659	149	398
	P	545	1429	685	1381	401	893	494	1095	NA	1135
(5) phosphoenol-pyruvate		NA	NA	NA	NA	NA	NA	NA	NA	NA	NA
ebA1105	T	141	80	76	69	115	67	103	70	49	81
	P	277	144	NA	261	NA	113	NA	NA	111	182
ebA5830	T	416	477	286	402	282	416	425	302	168	168
	P	776	1726	865	1522	438	893	675	798	107	602

Figure 14: Pyruvate decarboxylation and anaplerotic reactions connecting the citric acid cycle of *A. aromaticum* EbN1 with gluconeogenesis and other metabolic pathways
Growth conditions are abbreviated as substrate and electron acceptor: Ace = acetate, Ben = benzoate, Hbe = 3-hydroxybenzoate, HPP = 3-(4-hydroxyphenyl)propanoate, Phe = phenylalanine, NO_3 = nitrate, O_2 = oxygen; Metabolites are indicated in bold and numbered according to the pathway diagram, genes are identified by locus tag with T indicating expression values of transcription and P indicating mascot scores of proteins; All Omics data are classified in percentiles and color coded: Gray = below detection limit, light green = lowest 30%, bright green = medium 30%, green = higher 30%, dark green = top 10%, NA = not detected metabolite or protein

Malic enzyme (ebA4043) was detected in all samples with low to medium RNA transcription and protein scores, except during anaerobic 3-hydroxybenzoate degradation. Anaplerotic generation of pyruvate from malate via malic enzyme could be active, at least to a low degree, in all samples except during anaerobic 3-hydroxybenzoate degradation.

As first step from the citric acid cycle toward gluconeogenesis, generation of phosphoenolpyruvate from oxaloacetate is achieved by the reversible phosphoenolpyruvate carboxykinase (ebA4040). The gene showed high transcription throughout all samples, except during aerobic and anaerobic degradation of phenylalanine. Protein scores were generally elevated in aerobic samples and below the detection limit in anaerobic phenylalanine degrading cells.

Phosphoenolpyruvate synthetase (ebA5830), which catalyzes the ATP dependent formation of phosphoenolpyruvate from pyruvate, was detected as protein under all growth conditions. The enzyme was noticeably upregulated in cells degrading acetate or 3-hydroxybenzoate aerobically and during both aerobic and anaerobic benzoate degradation.

A pyruvate kinase (ebA1105), which catalyzes the reverse reaction from phosphoenolpyruvate to pyruvate, exhibited moderate gene expression in all samples. The protein was detected with low to moderate scores in most samples, excluding anaerobic benzoate, 3-hydroxybenzoate and both aerobic and anaerobic HPP degrading samples.

All in all, generation of pyruvate as precursor for several anabolic pathways is necessary under all growth conditions, except during aerobic 3-hydroxybenzoate degradation. This is reflected in the protein scores of malic enzyme ebA4043. Decarboxylation of pyruvate to acetyl-CoA as TCA entry point is a key process during aerobic 3-hydroxybenzoate degradation. This is consistent with the massive upregulation of all pyruvate dehydrogenase subunits under this growth condition.

3.2.2.3 Glycolysis/Gluconeogenesis

Gluconeogenesis has to be active under all growth conditions to provide building blocks for cell wall or lipopolysaccharide biosynthesis and precursors for several amino acid biosynthesis pathways. The pathway of gluconeogenesis and all related systems biology results are summarized in supplement 15.

The produced glucose was detected as glucose or 1,6-anhydro-glucose in all samples. The accumulation of glucose 6-phosphate in cells grown anaerobically with benzoate, correlated with the massive production of α-glucosylglycerol in these samples (see *3.2.4 Metabolic stress responses*).

Fructose 6-phosphate was detected in all anaerobic samples as well as in samples, aerobically degrading 3-hydroxybenzoate or HPP. Fructose 6-phosphate peak areas correlate with glucose 6-phosphate peak areas, indicating an enhanced gluconeogenesis for biosynthesis of α-glucosylglycerol. At the same time fructose was detectable in all samples but showed no correlation with fructose-6 phosphate concentrations.

All metabolic intermediates between fructose-6-phosphate and pyruvate were below the detection limit. These phosphorylated compounds tend to be unstable during sample preparation. Additionally, a tight regulation of the energy-consuming process of gluconeogenesis would avoid the unnecessary accumulation of intermediates.

On the transcriptomic and proteomic levels, no distinct regulation of gluconeogenesis was apparent. Most genes showed a medium level of transcript and protein throughout all samples. Only anaerobic phenylalanine samples showed reduced transcript and protein levels of gluconeogenesis enzymes. This could reflect the lower growth rate of *A. aromaticum* EbN1 under this condition and is in accordance with the reduced enzyme levels for phosphoenolpyruvate synthesis.

3.2.2.4 Respiration

A. aromaticum EbN1 is capable of aerobic and anaerobic respiration. In the systems biology experiments, growth with different substrates was investigated under aerobic respiration with air or under anaerobic respiration with nitrate as electron acceptor. The genome encodes numerous genes involved in respiration: Different terminal oxidases, different NADH dehydrogenases and a full enzymatic equipment for denitrification. These broad respiratory capabilities are described in detail by (Rabus, 2005). A summary of the annotation of all genes involved in respiration is given in supplement 16.

Average rates of nitrate consumption, nitrite formation and nitrite consumption were calculated from the measured nitrate and nitrite concentrations and from the growth rates in the exponential phase (Kathleen Trautwein, MPI) and are presented in figure 15. Of the

four enzymes necessary for denitrification, only nitrate reductase (ebA6282, ebA6285 and ebA6286) was regulated transcriptionally in response to nitrate availability. Transcription of cytochrome cd1 nitrite reductase (ebA488), nitric-oxide reductase (ebB6 and ebA179) and nitrous-oxide reductase (ebA6272) was detected in aerobic and anaerobic samples. Transcription of these genes did not correlate with either nitrate consumption rates or nitrite formation or consumption rates. A table of the expression values of all denitrification genes is presented in supplement 17. Since the denitrification complexes are membrane bound, these gene products are not included in the analysis of cytosolic protein.

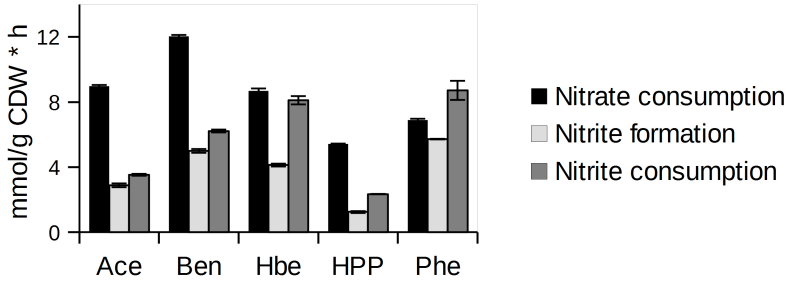

Figure 15: Nitrate consumption, nitrite consumtion and formation during anaerobic growth of *A. aromaticum* EbN1 as rates in mmol per gram cell dry weight and hour; Growth conditions are abbreviated as substrate: Ace = acetate, Ben = benzoate, Hbe = 3-hydroxybenzoate, HPP = 3-(4-hydroxyphenyl)propanoate, Phe = phenylalanine

Of the three proposed terminal oxidases in *A. aromaticum* EbN1, a cytochrome-c oxidase (ebA5131, ebA5132, ebA5134) showed the highest gene transcription, without discrimination between aerobic respiration and denitrification. Additional involvement of any or both of the other terminal oxidases could not be ruled out based the transcriptomic results, but this appears to be the preferred oxidase during aerobic growth and to be kept available during anaerobic growth. A table of gene expression values of all genes encoding terminal oxidases is presented in supplement 17. The data is in accordance with previous speculations, that this cytochrome-c oxidase (ebA5131, ebA5132, ebA5134) is the preferred terminal oxidase under low oxygen partial pressures (Rabus, 2005).

Gene transcription of NADH:quinone dehydrogenase (ebD11, ebA4835-ebA4848) and ATP-synthase (ebA2999-ebA3008) strongly correlated with each other. The highest transcription of both genes was detected in cells anaerobically degrading acetate. The second highest expression was detected during anaerobic HPP degradation and the lowest

values during anaerobic phenylalanine degradation. ATP concentrations along with the medium transcription value of NADH dehydrogenase and ATP synthase subunits are presented in figure 16. Transcription of the individual subunits was rather uniform and is included in supplement 18. ATP content per cell lies within the range reported for *E. coli* under different growth conditions and for various marine bacteria (see supplement 19) (Bennett *et al.*, 2009; Buckstein *et al.*, 2008; Hamilton and Holm-Hansen, 1967; Lowry *et al.*, 1971; Yaginuma *et al.*, 2014).

Both acetate cultures, both benzoate cultures and the anaerobic HPP culture showed low levels of ATP and higher transcription levels for NADH dehydrogenase and ATP synthase. This could indicate that ATP biosynthesis was the main restriction on growth under these conditions. However, even the lowest ATP concentrations are within the physiological range reported for other bacteria, thus a massive shortage of ATP seems not likely.

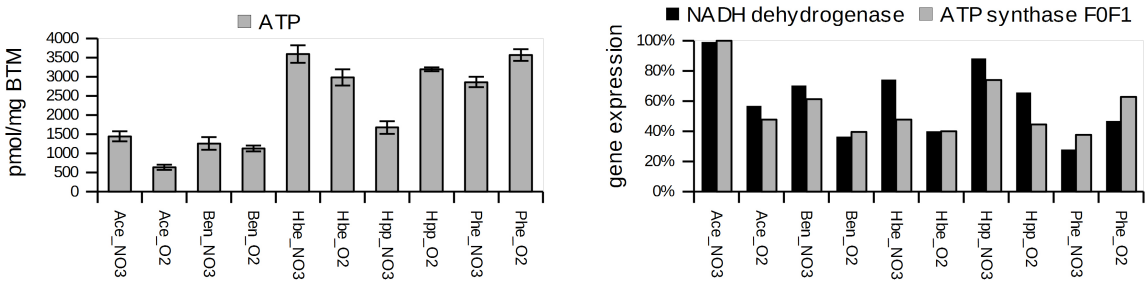

Figure 16: ATP content and medium gene expression of ATP synthase and NADH dehydrogenase
Gene expression is scaled to the maximum and given as mean value of all subunits; Growth conditions are abbreviated as substrate and electron acceptor: Ace = acetate, Ben = benzoate, Hbe = 3-hydroxybenzoate, Hpp = 3-(4-hydroxyphenyl)propanoate, Phe = phenylalanine, NO3 = nitrate, O2 = oxygen

3.2.2.5 Summary of the central metabolism

The central metabolism showed only minor variations in response to the different NADH-producing degradation pathways and to the mode of respiration. Anaerobic phenylalanine degradation appears to decelerate the citric acid cycle in response to NADH excess and restricted respiration, subsequently also reducing phosphoenolpyruvate biosynthesis and gluconeogenesis. Three enzyme systems with different cofactor usage are involved in the formation of succinyl-CoA from 2-oxoglutarate. These are regulated on trancriptional and translational level, according to the cofactor requirements of the

different degradation pathways.

Pyruvate was generated from malate via malic enzyme (ebA4043) under all growth conditions except during aerobic 3-hydroxybenzoate degradation, where pyruvate is a degradation product. Phosphoenolpyruvate formation from oxaloacetate appears specifically upregulated during aerobic growth.

Glyconeogenesis is active under all growth conditions and additionally upregulated during anaerobic benzoate degradation to allow for osmolyte biosynthesis.

3.2.3 β-oxidation

The process of β-oxidation is well known and studied in the context of fatty acid metabolism in most organisms. After activation to a CoA-ester, the substrate is sequentially oxidized at the β-carbon by dehydrogenation, hydratation and dehydratation before acetyl-CoA is cleaved off thiolytically (Voet *et al.*, 2002). The same sequential reactions are involved in the degradation of diverse CoA-bound carboxylic acid derivatives to acetyl-CoA.

In *A. aromaticum* EbN1, the β-oxidation parts of some metabolic pathways are not included in the respective gene clusters or operons but appear to be carried out by constitutive enzymes. This is the case in the pathways of aerobic benzoate and phenylalanine degradation and in anaerobic benzoate degradation: All three pathways lack a pathway specific enoyl-CoA hydratase (4.2.1.-). The last pathway additionally lacks one enoyl-CoA hydratase (4.2.1.-), one thiolase (2.3.1.-) and two 3-hydroxyacyl-CoA dehydrogenases (1.1.1.-). In contrast to that, full sets of pathway specific enzymes for β-oxidation sequences are included in the pathway of side chain removal of HPP. Table 6 shows an overview of all genes, related to β-oxidation processes and translated during the systems biology experiments with their assigned enzymatic roles. These 83 genes were submitted to cluster analysis of transcript and protein (supplement 20). Cluster analysis divided the genes into two larger groups. The top half showed largely unregulated transcription and translation (cluster A and B). The lower half of the analysis comprised of genes that showed differentiated protein profiles and either regulated (clusters E, F and H) or unregulated gene expression (clusters G, I, J and K).

One cluster (C) comprised of three genes, c2A174, c2A173 and c2A178 with elevated

transcription and translation during aerobic benzoate and HPP metabolism. These three genes were transcribed as one mRNA, including an enoyl-CoA hydratase (c2A174) that could perform the missing reaction in aerobic benzoate degradation. All in all, this cluster analysis revealed that a large number of β-oxidation enzymes were transcribed and translated under all growth conditions.

Table 6: Putative β-oxidation genes of *A. aromaticum* EbN1:
155 genes were annotated with a name or EC-number related to β-oxidation, 83 gene products were detected in the cytosolic protein fraction and are included in this table by enzyme function

Enzyme	Number
CoA ligase, ADP/AMP forming	14
acyl-CoA dehydrogenase	8
enoyl-CoA hydratase/isomerase	16
3-hydroxyacyl-CoA dehydrogenase	15
thiolase	10
electron transfer flavoproteins	4
other alcohol and aldehyde dehydrogenase	16

Since the cluster analysis of 83 gene transcripts and proteins resulted in a complex and difficult to interpret representation of the regulation, respective enzyme classes are discussed in detail below.

Enoyl-CoA hydratases catalyze the hydrolation of an enoyl-CoA-ester to a 3-hydroxyacyl-CoA-ester. 16 enoyl-CoA hydratases were transcribed and translated during the systems biology experiments. Of these, five enzymes are parts of the known gene clusters for anaerobic benzoate or 3-hydroxybenzoate degradation or aerobic benzoate degradation. Three more enzymes were not detected as protein while the degradation pathways lacking enoyl-CoA hydratases were active. This leaves eight putative enoyl-CoA hydratases, which are not assigned to substrate dependent pathways, and were translated under at least one of the growth conditions under investigation (table 7). Six of these enoyl-CoA hydratases were translated during anaerobic benzoate degradation. However, none of them showed distinct upregulation of gene transcription or protein translation during anaerobic benzoate degradation. Interestingly, ebA5296, the cyclohexa-1,5-dienecarbonyl-CoA hydratase from anaerobic benzoate degradation, also showed

unspecific gene transcription and protein translation, resulting in uniformly high protein mascot scores during all anaerobic aromatic degradations. Thus, any of the six putative enoyl-CoA hydratases could be involved in the hydrolation of crotonyl-CoA to 3-hydroxybutanoyl-CoA during anaerobic benzoate degradation. However, only ebA1321 and c2A174 were detected with high protein mascot scores.

Table 7: Hydratases whiche are not annotated as part of a specific degradation pathway

The enzymes are possibly involved in β-oxidation sequences from aerobic benzoate or phenylalanine degradation or anaerobic benzoate degradation;

Growth conditions are abbreviated as substrate and electron acceptor: Ace = acetate, Ben = benzoate, Hbe = 3-hydroxybenzoate, HPP = 3-(4-hydroxyphenyl)propanoate, Phe = phenylalanine, NO3 = nitrate, O2 = oxygen; Genes are identified by locus tag with T indicating expression values of transcription and P indicating mascot scores of proteins; Column Annotation gives the annotated gene name and Column EC gives the assigned EC-nuber, if available; All Omics data are classified in percentiles and color coded: Gray = below detection limit, light green = lowest 30%, bright green = medium 30%, green = higher 30%, dark green = top 10%, NA = not detected metabolite or protein

Gene	Annotation	EC		Ace NO_3	Ace O_2	Ben NO_3	Ben O_2	Hbe NO_3	Hbe O_2	HPP NO_3	HPP O_2	Phe NO_3	Phe O_2
ebA1321	enoyl-CoA hydratase/ isomerase (ech)	4.2.1.17	T	413	309	194	296	221	322	287	262	119	346
			P	589	630	547	535	502	510	517	634	571	620
c2A174	enoyl-CoA hydratase/ isomerase	4.2.1.17	T	11	13	15	104	18	29	34	44	21	46
			P	NA	NA	275	402	328	103	261	293	NA	NA
ebA6516	enoyl-CoA hydratase/ isomerase	4.2.1.17	T	105	98	78	85	105	127	89	83	159	114
			P	198	258	115	157	254	184	220	225	273	414
ebA4434	MaoC-like enoyl-CoA hydratase	putative	T	885	876	925	789	1188	1014	1070	915	1239	1570
			P	215	194	182	126	229	260	224	162	161	299
ebA2191	enoyl-CoA hydratase/ isomerase	4.2.1.17	T	29	33	25	44	26	42	25	27	29	30
			P	177	NA	152	NA	133	NA	75	NA	211	175
ebA2313	enoyl-CoA hydratase/ isomerase	4.2.1.17	T	185	149	90	92	90	120	104	101	63	93
			P	79	211	94	148	NA	126	202	92	80	NA
ebA3691	enoyl-CoA hydratase/ isomerase	4.2.1.17	T	6	7	28	25	11	13	27	14	44	16
			P	NA	NA	NA	NA	NA	NA	NA	NA	NA	64
ebA5671	MaoC-like enoyl-CoA hydratase	putative	T	29	41	31	47	30	55	30	31	81	76
			P	NA	NA	NA	NA	NA	NA	NA	NA	102	146
ebA5296	cyclohexa-1,5-dienecarbonyl-CoA hydratase	4.2.1.100	T	76	68	1563	487	547	345	1611	521	725	180
			P	283	182	641	364	634	501	658	569	579	364

Five enoyl-CoA hydratases, without known pathway affiliation, were translated during aerobic benzoate degradation. Of these, the same two enzymes showed high mascot scores under this growth condition. However, ebA1321 was expressed and translated with uniformly high scores throughout all growth conditions. The enzyme is annotated as *ech*

(catabolic enoyl-CoA hydratase) analogous to a subunit of the multifunctional enzyme complex from fatty acid degradation. Thus, a role in the respective aromatic degradation pathways appears less likely.

During aerobic phenylalanine degradation, seven enoyl-CoA hydratases were translated, any of which could be active during aerobic phenylalanine degradation. Besides ebA1321, two more enzymes, ebA6516 and ebA4434 showed high mascot scores. Enzyme ebA6516 is annotated as crotonase/enoyl-CoA hydratase superfamily protein and was translated under all growth conditions of the systems biology experiments. Both genes showed a mild upregulation of transcription and translation during aerobic phenylalanine degradation, thus suggesting involvement in this pathway.

Thiolases or acetyl-CoA C-acyltransferases are necessary to thiolytically cleave acetyl-CoA off from a 3-keto-acyl-CoA. In the lower pathway of anaerobic benzoate degradation, one such reaction is postulated without a specific enzymebeeing annotated, yet. Ten putative thiolases are included in the data set of translated genes from this study (supplement 21). All proteins that were detected during anaerobic benzoate degradation, were detected with higher mascot scores during aerobic benzoate degradation and were generally translated in all samples. Of these thiolases ebA5202, c2A172 and ebA3639 are not part of any known substrate specific gene cluster. Any of these enzymes could catalyze the cleaving of 3-ketopimeloyl-CoA to glutaryl-CoA and acetyl-Co during anaerobic benzoate degradation.

Lastly, two dehydrogenases are missing from the pathway of anaerobic benzoate degradation. Six genes that putatively encode hydroxyacyl-CoA dehydrogenases with no previously assigned role in degradation pathways, are translated during anaerobic benzoate degradation (supplement 22). All of these showed medium to high gene expression and translation under most growth conditions. Any of these enzymes could catalyze the two reactions during anaerobic benzoate degradation.

3.2.3.1 Summary of β-oxidation processes

A complex and redundant set of enzymes for β-oxidation processes was transcribed and translated in *A. aromaticum* EbN1 under all growth conditions. It appears most likely that several reactions from substrate specific β-oxidation sequences are catalyzed by multiple enzymes. However, this analysis points towards and involvement of c2A174, c2A173 and c2A178 in aerobic benzoyl-CoA degradation during growth with benzoate and HPP. Moreover, the enzymes could also be involved in the anaerobic benzoate degradation pathway. Furthermore, a role for enoyl-CoA hydratases ebA6516 and ebA4434 in aerobic phenylalanine degradation can be inferred from the systems biology data. Several enzymes were detected, that could fill in for the missing thiolase and 3-hydroxyacyl-CoA dehydrogenases from anaerobic benzoate degradation. These reactions appear to be catalyzed by redundant systems without distinct regulation.

3.2.4 Metabolic stress responses

Every aspect of the environment can constitute a challenge to bacterial growth, if a specific optimal range is not met. This includes temperature, which can be too low or too high; salinity, which can be below or above the preferred optimum; or oxygen partial pressure, which can deviate from the specific optimum. Adequate response to such challenges or stress factors is crucial for survival in changing environments and thus, numerous stress response mechanisms have evolved in bacteria (for a review see (Giuliodori *et al.*, 2007)).

In the systems biology experiments of this study most parameters, such as pH, temperature or salinity were kept in a narrow range near the growth optima of *A. aromaticum* EbN1. However, some observed metabolomic results resemble known bacterial stress responses like the accumulation of compatible solutes.

Massive accumulation of α-glucosylglycerol, putrescine, glutamate and β-glutamate was detected during anaerobic benzoate degradation. Lower levels of α-glucosylglycerol were also detectable during anaerobic HPP degradation and, even lower levels, during aerobic HPP degradation (Figure 17).

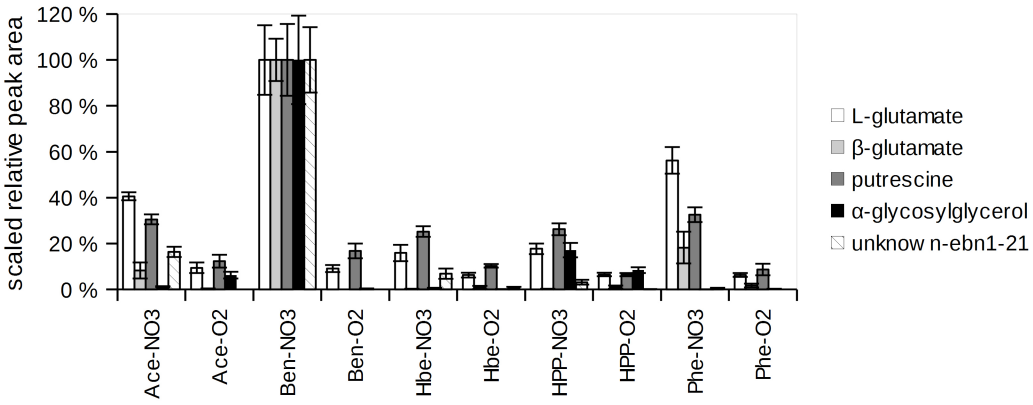

Figure 17: Accumulation of potential osmolytes during anaerobic growth with benzoate
Scaled relative peak areas of metabolites known as compatible solutes:white = L-glutamate, light gray = β-glutamate, dark gray = putrescine, black = α-glucosylglycerol,shaded = unknown-ebn1-21 tentatively identified as 2,4-diaminopentanoate ; Substrates are abbreviated: Ace = acetate, Ben = benzoate, Hbe = 3-hydroxybenzoate, HPP = 3-(4-hydroxyphenyl)propanoate; electron acceptors are indicated as appended _NO3 = nitrate or _O2 = oxygen

An additional compound, unknown-ebn1-21, which could not be identified via spectrum library comparison, showed a similar metabolic profile. The compound was elevated in all anaerobic cultures with a marked maximum during anaerobic benzoate degradation. The compound mass spectrum indicated an amino acid structure and is possibly an isomer of ornithine (*3.1.2 Analysis of unknown metabolites via GC-MS*).

If these compounds were synthesized and accumulated as compatible solutes to protect the cells or cell compounds from negative environmental influences, their biosynthesis could be expected to be regulated accordingly. Since none of the potential compatible solutes have been investigated in *A. aromaticum* EbN1, or a closely related organism so far, the biosynthesis pathways have not been described.

A predicted glycosyl transferase, ebA833, is the only gene with sufficient homology to glucosylglycerol biosynthesis enzymes. The gene showed low to moderate transcription in all samples with a maximum count of 31 during anaerobic benzoate degradation. The gene product was not detected in the cytosolic protein fraction of any sample.

Putrescine biosynthesis is not annotated in *A. aromaticum* EbN1 either. Additional BLAST queries could not provide candidate genes for ornithine decarboxylase (EC 4.1.1.17), agmatinase (EC 3.5.3.11), agmatine deaminase (EC 3.5.3.12) or N-carbamoylputrescine amidohydrolase (EC 3.5.1.53). Only one arginine decarboxylase (EC 4.1.1.19), ebA4413, and one putative arginase (EC 3.5.3.1), ebA3609, are annotated in *A.*

aromaticum EbN1. Both genes were transcribed with low to medium counts without substrate-specific regulation. Protein ebA4413 was the only putative putrescine biosynthesis enzyme, detected in this study during aerobic acetate degradation and with a low mascot score. Pathways for putrescine biosynthesis and all related systems biology results are presented in figure 18. In addition to the involved enzymes being ambiguous, ornithine, the only detected compound related to putrescine biosynthesis, showed no correlation to putrescine concentrations. Ornithine was only detected with very low signal intensities.

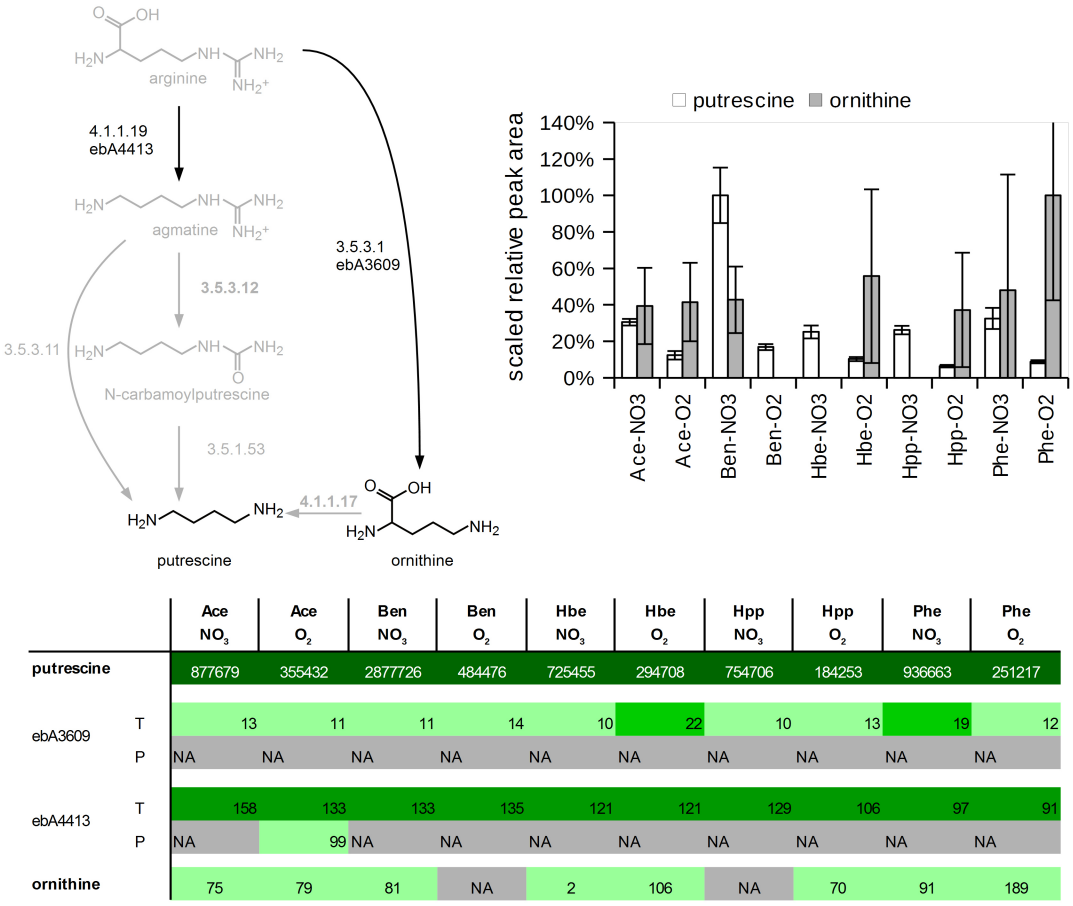

		Ace NO_3	Ace O_2	Ben NO_3	Ben O_2	Hbe NO_3	Hbe O_2	Hpp NO_3	Hpp O_2	Phe NO_3	Phe O_2
putrescine		877679	355432	2877726	484476	725455	294708	754706	184253	936663	251217
ebA3609	T	13	11	11	14	10	22	10	13	19	12
	P	NA	NA	NA	NA	NA	NA	NA	NA	NA	NA
ebA4413	T	158	133	133	135	121	121	129	106	97	91
	P	NA	99	NA	NA	NA	NA	NA	NA	NA	NA
ornithine		75	79	81	NA	2	106	NA	70	91	189

Figure 18: Putrescine biosynthesis pathways and scaled relative peak areas of detected compounds

Growth conditions are abbreviated as substrate and electron acceptor: Ace = acetate, Ben = benzoate, Hbe = 3-hydroxybenzoate, HPP = 3-(4-hydroxyphenyl)propanoate, Phe = phenylalanine, NO_3 = nitrate, O_2 = oxygen; bar plot: white = putrescine, gray = ornithine; systems biology data: Metabolites are indicated in bold, genes are identified by locus tag with T indicating expression values of transcription and P indicating mascot scores of proteins; All Omics data are classified in percentiles and color coded: Gray = below detection limit, light green = lowest 30%, bright green = medium 30%, green = higher 30%, dark green = top 10%, NA = not detected metabolite or protein

Biosynthesis of β-glutamate is even more unexplored. Only one pathway for the specific synthesis of this substance is described in C*lostridium difficile* (Ruzicka and Frey, 2007), which is no close relative of *A. aromaticum* EbN1. No homologous gene to the glutamate 2,3-aminomutase could be found in *A. aromaticum* EbN1. However, since the compound was positively identified by measurement of a synthetic standard and was detected with high signal intensities similar to glutamate, means of biosynthesis must be present in *A. aromaticum* EbN1.

α-Glucosylglycerol is an organic compatible solute, often associated with response to salt stress and nitrogen limitation in mesophilic bacteria and archaea (Empadinhas and da Costa, 2011). Glutamate and putrescine can also serve as compatible solutes (Kurz, 2008; Saum *et al.*, 2006) and β-glutamate was shown to accumulate as osmolyte in marine methanogenic bacteria (Robertson *et al.*, 1990). Neither salt concentration nor nitrogen availability differed significantly between the growth conditions and could explain the accumulation of compatible solutes during anaerobic benzoate degradation. Additionally, α-glucosylglycerol levels are much lower or undetectable in anaerobic HPP or phenylalanine degradation, where the same anaerobic benzoyl-CoA pathway is used under very similar growth conditions. None of the described compounds were previously detected in *A. aromaticum* EbN1, nor was the biosynthesis of these compounds or their role as osmolytes predicted or detected in *A. aromaticum* EbN1. A proteomics survey of solvent stress response of *A. aromaticum* EbN1 only indicated the potential biosynthesis of betaine as osmolytically active compound (Trautwein *et al.*, 2008).

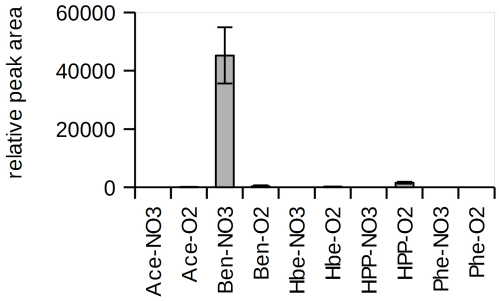

Figure 19: Intracellular levels of benzoate: Relative peak area of benzoic acid GC-MS signal; Substrates are abbreviated: Ace = acetate, Ben = benzoate, Hbe = 3-hydroxybenzoate, Hpp = 3-(4-hydroxyphenyl)propanoate; electron acceptors are indicated as appended -NO3 = nitrate or -O2 = oxygen

The reason for the notable accumulation of potential compatible solutes in *A. aromaticum* EbN1 during anaerobic degradation of benzoate, could be the high amount of intracellular benzoate (Figure 19). Benzoic acid has a well known biostatic effect (Lusk, 1911). The main mode of action is thought to be intracellular acidification, leading to enzyme inhibition, energy issues and induction of costly pH-homeostasis mechanisms (Barbour and Vincent, 1950; Krebs *et al.*, 1983). The preservative function of benzoate usually depends on low external pH values, facilitating diffusion of undissociated benzoic acid through the membrane. However, uptake systems in *A. aromaticum* EbN1 are pH-independent H^+ symporter, resulting in the high observed intracellular benzoate concentrations at neutral external pH (Collier *et al.*, 1997; Rabus, 2005; Tamang *et al.*, 2009). The high accumulation of intracellular benzoate during anaerobic growth was possibly enhanced by the higher substrate concentration in this experiment (*3.2.5 Physiological effects*). However, while the initial substrate concentration was 2.06 times higher in the anaerobic benzoate culture than in the aerobic culture, intracellular benzoate levels were 118 times higher in anaerobic benzoate degrading cells. Resistance to benzoate in *Salmonella typhimurium*, *Shigella flexneri*, and *Escherichia coli* was shown to be linked to acid stress response mechanisms, including a glutamate dependent system (Lin *et al.*, 1996, 1995). A similar system would explain the observed accumulation of glutamate in *A. aromaticum* EbN1 in response to the high intracellular levels of benzoate. Furthermore, for *E. coli* a contribution of osmolyte accumulation to pH-homeostasis was reported (Kitko *et al.*, 2010), which is in accordance with the hypothesis of compatible solutes as antidote to a benzoate-mediated pH shift. Beyond that, the general enzyme stabilizing effect of glucosylglycerol (Sawangwan *et al.*, 2010) could provide further protection against enzyme inhibition by pH shifts or by the benzoate anions themselves.

All in all, the extensive accumulation of potential osmolytes reflects the adaption of *A. aromaticum* EbN1 to competitively metabolize benzoate. Even when the metabolic capacities of degradation are exhausted, *A. aromaticum* EbN1 is able to retain the valuable substrate without suffering the common growth restricting side effects of intracellular benzoate accumulation. In the light of temporary substrate storage, accumulation of osmolytes, which can be metabolized again, appears to be a specifically useful strategy to circumvent benzoate toxicity.

In the context of the massive osmolyte accumulation, observed during anaerobic benzoate degradation, the proteomic and transcriptomic data were investigated regarding further typical stress responses.

Eight alternative sigma factors are annotated in *A. aromaticum* EbN1. They displayed various levels of transcription but no noticeable specificity for growth conditions. Only two proteins, rpoN1 and rpoD (ebA3393, ebA4365) were detectable and restricted to aerobic samples. The most thoroughly studied bacterial stress responses involve the alternative sigma factor RpoS to transcribe a, not yet fully described, large set of stress response genes. RpoS systems were studied in numerous bacteria and responded to several stress factors like osmolarity, temperature or starvation (Hengge-Aronis, 2002). However, no distinct role of sigma factor regulation in the osmolyte accumulation during anaerobic benzoate degradation in *A. aromaticum* EbN1 is apparent from the available transcriptomics and proteomic data.

Another typical response to oxidative or chemical stress is the translation of enzymes, that degrade toxic compounds, like reactive oxygen species. Catalase, ebA2102, showed average to high transcription, which was elevated in aerobic samples. The corresponding protein was detected with high mascot scores in anaerobic samples with maximum scores in anaerobic acetate and benzoate degrading cells. Superoxide dismutase, ebA5077, transcription was evenly high in all samples, with medium protein levels under all growth conditions. Five different peroxiredoxines are annotated in *A. aromaticum* EbN1. All of these showed medium to high transcription, independent of the growth conditions. The protein mascot scores ranged from below detection limit to medium high with no correlation to the osmolyte accumulation. An overview of all related transcription values and protein mascot scores is given in supplement 23. Neither catalase, nor any of the other enzymes appear to be connected to the osmolyte accumulation, as can be concluded from gene transcription and protein scores. Thus, the observed response during benzoate degradation is probably not caused by the formation of reactive oxygen species or other radical intermediates.

One more classical bacterial stress response involves the translation of chaperones and heat shock proteins. These serve to counteract diverse stress factors by stabilizing and refolding protein under denaturing influences. The products of 12 potential chaperones or heat shock proteins genes were detectable in the soluble protein fraction. None of these

correlated with the observed osmolyte accumulation. Transcription counts and protein scores of all potential chaperones are summarized in supplement 23.

In the context of the massive accumulation of osmolytes during anaerobic benzoate degradation, the lack of further stress responses was unexpected. However, the glutamate dependent acid stress response in *E. coli* was also found to be independent of the general stress response system through RpoS (Lin *et al.*, 1995). Moreover, the accumulation of intracellular benzoate in *A. aromaticum* EbN1 was caused by active transport and not passive diffusion and thus could be expected to be a controlled situation rather than a stressor triggering emergency defence mechanisms. Apparently, the accumulation of osmolytes was sufficient for metabolic stabilization under these conditions and no additional stress responses were required.

3.2.4.1 Summary of metabolic stress responses

Accumulation of several compatible solutes, especially α-glucosylglycerol, β-glutamate, glutamate and putrescine was observed during anaerobic benzoate degradation. This represented most likely a response to the high intracellular level of benzoate, which has a known bacteriostatic effect via decreasing the intracellular pH. The lack of additional stress responses indicates sufficient protective properties of the osmolytes to allow unhindered growth. Biosynthesis of putrescine, α-glucosylglycerol and β-glutamate in *A. aromaticum* EbN1 is reported for the first time and their biosynthesis pathways as well as the specific role of osmolytes demand further investigation.

3.2.5 Physiological effects

During the systems biological experiments, it became apparent that the morphology of *A. aromaticum* EbN1 changes with different growth conditions. Different sedimentation behavior and pellet stability was observed during cell harvest. Furthermore, microscopic monitoring (Kathleen Trautwein, MPI) revealed variations in cell size and shape under the different growth conditions. Microscopic images (supplement 24) showed that the cells were generally smaller during anaerobic growth than during aerobic growth. This effect was most pronounced with benzoate and acetate as substrate and only marginal with HPP as substrate. Additionally, the bacteria were found to form chains of four to six cells during

aerobic growth with benzoate and pairs of cells during aerobic growth with acetate. Over all, the cell form varied between oval to rod shaped with a length of 2 µm (3-hydroxybenzoate, anaerobic) to 5 µm (benzoate, aerobic). The differences in cell shape and size hardly reflected in the amount of dry biomass determined at the same optical density (Figure 20). Under most growth conditions, approximately 0.1 mg bio mass could be harvested from 1 ml culture broth at an optical density of 0.3 (660nm). Much lower yields were only generated during anaerobic cultivation with 3-hydroxybenzoate and HPP (0.58 and 0.62 mg/ml respectively). Bio dry mass, cell counts, growth curves and substrate uptake were determined and served to calculate growth rates, uptake rates and yields (supplement 25).

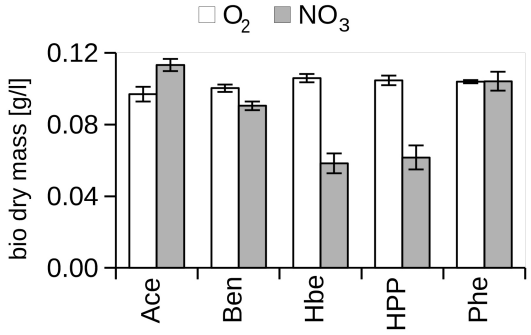

Figure 20: Concentration of dry biomass in culture broth:
Measurements were conducted by Kathleen Trautwein (MPI); Growth conditions are abbreviated as substrate and electron acceptor: Ace = acetate, Ben = benzoate, Hbe = 3-hydroxybenzoate, HPP = 3-(4-hydroxyphenyl)-propanoate, Phe = phenylalanine, NO_3 = nitrate, O_2 = oxygen

Based on previous laboratory experiences (Daniela Thieß, MPI Bremen) different initial substrate concentrations were provided for reproducible growth. In case of benzoate and phenylalanine higher substrate concentrations were supplied for anaerobic growth than for aerobic growth. This obviously influenced the exponential growth rates, but not the biomass yield (Figure 21). When the yield was normalized to the number of carbon atoms per molecule of substrates, aerobic growth generally resulted in better carbon utilization. The largest differences between aerobic and anaerobic yield per carbon atom were detected with benzoate and 3-hydroxybenzoate as substrates. This reflects the costly, ATP dependent reduction of the aromatic CoA-esters via benzoyl-CoA reductase. The same mechanism is active during anaerobic HPP and phenylalanine degradation but the effect is partially concealed by the effects of side chain metabolism from these substrates.

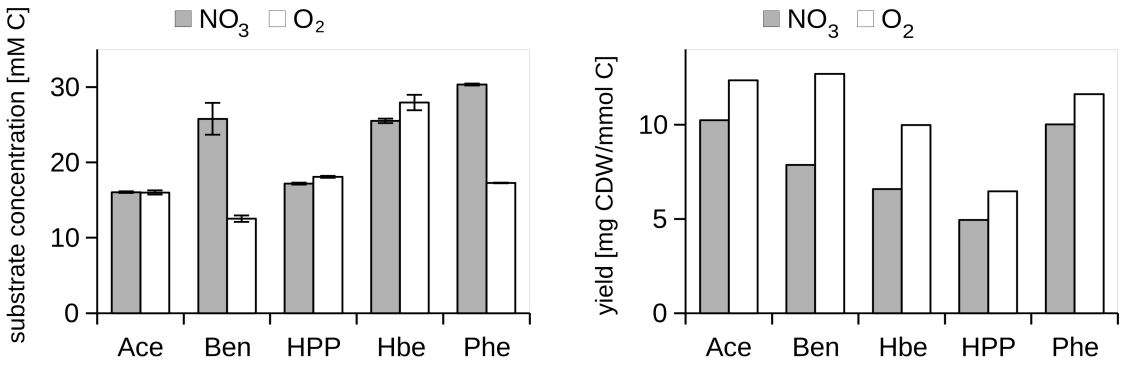

Figure 21: Initial substrate concentrations and bio mass yield
Substrate concentration is given as carbon concentration in mmol and yield in mg per mmol carbon at the time of systems biology sample generation (OD 0.3), measurements and calculations were conducted by Kathleen Trautwein (MPI); Growth conditions are abbreviated as substrate and electron acceptor: Ace = acetate, Ben = benzoate, Hbe = 3-hydroxybenzoate, HPP = 3-(4-hydroxyphenyl)propanoate, Phe = phenylalanine, NO_3 = nitrate, O_2 = oxygen

3.2.5.1 Biomass composition

In the light of the variable cell sizes and morphology, the over all biomass composition during all growth conditions was determined in the course of this work. The percentage of DNA, RNA, protein, lipid and poly-hydroxybutanoate (PHB) were measured and are presented in figure 22.

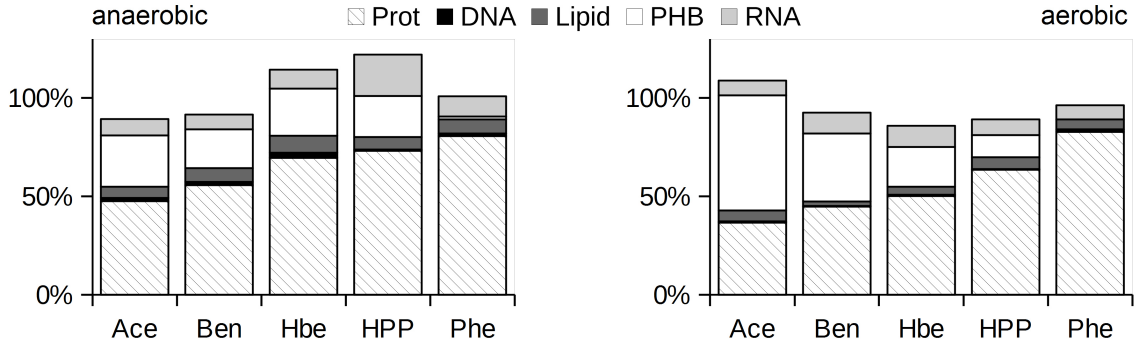

Figure 22: Substrate specific biomass composition during anaerobic and aerobic growth
Growth conditions are abbreviated as substrate: Ace = acetate, Ben = benzoate, Hbe = 3-hydroxybenzoate, Hpp = 3-(4-hydroxyphenyl)propanoate, Phe = phenylalanine; All values are relative to total dry biomass

The DNA content varied between 0.34% (benzoate, aerobic) and 2.51% (3-hydroxybenzoate, anaerobic). This value is lower than the average 3.1% described for *E. coli* (Neidhardt *et al.*, 1990). However, when the average cell weight was taken into account, values close to the described 9 fg/cell were achieved. Only aerobic HPP degrading cells and anaerobic cells degrading HPP or phenylalanine had considerably reduced DNA contents of 2.06, 3.04 and 3.08 fg/cell, respectively. These findings correlate well with the detected low growth rates under these growth conditions.

The detected lipid contends varied between 2.18% (benzoate, aerobic) and 8.75% (3-hydroxybenzoate, anaerobic), which was generally lower than the 9% described for *E.coli* (Neidhardt *et al.*, 1990). Over all, higher lipid content was measured in anaerobic cells. This reflects the changes in cell size, resulting in higher surface-to-volume ratios in the smaller anaerobic cells and thus increasing the relative amount of membrane lipid.

The RNA content of *A. aromaticum* EbN1 varied between 7.14% (phenylalanine, aerobic) and 10.60% (benzoate, aerobic) with the one exception of anaerobic HPP degradation (20.93%). Thus, the RNA content is generally only half as high as described for *E.coli* (Neidhardt *et al.*, 1990), except during anaerobic HPP degradation.

Protein content in *A. aromaticum* EbN1 cells differed from 36.57% (acetate, aerobic) to 82.83% (phenylalanine, aerobic). The lowest protein content correlated with the highest PHB content, which increases over all cell weight and thus decreases the relative amount of protein. In this context, protein content in most growth conditions is sufficiently similar to the 55% observed in *E. coli* (Neidhardt *et al.*, 1990). Most striking is the accumulation of extremely high protein levels during phenylalanine degradation, which coincides with the absence or very low levels of PHB. These extreme findings were verified by repeated protein quantification with different methods. At this point, we can only speculate, whether the observed protein accumulation represents some kind of storage or structure compound, or just reflects a complex and extensive set of protein, necessary for growth under these conditions.

3.2.5.2 Polyhydroxybutanoate

Poly-hydroxybutanoate (PHB) is a common bacterial storage polymer, which is often formed when respiratory capacity limits complete substrate oxidation. In this case, carbon can be stored as PHB, while NAD^+ or $NADP^+$ is regenerated independent of the respiratory

chain (Senior and Dawes, 1971). PHB metabolism, along with all related results from the systems biology experiments is shown in figure 23.

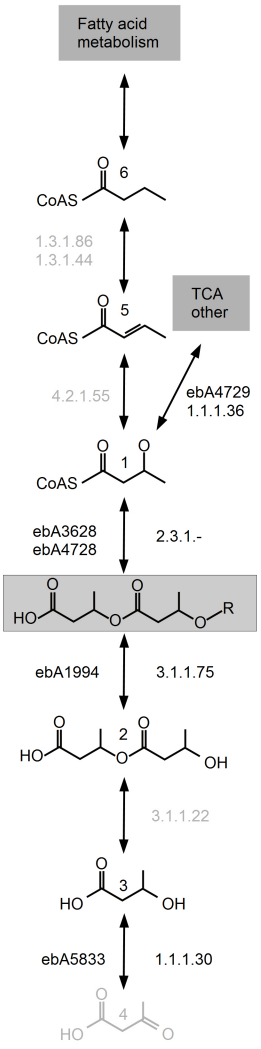

		Ace NO_3	Ace O_2	Ben NO_3	Ben O_2	Hbe NO_3	Hbe O_2	Hpp NO_3	Hpp O_2	Phe NO_3	Phe O_2
ebA4729	T	872	591	759	493	856	589	684	410	1365	1433
	P	934	710	705	856	764	958	788	786	887	1018
(1) 3-hydroxy-butanoyl-CoA		99840	231002	313354	165324	257168	46406	206375	172621	65728	11165
ebA3628	T	628	694	608	776	451	700	529	496	464	719
	P	NA	NA	NA	122	NA	NA	NA	NA	99	1214
ebA4728	T	231	211	280	177	252	204	264	155	247	225
	P	NA	NA	NA	NA	NA	NA	NA	NA	NA	463
PHB [% BDM]		26%	59%	20%	35%	24%	20%	21%	11%	2%	0%
ebA1994	T	27	28	19	26	20	25	21	23	14	25
	P	NA	NA	NA	NA	NA	NA	NA	NA	NA	NA
(2) unknown-ebn1-19		5812	2673	671	8621	1506	10986	4367	5308	4893	NA
4.2.1.55											
(3) 3-hydroxy-butanoate		11817	17036	160358	48643	10264	34977	51288	28260	7607	NA
ebA5833	T	207	186	142	147	189	146	199	156	155	114
	P	NA	NA	NA	NA	NA	NA	NA	NA	NA	NA
(4) acetoacetate		NA	NA	NA	NA	NA	NA	NA	NA	NA	NA
(5) crotonoyl-CoA		13412	21937	33520	18109	16046	7693	9258	19909	2914	801
(6) butanoyl-CoA		153131	166657	400467	205578	408200	255430	469347	655129	182646	32640

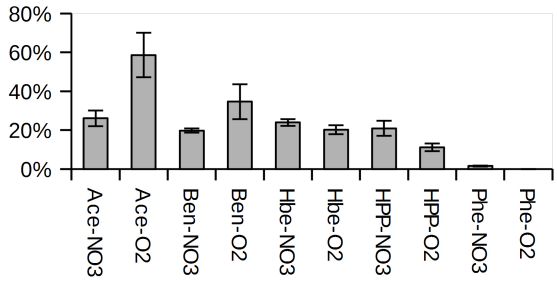

Figure 23: Poly-hydroxybutanoate (PHB) metabolism including PHB biosynthesis from 3-hydroxybutanoyl-CoA and degradation via 3-hydroxybutanoate dimer to acetoacetate.
PHB content is given as % of dry biomass and additionally visualized as bar chart; Growth conditions are abbreviated as substrate and electron acceptor: Ace = acetate, Ben = benzoate, Hbe = 3-hydroxybenzoate, HPP = 3-(4-hydroxyphenyl)propanoate, Phe = phenylalanine, NO_3 = nitrate, O_2 = oxygen; Metabolites are indicated in bold and numbered according to the pathway diagram, genes are identified by locus tag with T indicating expression values of transcription and P indicating mascot scores of proteins; All Omics data are classified in percentiles and color coded: Gray = below detection limit, light green = lowest 30%, bright green = medium 30%, green = higher 30%, dark green = top 10%, NA = not detected metabolite or protein

In *A. aromaticum* EbN1 intracellular PHB accumulated to approximately 20% of dry biomass under most analyzed growth conditions. Exceptions were aerobic acetate degradation and aerobic benzoate degradation with 58% and 34%, respectively. Lower PHB content was detected during aerobic HPP degradation (11%) and during both aerobic and anaerobic phenylalanine degradation (1.5% and 0%, respectively).

3-Hydroxybutanoyl-CoA, the precursor of PHB synthesis, was detected in all samples with medium to high signal intensities. Its maximum concentration was detected during anaerobic benzoate degradation, which is explained by 3-hydroxybutanoyl-CoA being an intermediate of the anaerobic benzoyl-CoA pathway. The lowest concentration was found during aerobic phenylalanine degradation, while signals during aerobic phenylalanine and hydroxybenzoate degradation were also reduced. Free 3-hydroxybutanoate was detectable in all samples except for aerobic phenylalanine degradation. A massive accumulation of the metabolite occurred during anaerobic benzoate degradation. This compound could originate from the degradation of PHB or its precursor, 3-hydroxybutanoyl-CoA, and might indicate activity of degrading enzymes. 3-hydroxybutanoate-dimer is a common intermediate of PHB de-polymerization. Unknown-ebn1-19 was tentatively identified as this dimer (*3.1.2 Analysis of unknown metabolites via GC-MS*). The putative dimer is absent from aerobic phenylalanine degrading samples, as is the PHB polymer. Apart from that, unknown-ebn1-19 showed no strong correlation with the intracellular PHB content (Figure 24).

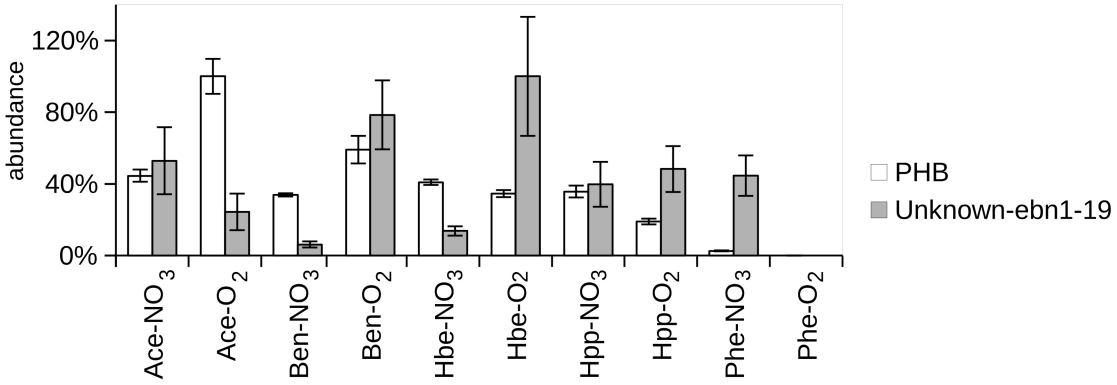

Figure 24: Relative PHB fraction and relative scaled peak area of unknown-ebn1-19
Relative peak area of unknown-19 and PHB content were scaled to the maximum values for comparability. Unknown-ebn1-19 was tentatively identified as 3-hydroxybutanoic acid dimer; Growth conditions are abbreviated as substrate and electron acceptor: Ace = acetate, Ben = benzoate, Hbe = 3-hydroxybenzoate, HPP = 3-(4-hydroxyphenyl)propanoate, Phe = phenylalanine, NO3 = nitrate, O2 = oxygen;

For PHB biosynthesis, two genes, ebA3628 and ebA4728, are annotated as poly-beta-hydroxybutanoate synthase/polymerase (2.3.1.-) in *A. aromaticum* EbN1. Both genes were translated under all growth conditions, which did not correlate with the observed content of intracellular PHB. High mascot scores were detected for ebA3628 during aerobic phenylalanine degradation, where no PHB accumulates in the cells. Only low mascot scores were detected for this enzyme during aerobic benzoate degradation and anaerobic phenylalanine degradation, while the protein was below detection limit in all other samples. Similarly, the amount of ebA4728 protein was high enough for detection during aerobic phenylalanine degradation but under no other growth condition. This finding is in accordance with the theory, that PHB-polymerase stays attached to the PHB-polymere, once polymerization is initialized (Leaf and Srienc, 1998). Acetoacetyl-CoA reductase, ebA4729, displayed high transcription under all growth conditions, which was noticeably elevated during aerobic and anaerobic phenylalanine degradation. Protein scores of ebA4729 were medium to high with a maximum during aerobic phenylalanine degradation. Gene ebA4732, annotated as a predicted polyhydroxyalkanoate synthesis repressor, showed uniformly high transcription in all samples but slightly reduced protein scores during aerobic phenylalanine, benzoate and acetate degradation.

Five genes are annotated as PHB-granule-associated proteins or phaseins (supplement 26). Three of these, ebA1323, ebA5033 and ebA2771, showed decreased protein scores during phenylalanine degradation. Protein ebA6852 also showed a reduced protein score during anaerobic phenylalanine degradation, but transcription and protein score were elevated during aerobic phenylalanine degradation. This was the only PHB related gene, showing noticeable changes in expression in response to growth conditions. The last gene, ebA6668, displays equally high transcription and protein scores throughout all samples. Phaseins have previously been correlated to the intracellular PHB content of *A. aromaticum* EbN1 (Trautwein *et al.*, 2008).

The data showed, that PHB was not produced in relevant amounts during phenylalanine degradation, the only nitrogen-containing substrate in the systems biology experiments. A known factor regulating PHB accumulation in *Alcaligenes latus* and other bacteria is the availability of nitrogen (Anderson and Dawes, 1990; Wang and Lee, 1997), with nitrogen limiting conditions promoting PHB production. Since all samples were taken during the

exponential growth phase, when plenty of substrate and all necessary medium compounds were available, a depletion of ammonium from the medium is unlikely.

The highest accumulation of PHB during aerobic acetate degradation correlated with the lowest detected ATP content. Overall, PHB accumulation and ATP content showed a negative correlation (-0.74). Moreover, PHB content and signal intensity of free coenzyme A showed a weak negative correlation (-0.45) but no correlation between measured acetyl-CoA abundances and PHB content was apparent (0.12). In most bacteria, PHB biosynthesis is positively correlated to acetyl-CoA concentration and negatively correlated to coenzyme A concentration, thus reacting to the activity of the citric acid cycle (Anderson and Dawes, 1990). However, acetyl-CoA was the most abundant signal in these HPLC-MS analyses, which could impair the quantitative validity of the data. All in all, the negative correlations to ATP content and free coenzyme A level, suggest a similar dependence of PHB production on the activity of the TCA and over all energetic condition of the cells. Thus, PHB production in *A. aromaticum* EbN1 responded to well known metabolic parameters, which are characterized in several organisms (for a review see (Anderson and Dawes, 1990; Senior and Dawes, 1971))

3.2.5.3 Summary of the physiological effects

The systems biology experiments showed a great influence of the growth conditions on cell size and biomass composition. Especially the content of protein and PHB varied massively and needs to be considered when interpreting systems biological data. While DNA, RNA and lipid content was generally lower than described for the model organism *E. coli*, protein content varied and was often much higher than in *E. coli*. PHB production in *A. aromaticum* EbN1 responded to the typical parameters citric acid cycle activity and nitrogen availability, as is common for this storage compound.

3.3 Degradation pathways

3.3.1 Aerobic benzoate degradation

Aerobic aromatic degradation is a process relevant in numerous environments. These structurally diverse compounds originate from macromolecules like lignine and other plant derived substances. Benzoate is the prototype of aromatic substrates and its aerobic degradation pathway via catechol has been studied since the 1970s (Reiner, 1971). The aerobic benzoate degradation pathway via benzoyl-CoA only emerged in the last 15 years (Mohamed *et al.*, 2001). This pathway was found to be preferred by facultative anaerobes and bacteria in micro-aerobic habitats, see (Ismail and Gescher, 2012) for a review.

Hitherto, no effort was made to observe the full pathway by integrating metabolites, proteins and transcripts simultaneously over different growth conditions, as in this study. The proposed pathway and the compiled systems biological results are illustrated in figure 25 and are discussed sequentially in the following section. In this study, not only benzoate was degraded aerobically via this pathway, but 3-(4-hydroxyphenyl)propanoate (HPP) was channeled into the benzoyl-CoA pathway, too. Additionally, benzoate and benzoyl-CoA were main or side products of anaerobic benzoate, HPP and phenylalanine degradation.

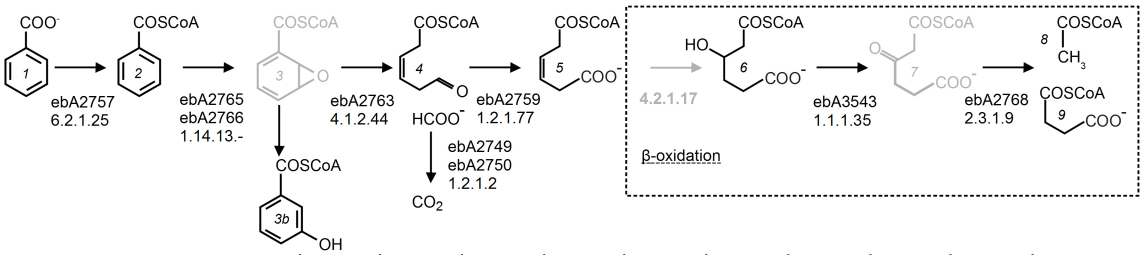

		Ace NO_3	Ace O_2	Ben NO_3	Ben O_2	Hbe NO_3	Hbe O_2	HPP NO_3	HPP O_2	Phe NO_3	Phe O_2
(1) benzoate		NA	94	45210	381	NA	212	NA	1561	NA	NA
ebA2757	T	63	20	425	255	606	46	623	57	724	85
	P	NA	289	NA	1568	NA	521	NA	1247	NA	979
(2) benzoyl-CoA		167146	3896	4105301	1469012	31071	105397	2013293	1042478	2842400	73503
ebA2765	T	552	160	9248	5343	10688	302	12067	614	15719	596
	P	NA	449	529	1865	330	753	367	1612	NA	1098
ebA2766	T	60	34	576	330	960	61	1288	66	1279	88
	P	NA	NA	NA	687	NA	146	NA	571	NA	202
(3) 2,3-epoxybenzoyl-CoA		NA	NA	NA	NA	NA	NA	NA	NA	NA	NA
(3b) 3-hydroxybenzoyl-CoA		NA	NA	8629	44008	2046058	155906	2637	14917	11254	9278
ebA2763	T	424	55	8230	1635	8739	136	7825	246	14203	271
	P	NA	464	474	1823	351	596	452	1475	223	934
ebA2749	T	10	11	11	81	12	23	18	48	20	27
	P	NA	NA	NA	548	NA	NA	NA	230	NA	NA
ebA2750	T	15	16	16	93	19	28	45	54	24	39
	P	71	NA	NA	737	NA	NA	NA	377	NA	190
(4) * 3,4-didehydroadipyl-CoA semialdehyde		2557.05	NA	1357.21	32056.4	567.33	3655.12	2663.75	29234.83	1176.97	NA
ebA2759	T	141	20	1347	170	1216	41	1232	80	1974	67
	P	NA	NA	404	1218	289	465	369	947	423	827
(5) * 3,4-didehydroadipyl-CoA		758.86	NA	44638.15	201615.29	734.23	NA	22788.45	123173.44	13357.82	15250
4.2.1.17	T + P										
(6) 3-hydroxyadipyl-CoA		2525	2774	18805	185994	904	3981	2474	67322	27563	48800
ebA3543	T	11	9	39	43	17	24	34	18	614	556
	P	NA	185	NA	295	NA	329	NA	NA	608	1385
(7) 3-oxoadipyl-CoA		NA	NA	NA	NA	168597	NA	NA	3612	NA	NA
ebA2768	T	42	54	150	234	268	82	871	99	346	98
	P	316	493	456	1276	227	653	289	1055	553	829
(8) acetyl-CoA		1328592	758914	846490	977224	1139162	1320983	589337	760534	886646	663864
(9) succinyl-CoA		322845	400537	329498	263021	369126	235378	173528	195625	222840	302463
ebA2762	T	547	52	10655	563	9686	69	8500	354	11138	114
	P	NA	NA	NA	93	NA	NA	NA	NA	NA	NA

Figure 25: Aerobic benzoate degradation via the benzoyl-CoA pathway: The pathway is subdivided into an upper and a lower pathway

Growth conditions are abbreviated as substrate and electron acceptor: Ace = acetate, Ben = benzoate, Hbe = 3-hydroxybenzoate, HPP = 3-(4-hydroxyphenyl)propanoate, Phe = phenylalanine, NO_3 = nitrate, O_2 = oxygen; Metabolites are indicated in bold and numbered according to the pathway diagram, genes are identified by locus tag with T indicating expression values of transcription and P indicating mascot scores of proteins; All Omics data are classified in percentiles and color coded: Gray = below detection limit, light green = lowest 30%, bright green = medium 30%, green = higher 30%, dark green = top 10%, NA = not detected metabolite or protein

In *A. aromaticum* EbN1, genes for aerobic benzoate degradation via benzoyl-CoA are organized in one cluster on the genome and show 83% to 92% protein sequence identity to the benzoate oxidation gene cluster (*box*) of *Azoarcus evansii*. Transcription of this gene cluster was found in all samples but generally increased under anoxic conditions. Only in cells grown with acetate, gene expression was reduced in anaerobically grown samples relative to the aerobically grown samples, resulting in the over all lowest gene expression values. Highest gene expression was detected in samples grown anaerobically with phenylalanine and HPP. In contrast to the gene expression, protein levels were reduced under anoxic conditions and several gene products could only be detected in cells grown aerobically. The highest protein mascot scores were measured in cells grown aerobically with benzoate and HPP. Relatively high transcription values were observed under all growth conditions. Mean relative peak areas of benzoyl-CoA, mean transcription values and mean protein mascot scores of the *box* genes are presented in figure 26A to illustrate the differences in transcription and protein levels

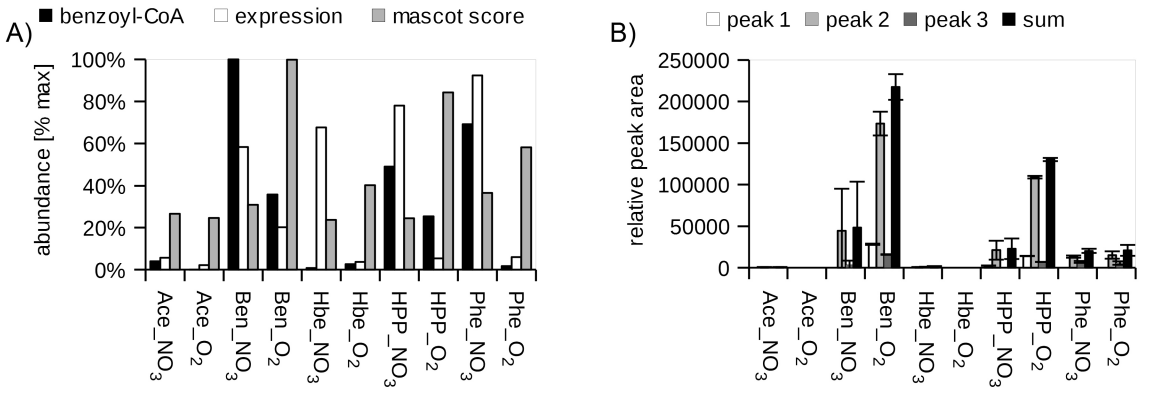

Figure 26: Selected metabolites, transcripts and proteins from the aerobic benzoyl-CoA degradation pathway

A) Substrate dependent transcription rate and protein abundance of the box gene cluster: black = relative peak area of benzoyl-CoA, white = relative mean expression rate of all box genes, gray = relative mean mascot score of all box gene products; B) HPLC-MS signals of putative 3,4-didehydroadipyl-CoA and isomers; Growth conditions are abbreviated as substrate and electron acceptor: Ace = acetate, Ben = benzoate, Hbe = 3-hydroxybenzoate, HPP = 3-(4-hydroxyphenyl)propanoate, Phe = phenylalanine, NO_3 = nitrate, O_2 = oxygen

Sequential metabolic pathway

(1) benzoate

Benzoate is a preferred carbon source for *A. aromaticum* EbN1. This predilection is revealed by the presence of two different benzoate uptake systems, allowing for optimum substrate uptake at different concentrations (Rabus *et al.*, 2005; Trautwein *et al.*, 2012a). In this systems biology experiments, both the H^+ symporter ebA5311 and the ABC-transportystem encoded in genes ebA5303-5309 showed high gene expression during aerobic benzoate degradation. Both transport systems were upregulated in the presence of aromatic substrates but not specifically during benzoate degradation. Three ABC-transporter subunits were detected within the cytosolic protein fraction but can not be expected to represent the actual protein pool, which is membrane localized. From these results, it can be concluded that benzoate was taken up actively and effectively but none of the transport systems could be assigned to be specific for this growth condition. Gene expression and protein scores of all benzoate transporter are given in supplement 27.

Intracellular benzoate was detected in samples aerobically degrading benzoate in medium high concentrations. The substance also accumulates during anaerobic benzoate degradation and during aerobic HPP and 3-hydroxybenzoate degradation.

(2) benzoyl-CoA

The first step of the aerobic benzoyl-CoA pathway is the activation of benzoate to benzoyl-CoA via benzoate:CoA ligase. Two genes are annotated as benzoate:CoA ligase in *A. aromaticum* EbN1. While ebA2757 is located in close proximity to the aerobic benzoate degradation genes, ebA5301 is located close to the anaerobic gene cluster and was thus assumed to participate in the respective pathway (Rabus *et al.*, 2005). Even though it is not located in the same operon, ebA2757 showed co-regulation with the *box* genes of aerobic benzoate degradation. Transcription was upregulated during anaerobic degradation of all aromatic substrates, but the protein was only detectable in aerobic samples with higher mascot scores during benzoyl-CoA degradation. Thus, the benzoate:CoA ligase ebA2757 appears to be specific for aerobic growth.

Low signals for benzoyl-CoA were detected in all samples but a substantial amount accumulated in response to benzoyl-CoA ligase activity on benzoate, both during aerobic and anaerobic growth.

(3) 2,3-epoxybenzoyl-CoA

In *A. evansii*, BoxA and BoxB were described to act together as benzoyl-CoA 2,3-epoxidase to perform the dearomatization of benzoyl-CoA using NADPH and O_2 as co-substrates. This is the energetically most demanding step in the pathway and was explored in more detail in *A. evansii* (Mohamed *et al.*, 2001; Zaar *et al.*, 2004). Transcriptomic and proteomic data confirmed a similar role of the enzyme in *A. aromaticum* EbN1.

Genes ebA2765 (*boxB*) and ebA2766 (*boxA*) are part of the *box* gene cluster and showed the typical regulation pattern. The genes are annotated as benzoyl-CoA 2,3-dioxygenase, showing protein sequence identities of 92% and 83.45% to BoxA and BoxB from *A. evansii,* respectively. The protein ebA2766 was only detectable in aerobic cells, while the ebA2765 protein was also detectable in most anaerobic cells, albeit with much lower mascot scores. Both gene products reached maximal protein levels in aerobically grown, benzoyl-CoA degrading cells (benzoate and HPP) but also accumulate in aerobic phenylalanine and 3-hydroxybenzoate degrading cells.

The expected reaction product 2,3-epoxybenzoyl-CoA was not detected in the systems biology experiments, however, elevated levels of 3-hydroxybenzoyl-CoA (3b) arose in all benzoyl-CoA degrading cells. Only very low cellular concentrations of the 2,3-epoxybenzoyl-CoA are likely to be present in the cells due to low stability and high reactivity of this intermediate. Additionally a strong product inhibition of the epoxidase was described in *A. evansii* (Rather *et al.*, 2011). Similar restrictions on the concentration of the epoxide intermediate in *A. aromaticum* EbN1 would explain why the metabolite could not be detected. At the same time, the elevated levels of 3-hydroxybenzoyl-CoA could be a by-product of epoxide decay in the cell and/or during sample preparation.

(4) 3,4-didehydroadipyl-CoA semialdehyde

The hydrolytic cleavage of 2,3-epoxybenzoyl-CoA to 3,4-didehydroadipyl-CoA semialdehyde is facilitated by benzoyl-CoA-dihydrodiol lyase and additionally yields formate (Gescher *et al.*, 2005). The sequence of ebA2763 shows 91% protein identity to benzoyl-CoA-dihydrodiol lyase BoxC from *A. evansii* and was co-regulated with the *box* regulon. Transcription was upregulated in the presence of all aromatic substrates during denitrification, while protein levels showed high signals during aerobic benzoyl-CoA degradation.

Genes ebA2749 (*fabA*) and ebA2750 (*fabB*) are annotated as formate dehydrogenase and showed distinct upregulation of gene transcripts and protein concentration during aerobic degradation of benzoyl-CoA. These genes are not part of the *box* regulon and upregulation was strictly limited to aerobic benzoyl-CoA degradation. Increased expression of formate dehydrogenase is in accordance with the formate producing reaction proposed for BoxC. Since the formate dehydrogenase genes are located close to the *box* genes, their involvement in further oxidation of the byproduct was predicted before but not confirmed experimentally (Rabus *et al.*, 2005)

For the exact mass of the reaction product, 3,4-didehydroadipyl-CoA semialdehyde, three different signals were detected. These signals could constitute different isomers of the newly linearized molecule and were summed for analysis. Highest signals were detected during aerobic degradation of benzoate and HPP, further supporting the identity as benzoyl-CoA degradation intermediate.

(5) 3,4-didehydroadipyl-CoA

The following oxidation of 3,4-didehydroadipyl-CoA semialdehyde to the aldehyde is facilitated by a specific aldehyde dehydrogenase. Gene ebA2759 shows 86% protein sequence identity to 3,4-dehydroadipyl-CoA semialdehyde dehydrogenase BoxD from *A. evansii* and was co-regulated with the *box* gene regulon in *A. aromaticum* EbN1. High levels of protein ebA2759 were detected during aerobic benzoyl-CoA degradation, while no protein was detectable during aerobic or anaerobic acetate degradation.

Three different signals were detected that correspond to the exact mass of 3,4-didehydroadipyl-CoA and isomers. All signals were strongest in samples grown aerobically with benzoate, followed by those grown aerobically with HPP and small signal intensities detectable in phenylalanine degrading cells. In this analysis, the peak areas were summed, since it was not possible to distinguish the isomers (Figure 26B). Overall, 3,4-didehydroadipyl-CoA was specifically elevated in cells aerobically degrading benzoyl-CoA, namely during aerobic growth with benzoate and HPP. Only a low signal was present in samples grown anaerobically with HPP.

Several studies proposed *cis*-3,4-didehydroadipyl-CoA as the product of ring-cleavage, before undergoing isomerization to *trans*-2,3-didehydroadipyl-CoA, followed by oxidation to 3-hydroxyadipyl-CoA (Gescher *et al.*, 2006; Zaar *et al.*, 2004, 2001). The systems

biology data could neither confirm nor disprove this hypothesis, because the isomers could not be distinguished by HPLC-MS analysis without synthetic standards. No specific enzyme is suggested for the isomerization in *A. evansii* or *A. aromaticum* EbN1. However, detection of multiple signals with the same mass points towards the presence of isomers. Aerobic phenylalanine degradation directly yields 2,3-dehydroadipyl-CoA from thiolytic cleavage of 3-oxo-5,6-dehydrosuberyl-CoA (Teufel *et al.*, 2010). This would normally result in only one isomeric signal in the samples. On the other hand, possible reversibility of producing and consuming reactions could lead to a mix of isomers as indicated by the multiple signals present during aerobic phenylalanine degradation. Thus, these samples could not serve to distinguish the isomeric signals from aerobic benzoate degradation.

(6) 3-hydroxyadipyl-CoA

Hydratation to 3-hydroxyadipyl-CoA is identical in aerobic phenylalanine and benzoate degradation, but no specific enoyl-CoA hydratase is annotated for either pathway in *A. aromaticum* EbN1. The reaction is the first in a series of typical β-oxidation reactions and marks the descent from upper to lower benzoyl-CoA pathway. Several enzymes that could convey this reaction are constitutively active in *A. aromaticum* EbN1 as described in *3.2.3 β-oxidation*. Possibly, several redundant enzymes catalyze the reaction either under all or only under specific growth conditions.

3-hydroxyadipyl-CoA was detected in all samples but showed the highest signal upon aerobic benzoate degradation with substantial signals during aerobic HPP degradation and aerobic phenylalanine degradation, followed by anaerobic phenylalanine degradation.

(7) 3-oxoadipyl-CoA

Reduction of 3-hydroxyadipyl-CoA to 3-oxoadipyl-CoA is again a typical β-oxidation reaction. No specific 3-hydroxyadipyl-CoA dehydrogenase is annotated in the pathway or could be identified from co-regulation with the *box* regulon in this study. Alternatively, the gene product of ebA3543, a 3-hydroxyacyl-CoA dehydrogenase from the *paa* gene cluster for aerobic phenylacetate degradation, could catalyze this reaction. Transcription and protein levels were elevated during aerobic benzoate and phenylalanine degradation as well as during 3-hydroxybenzoate degradation. In contrast to that, transcription and protein levels were not elevated during aerobic HPP degradation, though the same pathway is supposed to be active.

The expected product 3-oxoadipyl-CoA or an isomer thereof could only be detected in anaerobic, 3-hydroxybenzoate degrading samples and, to a lower extend, during aerobic HPP degradation. No signal was detected in samples aerobically degrading benzoate or phenylalanine and no metabolically relevant isomer for the substance is known. For other β-ketoacyl-CoAs low stability was observed during extraction and measurement (eg acetoacetyl-CoA, see *3.1.1 Analysis of CoA-esters*). This might explain the lack of 3-oxoadipyl-CoA detection during aerobic benzoyl-CoA degradation. The signal detected in samples degrading 3-hydroxybenzoate anaerobically was probably a natural isomer, specific for that degradation pathway.

The final thiolytic cleavage of 3-oxoadipyl-CoA to acetyl-CoA and succinyl-CoA could be catalyzed by acetyl-CoA C-acetyltransferase ebA2768. The gene is part of the *box* gene cluster in *A. aromaticum* EbN1 and showed co-regulation with the other *box* genes, while a high amount of protein was detectable during aerobic benzoyl-CoA and phenylalanine degradation. A role for ebA2768 in this reaction was proposed based on genomic evidence (Rabus *et al.*, 2005). Detection of specific transcription and cytosolic protein accumulation in this work confirm the proposed role of the enzyme in completing aerobic benzoyl-CoA degradation.

The products acetyl-CoA and succinyl-CoA were detectable in all samples in similar quantities. Both are part of the citric acid cycle and constitute the transition from the specific benzoyl-CoA pathway to central metabolism.

Transcription of the *box* regulon was elevated during anaerobic growth with aromatic substrates, while protein levels were reduced during anaerobic growth with a maximum during aerobic benzoate and HPP degradation. The observed transcription and protein regulation implicates mechanisms for substrate response and adaption to the mode of respiration on transcriptomic level and beyond. Regulator ebA2762 (BoxR) shows very high similarity (91%, (Rabus *et al.*, 2005)) to the substrate dependent regulatory repressor of the aerobic benzoate degradation genes, described in *Azoarcus* sp. CIB. The mechanism of regulation in *Azoarcus* sp. CIB was found to incorporate oxygen signaling in a still unknown way (Valderrama *et al.*, 2012). Similar regulatory mechanisms are possibly integrated in *A. aromaticum* EbN1 adaption to aerobic benzoate degradation.

Transcriptional repression would be lifted in the presence of a higher benzoyl-CoA concentration. Co-expression of the ebA2762 (*boxR*) with the *box* genes could impose a feedback regulation on the transcription, which would explain the reduced transcription observed during aerobic aromatic degradation compared to the anaerobic aromatic degradation. Regulation of the benzoyl-CoA degradation pathway genes in *A. aromaticum* EbN1 appears to extend far beyond transcriptional regulation and to include response to the availability of oxygen. This was demonstrated by the striking differences in transcription and protein scores found under the different growth conditions (Figure 26A). This elaborate regulation and the high amounts of transcript, present under all growth conditions, reflect the importance of the benzoyl-CoA degradation pathway for survival in swiftly changing sediment environments. Apparently, preparedness for aerobic aromatic degradation via the benzoyl-CoA pathway is beneficial, even under anoxic conditions or in the absence of a suitable substrate.

3.3.1.1 Summary of aerobic benzoate degradation

Genes for the upper aerobic benzoyl-CoA degradation pathway were co-expressed and appear to be subjected to complex regulation in response to aromatic substrates and modes of respiration. Combined metabolomic, transcriptomic and proteomic results constituted an upper aerobic benzoyl-CoA pathway as described for *T. aromatica*. The lower part of the pathway was not achieved by specifically regulated enzymes but possibly by generic and constitutively expressed β-oxidation enzymes. Out of the 10 expected intermediates of the aerobic benzoyl-CoA pathway, 7 were detected specifically during aerobic benzoate degradation.

3.3.2 Anaerobic benzoate degradation

Numerous habitats like sediments, stagnant waters or landfills provide anoxic zones, where no molecular oxygen is available to facilitate oxidation and dearomatization of the aromatic ring. Activation to CoA-esters allows for a reductive dearomatization of the aromatic ring, without the use of molecular oxygen. Anaerobic benzoyl-CoA degradation represents the prototype of CoA-mediated reductive dearomatization and serves as the

central degradation pathway, into which other aromatic degradation pathways are channeled.

A. aromaticum EbN1 degrades benzoate anaerobically via the benzoyl-CoA pathway. Additionally, during anaerobic growth, HPP and phenylalanine are channeled into this degradation pathway via benzoyl-CoA (Figure 27). Genes for anaerobic benzoate degradation in *A. aromaticum* EbN1 are organized in a large gene cluster (ebA5282-ebA5311) that displays high similarity to the (benzoate degradation) *bzd* operon of *A. evansii*. Transcriptomic analysis showed the mRNA to be split into four different units and two single genes. However, the analysis also showed that all of the mRNA molecules were co-regulated strongly, forming a regulatory unit. The gene cluster was highly transcribed throughout all growth conditions. Only moderate downregulation of transcription could be observed in acetate degrading cells and in aerobic samples. Protein levels closely followed the transcription pattern, without strong indication of additional regulation on the translational level.

Sequential metabolic pathway

(1) benzoate

Benzoate uptake is facilitated by active transport systems in *A. aromaticum* EbN1 and highest intracellular levels were observed during anaerobic growth with benzoate. This accumulation correlated with the accumulation of the following intermediate and reflects the restriction of the pathway by the rate limiting step of reductive dearomatization.

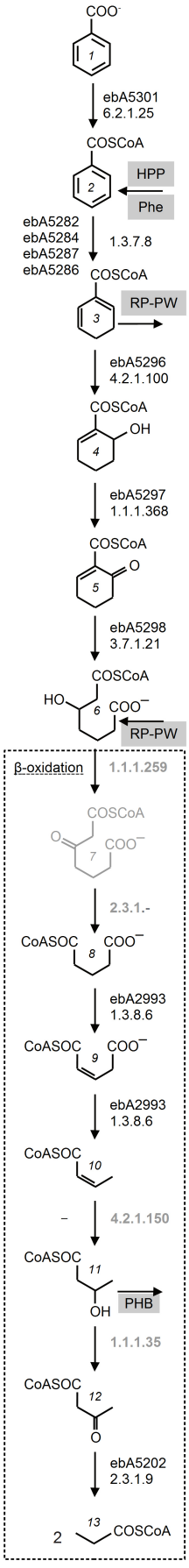

		Ace NO_3	Ace O_2	Ben NO_3	Ben O_2	Hbe NO_3	Hbe O_2	HPP NO_3	HPP O_2	Phe NO_3	Phe O_2
(1) benzoate		NA	94	45210	381	NA	212	NA	1561	NA	NA
ebA5301	T	39	17	620	219	272	128	682	266	398	77
	P	NA	NA	1226	205	983	329	1077	901	782	531
(2) benzoyl-CoA		167146	3896	4105301	1469012	31071	105397	2013293	1042478	2842400	73503
ebA5282	T	495	1062	8885	3209	3444	1831	9244	1810	14062	1047
	P	322	145	1701	659	1498	945	1703	1251	1557	306
ebA5284	T	373	911	9694	2678	3978	1474	10128	1480	13809	849
	P	80	NA	1426	625	984	512	1355	1199	1064	190
ebA742/ ebA5287	T	270	407	5062	1891	5731	907	6374	1540	4920	498
	P	795	767	1794	1144	1761	1161	1682	1319	1445	832
ebA744/ ebA5286	T	179	318	3765	1429	3866	662	4574	1030	4076	354
	P	545	642	1417	631	1557	831	1430	1073	1401	659
(3) cyclohexa-1,5-dienecarbonyl-CoA		NA	NA	59266	NA	NA	NA	9277	NA	3872	NA
ebA5296	T	76	68	1563	487	547	345	1611	521	725	180
	P	283	182	641	364	634	501	658	569	579	364
(4) 6-hydroxycyclohex-1-enecarbonyl-CoA		NA	NA	82462	NA	NA	NA	22394	NA	4546	NA
ebA5297	T	237	167	3972	1622	1631	829	4733	1293	1742	449
	P	138	121	782	360	718	348	777	504	619	279
(5) 6-ketoxycyclo hex-1-ene-1-carboxyl-CoA		NA	NA	68690	NA	NA	NA	35150	NA	12703	NA
ebA5298	T	261	164	3834	2399	1794	863	5569	2169	1887	444
	P	499	287	1071	749	936	745	941	843	799	549
(6) 3-hydroxypimelyl-CoA		NA	NA	417533	NA	77864	NA	131739	NA	22461	NA
1.1.1.259		NA	NA	NA	NA	NA	NA	NA	NA	NA	NA
(7) 3-ketopimelyl-CoA		NA	NA	NA	NA	NA	NA	NA	1190	NA	76491
2.3.1.-		NA	NA	NA	NA	NA	NA	NA	NA	NA	NA
(8) glutaryl-CoA		NA	NA	58243	NA	55611	NA	23728	NA	13753	NA
(9) glutaconyl-CoA		2187	NA	3567	945	5152	NA	2596	389	1872	1254
ebA2993	T	NA	220	1003	472	789	276	894	529	418	296
	P	44	80	223	186	205	70	1971	168	362	68
(10) crotonoyl-CoA		13412	21937	33520	18109	16046	7693	9258	19909	2914	801
4.2.1.150		NA	NA	NA	NA	NA	NA	NA	NA	NA	NA
(11) 3-hydroxy-butanoyl-CoA		99840	231002	313354	165324	257168	46406	206375	172621	65728	11165
3-hydroxybutanoate		11817	17036	160358	48643	10264	34977	51288	28260	7607	NA
1.1.1.157		NA	NA	NA	NA	NA	NA	NA	NA	NA	NA
(12) acetoacetyl-CoA		3076	7682	3776	4256	3621	2723	3023	1947	2174	1336
ebA5202	T	1530	1531	1292	1591	1377	1414	1431	1520	1165	1569
	P	1419	1489	1148	1528	1140	1300	1210	1449	718	1028
(13) acetyl-CoA		1328592	758914	846490	977224	1139162	1320983	589337	760534	886646	663864

Figure 27: Anaerobic benzoyl-CoA degradation pathway
Growth conditions are abbreviated as substrate and electron acceptor: Ace = acetate, Ben = benzoate, Hbe = 3-hydroxybenzoate, Hpp = 3-(4-hydroxyphenyl)propanoate, Phe = phenylalanine, NO3 = nitrate, O2 = oxygen; Metabolites are indicated in bold and numbered according to the pathway diagram, genes are identified by locus tag with T indicating expression values of transcription and P indicating mascot scores of proteins; All Omics data are classified in percentiles and color coded: Gray = below detection limit, light green = lowest 30%, bright green = medium 30%, green = higher 30%, dark green = top 10%, NA = not detected metabolite or protein

(2) benzoyl-CoA

Activation of benzoate to benzoyl-CoA can be catalyzed by two different predicted CoA-ligases. In the systems biology experiments, CoA-ligase ebA5301 (*bclA*) was expressed under all experimental conditions but showed the strongest upregulation with HPP and benzoate as substrates during anaerobic growth, while exhibiting very low expression with acetate as substrate. The ebA5301 protein was detected in all but the acetate samples with highest protein scores during anaerobic HPP and benzoate degradation. The second annotated benzoate-CoA ligase, ebA2757, was only detectable as protein in aerobic samples where highest scores were detected in samples accumulating benzoyl-CoA. These findings confirm the originally postulated role of ebA5301 (BclA) during anaerobic benzoate degradation (Rabus *et al.*, 2005; Wöhlbrand *et al.*, 2007), albeit the enzymes was not strictly limited to anaerobic benzoate degradation.

The activated benzoyl-CoA was detectable in very high quantity during aerobic and anaerobic benzoate and HPP degradation as well as during anaerobic phenylalanine degradation.

(3) cyclohexa-1,5-dienecarbonyl-CoA

Reduction of benzoyl-CoA to cyclohexa-1,5-dienecarbonyl-CoA is catalyzed by benzoyl-CoA reductase encoded by ebA5282, ebA5284, ebA5287 and ebA5286 (*bcrCBAD*). This type of benzoyl-CoA reductase is typical for facultative anaerobic bacteria that employ denitrification. The ATP dependent reaction proceeds via a radical intermediate, which is described in detail in a comprehensive review (Boll, 2004).

Transcripts and proteins corresponding to all four subunits were detected in all samples but accumulated during anaerobic benzoate, HPP and phenylalanine degradation. Subunits ebA5287 (BcrA) and ebA5286 (BcrD) display 100% protein sequence identity with the subunits from a different benzoyl-CoA reductase complex, specific for 3-hydroxybenzoyl-

CoA degradation (ebA5287 and ebA5286). Thus, transcript and protein measurements of these subunits cannot be assigned definitely to one or the other gene locus.

The expected reduction product cyclohexa-1,5-dienecarbonyl-CoA was detected specifically in anaerobic benzoyl-CoA degrading cells.

(4) 6-hydroxycyclohex-1-enecarbonyl-CoA

Hydratation of cyclohexa-1,5-dienecarbonyl-CoA to 6-hydroxycyclohex-1-enecarbonyl-CoA is facilitated by the cyclohexa-1,5-dienecarbonyl-CoA hydratase (ebA5296), which showed the typical expression and protein profiles from the *bzd* gene cluster. Transcription was upregulated in response to aromatic substrates and especially elevated in the presence of benzoyl-CoA, the protein concentration closely followed the gene expression profile.

6-hydroxycyclohex-1-enecarbonyl-CoA, or an isomer, was detected specifically during anaerobic benzoyl-CoA degradation.

(5) 6-ketoxycyclohex-1-ene-1-carboxyl-CoA

Dehydrogenation of 6-hydroxycyclohex-1-enecarbonyl-CoA to 6-ketoxycyclohex-1-ene-1-carboxyl-CoA is performed by 6-hydroxycyclohex-1-ene-1-carbonyl-CoA dehydrogenase (ebA5297). Transcription of the gene was high throughout all samples and additionally increased in cells degrading benzoyl-CoA anaerobically. The protein was detectable in all samples with elevated scores in the presence of aromatic substrates and under anoxic conditions.

The reaction product 6-ketoxycyclohex-1-ene-1-carboxyl-CoA was detected specifically during anaerobic benzoate degradation.

(6) 3-hydroxypimeloyl-CoA

The following ring cleavage of 6-ketoxycyclohex-1-ene-1-carboxyl-CoA to 3-hydroxypimeloyl-CoA is facilitated by the 6-oxo-cyclohex-1-ene-carbonyl-CoA hydrolase (ebA5298). This gene is co-localized with the gene cluster for anaerobic benzoyl-CoA degradation and showed the typical substrate dependent expression profile with protein accumulation during anaerobic degradation of aromatic substrates.

Product of the hydrolytic ring opening is 3-hydroxypimeloyl-CoA, which was detected in all anaerobic benzoyl-CoA degrading samples, as well as during anaerobic 3-

hydroxybenzoate degradation. 3-hydroxypimeloyl-CoA marks the beginning of the lower benzoyl-CoA pathway, which resembles a modified β-oxidation process of alternating dehydrogenation, hydration, dehydrogenation and thiolysis reactions. In contrast to the upper benzoyl-CoA pathway these genes are not organized in an operon in *A. aromaticum* EbN1.

(7) 3-ketopimelyl-CoA

No gene is annotated as 3-hydroxypimeloyl-CoA dehydrogenase (1.1.1.259) and the expected product, 3-ketopimeloyl-CoA, could not be detected. Resources for gene annotation based on sequence analysis are very limited, since many of the enzymes from anaerobic benzoyl-CoA degradation were only characterized for one or two organisms or by using partial EC-numbers. Where no specific gene is annotated, the pathway may also employ several constitutive or unspecific enzymes (*3.2.3 β-oxidation*). Additionally, the 3-keto-CoA intermediates, typical for β-oxidation, tend to be unstable during sample preparation, as described in section *3.1.1 Analysis of CoA-esters*.

(8) glutaryl-CoA and (9) glutaconyl-CoA

No gene is annotated as specific acetyl-CoA C-acyltransferase to perform the following thiolytical removal of acetyl-CoA from 3-ketopimelyl-CoA. The product, glutaryl-CoA, was elevated in cells anaerobically degrading benzoyl-CoA as well as 3-hydroxybenzoate. Reduction to glutaconyl-CoA and subsequent decarboxylation to crotonyl-CoA are expected to be catalysed by the same enzyme (ebA2993, GcdH) (Härtel *et al.*, 1993). While transcript and protein were present in abundance, the intermediate glutaconyl-CoA could only be detected in moderate amounts. Most likely, the intermediate does not leave the enzyme in between the two reactions.

(10) crotonyl-CoA

Crotonyl-CoA was only slightly elevated during anaerobic benzoate degradation but detectable in all samples. This metabolite is also involved in several amino acid degradation pathways and fatty acid degradation. Thus, the intracellular concentrations depend on numerous factor besides anaerobic benzoyl-CoA degradation.

(11) 3-hydroxybutanoyl-CoA

Oxidation of crotonyl-CoA to 3-hydroxybutanoyl-CoA typically occurs via a specific enoyl-CoA hydratase (EC 4.2.1.150), but no such enzyme is annotated in the *A. aromaticum* EbN1 genome.

However, the product 3-hydroxybutanoyl-CoA was detected in all samples and showed a maximum during anaerobic benzoate degradation. The metabolite is an important metabolic branching point, connecting the anaerobic benzoyl-CoA degradation to the poly-hydroxybutanoate (PHB) metabolism, where it plays a key role in the biosynthesis of the polymer (*3.2.5.2 Polyhydroxybutanoate*).

(12) acetoacetyl-CoA

The following reaction is a dehydrogenation of 3-hydroxybutanoyl-CoA to acetoacetyl-CoA, but no specific 3-hydroxybutanoyl-CoA dehydrogenase (EC 1.1.1.157) is annotated in *A. aromaticum* EbN1.

The reaction product, acetoacetyl-CoA, is a beta-ketoacyl-CoA, with very low stability under the given analytical conditions (*3.1.1 Analysis of CoA-esters*). Therefore, only moderate to medium concentrations of the metabolite were measured, which probably do not quantitatively represent the actual intracellular concentration.

The acetyl-CoA C-acetyltransferase (ebA5202, EC 2.3.1.9), annotated for the cleavage of acetoacetyl-CoA into two molecules of acetyl-CoA, appeared to be expressed constitutively with very high protein and transcript scores. This enzyme plays a role in PHB metabolism as well as in several other central metabolic routes.

The final product, acetyl-CoA, was also present in very high amounts in all samples since it is a key metabolite of the central metabolism as well as in most degradation pathways.

The potential regulator gene ebA5278 (*bzdR*) is no part of the gene cluster and showed high transcription in all samples with an additional elevation in anaerobic cells that degrade aromatic substrates. Protein levels of ebA5278 were below the detection limit in all aerobic samples, except for the HPP degrading cells, where low levels were detectable. Extensive studies regarding the regulation of anaerobic benzoate degradation in *Azoarcus sp.* CIB were conducted by other research groups (Durante-Rodríguez *et al.*, 2008, 2006; Valderrama *et al.*, 2014). These studies showed a benzoyl-CoA regulated de-repression of

transcription, mediated by the regulator BzdR. Furthermore, transcription was found to be regulated in response to oxygen availability and repressed by other carbon catabolites (Durante-Rodríguez et al., 2008, 2006; López Barragán et al., 2004).

However, regulation of the anaerobic benzoate degradation in the systems biology experiments appears to be less complex and less strict than both the regulation of aerobic benzoate degradation in *A. aromaticum* EbN1, observed in this study, and the regulation of anaerobic benzoate degradation, described for *Azoarcus sp*. CIB.

3.3.2.1 Rhodopseudomonas pathway

A second degradation pathway, analogue to that described in *Rhodopseudomonas palustris* (Pelletier and Harwood, 2000), could be involved in the further degradation of cyclohexa-1,5-dienecarbonyl-CoA (3). Any products from the hypothetical alternative *Rhodopseudomonas* pathway would rejoin the pathway through 3-hydroxypimeloyl-CoA (6). This pathway is similar to the anaerobic benzoyl-CoA degradation from *Thauera aromatica* and *Azoarcus evansii* but includes two hydration reactions prior to hydration of the last ring double bond and ring opening (Pelletier and Harwood, 2000; Perrotta and Harwood, 1994). The pathway requires higher energy input in form of ATP than the *Thauera/Azoarcus* pathway but employs the same set of enzymes as for the degradation of cyclohexancarboxylate. So far, this pathway was only observed in the obligate anaerobic phototrophic alphaproteobacterium *R. palustris*.

Genes similar to the *badHIJK* genes for anaerobic benzoyl-CoA degradation from *R. palustris* are annotated as one gene cluster (ebA1953-ebA1962) in *A. aromaticum* EbN1 (Rabus *et al.*, 2005). However, the key enzyme benzoyl-CoA reductase is not encoded in this cluster but in the *bzd* gene cluster of benzoyl-CoA degradation via the *Thauera/Azoarcus* pathway. Additionally, benzoyl-CoA reductase (ebA5282, ebA5284, ebA5287 and ebA5286) from *A. aromaticum* EbN1 shows much higher similarity to the enzymes of *Thauera* and *Azoarcus* than to the enzyme of *R. palustris* (Rabus *et al.*, 2005). The *bad* gene cluster of *A. aromaticum* EbN1 showed low to medium expression without any apparent upregulation in response to benzoate as substrate or intracellular benzoyl-CoA. None of the gene products were detected in the cytosolic protein fraction under any of the analyzed growth conditions.

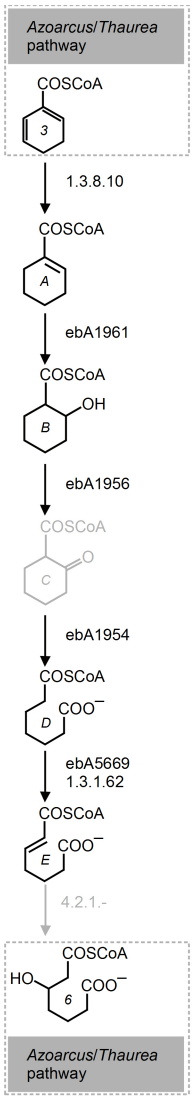

		Ace NO_3	Ace O_2	Ben NO_3	Ben O_2	Hbe NO_3	Hbe O_2	HPP NO_3	HPP O_2	Phe NO_3	Phe O_2
(3) cyclohexa-1,5-dienecarbonyl-CoA		NA	NA	59266	NA	NA	NA	9277	NA	3872	NA
(A) * cyclohex-1-ene-1-carboxyl-CoA		5729	NA	26652	NA	11674	13697	9861	15325	6696	1291
ebA1961	T	5	4	11	15	7	12	10	8	22	7
	P	NA	NA	NA	NA	NA	NA	NA	NA	NA	NA
(B) 2-hydroxycyclo-hexane-1-carboxyl-CoA		NA	NA	19276	NA	28285	NA	29289	NA	1839	NA
ebA1956	T	11	7	13	25	10	18	10	12	21	15
	P	NA	NA	NA	NA	NA	NA	NA	NA	NA	NA
(C) 2-ketocyclohexane-1-carboxyl-CoA		NA	NA	NA	NA	1117118	4784	1138	NA	934	2969
ebA1954	T	12	9	14	25	12	20	13	15	26	16
	P	NA	NA	NA	NA	NA	NA	NA	NA	NA	NA
(D) * pimeloyl-CoA		NA	544	220063	NA	198765	NA	199927	1426	89108	622
ebA5669	T	20	31	21	30	28	33	20	21	53	40
	P	NA	NA	NA	NA	NA	NA	NA	NA	NA	NA
(E) * 2,3-didehydro-pimeloyl-CoA		NA	NA	60482	NA	NA	NA	18944	NA	3010	1012
4.2.1.-		NA	NA	NA	NA	NA	NA	NA	NA	NA	NA
(6) 3-hydroxypimelyl-CoA		NA	NA	417533	NA	77864	NA	131739	NA	22461	NA

Figure 28: *Rhodopseudomonas* pathway of anaerobic benzoate degradation
Growth conditions are abbreviated as substrate and electron acceptor: Ace = acetate, Ben = benzoate, Hbe = 3-hydroxybenzoate, HPP = 3-(4-hydroxyphenyl)propanoate, Phe = phenylalanine, NO_3 = nitrate, O_2 = oxygen; Metabolites are indicated in bold and numbered according to the pathway diagram, genes are identified by locus tag with T indicating expression values of transcription and P indicating mascot scores of proteins; All Omics data are classified in percentiles and color coded: Gray = below detection limit, light green = lowest 30%, bright green = medium 30%, green = higher 30%, dark green = top 10%, NA = not detected metabolite or protein, * indicates metabolites with more than one signal in HPLC-MS, which could constitute isomers and are summed for this analysis

All in all, results from genetic, transcriptomic and proteomic analysis unanimously indicate that the *bad* enzymes play no active role in the anaerobic benzoate degradation of *A. aromaticum* EbN1 under the observed growth conditions. However, some putative intermediates of the *Rhodopseudomonas* pathway were detected and are discussed here (Figure 28).

Cyclohexa-1,5-dienecarbonyl-CoA (3) is the last mutual intermediate of both anaerobic benzoyl-CoA degradation pathways. In the *Rhodopseudomonas* pathway, the next step would be an additional double bond hydrogenation by the benzoyl-CoA reductase. This reaction involves the additional hydrolysis of two molecules of ATP and was so far only observed for the benzoyl-CoA reductase of *R. palustris*. The reaction product would be **cyclohex-1-ene-1-carboxyl-CoA (A)**. Two signals with the exact mass of this metabolite were detected in all samples except for aerobic benzoate and aerobic acetate degrading cultures. The highest signals were detected during anaerobic benzoate degradation. Mass spectrometry data indicates that the signals are indeed CoA-intermediates, possibly two isomer forms, but could not determine if a cyclohexane structure is present. Signal intensities for both possible isomers were summed for graphical representation.

The following hydratation of the last ring double bond would be performed by ebA1961 (BadC) and would yield **2-hydroxycyclohexane-1-carboxyl-CoA (B)**. Again, two signals for the mass of the putative metabolite were detected. One signal was strongest during anaerobic HPP degradation and detectable in all cells that anaerobically metabolize benzoyl-CoA or 3-hydroxybenzoyl-CoA. The second signal appeared to be specific for 3-hydroxybenzoate degradation and is not included in the representation of the *Rhodopseudomonas* pathway (Figure 28).

Dehydrogenation of 2-hydroxycyclohexane-1-carboxyl-CoA to **2-ketocyclohexane-1-carbonyl-CoA (C)** would be facilitated by a cyclohexane-1-carbonyl-CoA dehydrogenase (ebA1956). The reaction product would be 2-ketocyclohexane-1-carboxyl-CoA, an isomer to an intermediate of the main anaerobic benzoate degradation pathway, 6-hydroxycyclohex-1-enecarbonyl-CoA. Four different signals were recorded for the exact mass of 6-hydroxycyclohex-1-enecarbonyl-CoA, but only one signal correlated with anaerobic benzoyl-CoA degradation (supplement 28). This metabolite is most likely 6-hydroxycyclohex-1-enecarbonyl-CoA from the *Thauera* pathway, since the necessary enzymes for production and further catabolism of this intermediate are highly expressed in these samples. Thus, no signal corresponding to 2-ketocyclohexane-1-carboxyl-CoA from the *Rhodopseudomonas* pathway was detected.

Ring opening is presumably performed by 2-ketocyclohexanecarboxyl-CoA hydrolase (ebA1954, BadI) and would yield **pimeloyl-CoA (D)**. Two signals with the exact mass of

pimeloyl-CoA were detected and showed highest signal abundance upon anaerobic degradation of benzoyl-CoA. The signals were summed for graphical representation.

The next reaction would be a dehydrogenation by pimeloyl-CoA dehydrogenase (ebA5669), which is not part of the *bad* gene cluster and shows no specific regulation of expression. The ebA5669 protein was not detected in the cytosolic protein fraction of any sample. Two signals for the exact mass of the reaction product, **2,3-didehydro-pimeloyl-CoA (E)**, were detected and, based on mass spectrometric data, appeared to be CoA-intermediates. One signal appeared to be specific for anaerobic benzoyl-CoA degradation and could represent 2,3-didehydro-pimeloyl-CoA.

For the following hydroxylation of 2,3-didehydro-pimeloyl-CoA to produce **3-hydroxypimeloyl-CoA (6)**, no enzyme (EC 4.2.1.-) is annotated in the genome of *A. aromaticum* EbN1. The reaction product 3-hydroxypimeloyl-CoA marks the metabolic junction, where the *Rhodopseudomonas* pathway would reenter the *Thauera/Azoarcus* pathway of benzoyl-CoA degradation. It is an intermediate of both anaerobic benzoyl-CoA degradation pathways and was detected in high amounts in cells that anaerobically degrade benzoyl-CoA.

The hypothetical *bad* genes for the *Rhodopseudomonas* pathway in *A. aromaticum* EbN1 showed no transcriptional upregulation and no proteins accumulation. At the same time, all genes necessary for the more efficient *Thauera/Azoarcus* pathway were specifically transcribed and the necessary enzymes were detected in high concentrations. The mass signals detected for intermediates of the *Rhodopseudomonas* pathway mostly represented several isomer forms of the postulated metabolites. This contradicts the expectations of a concerted metabolic pathway with high throughput and specific reactions. Hence, the observed metabolites more likely represent byproducts of the *Thauera/Azoarcus* enzymes. All in all, it can be assumed that the *Thauera/Azoarcus* pathway is the main catabolic route active in anaerobic benzoate degradation in *A. aromaticum* EbN1. If reactions from the *Rhodopseudomonas* pathway occur during anaerobic benzoate degradation, they seem not to be purposefully induced and could only represent an ancillary or incomplete pathway. Possibly the genes play a role in anaerobic degradation of cyclohexancarboxylate, as in *R. palustris*. However, it was not yet tested, whether *A. aromaticum* EbN1 is capable of anaerobic growth with this substrate.

3.3.2.2 Summary of anaerobic benzoate degradation

The upper anaerobic benzoyl-CoA degradation pathway, including hydrolytic ring cleavage, was reconstructed without any gaps on metabolic, transcriptomic and proteomic level. From the lower pathway six out of seven metabolites were detected in this analysis, while only three genes out of seven are annotated, of which one appeared not to be regulated pathway dependent. The lower pathway was shown to occur via the postulated β-oxidation processes, employing constitutive and non-specific enzymes, as indicated by the detected metabolites.

Possibly, *A. aromaticum* EbN1 is also capable to degrade benzoyl-CoA via the *Rhodopseudomonas* pathway. However, this energetically more demanding pathway might constitute an ancillary pathway, while a major contribution to anaerobic benzoate degradation appears unlikely.

3.3.3 Aerobic and anaerobic HPP degradation

3-(4-hydroxyphenyl)propanoate belongs to a group of plant metabolites, relevant for the metabolism of secondary metabolite, the biosynthesis of lignin and many other compounds. In accordance with the broad natural availability, several aerobic and anaerobic bacterial degradation pathways for 3-phenylpropanoates were identified previously. The ability of *A. aromaticum* EbN1 to degrade 3-phenylpropanoates under denitrification, including 3-(4-hydroxyphenyl)propanoate (HPP), was previously described (Trautwein *et al.*, 2012b). It was speculated but not before investigated, that *A. aromaticum* EbN1 applies the same pathway under aerobic and anaerobic respiration.

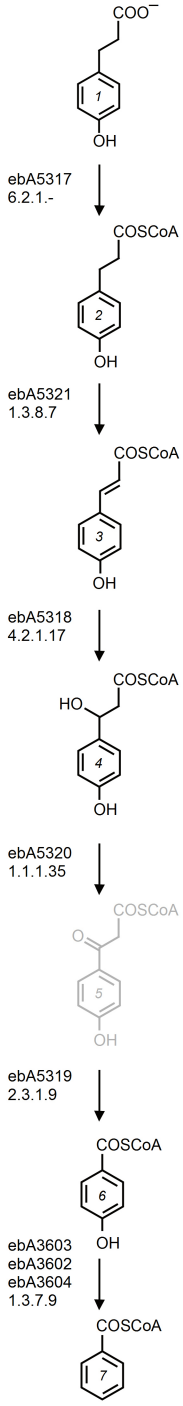

		Ace NO_3	Ace O_2	Ben NO_3	Ben O_2	Hbe NO_3	Hbe O_2	HPP NO_3	HPP O_2	Phe NO_3	Phe O_2
(1) 3-(4-hydroxyphenyl) propanoate		NA	NA	NA	NA	NA	NA	NA	3160	NA	NA
ebA5317	T	3	8	13	10	6	8	546	1050	23	22
	P	NA	NA	NA	NA	NA	NA	885	1237	NA	NA
(2) 3-(4-hydroxyphenyl) propanoyl-CoA		NA	NA	NA	NA	NA	NA	52239	51297	NA	NA
ebA5321	T	5	4	8	9	7	8	735	627	15	16
	P	NA	NA	NA	NA	NA	NA	645	836	NA	NA
(3) p-coumaroyl-CoA		NA	NA	NA	NA	NA	NA	2087	1597	NA	NA
ebA5318	T	6	14	19	18	12	14	1223	1492	32	35
	P	NA	NA	NA	NA	NA	NA	665	664	NA	136
(4) 3-hydroxy-3-(4-hydroxyphenyl)propanoyl-CoA		NA	NA	1842	NA	1217	NA	4903	NA	2527	NA
ebA5320	T	3	4	5	9	5	6	516	561	9	15
	P	NA	NA	NA	NA	NA	NA	1215	1257	133	227
(5) 4-hydroxyphenyl-acetyl-CoA		NA	NA	NA	NA	NA	NA	NA	NA	21419	NA
ebA5319	T	6	7	12	13	8	9	1017	995	20	25
	P	NA	NA	NA	NA	NA	NA	1386	1384	NA	92
(6) 4-hydroxybenzoyl-CoA		1967	NA	NA	NA	496	NA	45128	115360	11187	47317
4-hydroxybenzoate		NA	NA	NA	NA	NA	NA	1106	12670	NA	NA
ebA3603	T	2	1	1	4	26	3	9	70	5	2
	P	NA	NA	NA	NA	NA	NA	NA	176	NA	NA
ebA3602	T	1	0	1	2	11	1	9	49	2	1
	P	NA	NA	NA	NA	NA	NA	NA	150	NA	NA
ebA3604	T	4	1	3	5	46	5	14	148	5	2
	P	NA	NA	NA	NA	NA	NA	NA	NA	NA	NA
(7) benzoyl-CoA		167146	3896	4105301	1469012	31071	105397	2013293	1042478	2842400	73503

Figure 29: Aerobic and anaerobic degradation of 3-(4-hydroxyphenyl)propanoate to benzoyl-CoA

Growth conditions are abbreviated as substrate and electron acceptor: Ace = acetate, Ben = benzoate, Hbe = 3-hydroxybenzoate, HPP = 3-(4-hydroxyphenyl)propanoate, Phe = phenylalanine, NO_3 = nitrate, O_2 = oxygen; Metabolites are indicated in bold and numbered according to the pathway diagram, genes are identified by locus tag with T indicating expression values of transcription and P indicating mascot scores of proteins; All Omics data are classified in percentiles and color coded: Gray = below detection limit, light green = lowest 30%, bright green = medium 30%, green = higher 30%, dark green = top 10%, NA = not detected metabolite or protein

Metabolomic analysis covered most of the postulated intermediates, as illustrated in figure 29. The only missing intermediate was 4-hydroxyphenylacetyl-CoA but the following metabolite, 4-hydroxybenzoyl-CoA, and it's cleavage product 4-hydroxybenzoate were detected specifically in HPP degrading samples.

The HPP related gene cluster, ebA5317, ebA5318, ebA5319 and ebA5320, encodes acyl-CoA synthase, enoyl-CoA hydratase, acetyl-CoA C-acetyltransferase and 3-hydroxyacyl-CoA dehydrogenase, respectively. They were co-transcribed as one mRNA and showed specific upregulation of gene transcription and protein translation during aerobic and anaerobic degradation of HPP. A slight upregulation of gene transcription was also observed during phenylalanine degradation but did not lead to the production of high amounts of protein. Neither gene expression nor protein levels differed noticeably between aerobic and anaerobic HPP degradation.

The results confirm the β-oxidation-like removal of the HPP side chain via CoA-bound intermediates under oxic and anoxic growth conditions by detecting 4 of the 5 predicted metabolites. This work presents the first study of HPP side chain oxidation under oxic conditions in *A. aromaticum* EbN1. 4-Hydroxyphenylacetyl-CoA was the only intermediate that could not be detected, possibly because the β-keto group is sensitive to decomposition during extraction. Moreover, 4-hydroxyphenylacetate was also not detected by a GC-MS method applied in a previous study of anaerobic HPP degradation (Trautwein *et al.*, 2012b).

A remarkable observation during the systems biological experiments was the massive excretion of 4-hydroxybenzoate during aerobic HPP degradation. In this context, 4-hydroxybenzoyl-CoA reductase could play an important role. Under oxic conditions, 4-hydroxybenzoate from HPP was secreted into the medium at a rate similar to HPP consumption but was consumed partially after depletion of the substrate. However, only small amounts of 4-hydroxybenzoate were released into the medium under anoxic growth conditions. The results of HPLC-analysis of HPP and 4-hydroxybenzoate during aerobic and anaerobic cultivation (Kathleen Trautwein, MPI) are presented in figure 30.

Three genes, ebA3602, ebA3603 and ebA3604, are annotated as anaerobic 4-hydroxybenzoyl-CoA reductase and show 48% to 74% protein sequence identity to 4-hydroxybenzoyl-CoA reductase, HcrABC, from *Thauera aromatica*. All three genes show

a distinct upregulation of gene transcription during aerobic HPP degradation but not during anaerobic growth. Only moderate protein scores are detectable for two subunits in aerobic HPP degrading cells, while one subunit, ebA3604 (HcrC), is not detectable in any sample (Figure 29). The product, benzoyl-CoA, was detected during aerobic and anaerobic HPP degradation with signal intensities twice as high during anaerobic growth as during aerobic growth.

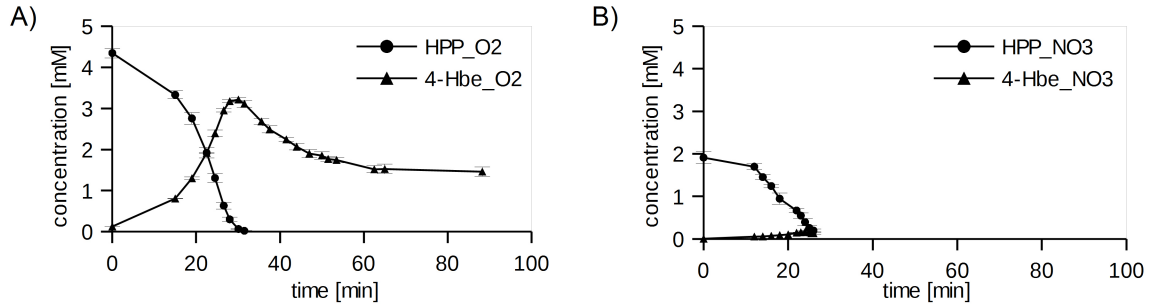

Figure 30: 3-(4-hydroxyphenyl)propanoate and 4-hydroxybenzoate concentrations during aerobic and anaerobicgrowth
Measurements and calculations by Kathleen Trautwein (MPI); A) Aerobic growth B) Anaerobic growth; HPP = 3-(4-hydroxyphenyl)propanoate, 4-Hbe = 4-hydroxybenzoate, _O_2 = aerobic, _NO_3 = anaerobic

The results confirm the proposed reduction of 4-hydroxybenzoyl-CoA to benzoyl-CoA under anoxic and oxic conditions by detecting both metabolites in high concentrations. The 4-hydroxybenzoyl-CoA reductase encoded by ebA3602-3604 was proposed to reduce 4-hydroxybenzoyl-CoA to benzoyl-CoA anaerobically (Rabus *et al.*, 2005), albeit the enzyme could not be detected in previous studies (Trautwein *et al.*, 2012b). However, the lack of detectable transcript or protein upregulation during anaerobic HPP degradation implies that a different enzyme is responsible for this reaction during anaerobic growth. Hypothetically, the anaerobic benzoyl-CoA reductase (ebA5287, ebA5286, ebA5284 and ebA5282) could catalyze the dehydroxylation of 4-hydroxybenzoate. All four subunits are highly expressed during HPP degradation. The reaction mechanisms used by benzoyl-CoA reductase and 4-hydroxybenzoate reductase are very similar, birch-like reductions that use radical intermediates but apply different enzymatic strategies (Boll, 2004; Boll and Fuchs, 2005). However, benzoyl-CoA reductase from *T. aromatica* is not able to use 4-hydroxybenzoate as substrate (Laempe *et al.*, 2001; Möbitz and Boll, 2002), thus enzyme assays would be necessary to investigate whether the *A. aromaticum* EbN1 enzyme acts on 4-hydroxybenzoyl-CoA.

The massive secretion of 4-hydroxybenzoyl-CoA during aerobic growth indicates a low capacity of the necessary reductase under this growth conditions, possibly due to the use of the originally anaerobic enzyme. This theory is further supported by the lower intracellular level of 4-hydroxybenzoate during anaerobic growth and by the fact that 4-hydroxybenzoate is not fully depleted during aerobic growth. No previous experiments or speculations have been made concerning the aerobic degradation pathway. Furthermore, HcrABC from *T. aromatica* was described to be highly oxygen sensitive (Brackmann and Fuchs, 1993; Breese and Fuchs, 1998). To date, no other enzyme is known to convert 4-hydroxybenzoyl-CoA to benzoate or benzoyl-CoA, either aerobically or anaerobically.

3.3.3.1 Summary of aerobic and anaerobic HPP degradation

Degradation of 3-(4-hydroxyphenyl)propanoate was demonstrated to proceed via the predicted β-oxidation of the side chain, both aerobically and anaerobically. The final reduction of 4-hydroxybenzoyl-CoA to benzoyl-CoA was confirmed by metabolomic data. However, the proposed 4-hydroxybenzoyl-CoA reductase shows no anaerobic upregulation, while the reaction appears to be constricted during aerobic growth.

3.3.4 Aerobic and anaerobic phenylalanine degradation

Phenylalanine is a proteinogenic aromatic amino acid and a commonly available substrate in diverse natural habitats. In bacteria, phenylalanine can be degraded via tyrosine when molecular oxygen is available. Alternatively, aerobic and anaerobic degradation of phenylalanine can proceed via phenylacetate and phenylacetyl-CoA. Anaerobic degradation of phenylacetate via phenylacetyl-CoA was first described in 1997 (Schneider *et al.*, 1997) while the aerobic pathway was only fully understood in 2010 (Teufel *et al.*, 2010). *A. aromaticum* EbN1 is predicted to employ aerobic and anaerobic degradation pathways via phenylacetyl-CoA (Rabus *et al.*, 2005).

3.3.4.1 Aerobic and anaerobic degradation of phenylalanine to phenylacetate

Different enzymes for the anaerobic degradation pathway of phenylalanine via phenylpyruvate and phenylacetaldehyde to phenylacetate in *A. aromaticum* EbN1 were previously suggested (Debnar-Daumler *et al.*, 2014; Rabus *et al.*, 2005; Wöhlbrand *et al.*, 2007). Additionally, an alternative route from phenylpyruvate directly to phenylacetyl-CoA via an indolepyruvate ferredoxin oxidoreductase complex (ebA121, ebA122) was proposed, based on genetic evidence (Rabus *et al.*, 2005). No predictions or experiments regarding the aerobic degradation of phenylalanine to phenylacetate in *A. aromaticum* EbN1 were previously made. The proposed aerobic and anaerobic degradation pathways from phenylalanine to phenylacetate and all related metabolomics, proteomics and transcriptomics data are presented in figure 31.

Sequential Metabolomic pathway

(1) phenylalanine

Intracellular phenylalanine was measured in highest concentrations in cells grown aerobically with phenylalanine as carbon source. Concentrations were lower in anaerobically grown cells and even lower but still detectable in the presence of all other substrates under aerobic respiration.

Neither the predicted aminotransferase (ebA596) nor any of 16 other annotated aminotransferases showed specific upregulation on transcriptional or proteomic level in this study. Since ebA596 protein was detected in all samples, it appears likely that this enzyme is constitutively active as part of the regular amino acid metabolism.

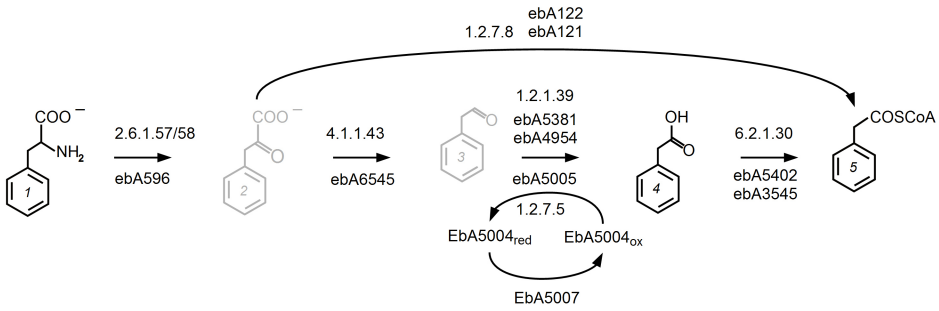

		Ace NO_3	Ace O_2	Ben NO_3	Ben O_2	Hbe NO_3	Hbe O_2	HPP NO_3	HPP O_2	Phe NO_3	Phe O_2
(1) phenylalanine		61	1386	764	1498	NA	1742	NA	473	2681	7990
ebA596	T	158	162	126	166	138	168	132	102	94	150
	P	436	499	461	466	506	468	373	392	384	606
(2) phenylpyruvate		NA	NA	NA	NA	NA	NA	NA	NA	NA	NA
ebA6545	T	26	32	47	35	31	36	28	25	1113	1091
	P	NA	NA	NA	NA	NA	NA	NA	NA	847	1347
ebA121	T	73	104	64	86	21	16	41	10	30	38
	P	253	NA	302	NA	398	NA	339	NA	427	NA
ebA122	T	201	374	144	245	47	51	103	31	57	155
	P	338	117	NA	NA	167	NA	NA	NA	208	NA
(3) phenylacetaldehyde		NA	NA	NA	NA	NA	NA	NA	NA	NA	NA
ebA4954	T	16	12	14	25	14	21	14	16	41	83
	P	NA	NA	NA	NA	NA	NA	NA	NA	NA	455
ebA5381	T	5	3	6	11	7	10	6	8	12	7
	P	NA	NA	NA	NA	NA	NA	NA	NA	NA	NA
ebA5004	T	151	207	205	342	225	352	210	222	3725	1202
	P	128	NA	123	NA	169	184	237	227	672	541
ebA5005	T	111	133	138	192	149	233	140	152	2756	793
	P	NA	NA	NA	NA	274	215	NA	199	1820	1028
ebA5007	T	21	21	19	25	26	36	19	27	522	145
	P	NA	NA	NA	NA	NA	NA	NA	NA	697	385
(4) phenylacetate		NA	NA	NA	NA	NA	NA	NA	NA	NA	495
ebA3545	T	110	130	156	368	131	261	151	130	1911	2170
	P	153	130	222	250	NA	332	151	221	588	876
ebA5727	T	7	3	7	15	7	17	5	11	19	99
	P	NA	NA	NA	NA	NA	NA	NA	NA	NA	504
ebA5402	T	64	45	60	79	131	100	208	111	1218	561
	P	101	NA	NA	NA	232	NA	404	424	907	751
(5) phenylacetyl-CoA		16097	3006	10006	NA	14172	1388	6336	1404	372495	730831

Figure 31: Aerobic and anaerobic degradation of phenylalanine to phenylacetate
Growth conditions are abbreviated as substrate and electron acceptor: Ace = acetate, Ben = benzoate, Hbe = 3-hydroxybenzoate, HPP = 3-(4-hydroxyphenyl)propanoate, Phe = phenylalanine, NO_3 = nitrate, O_2 = oxygen; Metabolites are indicated in bold and numbered according to the pathway diagram, genes are identified by locus tag with T indicating expression values of transcription and P indicating mascot scores of proteins; All Omics data are classified in percentiles and color coded: Gray = below detection limit, light green = lowest 30%, bright green = medium 30%, green = higher 30%, dark green = top 10%, NA = not detected metabolite or protein

(2) phenylpyruvate and (3) phenylacetaldehyde

The degradation products phenylpyruvate and phenylacetaldehyde were not detected by GC-MS analysis, possibly because of low intracellular concentrations of these reactive intermediates. The phenylpyruvate decarboxylase (ebA6545) was differentially upregulated on transcriptional and translational level when *A. aromaticum* EbN1 grew with phenylalanine, independent of the availability of oxygen. The originally predicted phenylacetaldehyde dehydrogenase (ebA5381) showed very low gene expression throughout all samples with no protein detectable in any sample during this study. An alternative phenylacetaldehyde dehydrogenase (ebA4954) showed transcriptional upregulation during growth in the presence of phenylalanine with a maximum during aerobic phenylalanine degradation. The protein, ebA4954, was only detectable during aerobic phenylalanine degradation with a moderate mascot score.

Aldehyde:ferredoxin oxidoreductase (ebA5005), as well as its specific ferredoxin (ebA5004) and the associated ferredoxin:NADH oxidoreductase (ebA5007) were upregulated during phenylalanine degradation, both transcriptionally and on protein level. Transcript and protein levels were highest in samples anaerobically degrading phenylalanine but also detectable in moderate to high amounts during aerobic respiration.

The putative indolepyruvate:ferredoxin oxidoreductase complex, ebA121 and ebA122 (*iorAB*) also appeared slightly upregulated transcriptionally and translationally during phenylalanine degradation. Both subunits were detectable in the cytosolic protein fraction during anaerobic phenylalanine degradation but also during anaerobic acetate and 3-hydroxybenzoate degradation.

In the systems biology experiments, of the four proposed pathway variants, only one phenylacetaldehyde dehydrogenase, ebA5381, was not expressed during either aerobic or anaerobic phenylalanine degradation. For this enzyme, a role in *p*-cresol degradation rather than phenylalanine degradation was hypothesized earlier (Wöhlbrand *et al.*, 2007).

In contrast to the literature, phenylacetaldehyde dehydrogenase ebA4954 protein was only detectable in aerobic samples. This contradicts the previous findings of cytosolic protein accumulation in *A. aromaticum* EbN1 during anaerobic growth but is in line with the finding that the enzyme is robust towards oxygen (Debnar-Daumler *et al.*, 2014).

The aldehyde:ferredoxin oxidoreductase ebA5005 was detected specifically during

phenylalanine degradation under both types of respiration and additionally upregulated during anaerobic growth. The tungsten-containing enzyme, ebA5005, was found to be surprisingly robust towards oxygen exposure (Debnar-Daumler *et al.*, 2014), thus a role in the aerobic metabolism of *A. aromaticum* EbN1 is likely. Whether the enzyme is involved in the actual metabolic pathway during one or both types of respiration, as postulated by Wöhlbrand *et al.* (2007) or plays a role in the degradation of toxic aldehyde byproducts, as hypothesized by Debnar-Daumler *et al.* (2014) remains to be determined.

The last alternative, IorAB mediated conversion of phenylpyruvate to phenylacetyl-CoA, was originally rejected by proteomic studies (Wöhlbrand *et al.*, 2007) but might be active during anaerobic phenylalanine degradation according to the data from this systems biology analysis. However, neither transcript nor protein abundance of both subunits appear to be regulated strictly substrate dependent. Therefore, proper enzymatic characterization would be necessary to prove or disprove this enzyme's role in phenylalanine degradation.

(5) phenylacetyl-CoA

Activation of phenylacetate to phenylacetyl-CoA could be achieved via three different predicted phenylacetate:CoA-ligases in *A. aromaticum* EbN1.

Gene ebA3545 (*paaK*) is co-located with the gene cluster annotated as aerobic phenylacetate degradation pathway. The gene showed high transcription counts and protein scores during phenylalanine degradation under oxic and anoxic conditions. Transcription levels were equally high during aerobic and anaerobic phenylalanine degradation, but the protein concentration was elevated under oxic conditions. Low to moderate protein scores were detected in all other samples except during anaerobic 3-hydroxybenzoate degradation, where no protein was detectable. This gene was originally proposed to be responsible for phenylacetyl-CoA formation under aerobic respiration and the protein was found to be differentially upregulated during aerobic phenylalanine degradation (Rabus *et al.*, 2005; Wöhlbrand *et al.*, 2007). However, data from this study suggests a role during both, aerobic and anaerobic phenylalanine degradation with only slight preference for the aerobic pathway.

The isoenzyme ebA5727 (*paaK2*) is transcribed to a far lower extend (50-100 times lower) than ebA3545 but shows a higher specificity for oxic conditions than ebA3545. The

corresponding protein is detected exclusively in aerobic phenylalanine samples. The gene was proposed to be involved in degradation of p-cresol rather than phenylacetate (Wöhlbrand *et al.*, 2007). Thus, the observed gene expression could be residual responsiveness of the transcriptional regulation to phenylacetate as the original substrate, even though now a different substrate specificity is likely.

Lastly, ebA5402 (*padJ*) is annotated as phenylacetate:CoA-ligase, co-located with the gene cluster for anaerobic phenylacetate degradation and showed strong upregulation in the presence of phenylalanine as substrate. Transcription was twice as high in the anaerobic phenylalanine samples as in the aerobic samples. The protein score of ebA5402 was only moderately elevated in the anaerobic samples compared to aerobic phenylalanine degradation.

Of the three predicted phenylacetate:CoA-ligases, ebA3545 and ebA5402 are present during aerobic and anaerobic phenylalanine degradation. Expression is not as specific for aerobic or anaerobic growth as originally assumed but shows moderate preferences for ebA3545 under aerobic respiration and ebA5402 during denitrification.

3.3.4.2 Aerobic degradation of phenylacetate

Aerobic phenylacetate degradation in *A. aromaticum* EbN1 was proposed to take place via the aerobic phenylacetyl-CoA pathway, which is common in microaerophilic bacteria (Teufel *et al.*, 2010). The pathway, along with all related experimental data, is represented in figure 32. In addition to its role during aerobic growth with phenylalanine as carbon source, the aerobic phenylacetyl-CoA pathway can be expected to be active under all oxic growth conditions as part of the normal amino acid metabolism. At the level of 2,3-didehydroadipyl-CoA, aerobic phenylacetate degradation and aerobic benzoate degradation merge. Downstream intermediates are identical in both pathways but some reactions are catalyzed by different, pathway specific enzymes.

In contrast to the genes for phenylalanine degradation to phenylacetate, the genes for aerobic phenylacetate degradation are organized in one gene cluster, resembling the phenylacetic acid (*paa*) operon originally described in *Azoarcus evansii* (Mohamed *et al.*, 2002). Transcription analysis indicates that the genes are divided into three separate mRNAs in *A. aromaticum* EbN1, but show a very high correlation of transcription and protein level (supplement 29).

Sequential metabolic pathway

(1) phenylacetate

Formation of phenylacetate from phenylalanine is discussed in the previous section. Phenylacetate was only detected in cells aerobically grown with phenylalanine as substrate.

(2) phenylacetyl-CoA

Activation of phenylacetate to phenylacetyl-CoA is facilitated by phenylacetate:CoA ligase ebA3545, which is part of the *paa* regulon in *A. aromaticum* EbN1 and shows strong co-regulation with the other genes from aerobic phenylacetyl-CoA degradation. Additionally, phenylacetate:CoA ligase ebA5402, from the anaerobic phenylacetate degradation pathway, is also expressed and translated during aerobic phenylalanine degradation and can catalyze this reaction.

Phenylacetyl-CoA was detected during aerobic and anaerobic phenylalanine degradation, where the relative peak area was twice as high in the aerobically grown samples. Additionally, the intermediate was detected in all samples except during aerobic benzoate degradation. In contrast to the phenylalanine degrading samples, phenylacetyl-CoA concentrations during degradation of other substrates were generally higher in anaerobic samples. The metabolite is an intermediate of the aerobic and anaerobic degradation pathways of phenylacetate and also expected to play a role in the amino acid metabolism under all growth conditions.

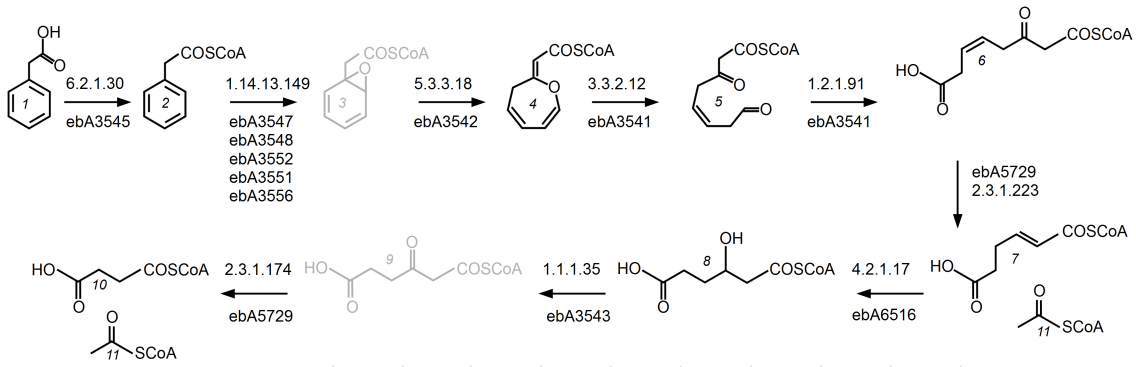

		Ace NO_3	Ace O_2	Ben NO_3	Ben O_2	Hbe NO_3	Hbe O_2	HPP NO_3	HPP O_2	Phe NO_3	Phe O_2
(1) phenylacetate		NA	NA	NA	NA	NA	NA	NA	NA	NA	495
ebA3545	T	110	130	156	368	131	261	151	130	1911	2170
	P	153	130	222	250	NA	332	151	221	588	876
(2) phenylacetyl-CoA		16097	3006	10006	NA	14172	1388	6336	1404	372495	730831
ebA3547	T	131	293	159	518	120	319	144	185	1903	2962
	P	129	167	NA	420	NA	402	NA	306	518	912
ebA3548	T	253	557	310	1123	261	663	296	332	3402	5512
	P	NA	83	NA	73	NA	78	NA	71	210	242
ebA3550	T	36	99	43	192	35	103	37	53	450	905
	P	126	247	121	407	137	378	104	239	479	696
ebA3551	T	26	47	25	146	24	62	22	33	223	664
	P	NA	NA	NA	75	NA	123	NA	77	285	373
ebA3553	T	20	41	21	108	20	52	15	32	193	534
	P	NA	NA	NA	496	NA	386	NA	223	311	1191
(3) 2-(1,2-epoxy-1,2-dihydrophenyl)acetyl-CoA		NA									
ebA3542	T	31	22	126	101	45	55	99	42	2012	1318
	P	NA	210	NA	297	NA	446	NA	322	781	1099
(4) 2-oxepin-2(3H)-ylideneacetyl-CoA		2656	NA	2353	NA	2059	NA	769	NA	1889	6556
ebA3541	T	33	45	87	190	40	72	76	49	684	737
	P	NA	634	92	1321	NA	863	NA	1146	361	1696
(5) * 3-oxo-5,6-dehydrosuberyl-CoA semialdehyde		NA	NA	NA	14626	NA	NA	NA	1503	13241	28262
ebA3541	T	33	45	87	190	40	72	76	49	684	737
	P	NA	634	92	1321	NA	863	NA	1146	361	1696
(6) * 3-oxo-5,6-dehydrosuberyl-CoA		NA	NA	NA	NA	NA	NA	NA	NA	3945	2816
ebA5729	T	2	1	2	4	1	3	2	2	4	35
	P	NA	NA	NA	NA	NA	NA	NA	NA	NA	546
(7) 2,3-didehydroadipyl-CoA		759	NA	44638	173296	734	NA	21205	109079	13358	15250
ebA6516	T	105	98	78	85	105	127	89	83	159	114
	P	198	258	115	157	254	184	220	225	273	414
(8) 3-hydroxyadipyl-CoA		2525	2774	18805	185994	904	3981	2474	67322	27563	48800
ebA3543	T	11	9	39	43	17	24	34	18	614	556
	P	NA	185	NA	295	NA	329	NA	NA	608	1385
(9) 3-oxoadipyl-CoA		NA	NA	NA	NA	168597	NA	NA	3612	NA	NA
ebA5729	T	2	1	2	4	1	3	2	2	4	35
	P	NA	NA	NA	NA	NA	NA	NA	NA	NA	546
(10) succinyl-CoA		322845	400537	329498	263021	369126	235378	173528	195625	222840	302463
(11) acetyl-CoA		1328592	758914	846490	977224	1139162	1320983	589337	760534	886646	663864

Figure 32: Aerobic phenylacetate degradation pathway
Growth conditions are abbreviated as substrate and electron acceptor: Ace = acetate, Ben = benzoate, Hbe = 3-hydroxybenzoate, HPP = 3-(4-hydroxyphenyl)propanoate, Phe = phenylalanine, NO_3 = nitrate, O_2 = oxygen; Metabolites are indicated in bold and numbered according to the pathway diagram, genes are identified by locus tag with T indicating expression values of transcription and P indicating mascot scores of proteins; All Omics data are classified in percentiles and color coded: Gray = below detection limit, light green = lowest 30%, bright green = medium 30%, green = higher 30%, dark green = top 10%, NA = not detected metabolite or protein, * indicates metabolites with more than one signal in HPLC-MS, which could constitute isomers and are summed for this analysis

(3) 2-(1,2-epoxy-1,2-dihydrophenyl)acetyl-CoA

Aerobic degradation of phenylacetyl-CoA is initiated by the multicomponent oxygenase PaaABCDE via NADPH dependent formation of 2-(1,2-epoxy-1,2-dihydrophenyl)acetyl-CoA with molecular oxygen (Teufel *et al.*, 2010). The genes ebA3547, ebA3548, ebA3550, ebA3551 and ebA3553 are annotated to encode the 1,2-phenylacetyl-CoA epoxidase subunits (*paaABCDE).* All subunits showed the highest transcription levels during aerobic phenylalanine degradation but were also transcribed and translated during anaerobic growth with this substrate. The subunit proteins could also be detected with the other aromatic substrates in aerobically but not in anaerobically grown samples. Subunit mascot scores during acetate degradation were much lower, with subunits ebA3551 and ebA3553 (PaaD and PaaE) below the detection limit. Transcription of the subunits showed strong co-regulation and indicate a substrate dependent regulation as well as transcriptional regulation in response to the respiratory mode. Additional regulation appears to further modulate protein levels according to substrate availability and respiration.

The expected product, 2-(1,2-epoxy-1,2-dihydrophenyl)acetyl-CoA, could not be detected, possibly because of the short-lived epoxy structure. Moreover, the amount of the epoxy intermediate was found to be strictly regulated in *Pseudomonas* sp. due to its toxicity and reactivity (Teufel *et al.*, 2012).

(4) 2-oxepin-2(3H)-ylideneacetyl-CoA

Isomerization of the epoxy-CoA to 2-Oxepin-2(3H)-ylideneacetyl-CoA is catalyzed by enoyl-CoA hydratase/isomerase ebA3542, which showed distinct substrate dependent transcription and translation, elevated during aerobic phenylalanine degradation. The isomerization product 2-Oxepin-2(3H)-ylideneacetyl-CoA (or one of its isomers) was detected in aerobic phenylalanine samples with the highest peak area.

(5) 3-oxo-5,6-dehydrosuberyl-CoA semialdehyde

The next catabolic step is hydrolytic ring cleavage of the C-O heterocycle by oxepin-CoA hydrolase, ebA3541, which showed the typical substrate and oxygen dependent regulation of the *paa* regulon.

3-Oxo-5,6-dehydrosuberyl-CoA semialdehyde, for which no isomers are known, was detected with two signals in cells grown with phenylalanine as substrate and, to a lower extend, in aerobically grown cells with benzoate as substrate. Both signals were summarized for graphical representation.

(6) 3-oxo-5,6-dehydrosuberyl-CoA

According to literature, dehydrogenation of 3-oxo-5,6-dehydrosuberyl-CoA semialdehyde to 3-oxo-5,6-dehydrosuberyl-CoA is catalyzed by the same bifunctional enzyme as the previous reaction, oxepin-CoA hydrolase PaaZ, ebA3541 (Teufel *et al.*, 2010).

The product 3-oxo-5,6-dehydrosuberyl-CoA was detected in cells aerobically and anaerobically degrading phenylalanine, with very similar signal intensities under both conditions. In a study with *E. coli*, no semialdehyde was detected. Therefore, a two-step conversion without the release of the semialdehyde intermediate was postulated (Teufel *et al.*, 2011, 2010). The detection of the metabolite contradicts this theory and suggests at least partial release of the intermediate from the enzyme in the systems biology experiments.

(7) 2,3-didehydroadipyl-CoA

No specific enzyme is annotated for the following thiolytical removal of acetyl-CoA in the gene cluster of aerobic phenylacetate degradation of *A. aromaticum* EbN1. In *E. coli* this reaction is catalyzed by PaaJ (2.3.1.223) but the gene is missing from the *paa* gene clusters of *A. aromaticum* EbN1 and *A. evansii* (Ismail *et al*., 2003). However, a second *paa* gene cluster is present in the genome of *A. aromaticum* EbN1, which includes a homologue to *paaJ*, ebA5729.

The reaction product 2,3-didehydroadipyl-CoA is also an intermediate of aerobic benzoyl-CoA degradation. Therefore, the highest signals were detected in aerobic benzoate samples, followed by aerobic 3-(4-hydroxyphenyl)propanoate (HPP) samples. In aerobic

phenylalanine samples, the signal was only about 10% of that in aerobic benzoate samples. No significant difference between aerobic and anaerobic phenylalanine degradation was detectable in regard to this intermediate and similar amounts were detected in anaerobic HPP samples.

(8) 3-hydroxyadipyl-CoA

Hydratation of 2,3-didehydroadipyl-CoA to 3-hydroxyadipyl-CoA is facilitated by 2,3-dehydroadipyl-CoA hydratase PaaF (4.2.1.17) in *Pseudomonas* sp. Y2 (Teufel *et al.*, 2010) but no such gene is annotated in *A. aromaticum* EbN1. The analysis of β-oxidation related genes and gene products (see *3.2.3 β-oxidation*) suggested a role of enoyl-CoA hydratase ebA6516 in the aerobic degradation of phenylalanine, which could catalyze this reaction. Gene transcription is not specific for aerobic phenylalanine degradation, but the protein mascot scores were elevated under this growth condition.

Even though the identity of the hydratase is not clear, the product 3-hydroxyadipyl-CoA was detectable in aerobic and anaerobic phenylalanine cells. The same was true for cells degrading benzoyl-CoA aerobically. Signal intensity in aerobic phenylalanine degrading cells was 26% of the relative peak area in aerobic benzoate degrading cells and 15% in anaerobic phenylalanine degrading cells.

(9) 3-oxoadipyl-CoA

The following oxidation to 3-oxoadipyl-CoA is catalyzed by 3-hydroxyacyl-CoA dehydrogenase ebA3543, which showed the typical expression pattern with the protein only being detectable in aerobic samples.

A HPLC-MS signal, representing 3-oxoadipyl-CoA or one of its isomers, was detected upon anaerobic 3-hydroxybenzoate degradation and to a low extent during aerobic HPP degradation but neither in aerobic phenylalanine degradation nor in aerobic benzoyl-CoA degradation. 3-oxoadipyl-CoA, like other β-ketoacyl-CoA, could be prone to decay during sample extraction (*3.1.1 Analysis of CoA-esters*). In this case, the signals detected during 3-hydroxybenzoate degradation would represent an isomer, possibly 4-oxoadipyl-CoA.

The last step in aerobic phenylacetate degradation is the cleavage of 3-oxoadipyl-CoA to acetyl-CoA and succinyl-CoA by a β-ketoadipyl-CoA thiolase. In *E. coli*, this reaction is

catalyzed by the same enzyme as the thiolysis of 3-oxo-5,6-dehydrosuberyl-CoA to 2,3-didehydroadipyl-CoA and acetyl-CoA (PaaJ) (Teufel *et al.*, 2010). Thus, a similar bifunctional role of ebA5729 in the aerobic phenylalanine degradation pathway appears likely.

The final products of aerobic phenylacetate degradation are acetyl-CoA and succinyl-CoA, both of which were detected in all samples in high concentrations. These metabolites are crucial for the central metabolism and their concentration in the cell is influenced by numerous anabolic and catabolic reactions and subject to strict regulation mechanisms.

3.3.4.3 Anaerobic phenylacetate degradation

Anaerobic phenylacetate degradation in *A. aromaticum* EbN1 was proposed to proceed via the anaerobic phenylacetyl-CoA pathway to benzoyl-CoA, which was previously confirmed by proteomics studies (Rabus *et al.*, 2005; Wöhlbrand *et al.*, 2007). The pathway and all related systems biology data are represented in figure 33.

The genes for anaerobic phenylacetate degradation were transcribed as one single mRNA with 12 genes in *A. aromaticum* EbN1. The operon includes phenylacetyl-CoA dehydrogenase (ebA5393, ebA5395, ebA5396), phenylglyoxylate:acceptor oxidoreductase (ebA5397, ebA5400, ebA5401), phenylacetate-CoA ligase (ebA5402) and several proteins with no assigned enzymatic function. Transcription of the operon was strongly upregulated in response to phenylalanine or one of its degradation products, possibly phenylacetyl-CoA. In the presence of oxygen, gene expression was reduced to 20-50% of the amount measured under anaerobic phenylalanine degradation. Basal expression with other substrates ranged from 0.5% to 10% with the exception of anaerobic HPP, where expression was slightly elevated.

Sequential metabolic pathway

(1) phenylacetate

Phenylacetate was detected solely during aerobic phenylalanine degradation. The lack of detection in cells grown anaerobically could be caused by variations in the sensitivity of GC-MS detection or by a lower rate of phenylacetate production from phenylalanine.

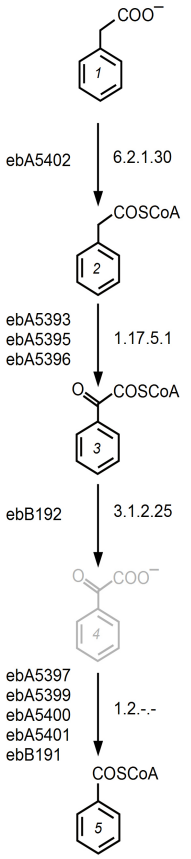

		Ace NO_3	Ace O_2	Ben NO_3	Ben O_2	Hbe NO_3	Hbe O_2	HPP NO_3	HPP O_2	Phe NO_3	Phe O_2
(1) phenylacetate		NA	NA	NA	NA	NA	NA	NA	NA	NA	495
ebA5402	T	64	45	60	79	131	100	208	111	1218	561
	P	101	NA	NA	NA	232	NA	404	424	907	751
(2) phenylacetyl-CoA		16097	3006	10006	NA	14172	1388	6336	1404	372495	730831
ebA5393	T	19	13	24	20	91	18	38	74	2047	510
	P	NA	NA	NA	NA	NA	NA	NA	NA	238	NA
ebA5395	T	13	9	14	14	48	14	32	46	921	185
	P	NA	NA	NA	NA	113	NA	179	NA	541	NA
ebA5396	T	13	7	14	14	42	12	38	43	668	176
	P	NA	NA	NA	NA	NA	NA	NA	NA	NA	NA
(3) phenylglyoxylyl-CoA		NA	NA	NA	NA	NA	NA	NA	NA	47833	4572
ebB192	T	28	18	22	31	58	42	84	65	502	244
	P	243	106	259	115	385	185	413	376	476	423
(4) phenylglyoxylate		NA	NA	NA	NA	NA	NA	NA	NA	NA	NA
ebA5397	T	25	18	25	30	79	40	95	67	1025	219
	P	NA	NA	NA	NA	127	NA	255	NA	654	177
ebA5399	T	23	13	19	28	59	30	77	50	682	169
	P	NA	NA	NA	NA	NA	NA	NA	NA	339	128
ebA5400	T	35	21	26	36	92	44	123	72	842	225
	P	NA	NA	NA	NA	120	NA	227	NA	715	155
ebA5401	T	38	23	32	46	89	55	131	76	900	284
	P	NA	NA	NA	NA	NA	NA	NA	NA	420	191
ebB191	T	43	34	45	62	115	75	139	128	1587	403
	P	NA	NA	NA	NA	65	NA	NA	NA	NA	NA
(5) benzoyl-CoA		167146	3896	4105301	1469012	31071	105397	2013293	1042478	2842400	73503

Figure 33: Anaerobic degradation of phenylacetate to benzoyl-CoA
Growth conditions are abbreviated as substrate and electron acceptor: Ace = acetate, Ben = benzoate, Hbe = 3-hydroxybenzoate, HPP = 3-(4-hydroxyphenyl)propanoate, Phe = phenylalanine, NO_3 = nitrate, O_2 = oxygen; Metabolites are indicated in bold and numbered according to the pathway diagram, genes are identified by locus tag with T indicating expression values of transcription and P indicating mascot scores of proteins; All Omics data are classified in percentiles and color coded: Gray = below detection limit, light green = lowest 30%, bright green = medium 30%, green = higher 30%, dark green = top 10%, NA = not detected metabolite or protein

(2) phenylacetyl-CoA

The formation of phenylacetyl-CoA from phenylacetate appears to be catalyzed by two phenylacetate:CoA-ligases ebA3545 and ebA5402 with only slight preferences for ebA5402 under anoxic conditions, as reflected by the protein scores. Phenylacetyl-CoA was detected in high concentrations upon aerobic and anaerobic phenylalanine degradation.

(3) phenylglyoxylyl-CoA

Alpha oxidation of phenylacetyl-CoA to phenylglyoxylyl-CoA is accomplished in one step by phenylacetyl-CoA dehydrogenase (ebA5393, ebA5395 and ebA5396). Transcription was specifically upregulated in anaerobic phenylalanine samples and proteins ebA5393 and ebA5395 were detectable only in those samples. The enzyme was found to be membrane bound in *T. aromatica* (Rhee and Fuchs, 1999; Schneider and Fuchs, 1998), explaining the absence of protein ebA5396 from the cytosolic protein preparation in the systems biology experiments.

Phenylglyoxylyl-CoA was detected in cells grown with phenylalanine under anoxic conditions and, reduced by factor 10, also in cells grown aerobically with phenylalanine.

(4) phenylglyoxylate

A predicted thioesterase (ebB192) is included in the operon, possibly catalyzing the thiolysis of phenylglyoxylyl-CoA. The gene was transcriptionally upregulated during anaerobic phenylalanine degradation, while the protein was detectable in equal concentrations during aerobic and anaerobic degradation of phenylalanine and 3-(4-hydroxyphenyl)propanoate and during anaerobic degradation of 3-hydroxybenzoate.

Free phenylglyoxylate was not detected in the GC-MS measurement. The substance is potentially not very stable during extraction and therefore difficult to detect.

(5) benzoyl-CoA

The following decarboxylation to benzoyl-CoA is carried out by phenylglyoxylate:acceptor oxidoreductase. Phenylglyoxylate:acceptor oxidoreductase subunits ebA5397, ebA5399, ebA5400, ebA5401 and ebB191, as part of the operon, showed distinct upregulation during anaerobic phenylalanine degradation. Four of the five subunits were also detectable as proteins with high mascot scores in anaerobic and low scores in aerobic phenylalanine samples. The last subunit, ebB191, was not detectable during anaerobic phenylalanine degradation. Phenylglyoxylate:acceptor oxidoreductase was previously studied in *Azoarcus evansii* and found to be membrane bound and highly sensitive to oxygen (Hirsch *et al.*, 1998). This is in accordance with the finding, that at least one subunit is not detectable in the cytosolic protein fraction.

The final product of this pathway, benzoyl-CoA, was detected in high abundance upon anaerobic degradation of phenylalanine. Degradation proceeds via the anaerobic benzoyl-CoA pathway, described in *3.3.2 Anaerobic benzoate degradation*.

3.3.4.4 Summary of aerobic and anaerobic phenylalanine degradation

According to the systems biological results, the most likely scenario for phenylalanine degradation to phenylacetate in *A. aromaticum* EbN1 is the existence of several redundant systems that act in concert under different environmental conditions. Only some of the enzymes appear to be specifically regulated in response to substrate availability, while other are expressed permanently or at least during several different degradation scenarios.

This study confirms the aerobic degradation of phenylacetate via the epoxy-CoA pathway. Nine out of eleven predicted intermediates were detected in cell extracts from aerobic phenylalanine degradation and the predicted catabolic genes showed transcript and protein levels to be specifically regulated. The lower part of the pathway was found to proceed partially via unspecific enzymes that are not included in the *paa* gene cluster for aerobic phenylacetate degradation. This is very similar to the β-oxidation sequences from other pathways in *A. aromaticum* EbN1.

The results confirm the pathway of anaerobic phenylacetate degradation in *A. aromaticum* EbN1 to proceed as described for *Pseudomonas sp* and *Thauera aromatica*. Four of the five predicted intermediates were detected in cell extracts from anaerobic phenylalanine degradation. The annotated genes were differentially transcribed and translated during anaerobic phenylalanine degradation, which confirms the previous predictions and proteomics studies (Rabus *et al.*, 2005; Wöhlbrand *et al.*, 2007).

3.3.5 Aerobic and anaerobic 3-hydroxybenzoate degradation

The hydroxylated phenolic compound 3-hydroxybenzoate can be derived from *m*-cresol degradation, 3-chlorobenzoate degradation or chemical pollution (Bonting *et al.*, 1995; Krooneman *et al.*, 1996). Aerobic degradation of 3-hydroxybenzoate via gentisate to fumarate and pyruvate is well known as the gentisate pathway (Goetz and Harmuth, 1992; Jones and Cooper, 1990). Anaerobic 3-hydroxybenzoate degradation via 3-

hydroxybenzoyl-CoA has previously been studied in *T. aromatica* and *R. palustris* (Gall *et al.*, 2013; Laempe *et al.*, 2001) but the detailed enzymatic pathway after initial dearomatization could not yet be elucidated.

3.3.5.1 Aerobic 3-hydroxybenzoate degradation pathway

Aerobic 3-hydroxybenzoate degradation in *A. aromaticum* EbN1 was previously shown to proceed via the gentisate pathway by proteomics studied (Wöhlbrand *et al.*, 2007). In this study, the pathway served as reference for aromatic degradation without the activation to CoA-esters and as control set up for the anaerobic 3-hydroxybenzoate degradation pathway (Figure 34).

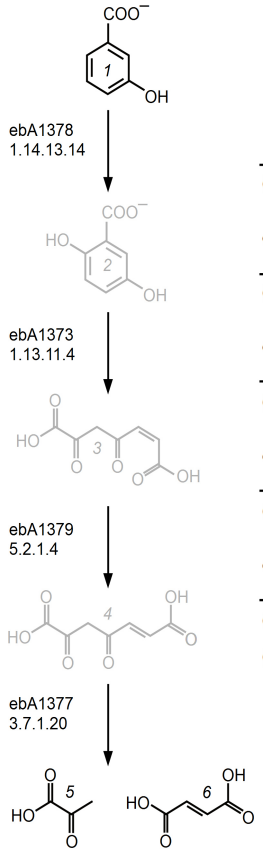

		Ace NO_3	Ace O_2	Ben NO_3	Ben O_2	Hbe NO_3	Hbe O_2	HPP NO_3	HPP O_2	Phe NO_3	Phe O_2
(1) 3-hydroxybenzoate		NA	NA	NA	NA	1410	1787	NA	NA	NA	NA
ebA1378	T	5	6	65	241	915	1360	12	24	35	43
	P	NA	NA	331	935	1045	1254	NA	354	NA	330
(2) gentisate		NA	NA	NA	NA	NA	NA	NA	NA	NA	NA
ebA1373	T	6	11	181	376	2616	1915	29	27	40	32
	P	NA	NA	318	657	612	825	NA	274	NA	86
(3) maleylpyruvate		NA	NA	NA	NA	NA	NA	NA	NA	NA	NA
ebA1379	T	4	7	61	251	824	1645	12	28	36	53
	P	NA	NA	175	613	724	921	NA	215	NA	243
(4) 3-fumarylpyruvate		NA	NA	NA	NA	NA	NA	NA	NA	NA	NA
ebA1377	T	21	28	304	1035	4242	4498	45	80	108	104
	P	NA	NA	373	698	672	813	NA	427	102	334
(5) pyruvate		499	933	1908	462	1720	1823	694	1085	NA	684
(6) fumarate		417	10042	5704	9032	2176	16778	1139	12477	629	2469

Figure 34: Aerobic degradation of 3-hydroxybenzoate via the gentisate pathway
Growth conditions are abbreviated as substrate and electron acceptor: Ace = acetate, Ben = benzoate, Hbe = 3-hydroxybenzoate, Hpp = 3-(4-hydroxyphenyl)propanoate, Phe = phenylalanine, NO3 = nitrate, O2 = oxygen; Metabolites are indicated in bold and numbered according to the pathway diagram, genes are identified by locus tag with T indicating expression values of transcription and P indicating mascot scores of proteins; All Omics data are classified in percentiles and color coded: Gray = below detection limit, light green = lowest 30%, bright green = medium 30%, green = higher 30%, dark green = top 10%, NA = not detected metabolite or protein

Intracellular 3-hydroxybenzoate was specifically detected in cells grown with this substrate aerobically or anaerobically in similar concentrations. The intermediates gentisate, maleylpyruvate and 3-fumarylpyruvate were not detected with the applied GC-MS analysis under any growth conditions. The final products fumarate and pyruvate were elevated in aerobic 3-hydroxybenzoate degrading cells. However, as important metabolites of the central metabolism, they are not specific to this catabolic pathway.

Four adjacent genes from *A. aromaticum* EbN1 are annotated as gentisate 1,2-dioxygenase (ebA1373), fumarylpyruvate hydrolase (ebA1377), salicylate-5-hydroxylase/ *m*-hydroxy-benzoate hydroxylase (ebA1378) and maleylpyruvate isomerase (ebA1379). The genes were detected as two separate mRNA strands but showed very high correlation of transcript abundance. Transcripts and protein levels of all four genes were massively upregulated in the presence of 3-hydroxybenzoate under aerobic respiration and denitrification. While the transcription was mostly independent of the oxygen availability, protein levels were reduced in the anaerobic samples. A moderate upregulation of all genes was also detected during the degradation of other aromatic compounds.

The results of this study confirm the gentisate pathway for aerobic 3-hydroxybenzoate degradation in *A. aromaticum* EbN1 as postulated previously (Rabus *et al.*, 2005; Wöhlbrand *et al.*, 2007). Of the investigated aromatic compounds, this is the only substrate that is not metabolized via a CoA-dependent but a classical aerobic dioxygenase pathway.

3.3.5.2 Anaerobic degradation of 3-hydroxybenzoate

Previous studies in *T. aromatica* showed that 3-hydroxybenzoyl-CoA was reduced by benzoyl-CoA reductase, but could not determine whether the product was the expected 3-hydroxycyclohex-1,5-diene-1-carbonyl-CoA or an isomer thereof (Laempe *et al.*, 2001). So far, no study investigated the details of 3-hydroxybenzoate degradation after the initial reductive dearomatization and none of the intermediates have previously been analyzed.

Based on enzyme homologies, the same pathway was predicted to be active in *A. aromaticum* EbN1 and enzyme function predictions were used to postulate a reaction sequence similar to β-oxidation, resulting in the formation of 4-oxopimeloyl-CoA (Rabus *et al.*, 2005; Wöhlbrand *et al.*, 2007).

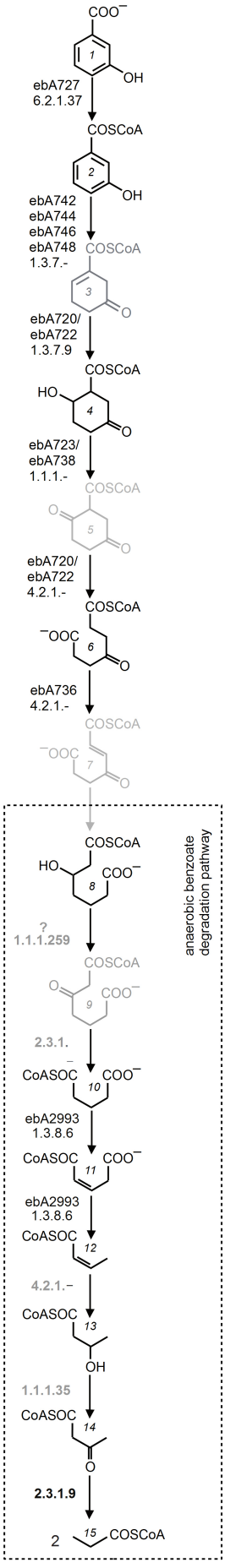

		Ace NO_3	Ace O_2	Ben NO_3	Ben O_2	Hbe NO_3	Hbe O_2	HPP NO_3	HPP O_2	Phe NO_3	Phe O_2
(1) 3-hydroxybenzoate		NA	NA	NA	NA	1410	1787	NA	NA	NA	NA
ebA727	T	28	9	14	20	753	23	14	22	36	21
	P	NA	NA	NA	NA	534	NA	NA	NA	NA	NA
(2) 3-hydroxybenzoyl-CoA		NA	NA	8629	44008	2046058	155906	2637	14917	11254	9278
ebA742	T	270	407	5062	1891	5731	907	6374	1540	4920	498
	P	795	767	1794	1144	1761	1161	1682	1319	1445	832
ebA744	T	179	318	3765	1429	3866	662	4574	1030	4076	354
	P	545	642	1417	631	1557	831	1430	1073	1401	659
ebA746	T	22	21	67	44	3743	29	69	67	129	21
	P	NA	NA	NA	NA	1083	NA	NA	NA	NA	NA
ebA748	T	18	17	91	46	1437	28	56	53	160	15
	P	NA	NA	NA	NA	1851	NA	NA	NA	NA	NA
(3) 2-ene-5-oxo-cyclohex-1-carbonyl-CoA		89012	16104	13069	21646	4257	5744	40752	5196	22078	2758
ebA720	T	4	4	5	8	242	6	4	6	13	6
	P	NA	NA	NA	NA	591	NA	NA	NA	NA	NA
(4) 2-hydroxy-5-oxo-cyclohex-1-carbonyl-CoA		NA	NA	97008	NA	187534	NA	19399	NA	7167	NA
ebA723	T	14	17	36	36	1181	21	18	15	118	16
	P	NA	NA	NA	NA	1356	128	160	NA	NA	NA
ebA738	T	34	9	30	24	423	12	21	22	96	10
	P	NA	NA	NA	NA	1039	NA	NA	NA	NA	NA
***(5) 2,5-dioxo-cyclohex-1-carbonyl-CoA**		5329.23	10008.83	12578.74	8333.55	6876.8	7964.72	2737.92	5112.14	5515.03	6220.79
ebA722	T	20	27	30	50	3204	28	19	21	87	20
	P	NA	NA	NA	NA	1165	253	NA	103	NA	91
(6) 4-oxopimeloyl-CoA_2		NA	NA	NA	NA	15408	NA	NA	NA	NA	NA
ebA736	T	22	6	19	21	277	13	15	18	71	11
	P	NA	NA	NA	NA	1235	NA	NA	326	NA	NA
(7) 2,3 dehydro-4-oxopimeloyl-CoA		NA	NA	NA	NA	NA	NA	NA	NA	NA	NA
(8) 3-hydroxypimelyl-CoA		NA	NA	417533	NA	77864	NA	131739	NA	22461	NA
1.1.1.259		NA	NA	NA	NA	NA	NA	NA	NA	NA	NA
(9) 3-ketopimelyl-CoA		NA	NA	NA	NA	NA	NA	NA	1190	NA	76491
2.3.1.-		NA	NA	NA	NA	NA	NA	NA	NA	NA	NA
(10) glutaryl-CoA		NA	NA	58243	NA	55611	NA	23728	NA	13753	NA
(11) glutaconyl-CoA		2187	NA	3567	945	5152	NA	2596	389	1872	1254
ebA2993	T	NA	220	1003	472	789	276	894	529	418	296
	P	44	80	223	186	205	70	1971	168	362	68
(12) crotonoyl-CoA		13412	21937	33520	18109	16046	7693	9258	19909	2914	801
4.2.1.150		NA	NA	NA	NA	NA	NA	NA	NA	NA	NA
(13) 3-hydroxy-butanoyl-CoA		99840	231002	313354	165324	257168	46406	206375	172621	65728	11165
1.1.1.157		NA	NA	NA	NA	NA	NA	NA	NA	NA	NA
(14) acetoacetyl-CoA		3076	7682	3776	4256	3621	2723	3023	1947	2174	1336
ebA5202	T	1530	1531	1292	1591	1377	1414	1431	1520	1165	1569
	P	1419	1489	1148	1528	1140	1300	1210	1449	718	1028
(15) acetyl-CoA		1328592	758914	846490	977224	1139162	1320983	589337	760534	886646	663864

Figure 35: Pathway of anaerobic 3-hydroxybenzoate degradation in *A. aromaticum* EbN1
The upper pathway is based on gene homologies to the 3-hydroxybenzoate degradation genes of *T. aromatica* and function prediction of the respective genes. The lower pathway is predicted based on metabolomic results from this study, suggesting a shared pathway of anaerobic benzoate and 3-hydroxybenzoate degradation via 3-hydroxypimeloyl-CoA
Growth conditions are abbreviated as substrate and electron acceptor: Ace = acetate, Ben = benzoate, Hbe = 3-hydroxybenzoate, HPP = 3-(4-hydroxyphenyl)propanoate, Phe = phenylalanine, NO_3 = nitrate, O_2 = oxygen; Metabolites are indicated in bold and numbered according to the pathway diagram, genes are identified by locus tag with T indicating expression values of transcription and P indicating mascot scores of proteins; All Omics data are classified in percentiles and color coded: Gray = below detection limit, light green = lowest 30%, bright green = medium 30%, green = higher 30%, dark green = top 10%, NA = not detected metabolite or protein;* indicates metabolites with more than one signal in HPLC-MS, which could constitute isomers and are summed for this analysis

A. aromaticum EbN1 genome encodes a gene cluster (ebA720-ebA748), ortholog to the 3-hydroxybenzoate degradation genes of *T. aromatica*. In this study, all genes of the 3-hydroxybenzoate cluster were found to be specifically expressed and translated during anaerobic 3-hydroxybenzoate degradation. These findings confirm the previously postulated role of the gene products in anaerobic degradation of 3-hydroxybenzoate. The pathway is presented in figure 35, along with a table of all related metabolomic, proteomic and transcriptomic data. The pathway metabolites are discussed sequentially below.

Sequential metabolomic pathway

(1) 3-hydroxybenzoate

Within the anaerobic 3-hydroxybenzoate gene cluster of *A. aromaticum* EbN1, genes for a C4-dicarboxylate transporter system and a putative Major-Facilitator-Superfamily (MFS) transporter are included (ebA725, ebA729 and ebA732). The genes are upregulated with the rest of the gene cluster specifically during anaerobic 3-hydroxybenzoate degradation and are probably responsible for substrate uptake under this growth condition.

Intracellular 3-hydroxybenzoate was detected specifically during 3-hydroxybenzoate degradation with similar signal intensities in aerobic and anaerobic cultures.

(2) 3-hydroxybenzoyl-CoA

After formation of a CoA-ester by the specific 3-hydroxybenzoate-CoA ligase (ebA727), highest levels of 3-hydroxybenzoyl-CoA were detected during anaerobic 3-hydroxybenzoate degradation. Thus, data are in full accordance with the reactions shown in *T. aromatica* and postulated for *A. aromaticum* EbN1 (Laempe *et al.*, 2001; Wöhlbrand *et al.*, 2007).

(3) 2-ene-5-oxo-cyclohex-1-carbonyl-CoA

Reduction of 3-hydroxybenzoyl-CoA in *A. aromaticum* EbN1 is proposed to proceed via a specific benzoyl-CoA reductase homologue, annotated as 3-hydroxybenzoyl-CoA reductase (ebA742, ebA744, ebA746 and ebA748). Subunits B and C (ebA746 and ebA748) are distinct from the enzyme of anaerobic benzoyl-CoA degradation and show highly specific transcription and translation during anaerobic 3-hydroxybenzoate degradation. In contrast to the substrate binding subunits, the ATP-binding subunits A and D (ebA742 and ebA744) show 100% sequence identity with the corresponding subunits of the benzoyl-CoA degrading enzyme, thus generating mixed transcriptomic and proteomic data. The distinct upregulation of transcription and translation during anaerobic 3-hydroxybenzoate degradation supports the role as a specific 3-hydroxybenzoyl-CoA reductase.

The proposed product of the reduction is 2-ene-5-oxocyclohex-1-carbonyl-CoA, an isomer to 6-oxocyclohex-1-ene-1-carboxyl-CoA, which is an intermediate of the anaerobic benzoyl-CoA pathway. Two signals with the exact mass of the oxocyclohexen-CoA isomers were detected by HPLC-MS analysis. One signal was specific for cells anaerobically degrading benzoyl-CoA and was thus tentatively identified as 6-oxocyclohex-1-ene-1-carboxyl-CoA. The other signal showed no clear substrate specificity. It was detected in all samples with a maximum during anaerobic acetate degradation and only medium signal intensities were detected during anaerobic 3-hydroxybenzoate degradation (supplement 30). All in all, the HPLC-MS data can neither confirm nor exclude the formation of 2-ene-5-oxo-cyclohex-1-carbonyl-CoA in the course of anaerobic 3-hydroxybenzoate degradation in *A. aromaticum* EbN1.

(4) 2-hydroxy-5-oxo-cyclohex-1-carbonyl-CoA

Hydrogenation of 2-ene-5-oxo-cyclohex-1-carbonyl-CoA to 2-hydroxy-5-oxo-cyclohex-1-carbonyl-CoA was proposed to be catalyzed by one of two enoyl-CoA hydratases, encoded in the 3-hydroxybenzoate degradation gene cluster, ebA720 or ebA722 (Wöhlbrand *et al.*, 2007). Both hydratases show specific upregulation of transcript and protein levels.

The product 2-hydroxy-5-oxo-cyclohex-1-carbonyl-CoA is an isomer to 2,3-didehydro-pimeloyl-CoA, which is an intermediate of the *Rhodopseudomonas* pathway of anaerobic

benzoyl-CoA degradation. In this analysis, five signals with the exact mass of 2-hydroxy-5-oxo-cyclohex-1-carbonyl-CoA were detected. One signal was found to be specifically elevated during anaerobic degradation of 3-hydroxybenzoate. Thus, the signal is tentatively identified as 2-hydroxy-5-oxo-cyclohex-1-carbonyl-CoA. Relative peak areas of all five signals are presented in supplement 31 and more details on the specific peak identification can be found in *3.1.1 Analysis of CoA-esters*.

(5) 2,5-dioxo-cyclohex-1-carbonyl-CoA

Dehydrogenation by one of the putative alcohol dehydrogenases, ebA723 or ebA738, which are both specifically transcribed and translated, would yield 2,5-dioxo-cyclohex-1-carbonyl-CoA. Four signals were detected with the exact mass of 2,5-dioxo-cyclohex-1-carbonyl-CoA or the isomer 2,3-dihydro-2,3-dihydroxybenzoyl-CoA from aerobic benzoate degradation (supplement 32). None of the signals was strong enough to yield MS2 data for further structure elucidation and none of the signals was specific for anaerobic 3-hydroxybenzoate degradation. However, the signal of peak 3 appeared to be specific for aerobic phenylalanine degradation. This signal most likely represents a byproduct of the epoxy-opening of the aromatic ring during aerobic phenylalanine degradation, as previous studies suggest that the reaction is prone to the production of unspecific byproducts (Teufel *et al.*, 2012). Based on this data, a role of 2,5-dioxo-cyclohex-1-carbonyl-CoA in the anaerobic 3-hydroxybenzoate degradation pathway can neither be confirmed nor denied. For representation in the pathway (Figure 35), relative peak areas of peak 1, peak 2 and peak 4 were summed.

(6) 4-oxopimeloyl-CoA

Hydrolytic ring opening by one of the predicted enoyl-CoA hydratases, ebA720 or ebA722, would yield 4-oxopimeloyl-CoA. This metabolite is an isomer of 3-oxopimeloyl-CoA, which is an intermediate of the anaerobic benzoate degradation pathway. Three signals with the exact mass of 4-oxopimeloyl-CoA were detected in the systems biological experiments. The 3-oxo-isomer could not be detected during anaerobic benzoyl-CoA degradation, probably because of the low stability of some β-oxo-CoAs, such as acetoacetyl-CoA (*3.1.1 Analysis of CoA-esters*). One signal was elevated during aerobic phenylalanine degradation and could constitute a byproduct of the epoxydase reaction. The

second signal was detected during aerobic benzoate degradation and during both aerobic and anaerobic phenylalanine degradation. The last peak was specific for anaerobic 3-hydroxybenzoate degradation and could thus represent 4-oxopimeloyl-CoA. Since no signal was detected during anaerobic benzoate degradation, the signal detected during anaerobic 3-hydroxybenzoate degradation is most likely not the 3-oxo-isomer, further supporting the postulated 4-oxo-structure.

All in all, metabolomic evidence points towards 4-oxopimelyl-CoA to be the isomeric intermediate of anaerobic 3-hydroxybenzoate degradation. However, this metabolite cannot be channeled into classical β-oxidation and no enzyme has previously been described to metabolize 4-oxopimeloyl-CoA.

(7) 2,3-dehydro-4-oxopimeloyl-CoA

The hypothetical reduction of 4-oxopimeloyl-CoA by the predicted acyl-CoA dehydrogenase ebA736 would yield 2,3-dehydro-4-oxopimeloyl-CoA, if the pathway proceeded via the typical β-oxidation sequence and the oxo-group at the fourth carbon atom would pose no hindrance. No signal with the exact mass of 2,3-dehydro-4-oxopimeloyl-CoA was detected. The metabolomic data cannot confirm this hypothetical step in anaerobic 3-hydroxybenzoate degradation. Since the 4-keto group would hamper a classical β-oxidation, it appears more likely that additional enzymatic reactions are necessary to channel the pathway toward 3-hydroxypimeloyl-CoA.

Lower pathway

4-oxopimeloyl-CoA is the last metabolite of the upper specific pathway of anaerobic 3-hydroxybenzoate degradation. Metabolomic data suggests, that the metabolite is converted to 3-hydroxypimeloyl-CoA and degradation then proceeds via the same pathway as anaerobic benzoyl-CoA degradation. Even though the enzymes for this sequence of β-oxidation reactions are not annotated without gaps, every known enzyme and every detectable intermediate that was found during anaerobic benzoyl-CoA degradation was also detected during anaerobic 3-hydroxybenzoate degradation. The lower pathway with all related metabolomic, transcriptomic and proteomic data is included in figure 35. For a detailed description of the reaction sequence, see *3.3.2 Anaerobic benzoate degradation*.

3.3.5.3 Summary of anaerobic 3-hydroxybenzoate degradation

The systems biological results confirm the anaerobic degradation of 3-hydroxybenzoate to proceed via 3-hydroxybenzoyl-CoA as described for *T. aromatica*. Furthermore, first metabolomic evidence is provided to support the predicted catabolic pathway via alternating reduction and oxidation steps to yield 4-oxopimeloyl-CoA. Of the six proposed intermediates, four were tentatively identified by their accurate mass and found to be specific for anaerobic degradation of 3-hydroxybenzoate.

Even though the exact reactions and enzymes, responsible for the further degradation of 4-oxopimeloyl-CoA, remain elusive, the systems biological data from this study suggests a lower pathway of anaerobic 3-hydroxybenzoate degradation. This newly postulated lower pathway merges anaerobic 3-hydroxybenzoate degradation and the lower anaerobic benzoate degradation at the intermediate 3-hydroxypimeloyl-CoA.

4 Conclusions

Aerobic and anaerobic biodegradation of aromatic compounds forms a complex network of peripheral and central pathways, affecting the central metabolism and cell physiology. Previous research in this area focused on single reactions and pathways, leaving several gaps in the understanding of the metabolomic network. This study aimed to gain further insights into the complexity of aromatic degradation, influencing the whole bacterial cell. To shed light on the more interrelated aspects of aromatic metabolism beyond isolated pathway analysis, the metabolism of *A. aromaticum* EbN1 was studied in detail by combining metabolomic, transcriptomic and proteomic data with physiological analyses to create a systems biological view. Thereby, the gap left by previous research was closed to gain further insights into the complexity of aerobic and anaerobic aromatic degradation. Key findings of this study regard the importance of CoA-ester analysis, adaption to the typical environment, accumulation of putative osmolytes and details on anaerobic 3-hydroxybenzoate metabolism as well as on 3-(4hydroxyphenyl)propanoate degradation. These are contemplated below.

The first important step in this work was to establish a method for the analysis of CoA-esters. Only the combination of classical GC-MS based metabolomics with CoA-ester analysis allowed to comprehensively monitor CoA-ester-based degradation pathways and the central cellular metabolism. The results stress the importance of the aerobic and anaerobic benzoyl-CoA pathways as key routes in aromatic degradation.

The fine-tuned regulation of the pathways, as well as the high transcription of specific genes even under non-benzoate-degrading conditions, reflects the adaption of *A. aromaticum* EbN1 to its natural habitat. In aqueous sediments, sudden disturbances can lead to swift changes in oxygen entry and nutrient availability. Thus, readily transcribed genes for the benzoyl-CoA pathways could save valuable time in the adaption to a changing environment.

Secondly, the accumulation of putative osmolytes during anaerobic benzoate degradation was a particular result of the comprehensive metabolomic analysis. Biosynthesis of putrescine, β-glutamate and α-glucosylglycerol were previously neither

observed nor predicted in *A. aromaticum* EbN1. The accumulation of these osmolytes correlated with a high intracellular concentration of benzoate and could present a novel mechanism of cell protection against the biostatic effects of this compound.

The detection of the putative osmolytes contributes to the understanding of the biosynthetic capabilities of the organism, in a way that could not previously be addressed by genomic and proteomic analysis. Enzymes for the biosynthesis of putrescine, β-glutamate and α-glucosylglycerol in *A. aromaticum* EbN1 could not be identified by genomic analysis. However, means of effective biosynthesis are present and further research regarding these pathways could lead to the discovery of new specific enzymatic strategies. Especially the biosynthesis of α-glucosylglycerol would be of biotechnological interest, since glucosidic compounds are increasingly investigated as enzyme stabilizing agents, food and cosmetic additives (Luley-Goedl and Nidetzky, 2011). Biosynthesis in mesophilic facultative anaerobic bacteria could provide different enzymatic strategies and allow for production outside of thermophilic organisms with exclusive nutritional requirements.

Furthermore, the accumulation of putative osmolytes during anaerobic benzoate degradation could present the first observation of a novel mechanism of benzoate tolerance in bacteria. Benzoate has been used as preservative for a long time and the studied bacterial defense mechanism include means of pH-homeostasis and efflux systems. In contrast to that, the active accumulation of benzoate in cells of *A. aromaticum* EbN1 and the apparent countervailing of its negative effects with osmolyte accumulation, represent a completely new strategy. The capability to accumulate and store the toxic, yet highly energetic substrate could be of great advantage to the organism under swiftly changing growth conditions when competing for nutrients.

Thus, this work presents the indication to further investigate the correlation of osmolyte accumulation in *A. aromaticum* EbN1 with varying benzoate concentrations. Furthermore, research regarding the biosynthesis pathways for the newly detected osmolytes could be promising for biotechnological applications. Additionally, if the accumulation of osmolytes poses a distinct advantage in the biodegradation of varying concentrations of aromatic nutrients, the mechanisms in *A. aromaticum* EbN1 and related organisms would be of interest regarding the optimization of bioremediation applications.

Additional findings of the metabolomic analysis regard the anaerobic degradation of 3-hydroxybenzoate. The predicted pathway in *A. aromaticum* EbN1 was based on differential protein expression and enzyme function predictions but no metabolomic data was available. In this thesis, anaerobic degradation of 3-hydroxybenzoate was found to proceed via 3-hydroxybenzoyl-CoA to 4-oxopimeloyl-CoA and 3-hydroxypimeloyl-CoA. For the first time, four out of the six intermediates were detected and represent the pathway in *A. aromaticum* EbN1 on a metabolomic level.

Thus, the results of this study served to narrow down the open questions in anaerobic 3-hydroxybenzoate degradation to the conversion of 4-oxopimeloyl-CoA to 3-hydroxypimeloyl-CoA. So far, 4-oxopimeloyl-CoA has not been described as metabolic intermediate of any biodegradation pathway, except as hypothetical intermediate (Rabus *et al.*, 2005; Wöhlbrand *et al.*, 2007). Sequential β-oxidation of the compound would be made difficult by the keto-group at the γ-carbon atom. However, metabolomic data strongly indicate the formation of 3-hydroxypimeloyl-CoA, which is a suitable substrate for further β-oxidation. These findings raise the question how 4-oxopimeloyl-CoA is converted to 3-hydroxypimeloyl-CoA. Acyl-CoA mutases or reductoisomerases could catalyze the rearrangement of methyl-groups, but not typically the transfer of a keto- or hydroxy-group within the molecule. Alternatively, sequential oxidation of the keto-group and elimination of the resulting hydroxy-group could give rise to 3,4-dehydropimeloyl-CoA, which in turn could be hydroxylated to 3-hydroxypimeloyl-CoA. However, none of the putative intermediates of this reaction sequence were detected in this study.

Despite the open questions regarding the formation of 3-hydroxypimeloyl-CoA, the systems biological data revealed a distinct lower pathway of anaerobic 3-hydroxybenzoate degradation. This reaction sequence is analogue to the lower pathway of anaerobic benzoyl-CoA degradation and ultimately converts 3-hydroxypimeloyl-CoA to three molecules of acetyl-CoA.

Lastly, the systems biological data from this thesis shed new light on the predicted dehydroxylation of 4-hydroxybenzoyl-CoA during HPP degradation. The data showed that the predicted 4-hydroxybenzoyl-CoA reductase transcription and translation was not upregulated during anaerobic HPP degradation and the reaction appeared impaired during aerobic growth. Thus, the data from this study indicate a reaction different from the

predicted 4-hydroxybenzoyl-CoA reductase mediated dehydroxylation.

So far, the only characterized 4-hydroxybenzoyl-CoA reductase in literature is the enzyme from *T. aromatica*. 4-hydroxybenzoyl-CoA reduction and benzoyl-CoA reduction are both catalyzed by enzymes employing birch-like radical reaction mechanism (Boll, 2004; Boll and Fuchs, 2005). However, activity on 4-hydroxybenzoyl-CoA has been experimentally ruled out for the benzoyl-CoA reductase from *T. aromatica*. Homologs for both enzymes are annotated in *A. aromaticum* EbN1 with high similarities but were not biochemically characterized regarding their substrate spectrum. In the light of the systems biological data from this study, it appears possible that the benzoyl-CoA reductase of *A. aromaticum* EbN1 is involved in the reduction of 4-hydroxybenzoyl-CoA during anaerobic and/or aerobic HPP degradation. Future investigation of the substrate specificity of this enzyme could provide new insight into the mechanisms of radical assisted anaerobic reduction; a research area with only moderate coverage but possibly great value for biotechnological applications.

References

Allet, N., Barrillat, N., Baussant, T., Boiteau, C., Botti, P., Bougueleret, L., Budin, N., Canet, D., Carraud, S., Chiappe, D., Christmann, N., Colinge, J., Cusin, I., Dafflon, N., Depresle, B., Fasso, I., Frauchiger, P., Gaertner, H., Gleizes, A., Gonzalez-Couto, E., Jeandenans, C., Karmime, A., Kowall, T., Lagache, S., Mahé, E., Masselot, A., Mattou, H., Moniatte, M., Niknejad, A., Paolini, M., Perret, F., Pinaud, N., Ranno, F., Raimondi, S., Reffas, S., Regamey, P.-O., Rey, P.-A., Rodriguez-Tomé, P., Rose, K., Rossellat, G., Saudrais, C., Schmidt, C., Villain, M., Zwahlen, C., 2004. In vitro and in silico processes to identify differentially expressed proteins. PROTEOMICS 4, 2333–2351.

Allwood, J.W., Goodacre, R., 2010. An introduction to liquid chromatography–mass spectrometry instrumentation applied in plant metabolomic analyses. Phytochem. Anal. 21, 33–47.

Altenschmidt, U., Oswald, B., Fuchs, G., 1991. Purification and characterization of benzoate-coenzyme A ligase and 2-aminobenzoate-coenzyme A ligases from a denitrifying *Pseudomonas* sp. J. Bacteriol. 173, 5494–5501.

Altenschmidt, U., Oswald, B., Steiner, E., Herrmann, H., Fuchs, G., 1993. New aerobic benzoate oxidation pathway via benzoyl-coenzyme A and 3-hydroxybenzoyl-coenzyme A in a denitrifying *Pseudomonas* sp. J. Bacteriol. 175, 4851–4858.

Anders, H.-J., Kaetzke, A., Kämpfer, P., Ludwig, W., Fuchs, G., 1995. Taxonomic Position of Aromatic-Degrading Denitrifying *Pseudomonad* Strains K 172 and KB 740 and Their Description as New Members of the Genera *Thauera*, as *Thauera aromatica* sp. nov., and *Azoarcus*, as *Azoarcus evansii* sp. nov., Respectively, Members of the Beta Subclass of the Proteobacteria. Int. J. Syst. Bacteriol. 45, 327–333.

Anderson, A.J., Dawes, E.A., 1990. Occurrence, metabolism, metabolic role, and industrial uses of bacterial polyhydroxyalkanoates. Microbiol. Rev. 54, 450–472.

Armando, J. w., Boghigian, B. a., Pfeifer, B. a., 2012. LC-MS/MS quantification of short-chain acyl-CoA's in *Escherichia coli* demonstrates versatile propionyl-CoA synthetase substrate specificity. Lett. Appl. Microbiol. 54, 140–148.

Bantscheff, M., Lemeer, S., Savitski, M.M., Kuster, B., 2012. Quantitative mass spectrometry in proteomics: critical review update from 2007 to the present. Anal. Bioanal. Chem. 404, 939–965.

Barbour, T.G.H., Vincent, J.M., 1950. The bacteriostatic action of phenol, benzoic acid and related compounds on *Bacterium aerogenes*. J. Gen. Microbiol. 4, 110–121.

Bennett, B.D., Kimball, E.H., Gao, M., Osterhout, R., Van Dien, S.J., Rabinowitz, J.D., 2009. Absolute metabolite concentrations and implied enzyme active site occupancy in *Escherichia coli*. Nat. Chem. Biol. 5, 593–599.

Benton, H.P., Want, E.J., Ebbels, T.M.D., 2010. Correction of mass calibration gaps in liquid chromatography–mass spectrometry metabolomics data. Bioinformatics 26, 2488–2489.

Boll, M., 2004. Key enzymes in the anaerobic aromatic metabolism catalysing Birch-like reductions. Biochim. Biophys. Acta BBA - Bioenerg., Functional Redox Radicals in Proteins 1707, 34–50.

Boll, M., Fuchs, G., 2005. Unusual reactions involved in anaerobic metabolism of phenolic compounds. Biol. Chem. 386, 989–997.

Boll, M., Fuchs, G., 1995. Benzoyl-Coenzyme A Reductase (Dearomatizing), a Key Enzyme of Anaerobic Aromatic Metabolism. Eur. J. Biochem. 234, 921–933.

Boll, M., Löffler, C., Morris, B.E.L., Kung, J.W., 2014. Anaerobic degradation of homocyclic aromatic compounds via arylcarboxyl-coenzyme A esters: organisms, strategies and key enzymes. Environ. Microbiol.

Bolten, C.J., Kiefer, P., Letisse, F., Portais, J.-C., Wittmann, C., 2007. Sampling for Metabolome Analysis of Microorganisms. Anal. Chem. 79, 3843–3849.

Bonting, C.F.C., Schneider, S., Schmidtberg, G., Fuchs, G., 1995. Anaerobic degradation ofm-cresol via methyl oxidation to 3-hydroxybenzoate by a denitrifying bacterium. Arch. Microbiol. 164, 63–69.

Brackmann, R., Fuchs, G., 1993. Enzymes of anaerobic metabolism of phenolic compounds. Eur. J. Biochem. 213, 563–571.

Breese, K., Fuchs, G., 1998. 4-Hydroxybenzoyl-CoA reductase (dehydroxylating) from the denitrifying bacterium *Thauera aromatica.* Eur. J. Biochem. 251, 916–923.

Buckstein, M.H., He, J., Rubin, H., 2008. Characterization of Nucleotide Pools as a Function of Physiological State in *Escherichia coli*. J. Bacteriol. 190, 718–726.

Cao, B., Nagarajan, K., Loh, K.-C., 2009. Biodegradation of aromatic compounds: current status and opportunities for biomolecular approaches. Appl. Microbiol. Biotechnol. 85, 207–228.

Carroll, D.I., Dzidic, I., Stillwell, R.N., Horning, M.G., Horning, E.C., 1974. Subpicogram detection system for gas phase analysis based upon atmospheric pressure ionization (API) mass spectrometry. Anal. Chem. 46, 706–710.

Collier, L.S., Nichols, N.N., Neidle, E.L., 1997. benK encodes a hydrophobic permease-like protein involved in benzoate degradation by *Acinetobacter* sp. strain ADP1. J. Bacteriol. 179, 5943–5946.

Conesa, A., Mortazavi, A., 2014. The common ground of genomics and systems biology. BMC Syst. Biol. 8, S1.

Cunningham, L., Gruer, M.J., Guest, J.R., 1997. Transcriptional regulation of the aconitase genes (acnA and acnB) of *Escherichia coli*. Microbiol. Read. Engl. 143 (Pt 12), 3795–3805.

Debnar-Daumler, C., Seubert, A., Schmitt, G., Heider, J., 2014. Simultaneous Involvement of a Tungsten-Containing Aldehyde:Ferredoxin Oxidoreductase and a Phenylacetaldehyde Dehydrogenase in Anaerobic Phenylalanine Metabolism. J. Bacteriol. 196, 483–492.

DeJongh, D.C., Radford, T., Hribar, J.D., Hanessian, S., Bieber, M., Dawson, G., Sweeley, C.C., 1969. Analysis of trimethylsilyl derivatives of carbohydrates by gas chromatography and mass spectrometry. J. Am. Chem. Soc. 91, 1728–1740.

Dettmer, K., Aronov, P.A., Hammock, B.D., 2007. Mass spectrometry-based metabolomics. Mass Spectrom. Rev. 26, 51–78.

Díaz, E., Jiménez, J.I., Nogales, J., 2013. Aerobic degradation of aromatic compounds. Curr. Opin. Biotechnol. 24, 431–442.

Durante-Rodríguez, G., Zamarro, M.T., García, J.L., Díaz, E., Carmona, M., 2008. New insights into the BzdR-mediated transcriptional regulation of the anaerobic catabolism of benzoate in *Azoarcus* sp. CIB. Microbiol. Read. Engl. 154, 306–316.

Durante-Rodríguez, G., Zamarro, M.T., García, J.L., Díaz, E., Carmona, M., 2006. Oxygen-Dependent Regulation of the Central Pathway for the Anaerobic Catabolism of Aromatic Compounds in *Azoarcus* sp. Strain CIB. J. Bacteriol. 188, 2343–2354.

Dutton, P.L., Evans, W.C., 1970. Inhibition of aromatic photometabolism in *Rhodopseudomonas palustris* by fatty acids. Arch. Biochem. Biophys. 136, 228–232.

Dutton, P.L., Evans, W.C., 1968. The photometabolism of benzoic acid by *Rhodopseudomonas palustris*: a new pathway of aromatic ring metabolism. Biochem. J. 109, 5P–6P.

Ebenau-Jehle, C., Boll, M., Fuchs, G., 2003. 2-Oxoglutarate:NADP(+) oxidoreductase in *Azoarcus evansii*: properties and function in electron transfer reactions in aromatic ring reduction. J. Bacteriol. 185, 6119–6129.

Empadinhas, N., da Costa, M.S., 2011. Diversity, biological roles and biosynthetic pathways for sugar-glycerate containing compatible solutes in bacteria and archaea. Environ. Microbiol. 13, 2056–2077.

Fiehn, O., 2002. Metabolomics--the link between genotypes and phenotypes. Plant Mol. Biol. 48, 155–171.

Fiehn, O., Kopka, J., Dörmann, P., Altmann, T., Trethewey, R.N., Willmitzer, L., 2000a. Metabolite profiling for plant functional genomics. Nat. Biotechnol. 18, 1157–1161.

Fiehn, O., Kopka, J., Trethewey, R.N., Willmitzer, L., 2000b. Identification of Uncommon Plant Metabolites Based on Calculation of Elemental Compositions Using Gas Chromatography and Quadrupole Mass Spectrometry. Anal. Chem. 72, 3573–3580.

Fuchs, G., Boll, M., Heider, J., 2011. Microbial degradation of aromatic compounds — from one strategy to four. Nat. Rev. Microbiol. 9, 803–816.

Gall, D.L., Ralph, J., Donohue, T.J., Noguera, D.R., 2013. Benzoyl Coenzyme A Pathway-Mediated Metabolism of meta-Hydroxy-Aromatic Acids in *Rhodopseudomonas palustris*. J. Bacteriol. 195, 4112–4120.

Gescher, J., Eisenreich, W., Wörth, J., Bacher, A., Fuchs, G., 2005. Aerobic benzoyl-CoA catabolic pathway in *Azoarcus evansii*: studies on the non-oxygenolytic ring cleavage enzyme. Mol. Microbiol. 56, 1586–1600.

Gescher, J., Ismail, W., Olgeschlager, E., Eisenreich, W., Worth, J., Fuchs, G., 2006. Aerobic Benzoyl-Coenzyme A (CoA) Catabolic Pathway in *Azoarcus evansii*: Conversion of Ring Cleavage Product by 3,4-Dehydroadipyl-CoA Semialdehyde Dehydrogenase. J. Bacteriol. 188, 2919–2927.

Gilibili, R.R., Kandaswamy, M., Sharma, K., Giri, S., Rajagopal, S., Mullangi, R., 2011. Development and validation of a highly sensitive LC-MS/MS method for simultaneous quantitation of acetyl-CoA and malonyl-CoA in animal tissues. Biomed. Chromatogr. 25, 1352–1359.

Giuliodori, A.M., Gualerzi, C.O., Soto, S., Vila, J., Tavío, M.M., 2007. Review on Bacterial Stress Topics. Ann. N. Y. Acad. Sci. 1113, 95–104.

Goetz, F.E., Harmuth, L.J., 1992. Gentisate pathway in *Salmonella typhimurium*: metabolism of m-hydroxybenzoate and gentisate. FEMS Microbiol. Lett. 97, 45–49.

Halket, J.M., Waterman, D., Przyborowska, A.M., Patel, R.K.P., Fraser, P.D., Bramley, P.M., 2005. Chemical derivatization and mass spectral libraries in metabolic profiling by GC/MS and LC/MS/MS. J. Exp. Bot. 56, 219–243.

Hamilton, R.D., Holm-Hansen, O., 1967. Adenosine Triphosphate Content of Marine Bacteria1. Limnol. Oceanogr. 12, 319–324.

Härtel, U., Eckel, E., Koch, J., Fuchs, G., Linder, D., Buckel, W., 1993. Purification of glutaryl-CoA dehydrogenase from *Pseudomonas* sp., an enzyme involved in the anaerobic degradation of benzoate. Arch. Microbiol. 159, 174–181.

Heider, J., Fuchs, G., 1997. Anaerobic Metabolism of Aromatic Compounds. Eur. J. Biochem. 243, 577–596.

Hengge-Aronis, R., 2002. Signal Transduction and Regulatory Mechanisms Involved in Control of the σS (RpoS) Subunit of RNA Polymerase. Microbiol. Mol. Biol. Rev. 66, 373–395.

Hille, R., Hall, J., Basu, P., 2014. The Mononuclear Molybdenum Enzymes. Chem. Rev. 114, 3963–4038.

Hiller, K., Hangebrauk, J., Jäger, C., Spura, J., Schreiber, K., Schomburg, D., 2009. MetaboliteDetector: Comprehensive Analysis Tool for Targeted and Nontargeted GC/MS Based Metabolome Analysis. Anal. Chem. 81, 3429–3439.

Hirsch, W., Schägger, H., Fuchs, G., 1998. Phenylglyoxylate:NAD+ oxidoreductase (CoA benzoylating), a new enzyme of anaerobic phenylalanine metabolism in the denitrifying bacterium *Azoarcus evansii*. Eur. J. Biochem. FEBS 251, 907–915.

Holms, W.H., 1987. Control of flux through the citric acid cycle and the glyoxylate bypass in *Escherichia coli*. Biochem. Soc. Symp. 54, 17–31.

Hungate, R.E., 1969. Chapter IV A Roll Tube Method for Cultivation of Strict Anaerobes, in: Ribbons, J.R.N. and D.W. (Ed.), Methods in Microbiology. Academic Press, pp. 117–132.

Ismail, W., El-Said Mohamed, M., Wanner, B.L., Datsenko, K.A., Eisenreich, W., Rohdich, F., Bacher, A., Fuchs, G., 2003. Functional genomics by NMR spectroscopy. Phenylacetate catabolism in *Escherichia coli*. Eur. J. Biochem. FEBS 270, 3047–3054.

Ismail, W., Gescher, J., 2012. Epoxy Coenzyme A Thioester pathways for degradation of aromatic compounds. Appl. Environ. Microbiol. 78, 5043–5051.

Issaq, H.J., Van, Q.N., Waybright, T.J., Muschik, G.M., Veenstra, T.D., 2009. Analytical and statistical approaches to metabolomics research. J. Sep. Sci. 32, 2183–2199.

Jellum, E., Kvittingen, E.A., Stokke, O., 1988. Mass spectrometry in diagnosis of metabolic disorders. Biomed. Environ. Mass Spectrom. 16, 57–62.

Jones, D.C.N., Cooper, R.A., 1990. Catabolism of 3-hydroxybenzoate by the gentisate pathway in *Klebsiella pneumoniae* M5a1. Arch. Microbiol. 154, 489–495.

Kell, D.B., 2004. Metabolomics and systems biology: making sense of the soup. Curr. Opin. Microbiol. 7, 296–307.

Kelleher, D.E., Mohr, P.J., Martin, W.C., Wiese, W.L., Sugar, J., Fuhr, J.R., Olsen, K., Musgrove, A., Reader, J., Sansonetti, C.J., Dalton, G.R., 1999. New NIST Atomic Spectra Database. pp. 170–179.

Kim, J., Darley, D., Buckel, W., 2005. 2-Hydroxyisocaproyl-CoA dehydratase and its activator from *Clostridium difficile*. FEBS J. 272, 550–561.

Kind, T., Wohlgemuth, G., Lee, D.Y., Lu, Y., Palazoglu, M., Shahbaz, S., Fiehn, O., 2009. FiehnLib – mass spectral and retention index libraries for metabolomics based on quadrupole and time-of-flight gas chromatography/mass spectrometry. Anal. Chem. 81, 10038–10048.

Kitko, R.D., Wilks, J.C., Garduque, G.M., Slonczewski, J.L., 2010. Osmolytes Contribute to pH Homeostasis of *Escherichia coli*. PLoS ONE 5, e10078.

Koch, J., Fuchs, G., 1992. Enzymatic reduction of benzoyl-CoA to alicyclic compounds, a key reaction in anaerobic aromatic metabolism. Eur. J. Biochem. 205, 195–202.

Kolkmann, R., Leistner, E., 1987. Synthesis, Analysis and Characterization of the Coenzyme A Esters of o-SuccinylIbenzoic Acid, an Intermediate in Vitamin K2 (Menaquinone) Biosynthesis. Z. Für Naturforschung C 42, 542–552.

Kopka, J., Schauer, N., Krueger, S., Birkemeyer, C., Usadel, B., Bergmüller, E., Dörmann, P., Weckwerth, W., Gibon, Y., Stitt, M., Willmitzer, L., Fernie, A.R., Steinhauser, D., 2005. GMD@CSB.DB: the Golm Metabolome Database. Bioinformatics 21, 1635–1638.

Kováts, E., 1958. Gas-chromatographische Charakterisierung organischer Verbindungen. Teil 1: Retentionsindices aliphatischer Halogenide, Alkohole, Aldehyde und Ketone. Helv. Chim. Acta 41, 1915–1932.

Krebs, H.A., Wiggins, D., Stubbs, M., Sols, A., Bedoya, F., 1983. Studies on the mechanism of the antifungal action of benzoate. Biochem. J. 214, 657–663.

Krooneman, J., Wieringa, E.B., Moore, E.R., Gerritse, J., Prins, R.A., Gottschal, J.C., 1996. Isolation of *Alcaligenes* sp. strain L6 at low oxygen concentrations and degradation of 3-chlorobenzoate via a pathway not involving (chloro)catechols. Appl. Environ. Microbiol. 62, 2427–2434.

Kurz, M., 2008. Compatible solute influence on nucleic acids: Many questions but few answers. Saline Syst. 4, 6.

Laass, S., Kleist, S., Bill, N., Drüppel, K., Kossmehl, S., Wöhlbrand, L., Rabus, R., Klein, J., Rohde, M., Bartsch, A., Wittmann, C., Schmidt-Hohagen, K., Tielen, P., Jahn, D., Schomburg, D., 2014. Gene Regulatory and Metabolic Adaptation Processes of *Dinoroseobacter shibae* DFL12T during Oxygen Depletion. J. Biol. Chem. 289, 13219–13231.

Laempe, D., Jahn, M., Breese, K., Schägger, H., Fuchs, G., 2001. Anaerobic Metabolism of 3-Hydroxybenzoate by the Denitrifying Bacterium *Thauera aromatica*. J. Bacteriol. 183, 968–979.

Leaf, T.A., Srienc, F., 1998. Metabolic modeling of polyhydroxybutyrate biosynthesis. Biotechnol. Bioeng. 57, 557–570.

Lin, J., Lee, I.S., Frey, J., Slonczewski, J.L., Foster, J.W., 1995. Comparative analysis of extreme acid survival in *Salmonella typhimurium*, *Shigella flexneri*, and *Escherichia coli*. J. Bacteriol. 177, 4097–4104.

Lin, J., Smith, M.P., Chapin, K.C., Baik, H.S., Bennett, G.N., Foster, J.W., 1996. Mechanisms of acid resistance in enterohemorrhagic *Escherichia coli*. Appl. Environ. Microbiol. 62, 3094–3100.

Löffler, F., Müller, R., Lingens, F., 1992. Purification and properties of 4-halobenzoate-coenzyme A ligase from *Pseudomonas* sp. CBS3. Biol. Chem. Hoppe. Seyler 373, 1001–1007.

López Barragán, M.J., Carmona, M., Zamarro, M.T., Thiele, B., Boll, M., Fuchs, G., García, J.L., Díaz, E., 2004. The bzd gene cluster, coding for anaerobic benzoate catabolism, in *Azoarcus* sp. strain CIB. J. Bacteriol. 186, 5762–5774.

Lowry, O.H., Carter, J., Ward, J.B., Glaser, L., 1971. The Effect of Carbon and Nitrogen Sources on the Level of Metabolic Intermediates in *Escherichia coli*. J. Biol. Chem. 246, 6511–6521.

Luley-Goedl, C., Nidetzky, B., 2011. Glycosides as compatible solutes: biosynthesis and applications. Nat. Prod. Rep. 28, 875–896.

Lusk, G., 1911. The use of sodium benzoate as a preservative of food. Science 34, 759–760.

Magnes, C., Suppan, M., Pieber, T.R., Moustafa, T., Trauner, M., Haemmerle, G., Sinner, F.M., 2008. Validated comprehensive analytical method for quantification of coenzyme A activated compounds in biological tissues by online solid-phase extraction LC/MS/MS. Anal. Chem. 80, 5736–5742.

Mäkelä, M.R., Donofrio, N., de Vries, R.P., 2014. Plant biomass degradation by fungi. Fungal Genet. Biol., Biomass Degradation by Fungi 72, 2–9.

Martínez-Blanco, H., Reglero, A., Rodriguez-Aparicio, L.B., Luengo, J.M., 1990. Purification and biochemical characterization of phenylacetyl-CoA ligase from *Pseudomonas putida*. A specific enzyme for the catabolism of phenylacetic acid. J. Biol. Chem. 265, 7084–7090.

Mashego, M.R., Rumbold, K., Mey, M.D., Vandamme, E., Soetaert, W., Heijnen, J.J., 2006. Microbial metabolomics: past, present and future methodologies. Biotechnol. Lett. 29, 1–16.

Matrix Science Inc, 2015. MS/MS Results Interpretation. http://www.matrixscience.com.

Matyash, V., Liebisch, G., Kurzchalia, T.V., Shevchenko, A., Schwudke, D., 2008. Lipid extraction by methyl-tert-butyl ether for high-throughput lipidomics. J. Lipid Res. 49, 1137–1146.

McClure, R., Balasubramanian, D., Sun, Y., Bobrovskyy, M., Sumby, P., Genco, C.A., Vanderpool, C.K., Tjaden, B., 2013. Computational analysis of bacterial RNA-Seq data. Nucleic Acids Res. 41, e140–e140.

Michal, G., Schomburg, D., 2012. Biochemical Pathways: An Atlas of Biochemistry and Molecular Biology, 2. Auflage. ed. John Wiley & Sons, Hoboken, N.J.

Minkler, P.E., Kerner, J., Kasumov, T., Parland, W., Hoppel, C.L., 2006. Quantification of malonyl-coenzyme A in tissue specimens by high-performance liquid chromatography/mass spectrometry. Anal. Biochem. 352, 24–32.

Möbitz, H., Boll, M., 2002. A Birch-like Mechanism in Enzymatic Benzoyl-CoA Reduction: A Kinetic Study of Substrate Analogues Combined with an ab Initio Model†. Biochemistry (Mosc.) 41, 1752–1758.

Mohamed, M.E., Zaar, A., Ebenau-Jehle, C., Fuchs, G., 2001. Reinvestigation of a new type of aerobic benzoate metabolism in the proteobacterium *Azoarcus evansii*. J. Bacteriol. 183, 1899–1908.

Mohamed, M., Ismail, W., Heider, J., Fuchs, G., 2002. Aerobic metabolism of phenylacetic acids in *Azoarcus evansii*. Arch. Microbiol. 178, 180–192.

Muhr, E., Schühle, K., Clermont, L., Sünwoldt, K., Kleinsorge, D., Seyhan, D., Kahnt, J., Schall, I., Cordero, P.R., Schmitt, G., Heider, J., 2015. Enzymes of anaerobic ethylbenzene and p-ethylphenol catabolism in "*Aromatoleum aromaticum*": differentiation and differential induction. Arch. Microbiol. 197, 1051–1062.

Neidhardt, F.C., Ingraham, J.L., Schaechter, M., 1990. Physiology of the Bacterial Cell: A Molecular Approach. Sinauer Associates Inc.,U.S., Sunderland, Mass.

Onorato, J., Chen, L., Shipkova, P., Ma, Z., Azzara, A., Devenny, J., Liang, N., Haque, T., Cheng, D., 2010. Liquid-liquid extraction coupled with LC/MS/MS for monitoring of malonyl-CoA in rat brain tissue. Anal. Bioanal. Chem. 397, 3137–3142.

Pelletier, D.A., Harwood, C.S., 2000. 2-Hydroxycyclohexanecarboxyl Coenzyme A Dehydrogenase, an Enzyme Characteristic of the Anaerobic Benzoate Degradation Pathway Used by *Rhodopseudomonas palustris*. J. Bacteriol. 182, 2753 –2760.

Perkins, D.N., Pappin, D.J.C., Creasy, D.M., Cottrell, J.S., 1999. Probability-based protein identification by searching sequence databases using mass spectrometry data. ELECTROPHORESIS 20, 3551–3567.

Perrotta, J.A., Harwood, C.S., 1994. Anaerobic Metabolism of Cyclohex-1-Ene-1-Carboxylate, a Proposed Intermediate of Benzoate Degradation, by *Rhodopseudomonas palustris*. Appl. Environ. Microbiol. 60, 1775–1782.

Peyraud, R., Kiefer, P., Christen, P., Massou, S., Portais, J.-C., Vorholt, J.A., 2009. Demonstration of the ethylmalonyl-CoA pathway by using 13C metabolomics. Proc Natl Acad Sci U S A 106, 4846–4851.

Philipp, B., Schink, B., 2012. Different strategies in anaerobic biodegradation of aromatic compounds: nitrate reducers versus strict anaerobes. Environ. Microbiol. Rep. 4, 469–478.

Quester, S., Schomburg, D., 2011. EnzymeDetector: an integrated enzyme function prediction tool and database. BMC Bioinformatics 12, 376.

Rabus, R., 2005. Functional genomics of an anaerobic aromatic-degrading denitrifying bacterium, strain EbN1. Appl. Microbiol. Biotechnol. 68, 580–587.

Rabus, R., Kube, M., Heider, J., Beck, A., Heitmann, K., Widdel, F., Reinhardt, R., 2005. The genome sequence of an anaerobic aromatic-degrading denitrifying bacterium, strain EbN1. Arch. Microbiol. 183, 27–36.

Rabus, R., Trautwein, K., Wöhlbrand, L., 2014. Towards habitat-oriented systems biology of "*Aromatoleum aromaticum*" EbN1 : Chemical sensing, catabolic network modulation and growth control in anaerobic aromatic compound degradation. Appl. Microbiol. Biotechnol.

Rabus, R., Widdel, F., 1995. Anaerobic degradation of ethylbenzene and other aromatic hydrocarbons by new denitrifying bacteria. Arch. Microbiol. 163, 96–103.

Rather, L.J., Knapp, B., Haehnel, W., Fuchs, G., 2010. Coenzyme A-dependent aerobic metabolism of benzoate via epoxide formation. J. Biol. Chem. 285, 20615–20624.

Rather, L.J., Weinert, T., Demmer, U., Bill, E., Ismail, W., Fuchs, G., Ermler, U., 2011. Structure and Mechanism of the Diiron Benzoyl-Coenzyme A Epoxidase BoxB. J. Biol. Chem. 286, 29241–29248.

Reed, L.J., Cox, D.J., 1970. 4 Multienzyme Complexes, in: Boyer, P.D. (Ed.), The Enzymes. Academic Press, pp. 213–240.

Reiner, A.M., 1971. Metabolism of benzoic acid by bacteria: 3,5-cyclohexadiene-1,2-diol-1-carboxylic acid is an intermediate in the formation of catechol. J. Bacteriol. 108, 89–94.

Reszko, A.E., Kasumov, T., Comte, B., Pierce, B.A., David, F., Bederman, I.R., Deutsch, J., Des Rosiers, C., Brunengraber, H., 2001. Assay of the Concentration and 13C-Isotopic Enrichment of Malonyl–Coenzyme A by Gas Chromatography–Mass Spectrometry. Anal. Biochem. 298, 69–75.

Rhee, S.K., Fuchs, G., 1999. Phenylacetyl-CoA:acceptor oxidoreductase, a membrane-bound molybdenum-iron-sulfur enzyme involved in anaerobic metabolism of phenylalanine in the denitrifying bacterium *Thauera aromatica*. Eur. J. Biochem. FEBS 262, 507–515.

Robertson, D.E., Roberts, M.F., Belay, N., Stetter, K.O., Boone, D.R., 1990. Occurrence of beta-glutamate, a novel osmolyte, in marine methanogenic bacteria. Appl. Environ. Microbiol. 56, 1504–1508.

Ruzicka, F.J., Frey, P.A., 2007. Glutamate 2,3-aminomutase: A new member of the radical SAM superfamily of enzymes. Biochim. Biophys. Acta BBA - Proteins Proteomics 1774, 286–296.

Saum, S.H., Sydow, J.F., Palm, P., Pfeiffer, F., Oesterhelt, D., Müller, V., 2006. Biochemical and molecular characterization of the biosynthesis of glutamine and glutamate, two major compatible solutes in the moderately halophilic bacterium *Halobacillus halophilus*. J. Bacteriol. 188, 6808–6815.

Sawangwan, T., Goedl, C., Nidetzky, B., 2010. Glucosylglycerol and glucosylglycerate as enzyme stabilizers. Biotechnol. J. 5, 187–191.

Schneider, S., Fuchs, G., 1998. Phenylacetyl-CoA:acceptor oxidoreductase, a new alpha-oxidizing enzyme that produces phenylglyoxylate. Assay, membrane localization, and differential production in *Thauera aromatica*. Arch. Microbiol. 169, 509–516.

Schneider, S., Mohamed, M.E., Fuchs, G., 1997. Anaerobic metabolism of L-phenylalanine via benzoyl-CoA in the denitrifying bacterium *Thauera aromatica*. Arch. Microbiol. 168, 310–320.

Senior, P.J., Dawes, E.A., 1971. Poly-β-hydroxybutyrate biosynthesis and the regulation of glucose metabolism in *Azotobacter beijerinckii*. Biochem. J. 125, 55–66.

Smith, C.A., Want, E.J., O'Maille, G., Abagyan, R., Siuzdak, G., 2006. XCMS: Processing Mass Spectrometry Data for Metabolite Profiling Using Nonlinear Peak Alignment, Matching, and Identification. Anal. Chem. 78, 779–787.

Sorek, R., Cossart, P., 2010. Prokaryotic transcriptomics: a new view on regulation, physiology and pathogenicity. Nat. Rev. Genet. 11, 9–16.

Strehmel, N., Kopka, J., Scheel, D., Böttcher, C., 2013. Annotating unknown components from GC/EI-MS-based metabolite profiling experiments using GC/APCI(+)-QTOFMS. Metabolomics 10, 324–336.

Tamang, D.G., Rabus, R., Barabote, R.D., Saier, M.H., 2009. Comprehensive Analyses of Transport Proteins Encoded Within the Genome of "*Aromatoleum aromaticum*" Strain EbN1. J. Membr. Biol. 229, 53–90.

Tarvin, D., Buswell, A.M., 1934. The Methane Fermentation of Organic Acids and Carbohydrates1,2. J. Am. Chem. Soc. 56, 1751–1755.

Tautenhahn, R., Böttcher, C., Neumann, S., 2008. Highly sensitive feature detection for high resolution LC/MS. BMC Bioinformatics 9, 504.

Teufel, R., Friedrich, T., Fuchs, G., 2012. An oxygenase that forms and deoxygenates toxic epoxide. Nature 483, 359–362.

Teufel, R., Gantert, C., Voss, M., Eisenreich, W., Haehnel, W., Fuchs, G., 2011. Studies on the mechanism of ring hydrolysis in phenylacetate degradation: a metabolic branching point. J. Biol. Chem. 286, 11021–11034.

Teufel, R., Mascaraque, V., Ismail, W., Voss, M., Perera, J., Eisenreich, W., Haehnel, W., Fuchs, G., 2010. Bacterial phenylalanine and phenylacetate catabolic pathway revealed. Proc. Natl. Acad. Sci. U. S. A. 107, 14390–14395.

Tjaden, B., 2015. De novo assembly of bacterial transcriptomes from RNA-seq data. Genome Biol. 16, 1.

Trautwein, K., Kühner, S., Wöhlbrand, L., Halder, T., Kuchta, K., Steinbüchel, A., Rabus, R., 2008. Solvent Stress Response of the Denitrifying Bacterium "*Aromatoleum aromaticum*" Strain EbN1. Appl. Environ. Microbiol. 74, 2267–2274.

Trautwein, K., Lahme, S., Wöhlbrand, L., Feenders, C., Mangelsdorf, K., Harder, J., Steinbüchel, A., Blasius, B., Reinhardt, R., Rabus, R., 2012a. Physiological and proteomic adaptation of "*Aromatoleum aromaticum*" EbN1 to low growth rates in benzoate-limited, anoxic chemostats. J. Bacteriol. 194, 2165–2180.

Trautwein, K., Wilkes, H., Rabus, R., 2012b. Proteogenomic evidence for β-oxidation of plant-derived 3-phenylpropanoids in "*Aromatoleum aromaticum*" EbN1. PROTEOMICS 12, 1402–1413.

Valderrama, J.A., Durante-Rodríguez, G., Blázquez, B., García, J.L., Carmona, M., Díaz, E., 2012. Bacterial Degradation of Benzoate Cross-regulation between aerobic and anaerobic pathways. J. Biol. Chem. 287, 10494–10508.

Valderrama, J.A., Shingler, V., Carmona, M., Díaz, E., 2014. AccR is a master regulator involved in carbon catabolite repression of the anaerobic catabolism of aromatic compounds in *Azoarcus* sp. CIB. J. Biol. Chem. 289, 1892–1904.

van Gulik, W.M., 2010. Fast sampling for quantitative microbial metabolomics. Curr. Opin. Biotechnol. 21, 27–34.

Voet, D.J., Voet, J.G., Pratt, C.W., 2002. Lehrbuch der Biochemie, 2. Auflage. ed. Wiley-VCH Verlag GmbH & Co. KGaA, Weinheim.

Vranova, V., Rejsek, K., Formanek, P., 2013. Aliphatic, Cyclic, and Aromatic Organic Acids, Vitamins, and Carbohydrates in Soil: A Review. Sci. World J. 2013.

Wang, F., Lee, S.Y., 1997. Poly(3-Hydroxybutyrate) Production with High Productivity and High Polymer Content by a Fed-Batch Culture of *Alcaligenes latus* under Nitrogen Limitation. Appl. Environ. Microbiol. 63, 3703–3706.

Ward, J.H., 1963. Hierarchical Grouping to Optimize an Objective Function. J. Am. Stat. Assoc. 58, 236–244.

Warnes, G.R., Bolker, B., Bonebakker, L., Gentleman, R., Liaw, W.H.A., Lumley, T., Maechler, M., Magnusson, A., Moeller, S., Schwartz, M., Venables, B., 2015. gplots: Various R Programming Tools for Plotting Data.

Werf, M.J. van der, Overkamp, K.M., Muilwijk, B., Coulier, L., Hankemeier, T., 2007. Microbial metabolomics: Toward a platform with full metabolome coverage. Anal. Biochem. 370, 17–25.

Whittle, P.J., Lunt, D.O., Evans, W.C., 1976. Anaerobic Photometabolism of Aromatic Compounds by *Rhodopseudomonas* sp. Biochem. Soc. Trans. 4, 490–491.

Widdel, F., Bak, F., 1992. Gram-Negative Mesophilic Sulfate-Reducing Bacteria, in: Balows, A., Trüper, H.G., Dworkin, M., Harder, W., Schleifer, K.-H. (Eds.), The Prokaryotes. Springer New York, pp. 3352–3378.

Wöhlbrand, L., Kallerhoff, B., Lange, D., Hufnagel, P., Thiermann, J., Reinhardt, R., Rabus, R., 2007. Functional proteomic view of metabolic regulation in "*Aromatoleum aromaticum*" strain EbN1. Proteomics 7, 2222–2239.

Wöhlbrand, L., Trautwein, K., Rabus, R., 2013. Proteomic tools for environmental microbiology - a roadmap from sample preparation to protein identification and quantification. Proteomics 13, 2700–2730.

Yaginuma, H., Kawai, S., Tabata, K.V., Tomiyama, K., Kakizuka, A., Komatsuzaki, T., Noji, H., Imamura, H., 2014. Diversity in ATP concentrations in a single bacterial cell population revealed by quantitative single-cell imaging. Sci. Rep. 4.

Yang, S., Sadilek, M., Lidstrom, M.E., 2010. Streamlined pentafluorophenylpropyl column liquid chromatography-tandem quadrupole mass spectrometry and global 13C-labeled internal standards improve performance for quantitative metabolomics in bacteria. J. Chromatogr. A 1217, 7401–7410.

Zaar, A., Eisenreich, W., Bacher, A., Fuchs, G., 2001. A novel pathway of aerobic benzoate catabolism in the bacteria *Azoarcus evansii* and *Bacillus stearothermophilus*. J. Biol. Chem. 276, 24997–25004.

Zaar, A., Gescher, J., Eisenreich, W., Bacher, A., Fuchs, G., 2004. New enzymes involved in aerobic benzoate metabolism in *Azoarcus evansii*. Mol. Microbiol. 54, 223–238.

Zhang, W., Li, F., Nie, L., 2010. Integrating multiple "omics" analysis for microbial biology: application and methodologies. Microbiology 156, 287–301.

Supplementary Material

supplement 1: Mass spectrometer settings for GC-APCI-MS

Mass spectrometer setting for GC-APCI-MS	
mode	positive
mass range	100-1550 *m/z*
spectra rate	0.4 Hz
end plate offset	-500 V
capillary	-1000 V
corona	3000 nA
nebuliser	4 bar
dry gas	4 L/min
dry temperature	180 °C
funnel 1/2 RF	200 Vpp
in-source CID energy	0 V
hexapole RF	150 Vpp
quadrupole ion energy	5 eV
collision energy	7 eV
collision RF	140 Vpp
transfer time	80 µs
pre puls storage	5 µs

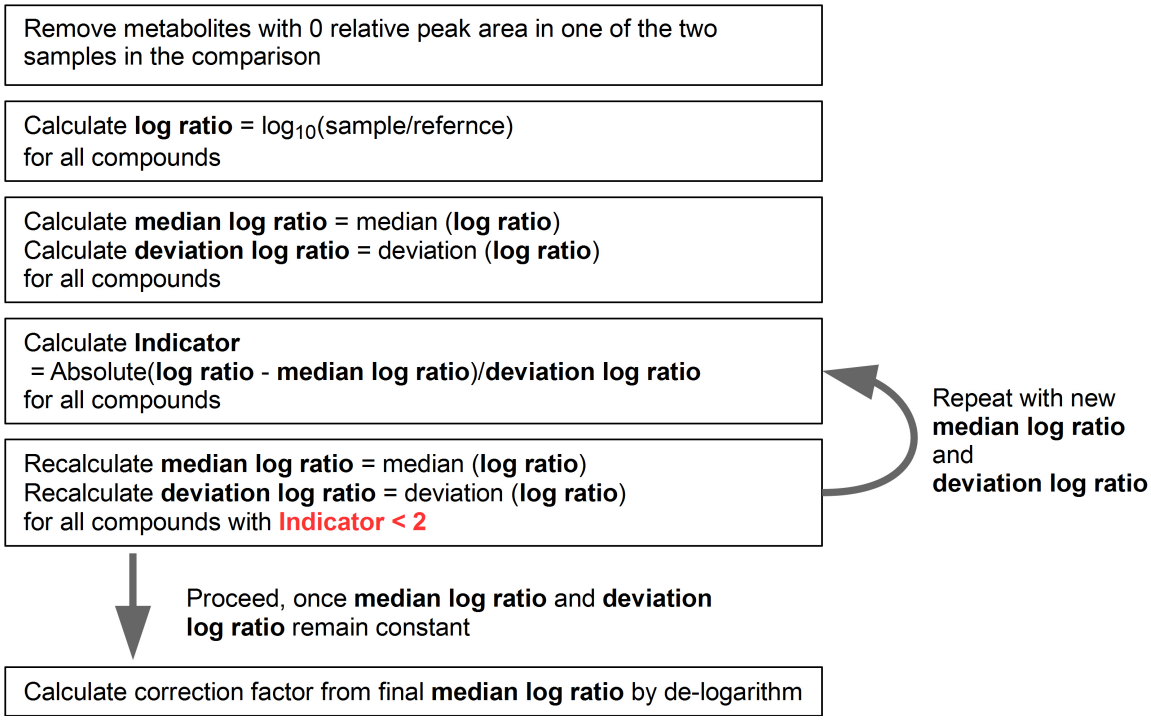

supplement 2: Normal centralization

supplement 3: R-script for Normal centralization of metabolomic data

#Definitionen:

input.file <- "150423-zentralisierung.csv"

```
# WICHTIG: Alle  ehemaligen Nullstellen müssen wieder 0 sein, damit sie automatisch erkannt und von der Zentralisierung ausgeschlossen werden können, Feldtrenner ist tab "\t", Dezimaltrenner ist der Punkt "."
output.file <- "150423-zusammen-out.csv"
# Ausführliche Ergebnisstabelle mit der Anzahl der Iterationen und einigen Zwischenergebnissen um die Rechnungen nachvollziehen zu können.
summary.file <- paste("summary", "_", input.file, sep = "")
# Enthält nur die ermittelten Faktoren, die einfach in die Auswertetabelle kopiert werden können
iterations <- 10
# Anzahl der Iteration wenn kein stabiler Wert gefunden wird
Referenz <- "Mittelwert"
#name der probe, auf die zentralisiert werden soll

# 1) Daten einlesen und Outputfiles definieren
data <- read.table(file = input.file, head=TRUE, sep="\t", dec=".",row.names=1)
final <- as.data.frame(matrix(data = NA, nrow = 1, ncol = iterations+2))
colnames(final) <- c("sample", "LogRatio", paste("Abs", 1:iterations))
summary <-as.data.frame(matrix(data = NA, nrow = 1, ncol = ncol(data)))
colnames(summary) <- colnames(data)
rownames(summary) <- c("Factor")
summary[1,Referenz] <- 1
proben <- colnames(data)
proben <- proben[! proben %in% Referenz]

#2) Proben einzeln einlesen, Nullstellen entfernen, probenspezifischen Output vorbereiten, LogRatio und ersten Median sowie Stabw berechnen, erste Spalte Results eintragen
for (samp in proben){
        output <- as.data.frame(matrix(data = NA, nrow=nrow(data), ncol = iterations+3))
        namen <- c(paste("Ref:", Referenz), samp, paste(samp, "LogRatio"), paste(samp, "Abs", 1:iterations, sep = ""))
        colnames(output) <- namen
        rownames(output) <- rownames(data)
        output[,1] <- data[,Referenz]
        output[,samp] <- data[,samp]
        metabolite <- c(row.names(output))
        nullen <- metabolite[which(output[,1] == 0 | output[,2] == 0)]
        nullen.df <- output[nullen,]
        output <- output[setdiff(rownames(output),rownames(nullen.df)),]
        anzahl <- nrow(output)

        metabolite <- c(row.names(output))
        output[,3] <- log((output[,1]/output[,2]),10)          #log ratio
        med <- median(output[,3])                    #median log ratio
        stabw <- sd(output[,3])                              #deviation log ratio
        stabw.now <- stabw
        median1 <- med
        result <- as.data.frame(matrix(data = NA, nrow = 7, ncol = iterations+2))
        colnames(result) <- c("sample", "LogRatio", paste("Abs", 1:iterations))
        rownames(result) <- c("Median", "STABW", "Excludet", "median_stabil", "Nullen", "Rest%", "LOG10")

        result$sample <- samp
```

```
        result[1,2] <- median1
        result[2,2] <- stabw.now
        result[3,2] <- "NA"
        result[4,2] <- "NA"
        result[5,2] <- toString(nullen)
        result[7,2] <- 10^median1

#3) Berechnung der Absolutwerte: es werden für die nächste Berechnungen alle LogRatios vom Median
und Standardabweichung ausgeschlossen deren Absolutwert größer als 2 ist; Die maximale Anzahl der
Iterationen ist mit "iterations" s.o. beschränkt, es wird abgebrochen sobald der Median stabil bleibt; In der
Ergebnistabelle werden Median, Standarabweichung, ausgeschlossene Metabolite, der Vergleich mit dem
letzten Median und der entlogarithmierte Median jeder einzelnen Iteration zusammengefasst sowie die wegen
Nullstellen ausgeschlossenen Metabolite aufgefügt.
        for ( i in 1:iterations) {
                n <- i+3
                output[,n] <- abs((output[,3] - med) / stabw.now)                    #Indicator
                exclude <- metabolite[which(output[,n] > 2)]
                exclude.df <- output[exclude,]
                dings.b <- output[setdiff(rownames(output),rownames(exclude.df)),]
                median2 <- median(dings.b[,3])
                stabw.now <- sd(dings.b[,3])
                rest <- nrow(dings.b)/anzahl
                result[1, i+2] <- median2
                result[2, i+2] <- stabw.now
                result[3, i+2] <- toString(exclude)
                result[4, i+2] <- median1 == median2
                result[6, i+2] <- rest
                result[7, i+2] <- 10^median2
                if(median1 == median2) {
                        factor <- 10^median2
                        summary[1,samp] <- factor
                        break}
                median1 <- median2
        }
# csv aller berechneten Werte für jede einzelne Probe wird automatisch generiert
        output2 <- output[order(output[,4]),]
        file <- paste(samp, "-R-cent-data.csv")
        write.csv(output2, file)
        final <- rbind(final, result)
}
write.csv(final,output.file ,row.names = TRUE)
write.csv(summary,summary.file ,row.names = TRUE)
```

supplement 4: R-script for the application of R XCMS for peak detection, alignment and base line integration for not-detected peaks

```
library(xcms)
library(multtest)

batch.table <- "141013_batch_ppm15-untargeted.csv"
#Name für die untargeted batch tabelle mit der später weiter gearbeitet wird
R.name <- "141013-peakdetection.RData"
#Name für das workspace image, das alle zwischenschritte der Peakdetection enthält so dass man ab einem
beliebigen punkt wieder einsteigen kann wenn zB die RT-korrection mist ist
mz_min <- 340
# Massen unter diesem Wert werden ausgeschlossen, Untergrenze ist wichtig wenn man auch Cofactoren
```

```
sehen will, da spielt aber auch der Scanrange eine wichtige Rolle!
mz_max <- 950
#Obergrenze der Massen ist wichtig wenn man automatisch M+H detektieren will. Hohe Grenze dauert aber viel länger beim rechnen!!
# !! ACHTUNG: als workspace muss der Ordner mit den mzXML daten ausgewählt sein. Replika-gruppen werden durch die Ordnerstruktur vorgegeben, XCMS bezieht alle Unterordner mit brauchbaren daten mit in die Btch ein

#Parameter für Peak Detection cent.wave:
ppm=15                  #sehr hoher Wert hier(15ppm ist extrem viel) verhindert zerfleddern von Peaks wenn die Mssengenauigkeit schwankt, durch ausprobieren ermittelt
peakwidth=c(6,30)       #range für peakbreiten in sec selbst die kleinsten sind normalerweise etwa 10 sec breit, große etwa 20sec
snthresh=1              #extrem niedrig weil ich dem Rauschen nicht immer traue
prefilter=c(1,200)      #kann das ganze schneller machen, massenspur muss mindestens 1 peak mit intensität 200 enthalten um weiter ausgewertet zu werden
mzCenterFun="wMeanApex3"#mz wird an Spitze des peaks +/- 1 scan gemittelt
integrate=1             #robustere aber ggf etwas rauschigere Integrationsmethode
mzdiff=0.2              #Massen müssen sich um mindestens diesen Wert unterscheiden um als unterschiedliche überlagerte peaks kzeptiert zu werden
fitgauss=TRUE           #frisst zwar rechenzeit macht ber bessere ergebnisse
scanrange= c(700, 5000) #RT begrenzung für die peakdetection in Scans nicht sec!
noise=0                 #muss man hinterher selber sehen
sleep=0                 #überflüssig, lässt die Graphen zwischendurch auf dem Bildschirm stehen und verzögert extrem
verbose.columns=FALSE   #irgendws mit metdaten und deren Speicherung
ROI.list=list()         #keine vorgefertigte liste für Regions Of Interrest

xset1 <- xcmsSet(method = "centWave", ppm = ppm, peakwidth = peakwidth, snthresh = snthresh, prefilter = prefilter, mzCenterFun = mzCenterFun, integrate = integrate, mzdiff = mzdiff, fitgauss = fitgauss, scanrange = scanrange, noise = noise, sleep = sleep, verbose.columns = verbose.columns, ROI.list = ROI.list )
#hier reduziere ich manuell die anzahl der peaks auf einen masseberich der nur die M+2H ionen enthält um die folgenden Schritte zu beschleunigen Der schritt knn auch ausgelassen werden um wirklich alle peaks zu erhalten, dann wird die batch aber unterumständen gigantisch
dings <- xset1@peaks
dings2 <- dings[which(dings[,"mz"]< mz_max & dings[,"mz"]> mz_min),]
xset <- xset1
xset@peaks <- dings2
#peaks mit gleicher masse und RT werden gruppiert = alignement
xset <- group(xset, method = "nearest", mzVsRTbalance = 15, mzCheck = 0.05, rtCheck = 25, kNN = 15)
#korrigiert die retentionszeit von peaks die zusmmen gruppiert wurden aber nicht genau die selbe RT haben; wie RI clibrtion nur ohne Alkan und gibt ein Bild der RT correction..
xset2 <- retcor(xset, missing = 3, extra = 2, smooth = "loess", span = 0.2, family = "symmetric", plottype = "mdevden")
        png(file = "rt_correctionNo1.png", bg = "transparent")
        plotrt(xset2)
        graphics.off()
#zweite iterration der RT korrektion mit etwas strafferen prametern
xset2 <- group(xset2, method = "nearest", mzVsRTbalance = 15, mzCheck = 0.05, rtCheck = 15, kNN = 10)
xset3 <- retcor(xset2, missing = 1, extra = 0, smooth = "loess", span = 0.2, family = "symmetric", plottype = "mdevden")
        png(file = "rt_correctionNo2.png", bg = "transparent")
        plotrt(xset3)
        graphics.off()
xset3 <- group(xset3, method = "nearest", mzVsRTbalance = 15, mzCheck = 0.1, rtCheck = 10, kNN = 10)
#hier werden Nullstellen Automatisch durch integration der entsprechenden Ionenspur an der RT aufgefüllt. Information, was eine Nullstelle war geht leider verloren, nur die gesmtzahl an Nullstellen eines peaks in
```

```
einer replikatgruppe belibt erhalten
xset4 <- fillPeaks(xset3)
pks2 <- peakTable(xset4)
#export der peaktabelle untargeted und des R-imges
write.table (pks2, file = batch.table, row.names = FALSE)
save.image(file = R.name, version = NULL, ascii = FALSE, compress = FALSE, safe = TRUE)
```

supplement 5: R-script for the comparison of peak detection results with CoA-library in CSV format

```
#Variablen für die Identifizierung
delta_mz <- 0.05                        #u Bereich der +/- angewendet wird um zu identifizieren
delta_rt <- 20                          #sec Bereich der +/- angewendet wird um zu identifizieren
library <- "D:/LC Daten/Sso_raw data/xml/CasAA/150707_Intermediate_CSV_2.csv"
        #csv tabelle mit den massen und retetionszeiten zur Identifizierung, tab-getrennt, spalte 1 = name,
spalte 4 = referenz für identifizierung, spalte 8 = identifikationsnummer der isomergruppe
input_data <- "141014_batch_untargeted_ppm15.csv"       #output tabelle der peakdetetction
filename <- "150810_batch_identified2.csv"
        #Filename unter dem die Ergebnistabelle mit Identifikationen gespeichert wird

#Funktion Identifizierung:
identification <- function(daten, ziel, delta_mz, delta_rt){
        Ergebnis <- data.frame()
        y <- nrow(ziel)
        pks <- daten
        for (z in 1:y){
                CoA <- data.frame()
                t <- data.frame()
                mz_min <- ziel[[13]][z]-delta_mz
                mz_max <- ziel[[13]][z]+delta_mz
                rt_min <- ziel[[14]][z]-delta_rt
                rt_max <- ziel[[14]][z]+delta_rt
                name <- as.vector(ziel[[1]][z], mode = "character")
                isomer_grp <- ziel[[9]][z]
                ref <- ziel[[5]][z]
                pathways <- ziel[[10]][z]
                CoA <- subset(pks, pks[,4] < rt_max & pks[,4] > rt_min & pks[,1] > mz_min & pks[,1] <
mz_max)
                a <- nrow(CoA)
                if ( a > 0){
                t <- as.data.frame(cbind(name, ref, pathways, isomer_grp, CoA))
                Ergebnis <- rbind(Ergebnis, t)
                }
        }
        return(Ergebnis)
}

#Funktion zum Isomere sortieren:
isomere1 <- function(identifizierte, ziel){
Ergebnis <- identifizierte
name_doppelt <- as.vector(droplevels(Ergebnis[duplicated(Ergebnis$name),1]))
iso_doppelt <- as.vector(unique(Ergebnis[duplicated(Ergebnis$name),4]))
rest <- subset(Ergebnis, ! Ergebnis$isomer_grp %in% iso_doppelt)
korr <- data.frame()

for (d in iso_doppelt){
```

```
        sub <- subset(ziel, ziel$Isomergruppe == d)
        a <- nrow(sub)
        erg <- subset(Ergebnis, Ergebnis$isomer_grp == d)
        erg2 <- subset(erg, ! duplicated(erg$rt), select = -c(name, ref, pathways, isomer_grp))
        b <- nrow(erg2)
        if(a > 1){
                soll <- as.vector(sub$RT)
                ist <- as.vector(erg2$rt)
                c <- length(ist)
                for (f in 1:c){
                        e <- ist[f]
                        diff <- abs(e - t(soll))
                        isomer <- which.min(diff)
                        id <- sub[isomer,]
                        name <-as.vector(id[[1]][1], mode = "character")
                        isomer_grp <- id[[9]][1]
                        ref <- id[[5]][1]
                        pathways <- id[[10]][1]
                        peak <- erg2[f,]
                        t <- as.data.frame(cbind(name, ref, pathways, isomer_grp, peak))
                        korr <- rbind(korr, t)
                                }
        }
        else{
        erg3 <- subset(erg, ! duplicated(erg$rt))
        korr <- rbind(korr,erg3)
        }
}
Ergebnis3 <- rbind(rest, korr)
return(Ergebnis3)
}

#Anwendung der beiden Funktionen: und Datenausgabe
tabelle1 <- read.table(file = library, header = TRUE, sep = "\t", dec= ".")
tabelle <- subset(tabelle1, tabelle1$RT != "NA")
peaks <- read.table(file = input_data, header = TRUE)
test <- identification(daten=peaks, ziel=tabelle, delta_mz=delta_mz, delta_rt=delta_rt)
test3 <- isomere1(identifizierte=test, ziel=tabelle)
write.table (test3, file = filename, row.names = FALSE)
```

supplement 6: Recovery rates of available synthetic CoA-ester standards determined for the applied SPE extraction method

CoA ester	Recoveryrate	standard deviation
CoA	n.d.	
acetyl-CoA	n.d.	
propanoyl-CoA	56.57%	± 7.73%
crotonyl-CoA	21.00%	± 3.37%
butanoyl/isobutanoyl-CoA	63.30%	± 6.91%
2methylcrotonyl-CoA	55.95%	± 3.91%
acetoacetyl-CoA	1.80%	± 1.05%
isovaleryl-CoA	21.98%	± 7.72%
malonyl-CoA	60.42%	± 10.32%
succinyl/methylmalonyl-CoA	n.d.	
benzoyl-CoA	57.61%	± 4.70%
glutaryl-CoA	46.94%	± 6.76%
phenylacetyl-CoA	46.53%	± 5.07%
3-hydroxybutanoyl-CoA	50.93%	± 8.12%

supplement 7: CoA-ester synthetic standards

Name	Sum formula	M+H	M+2H	RT(sec)
benzoyl-CoA	C28H40N7O17P3S	872.15	436.58	1472
glutaryl-CoA	C26H42N7O19P3S	882.15	441.58	547.5
crotonoyl-CoA	C25H40N7O17P3S	836.15	418.58	1126.5
3-hydroxybutanoyl-CoA	C25H42N7O18P3S	854.16	427.58	782.5
acetoacetyl-CoA	C25H40N7O18P3S	852.14	426.58	702.5
acetyl-CoA	C23H38N7O17P3S	810.13	405.57	720
phenylacetyl-CoA	C29H42N7O17P3S	886.16	443.59	1476.5
coenzyme A	C21H36N7O16P3S	768.12	384.56	478.85
isobutanoyl-CoA	C25H42N7O17P3S	838.16	419.59	1222
butanoyl-CoA	C25H42N7O17P3S	838.16	419.59	1241
isovaleryl-CoA	C26H44N7O17P3S	852.18	426.59	1459
malonyl-CoA	C24H38N7O19P3S	854.12	427.57	338.5
propanoyl-CoA	C24H40N7O17P3S	824.15	412.58	961.5
succinyl-CoA	C25H40N7O19P3S	868.14	434.57	446
methylmalonyl-CoA	C25H40N7O19P3S	868.14	434.57	496.67
CoA-disulfide	C42H70N14O32P6S2	1533.22	767.11	756
dephospho-CoA	C21H35N7O13P2S	688.16	344.58	852

supplement 8: Identification of CoA-esters without synthetic standards

Name	Sum formula	M+H	M+2H	RT(sec)	Identification	M+H	MS2	mSigma	err(ppm)	specifity
3-hydroxypimelyl-CoA	C28H46N7O20P3S	926.18	463.59	592	***	ok	**ja**	**5.9**	**-1.8**	+
2-hydroxy-5-oxo-cyclohex-1-carbonyl-CoA	C28H44N7O19P3S	908.17	454.59	936	***	ok	**ja**	**17**	**-0.2**	0
pimeloyl-CoA_3	C28H46N7O19P3S	910.19	455.6	846	***	ok	**ja**	**7.3**	**0.1**	+
6-hydroxycyclohex-1-enecarbonyl-CoA_1	C28H44N7O18P3S	892.17	446.59	1170	***	ok	**ja**	**5.6**	**-2.5**	-
5-carboxy-2-pentenoyl-CoA	C27H42N7O19P3S	894.15	447.58	625	***	ok	**ja**	**4.2**	**0.9**	0
3-hydroxyadipyl-CoA	C27H44N7O20P3S	912.16	456.59	475.54	***	ok	**ja**	**6.3**	**-2.9**	-
4-hydroxybenzoyl-CoA_1	C28H40N7O18P3S	888.14	444.58	1205	***	ok	**ja**	**4.8**	**-2.4**	+
3-hydroxybenzoyl-CoA	C28H40N7O18P3S	888.14	444.58	1294	***	ok	**ja**	**1.1**	**-4.2**	+
adipoyl-CoA	C27H44N7O19P3S	896.17	448.59	687.99	***	ok	**ja**	**11.6**	**-1.7**	
cyclohexa-1,5-dienecarbonyl-CoA	C28H42N7O17P3S	874.16	437.59	1500	**	ok	no	**18**	**0.2**	-
6-oxocyclohex-1-ene-1-carboxyl-CoA	C28H42N7O18P3S	890.16	445.58	979	**	ok	no	**18.3**	**1.1**	+
2,3-didehydro-pimeloyl-CoA_3	C28H44N7O19P3S	908.17	454.59	1252	**	ok	no	**17.7**	**0.7**	-
pimeloyl-CoA_1	C28H46N7O19P3S	910.19	455.6	496	**	ok	no	**29.7**	**-2.5**	
2-oxocyclohexane-1-carboxyl-CoA	C28H44N7O18P3S	892.17	446.59	1095	**	ok	**ja**	**5.5**	7.5	-
2-hydroxycyclohexanecarbonyl-CoA	C28H46N7O18P3S	894.19	447.6	1151	**	ok	no	**26.9**	**-2.6**	-
3,4-didehydroadipyl-CoA	C27H42N7O19P3S	894.15	447.58	650	**	ok	no	**16.8**	**0.4**	+
phenylglyoxylyl-CoA	C29H40N7O18P3S	900.14	450.58	973	**	ok	**ja**	32.9	**-5**	+
3-oxo-5,6-dehydrosuberyl-CoA semialdehyde_1	C29H44N7O19P3S	920.17	460.59	895	**	ok	no	**17.6**	**-4.4**	+
CoA-glutathione	C31H51N10O22P3S2	1073.19	537.1	399	**	ok	**ja**	**14.5**	-5.6	0
4-hydroxybenzoyl-CoA_2	C28H40N7O18P3S	888.14	444.58	1230	**	ok	**ja**	**21.2**	7.2	+
3-(4-hydroxyphenyl)propanoyl-CoA	C30H44N7O18P3S	916.17	458.59	1402	**	ok	**ja**	**9.4**	-5.6	+
3-hydroxy-5-oxohexanoyl-CoA	C27H44N7O19P3S	896.17	448.59	1189	**	ok	no	**15.8**	**1.2**	

supplement 8 continued: Identification of CoA-esters without synthetic standards

Name	Sum formula	M+H	M+2H	RT(sec)	Identification	M+H	MS2	mSigma	err(ppm)	specifity
6-hydroxycyclohex-1-enecarbonyl-CoA_2	C28H44N7O18P3S	892.17	446.59	1040	0	ok	no	54.3	11	+
cyclohex-1-ene-1-carboxyl-CoA_1	C28H44N7O17P3S	876.18	438.59	1220	0	ok	no	x	x	0
cyclohex-1-ene-1-carboxyl-CoA_2	C28H44N7O17P3S	876.18	438.59	1241	0	ok	no	x	x	0
2,5-dioxo-cyclohex-1-carbonyl-CoA_1	C28H42N7O19P3S	906.15	453.58	910	0	no	no	x	x	-
2,5-dioxo-cyclohex-1-carbonyl-CoA_2	C28H42N7O19P3S	906.15	453.58	926	0	ok	no	67.9	14.3	-
2,3-dihydro-2,3-dihydroxybenzoyl-CoA-isomer	C28H42N7O19P3S	906.15	453.58	502	0	ok	no	x	x	0
2,3-dihydro-2,3-dihydroxybenzoyl-CoA	C28H42N7O19P3S	906.15	453.58	451	0	ok	no	x	x	0
3,4-didehydroadipyl-CoA semialdehyde-1	C27H42N7O18P3S	878.16	439.58	863	0	ok	no	x	x	+
3-oxoadipyl-CoA	C27H42N7O20P3S	910.14	455.57	749	0	ok	**ja**	x	x	-
2-oxepin-2(3h)-ylideneacetyl-CoA	C29H42N7O18P3S	902.16	451.58	1221	0	ok	no	68.1	-12.6	+
3-oxo-5,6-dehydrosuberyl-CoA semialdehyde_2	C29H44N7O19P3S	920.17	460.59	866.5	0	ok	no	121.6	-9.3	+
3-oxo-5,6-dehydrosuberyl-CoA_2	C29H44N7O20P3S	936.16	468.59	627.7	0	no	no	x	6.9	+
3-oxo-5,6-dehydrosuberyl-CoA_1	C29H44N7O20P3S	936.16	468.59	747	0	ok	no	68.8	-6.5	+
geranoyl-CoA	C31H50N7O17P3S	918.23	459.62	1407	0	ok	no	**12.2**	36.5	0
4-hydroxybenzoylacetyl-CoA	C30H42N7O19P3S	930.15	465.58	1100	0	no	no	x	x	+

supplement 8 continued: Identification of CoA-esters without synthetic standards

Name	Sum formula	M+H	M+2H	RT(sec)	Identification	M+H	MS2	mSigma	err(ppm)	specifity
6-hydroxycyclohex-1-enecarbonyl-CoA_2	C28H44N7O18P3S	892.17	446.59	1040	0	ok	no	54.3	11	+
cyclohex-1-ene-1-carboxyl-CoA_1	C28H44N7O17P3S	876.18	438.59	1220	0	ok	no	x	x	0
cyclohex-1-ene-1-carboxyl-CoA_2	C28H44N7O17P3S	876.18	438.59	1241	0	ok	no	x	x	0
2,5-dioxo-cyclohex-1-carbonyl-CoA_1	C28H42N7O19P3S	906.15	453.58	910	0	no	no	x	x	-
2,5-dioxo-cyclohex-1-carbonyl-CoA_2	C28H42N7O19P3S	906.15	453.58	926	0	ok	no	67.9	14.3	-
2,3-dihydro-2,3-dihydroxybenzoyl-CoA-isomer	C28H42N7O19P3S	906.15	453.58	502	0	ok	no	x	x	0
2,3-dihydro-2,3-dihydroxybenzoyl-CoA	C28H42N7O19P3S	906.15	453.58	451	0	ok	no	x	x	0
3,4-didehydroadipyl-CoA semialdehyde-1	C27H42N7O18P3S	878.16	439.58	863	0	ok	no	x	x	+
3-oxoadipyl-CoA	C27H42N7O20P3S	910.14	455.57	749	0	ok	**ja**	x	x	-
2-oxepin-2(3h)-ylideneacetyl-CoA	C29H42N7O18P3S	902.16	451.58	1221	0	ok	no	68.1	-12.6	+
3-oxo-5,6-dehydrosuberyl-CoA semialdehyde_2	C29H44N7O19P3S	920.17	460.59	866.5	0	ok	no	121.6	-9.3	+
3-oxo-5,6-dehydrosuberyl-CoA_2	C29H44N7O20P3S	936.16	468.59	627.7	0	no	no	x	6.9	+
3-oxo-5,6-dehydrosuberyl-CoA_1	C29H44N7O20P3S	936.16	468.59	747	0	ok	no	68.8	-6.5	+
geranoyl-CoA	C31H50N7O17P3S	918.23	459.62	1407	0	ok	no	**12.2**	36.5	0
4-hydroxybenzoylacetyl-CoA	C30H42N7O19P3S	930.15	465.58	1100	0	no	no	x	x	+

supplement 9: Unknown compounds from GC-MS metabolomic analysis

No.	Comment	original identification	Growth condition
01	low quality	5-Hydroxypentanoic-acid_2TMS_1341.49	Hbe_NO_3
02	iso-glutamate 2TMS	Butanoic_acid,_4-acetamido-_(1TMS)_1517.09	Ben_NO_3
03	unknown in library	D226501_2270.1	Ace_O_2
04		D228685_2290.51	Ace_O_2
05	low quality	Imidazole-4-acetic_acid_(1TMS)_1563.99	Ben_O_2
06	low quality	Kojic_acid_(2TMS)_1692.62	Hbe_NO_3
07	low quality	NA_234_161_81_1894.71	HPP_O_2
08		NA197	Hbe_NO_3
09		NA226	Ben_NO_3
10		NA228	Phe_NO_3
11	low quality	NA374	Ben_NO_3
12		NA459	HPP_NO_3
13	iso-glutamate 3TMS	Ornithine_(3TMS)_(Derivate_not_found)_1621.8	Ben_NO_3
14	unknown in library	Phytol_(1TMS)_BP_2137.11	HPP_NO_3
15	Contaminant	Unknown#1169.8-pae-bth_013	Hbe_O_2
16	Contaminant	Unknown#1248.7-cgl-sst_008	HPP_O_2
17		Unknown#1392.1-pin-mhe_012	Hbe_O_2
18		Unknown#1496.63-ypy-mse_010	Hbe_O_2
19	3-hydroxybutanoate-dimer, tentative	Unknown#1594.3-pin-mhe_030	Hbe_O_2
20	unknown in library	Unknown#1654.8-cgl-sst_043	Hbe_NO_3
21		Unknown#1878.81-ypy-mse_031	Ben_NO_3
22		Unknown#2269.25-ypy-mse_027	Ben_NO_3
23		Unknown#2551.4-cgl-sst_119	Ben_NO_3
24	low quality	Butanoic_acid,_2-amino-_(2TMS)_1157.12	Hbe_O_2
25		Mannosylglycerate_(6TMS)_2229.85	HPP_O_2
26		Glycerol,_2-glucosyl-_(6TMS)_putative_BP3_2340.95	Ace_O_2
27		Glycerol,_2-galactosyl-O-_(6TMS)_2301.66	Ace_O_2

supplement 10: Results of exometabolome analysis
s indicates samples with microbial growth, c indicates control samples of medium without microbial growth

Derivative_Group	Ace NO3 s	Ace NO3 c	Ace O2 s	Ace O2 c	Ben NO3 s	Ben NO3 c	Ben O2 s	Ben O2 c	Hbe NO3 s	Hbe NO3 c	Hbe O2 s	Hbe O2 c	HPP NO3 s	HPP NO3 c	HPP O2 s	HPP O2 c	Phe NO3 s	Phe NO3 c	Phe O2 s	Phe O2 c
3-hydroxybenzoate	n.d.	n.d.	n.d.	n.d.	n.d.	n.d.	n.d.	n.d.	0.0	n.d.	n.d.	n.d.	n.d.	n.d.	n.d.	n.d.	n.d.	n.d.	n.d.	n.d.
4-hydroxybenzoate	n.d.	n.d.	n.d.	n.d.	n.d.	n.d.	n.d.	n.d.	n.d.	n.d.	n.d.	n.d.	n.d.	n.d.	0.1	n.d.	n.d.	n.d.	n.d.	n.d.
benzoate	n.d.	n.d.	n.d.	n.d.	73.6	201.2	0.5	0.4	n.d.	n.d.	0.0	n.d.	n.d.	n.d.	n.d.	n.d.	n.d.	n.d.	n.d.	n.d.
dehydroascorbic acid	0.02	0.1	0.0	0.0	12.7	0.7	0.0	0.0	0.8	0.0	0.0	0.0	0.3	0.0	0.0	0.0	2.2	0.0	0.0	0.0
hydroxylamine	0.07	1.4	0.1	0.3	2.3	13.8	0.2	0.2	0.3	0.8	0.5	2.1	0.1	0.3	0.4	0.2	0.2	1.9	0.2	0.3
lactate	0.08	0.4	0.0	0.0	4.4	3.1	0.1	0.1	0.3	0.2	0.2	0.9	0.1	0.4	0.2	0.1	0.1	0.5	0.1	0.2
oxalate	n.d.	n.d.	n.d.	n.d.	n.d.	n.d.	n.d.	n.d.	n.d.	n.d.	n.d.	n.d.	n.d.	0.0	n.d.	n.d.	n.d.	0.0	n.d.	n.d.
phosphate	46.64	241.7	79.8	28.1	1655.8	4208.3	118.0	26.4	421.6	158.5	106.7	86.7	80.6	100.8	304.8	52.5	1467.3	618.0	141.2	54.5
xylitol	n.d.	0.1	n.d.	n.d.	0.0	n.d.	n.d.	n.d.	0.0	n.d.	n.d.	0.1	n.d.	0.0	0.0	n.d.	0.0	n.d.	n.d.	n.d.
NA109003_(classified_unknown)_1104.91	0.02	0.2	0.1	0.5	0.8	1.7	0.0	0.0	0.1	0.0	0.1	0.2	0.0	0.1	0.1	0.0	0.1	0.6	0.0	0.1
NA46	0	0.0	0.0	0.0	0.1	0.1	0.0	0.0	n.d.	n.d.	n.d.	n.d.	n.d.	n.d.	0.0	n.d.	n.d.	n.d.	0.0	0.0
no_match_1255.31_150504_kmu_08_1608215000	n.d.	n.d.	n.d.	n.d.	n.d.	n.d.	n.d.	n.d.	0.1	n.d.	n.d.	n.d.	n.d.	n.d.	n.d.	n.d.	n.d.	n.d.	n.d.	n.d.
Unknown#1169.8-pae-bth_013	0.12	0.4	0.1	0.1	5.1	3.2	0.2	0.1	0.5	0.2	0.3	0.2	0.1	0.2	0.3	0.1	0.4	0.9	0.2	0.2

supplement 11: Metabolomics results GC-MS and HPLC-MS

Metabolite	Ace_NO3	Ace_O2	Ben_NO3	Ben_O2	Hbe_NO3	Hbe_O2	HPP_NO3	HPP_O2	Phe_NO3	Phe_O2
(4-hydroxyphenyl)acetate	NA	NA	NA	NA	13	NA	NA	NA	78	91
1-hexadecanol	761	885	238	556	642	283	633	1132	870	1613
1-pyrroline-3-hydroxy-5-carboxylic-acid	36633	NA	18325	NA	11282	NA	26550	NA	55712	NA
1,6-anhydro-glucose	283	366	194	741	188	364	224	531	NA	284
2-ene-5-oxo-cyclohex-1-carbonyl-CoA	89012	16104	13069	21646	4257	5744	40752	5196	22078	2758
2-hydroxy-5-oxo-cyclohex-1-carbonyl-CoA	NA	NA	97008	NA	187534	NA	19399	NA	7167	NA
2-Hydroxycyclohexane-1-carboxyl-CoA	NA	NA	19276	NA	843	NA	29289	NA	1839	NA
2-Hydroxycyclohexanecarbonyl-CoA	NA	NA	NA	NA	27441	NA	NA	NA	NA	NA
2-isocaprenoyl-CoA	NA	NA	NA	NA	NA	NA	904	6481	NA	NA
2-isopropylmalic acid	NA	NA	NA	NA	427	NA	NA	NA	NA	NA
2-Ketocyclohexane-1-carboxyl-CoA	NA	NA	NA	NA	1117118	4784	1138	NA	934	2969
2-O-alpha-glucosylglycerol	20163	119533	1685283	3532	10523	2395	288676	141829	1007	3730
2-Oxepin-2(3H)-ylideneacetyl-CoA	2656	NA	2353	NA	2059	NA	769	NA	1889	6556
2-oxoglutarate	242	36	92	66	161	142	135	329	NA	46
2,3-Didehydro-pimeloyl-CoA_1	36511	9751	14859	26314	18385	37019	16355	20007	33572	9792
2,3-Didehydro-pimeloyl-CoA_2	NA	NA	60482	NA	NA	NA	18944	NA	3010	1012
2,3-Didehydro-pimeloyl-CoA_3	NA	NA	19116	183865	NA	NA	3237	68010	3590	5397
2,3-Dihydro-2,3-dihydroxybenzoyl-CoA	3665	10009	9556	6264	3759	5314	2738	3543	2862	4779
2,3-Dihydro-2,3-dihydroxybenzoyl-CoA-Isomer	1664	NA	3023	2070	1871	2650	NA	701	1276	NA
2,5-dioxo-cyclohex-1-carbonyl-CoA_1	NA	NA	NA	NA	NA	NA	NA	NA	NA	11772
2,5-dioxo-cyclohex-1-carbonyl-CoA_2	NA	NA	NA	NA	1246	NA	NA	868	1377	1442
2,6-Dihydroxycyclohexane-1-carboxyl-CoA	NA	NA	5868	NA	18811	NA	1969	NA	NA	NA
3-(4-hydroxyphenyl)propanoate	NA	NA	NA	NA	NA	NA	NA	3160	NA	NA
3-(4-hydroxyphenyl)propanoyl-CoA	NA	NA	NA	NA	NA	NA	52239	51297	NA	NA
3-Hydroxy-2-methylbutanoyl-CoA	17726	1999	2909	NA	27550	4617	1613	8746	40207	25208
3-hydroxy-3-(4-hydroxyphenyl)propanoyl-CoA	NA	NA	1842	NA	1217	NA	4903	NA	2527	NA
3-Hydroxy-5-oxohexanoyl-CoA	11991	21700	14931	30108	20019	45541	29275	31015	7467	808
3-hydroxy-decanoate	352	45	NA	71	257	32	366	34	754	4
3-Hydroxyadipyl-CoA	2525	2774	18805	185994	904	3981	2474	67322	27563	48800
3-hydroxybenzoate	NA	NA	NA	NA	1410	1787	NA	NA	NA	NA
3-Hydroxybenzoyl-CoA	NA	NA	8629	44008	2046058	155906	2637	14917	11254	9278
3-hydroxybutanoate	11817	14354	160358	46044	10264	34977	51288	28260	7607	NA
3-Hydroxybutanoyl-CoA	99840	231002	313354	165324	257168	46406	206375	172621	65728	11165
3-Hydroxypimelyl-CoA	NA	NA	417533	NA	77864	NA	131739	NA	22461	NA
3-Ketopimelyl-CoA	NA	NA	NA	NA	NA	NA	NA	1190	NA	76491
3-Methylglutaconyl-CoA	NA	NA	3495	15916	1005	NA	NA	7024	6897	5719
3-Oxo-5,6-dehydrosuberyl-CoA semialdehyde_1	NA	NA	NA	NA	NA	NA	NA	NA	3577	5359
3-Oxo-5,6-dehydrosuberyl-CoA semialdehyde_2	NA	NA	NA	14626	NA	NA	NA	1503	9665	22903
3-Oxo-5,6-dehydrosuberyl-CoA_1	NA	NA	NA	NA	NA	NA	NA	NA	727	952
3-Oxo-5,6-dehydrosuberyl-CoA_2	NA	NA	NA	NA	NA	NA	NA	NA	3218	1863
3-Oxoadipyl-CoA	NA	NA	NA	NA	168597	NA	NA	3612	NA	NA
3-phenyllactate	NA	NA	NA	NA	NA	NA	757	NA	187	NA
3,4-Didehydroadipyl-CoA	NA	NA	NA	28319	NA	NA	1584	14095	NA	NA
3,4-Didehydroadipyl-CoA semialdehyde-1	2557	NA	1357	5486	567	3655	1849	1333	1177	NA
3,4-Didehydroadipyl-CoA semialdehyde-2	NA	NA	NA	16920	NA	NA	814	16316	NA	NA
3,4-Didehydroadipyl-CoA semialdehyde-3	NA	NA	NA	9651	NA	NA	NA	11586	NA	NA
4-hydroxybenzoate	NA	NA	NA	NA	NA	NA	1106	12670	NA	NA
4-hydroxybenzoyl-CoA_1	NA	NA	NA	NA	496	NA	NA	115360	NA	47317
4-hydroxybenzoyl-CoA_2	1967	NA	NA	NA	NA	NA	45128	NA	11187	NA

supplement 11 continued: Metabolomics results GC-MS and HPLC-MS

Metabolite	Ace_NO3	Ace_O2	Ben_NO3	Ben_O2	Hbe_NO3	Hbe_O2	HPP_NO3	HPP_O2	Phe_NO3	Phe_O2
4-hydroxybenzoylacetyl-CoA	NA	NA	NA	NA	9094	NA	NA	NA	NA	NA
4-Hydroxyphenylacetyl-CoA	NA	NA	NA	NA	NA	NA	NA	NA	21419	NA
4-Oxopimeloyl-CoA_1	NA	NA	NA	1377	NA	NA	NA	NA	632	3229
4-Oxopimeloyl-CoA_2	NA	NA	NA	NA	15408	NA	NA	NA	NA	NA
5-Carboxy-2-pentenoyl-CoA	759	NA	44638	173296	734	NA	21205	109079	13358	15250
5-Methyl-3-oxo-4-hexenoyl-CoA	NA	NA	NA	NA	114362	886	NA	NA	NA	NA
6-deoxy-mannose	186	NA	178	NA	77	135	NA	NA	NA	NA
6-Hydroxycyclohex-1-enecarbonyl-CoA_1	NA	NA	NA	NA	7275	NA	NA	NA	NA	NA
6-Hydroxycyclohex-1-enecarbonyl-CoA_2	NA	NA	82462	NA	NA	NA	22394	NA	4546	NA
6-Ketoxycyclohex-1-ene-1-carboxyl-CoA	NA	NA	68690	NA	NA	NA	35150	NA	12703	NA
6-Oxo-2-hydroxycyclohexane-1-carboxyl-CoA	NA	NA	25958	NA	9674	NA	3873	NA	1010	NA
Acetoacetyl-CoA	3076	7682	3776	4256	3621	2723	3023	1947	2174	1336
Acetyl-CoA	1328592	758914	846490	977224	1139162	1320983	589337	760534	886646	663864
adenosine	NA	NA	196	NA	NA	NA	NA	NA	NA	NA
Adipoyl-CoA	2366	2499	9897	52632	8022	3676	10696	79453	11664	10835
alanine	9562	10406	46550	8910	17815	8056	14449	10151	9514	14528
arabinonate	156	NA	NA	NA	NA	NA	123	NA	NA	NA
aspartate	880	8290	1055	12731	23	12343	653	7314	1186	15030
benzoate	NA	95	45210	382	NA	212	NA	1561	NA	NA
Benzoyl-CoA	167146	3896	4105301	1469012	31071	105397	2013293	1042478	2842400	73503
beta-Alanine	NA	NA	133	NA	NA	988	524	4910	64	15185
Beta-alanyl-CoA	8872	2860	2181	5353	1441	3201	9889	2636	13320	2795
Butanoyl-CoA	153131	166657	400467	205578	408200	255430	469347	655129	182646	32640
cadaverine	280	NA	1060	NA	NA	867	NA	256	253	913
citrate	68	NA	130	NA	190	NA	121	122	801	36
CoA-disulfide	1672179	1914517	1200539	1725926	1325694	1312706	1825189	1403107	1991479	1954251
CoA-glutathione	156281	641934	267992	304696	225213	240237	449966	110580	485620	395062
CoenzymeA	823540	623605	1124084	1031106	1063360	1158157	838322	859465	742654	1317761
Crotonoyl-CoA	13412	21937	33520	18109	16046	7693	9258	19909	2914	801
Cyclohex-1-ene-1-carboxyl-CoA_1	2891	NA	16059	NA	5697	7782	5784	9747	3999	1291
Cyclohex-1-ene-1-carboxyl-CoA_2	2838	NA	10593	NA	5977	5915	4077	5578	2697	NA
Cyclohexa-1,5-dienecarbonyl-CoA	NA	NA	59266	NA	NA	NA	9277	NA	3872	NA
dehydroascorbic acid	NA	NA	7082	NA	4326	NA	NA	NA	NA	NA
Dephospho-CoA	40318	44052	110978	49634	61812	47300	67549	48165	28556	76125
Diethanolamine	NA	640	NA	142	NA	574	NA	284	NA	132
dihydroxyacetone phosphate	NA	63	46	NA	85	64	36	110	NA	25
dodecanoate	452	621	70	5038	383	344	NA	447	509	341
dodecanol	NA	NA	216	NA	386	106	NA	10	NA	NA
erythronic acid	155	NA	62	NA	129	NA	109	NA	456	NA
erythronic acid-1,4-lactone	120	104	104	NA	495	NA	NA	NA	308	NA
ethanolamine	235	627	600	996	424	1090	561	735	489	662
ethanolaminephosphate	424	313	141	NA	625	326	542	591	494	461
Ethylmalonyl-CoA	NA	NA	NA	NA	NA	NA	NA	688	NA	652
fructose	296	190	102	195	366	354	322	210	152	130
fructose-6-phosphate	386	130	1224	NA	360	26	315	569	43	NA
fumarate	417	9808	5704	9053	2176	16778	1139	12477	629	2469
Geranoyl-CoA	NA	NA	NA	NA	19381	NA	7282	7130	NA	NA
glucose	2345	2263	2454	2205	2776	1641	3034	1862	2004	2103
glucose-6-phosphate	9645	1704	53256	NA	10525	123	10306	4988	744	1284

supplement 11 continued: Metabolomics results GC-MS and HPLC-MS

Metabolite	Ace_NO3	Ace_O2	Ben_NO3	Ben_O2	Hbe_NO3	Hbe_O2	HPP_NO3	HPP_O2	Phe_NO3	Phe_O2
Glutaconyl-1-CoA	2187	NA	3567	945	5152	NA	2596	389	1872	1254
glutamate	652770	160509	1607144	136164	255715	100591	284767	104584	903730	100998
Glutaryl-CoA	NA	NA	58243	NA	55611	NA	23728	NA	13753	NA
glyceraldehyde	136	NA	1101	NA	417	NA	377	NA	NA	NA
glycerate	44	26	NA	13	NA	43	139	52	83	46
glycerol	666	NA	1479	NA	1135	NA	1391	NA	4252	NA
glycerol-3-phosphate	442	738	106	251	759	411	795	393	1135	1540
glycine	4299	5351	8828	6709	5880	8382	7465	4620	6601	5927
glycylglycine	18163	NA	31349	NA	12179	NA	5576	183	NA	NA
hexadecanoate	1317	1425	1447	19	811	NA	1163	1423	1129	3461
hydroxylamine	NA	NA	NA	NA	NA	NA	NA	NA	269	NA
iminodiacetate	NA	NA	NA	NA	271	NA	234	914	4908	3433
Isobutanoyl-CoA	225429	178796	540194	249284	276564	324094	656287	1227440	292206	39665
isoleucine	209	1852	2040	1361	945	1818	677	2407	1023	2819
Isovaleryl-CoA	2711	NA	NA	NA	6410	NA	NA	1325	1169	7401
lactate	342	51	105	1043	504	NA	1234	NA	1894	NA
leucine	NA	5841	NA	1549	NA	2843	NA	2341	NA	2077
lysine	3299	117	4874	NA	NA	922	NA	662	NA	4538
lyxonic acid	177	NA	NA	NA	NA	NA	174	NA	NA	NA
malate	1083	1414	1159	1407	3034	1279	2698	1108	415	312
Malonyl-CoA	35709	15596	4970	NA	32023	3221	10575	3252	3671	9580
mannose	133	776	211	952	189	162	184	42	373	NA
mannose-6-phosphate	1543	177	3008	NA	1683	9	1344	521	NA	324
methionine	NA	1212	NA	1500	NA	2319	NA	1850	NA	1753
Methylmalonyl-CoA	93594	58259	67118	51036	98176	81263	33946	27867	62347	46286
Methylsuccinyl-CoA	1841	1398	2257	968	5342	1750	1539	4859	NA	NA
N-acetyl-glucosamine	148	139	32	23	55	124	45	81	29	65
N-acetyl-glutamate	642	683	483	NA	NA	427	NA	127	80	310
N-acetyl-muramate	57	NA	215	NA	91	NA	116	NA	NA	NA
n-heptadecanol	NA	NA	NA	NA	4	NA	1	NA	125	NA
n-hexadecenoate	41	NA	5	NA	77	NA	NA	NA	NA	NA
norvaline	NA	1455	40	440	517	1583	NA	1131	NA	2634
octadecanoate	118	743	20	NA	10	NA	72	987	62	3539
octadecanol	NA	NA	NA	NA	NA	NA	NA	NA	5	NA
ornithine	75	135	81	NA	2	106	NA	70	91	189
p-Coumaroyl-CoA	NA	NA	NA	NA	NA	NA	2087	1597	NA	NA
pentadecanoate	135	152	31	20	64	80	NA	93	68	90
Pentanoyl-CoA	2323	6093	1883	6026	15395	3718	2162	8399	1889	8267
Phenoxyacetyl-CoA	NA	NA	NA	NA	NA	NA	NA	NA	7825	NA
phenylacetate	NA	NA	NA	NA	NA	NA	NA	NA	NA	495
Phenylacetyl-CoA	16097	3006	10006	NA	14172	1388	6336	1404	372495	730831
phenylalanine	61	1259	764	1540	NA	1742	NA	473	2681	7990
phenylethylamine	1420	1617	NA	540	NA	1985	675	1403	1832	1801
Phenylglyoxylyl-CoA	NA	NA	NA	NA	NA	NA	NA	NA	47833	4572
Pimeloyl-CoA_1	NA	544	6748	NA	2483	NA	1961	NA	25848	622
Pimeloyl-CoA_3	NA	NA	213315	NA	196282	NA	197966	1426	63260	NA
proline	423	1315	347	1431	182	2523	287	1637	563	2069
Propanoyl-CoA	66578	15207	34103	17857	31395	51325	22782	37352	53384	44171
putrescine	877679	333179	2877726	435140	725455	294708	754706	184253	936663	251217

supplement 11 continued: Metabolomics results GC-MS and HPLC-MS

Metabolite	Ace_NO3	Ace_O2	Ben_NO3	Ben_O2	Hbe_NO3	Hbe_O2	HPP_NO3	HPP_O2	Phe_NO3	Phe_O2
pyroglutamate	5020	248440	3904	260672	538	164027	NA	146786	11490	143887
pyruvate	499	955	1908	426	1720	1823	694	1085	NA	684
ribose	65	NA	29	NA	35	NA	45	NA	NA	NA
serine	NA	2140	521	2826	NA	2384	NA	2450	NA	3867
sorbose	241	316	166	329	344	595	326	314	136	222
succinate	1072	11898	7665	11217	5636	11023	3102	9022	587	8639
Succinyl-CoA	322845	400537	329498	263021	369126	235378	173528	195625	222840	302463
tetradecan-1-ol	NA	41	NA	15	680	18	55	10	18	NA
tetradecanoate	172	70	44	NA	80	12	78	26	NA	163
threonate	1830	NA	379	NA	251	NA	2780	NA	2893	NA
threonine	372	3709	1273	4798	875	4535	850	6528	1442	9465
thymine	NA	11244	88	14546	NA	7329	NA	2925	138	8120
Unknown-ebn1-01	NA	NA	NA	NA	1102	NA	NA	NA	NA	NA
Unknown-ebn1-02	87253	NA	201179	NA	71549	NA	98700	NA	196721	NA
Unknown-ebn1-03	NA	7394	NA	183	NA	129	NA	6642	NA	194
Unknown-ebn1-04	NA	2595	NA	NA	NA	NA	NA	99	NA	NA
Unknown-ebn1-05	NA	NA	NA	4789	NA	NA	NA	3480	NA	3689
Unknown-ebn1-06	NA	NA	NA	NA	163	NA	NA	NA	NA	NA
Unknown-ebn1-07	1065	8661	1401	9006	1537	45324	1217	33465	464	49256
Unknown-ebn1-08	NA	NA	75	NA	191	NA	NA	NA	NA	NA
Unknown-ebn1-09	NA	1930	3903	1335	NA	1653	NA	2242	1256	1979
Unknown-ebn1-10	NA	1123	NA	777	NA	1192	2479	1606	3031	1085
Unknown-ebn1-11	208	125	419	37	211	160	302	300	196	165
Unknown-ebn1-12	NA	4	101	NA	NA	NA	604	NA	NA	NA
Unknown-ebn1-13	2896	152	35132	NA	50	297	79	328	6404	601
Unknown-ebn1-14	4485	1623	2316	NA	3156	1250	6400	1318	338	2529
Unknown-ebn1-15	NA	5215	NA	5113	NA	7012	5	5615	NA	4429
Unknown-ebn1-16	1808	12428	6998	2352	4615	7625	2730	18151	361	11278
Unknown-ebn1-17	NA	600	NA	4046	NA	4317	NA	2145	NA	33
Unknown-ebn1-18	157	1007	564	408	498	1885	575	414	628	287
Unknown-ebn1-19	5812	1843	671	8845	1506	10986	4367	5308	4893	NA
Unknown-ebn1-20	NA	NA	NA	NA	538	NA	NA	NA	NA	NA
Unknown-ebn1-21	55273	51	337697	NA	23123	1829	10701	177	1720	NA
Unknown-ebn1-22	1488	33	2135	NA	969	NA	1208	109	NA	NA
Unknown-ebn1-23	59	NA	1327	NA	254	NA	216	NA	NA	NA
Unknown-ebn1-24	498	1554	1377	665	2554	4005	NA	2558	499	1260
Unknown-ebn1-25	100	5086	141	102	36	91	641	5625	328	158
Unknown-ebn1-26	NA	4161	NA	87	NA	48	NA	3357	NA	99
Unknown-ebn1-27	NA	4447	NA	104	NA	70	NA	4201	NA	91
Uracil	NA	1363	56	706	NA	1432	NA	999	NA	918
uridine	4	NA	38	NA	NA	NA	NA	NA	NA	NA
valine	5663	11065	42344	7465	90750	8283	20767	9527	78331	23625
xylulose-5-phosphate	128	286	61	NA	85	22	53	140	18	93

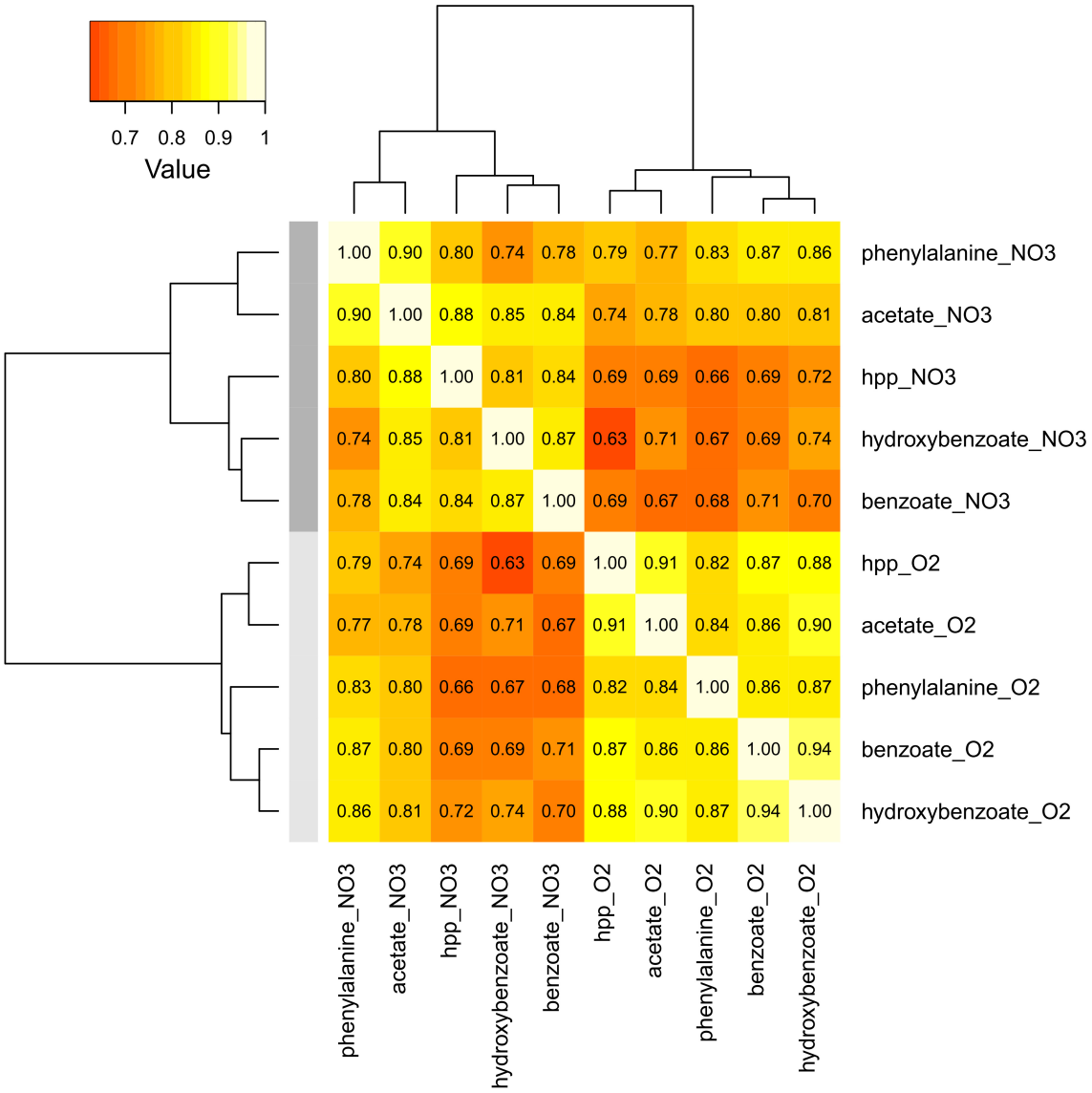

supplement 12: Correlation analysis of the metabolic profiles after transformation of the peak areas to the logarithm 2

supplement 13: Fold-changes of all metabolites >10

Derivative_Group	comment	Ace NO_3	Ace O_2	Ben NO_3	Ben O_2	Hbe NO_3	Hbe O_2	HPP NO_3	HPP O_2	Phe NO_3	Phe O_2
unknown-ebn1-01	unknown	NA	NA	NA	NA	1205	NA	NA	NA	NA	NA
unknown-ebn1-03	unknown	NA	101.8	NA	2.8	NA	2.0	NA	102.6	NA	3.0
unknown-ebn1-04	unknown	NA	3993	NA	NA	NA	NA	NA	152.8	NA	NA
unknown-ebn1-05	unknown	NA	1267	NA	6570	NA	NA	NA	5010	NA	5310
unknown-ebn1-12	unknown	NA	NA	98.0	NA	NA	NA	586.7	NA	NA	NA
unknown-ebn1-13	unknown	9.3	0.2	112.4	NA	0.2	0.9	0.3	1.1	20.5	1.9
unknown-ebn1-17	unknown	NA	67.8	NA	239.0	NA	262.4	NA	130.4	NA	2.0
unknown-ebn1-20	unknown	NA	NA	NA	NA	588.8	NA	NA	NA	NA	NA
unknown-ebn1-21	unknown	31.1	NA	190.3	NA	13.0	1.0	6.0	0.1	1.0	NA
unknown-ebn1-22	unknown	23.5	0.3	33.8	NA	15.3	NA	19.1	1.7	NA	NA
unknown-ebn1-23	unknown	32.4	NA	725.4	NA	139.0	NA	117.9	NA	NA	NA
Unknown-ebn1-25	unknown	0.7	29.4	0.9	0.7	0.2	0.6	4.3	37.6	2.2	1.1
Unknown-ebn1-26	unknown	NA	151.0	NA	3.6	NA	2.0	NA	138.3	NA	4.1
Unknown-ebn1-27	unknown	NA	111.1	NA	2.9	NA	2.0	NA	118.7	NA	2.6
alpha-glycosylglycerol	osmolyte	1.3	6.9	109.8	0.2	0.7	0.2	18.8	9.2	0.1	0.2
dodecanol	fatty acid	NA	NA	186.4	NA	332.6	90.9	NA	7.7	NA	NA
octadecanoate	fatty acid	1.8	7.8	0.3	NA	0.1	NA	1.1	14.7	0.9	52.5
tetradecan-1-ol	fatty acid	NA	2.7	NA	0.9	45.1	1.1	3.6	0.6	1.2	NA
dodecanoate	fatty acid	1.1	3.6	0.2	14.0	0.9	0.8	NA	1.1	1.2	0.8
3-hydroxy-decanoate	fatty acid	5.5	0.8	NA	1.2	4.0	0.5	5.7	0.5	11.7	NA
erythronic acid	artifact	4.8	NA	1.9	NA	4.0	NA	3.4	NA	14.2	NA
glycerol	artifact	2.0	NA	4.4	NA	3.4	NA	4.2	NA	12.7	NA
dehydroascorbic acid	artifact	NA	NA	3437	NA	2099	NA	NA	NA	NA	NA
hydroxylamine	artifact	NA	NA	NA	NA	NA	NA	NA	NA	294.3	NA
iminodiacetate	artifact	NA	NA	NA	NA	2.3	NA	2.0	7.7	41.6	29.1
2,5-dioxo-cyclohex-1-carbonyl-CoA_1	byproduct	NA	NA	NA	NA	NA	NA	NA	NA	NA	37.7
3-oxoadipyl-CoA	byproduct	NA	NA	NA	NA	338.2	NA	NA	7.2	NA	NA
4-hydroxyphenylacetyl-CoA	byproduct	NA	NA	NA	NA	NA	NA	NA	NA	45.5	NA
phenoxyacetyl-CoA	byproduct	NA	NA	NA	NA	NA	NA	NA	NA	31.6	NA
2-ketocyclohexane-1-carboxyl-CoA	byproduct	NA	NA	NA	NA	1586	6.8	1.6	NA	1.3	4.2
geranoyl-CoA	byproduct	NA	NA	NA	NA	69.1	NA	26.0	25.4	NA	NA
3-ketopimelyl-CoA	byproduct	NA	NA	NA	NA	NA	NA	NA	4.2	NA	271.5
4-hydroxy-benzoylacetyl-CoA	byproduct	NA	NA	NA	NA	20.7	NA	NA	NA	NA	NA
2,3-didehydro-pimeloyl-CoA_3	byproduct	NA	NA	5.6	53.9	NA	NA	0.9	19.9	1.1	1.6
2,6-dihydroxycyclo-hexane-1-carboxyl-CoA	byproduct	NA	NA	21.9	NA	70.2	NA	7.4	NA	NA	NA
pimeloyl-CoA_1	byproduct	NA	0.4	5.2	NA	1.9	NA	1.5	NA	20.0	0.5

supplement 13 continued: Fold-changes of all metabolites >10

Derivative_Group	comment	Ace NO_3	Ace O_2	Ben NO_3	Ben O_2	Hbe NO_3	Hbe O_2	HPP NO_3	HPP O_2	Phe NO_3	Phe O_2
5-methyl-3-oxo-4-hexenoyl-CoA	byproduct	NA	NA	NA	NA	242.1	1.9	NA	NA	NA	NA
2-hydroxycyclo-hexanecarbonyl-CoA	byproduct	NA	NA	NA	NA	116.1	NA	NA	NA	NA	NA
2-hydroxycyclohexane-1-carboxyl-CoA	byproduct	NA	NA	64.4	NA	2.8	NA	97.8	NA	6.1	NA
3-phenyllactate		NA	NA	NA	NA	NA	NA	734.9	NA	181.9	NA
2-isocaprenoyl-CoA		NA	NA	NA	NA	NA	NA	2.0	14.1	NA	NA
beta-alanine	amino acid	NA	NA	1.4	NA	NA	10.1	5.3	49.9	0.6	154.5
lysine	amino acid	9.9	NA	14.7	NA	NA	2.8	NA	2.0	NA	13.7
glycylglycine	dipeptide	195.8	NA	337.9	NA	131.3	NA	60.1	2.0	NA	NA
glucose-6-phosphate	gluco-neogenesis	3.1	0.3	17.0	NA	3.4	0.0	3.3	1.6	0.2	0.4
glyceraldehyde	gluco-neogenesis	37.2	NA	300.8	NA	113.9	NA	102.9	NA	NA	NA
thymine	nucleobase	NA	8.2	0.1	10.7	NA	4.8	NA	1.9	0.1	5.3
2-isopropylmalic acid	organic acid	NA	NA	NA	NA	466.5	NA	NA	NA	NA	NA

supplement 14: Fold-changes of pathway specific metabolites

Metabolite	pathway	Ace NO_3	Ace O_2	Ben NO_3	Ben O_2	Hbe NO_3	Hbe O_2	HPP NO_3	HPP O_2	Phe NO_3	Phe O_2
6-oxo-2-hydroxycyclohexane-1-carboxyl-CoA	Ben NO_3	NA	NA	88.8	NA	33.1	NA	13.2	NA	3.5	NA
3-hydroxypimelyl-CoA	Ben NO_3	NA	NA	1109	NA	206.8	NA	349.9	NA	59.7	NA
benzoate	Ben NO_3	NA	2.0	947.2	8.0	NA	4.4	NA	32.7	NA	NA
6-hydroxycyclohex-1-enecarbonyl-CoA_2	Ben NO_3	NA	NA	392.8	NA	NA	NA	106.7	NA	21.7	NA
pimeloyl-CoA_3	Ben NO_3	NA	NA	203.0	NA	186.8	NA	188.4	1.4	60.2	NA
glutaryl-CoA	Ben NO_3	NA	NA	127.1	NA	121.3	NA	51.8	NA	30.0	NA
2,3-didehydro-pimeloyl-CoA_2	Ben NO_3	NA	NA	95.9	NA	NA	NA	30.0	NA	4.8	1.6
6-ketoxycyclohex-1-ene-1-carboxyl-CoA	Ben NO_3	NA	NA	89.9	NA	NA	NA	46.0	NA	16.6	NA
cyclohexa-1,5-dienecarbonyl-CoA	Ben NO_3	NA	NA	80.6	NA	NA	NA	12.6	NA	5.3	NA
3,4-didehydroadipyl-CoA semialdehyde-2	Ben O_2	NA	NA	NA	21.2	NA	NA	1.0	20.5	NA	NA
3-hydroxyadipyl-CoA	Ben O_2	0.2	0.2	1.7	16.3	0.1	0.3	0.2	5.9	2.4	4.3

supplement 14 continued: Fold-changes of pathway specific metabolites

Metabolite	pathway	Ace NO_3	Ace O_2	Ben NO_3	Ben O_2	Hbe NO_3	Hbe O_2	HPP NO_3	HPP O_2	Phe NO_3	Phe O_2
5-carboxy-2-pentenoyl-CoA	Ben O_2	0.1	NA	3.1	12.1	0.1	NA	1.5	7.6	0.9	1.1
3,4-didehydroadipyl-CoA	Ben O_2	NA	NA	NA	10.6	NA	NA	0.6	5.3	NA	NA
2-hydroxy-5-oxo-cyclohex-1-carbonyl-CoA	Hbe NO_3	NA	NA	149.8	NA	289.5	NA	29.9	NA	11.1	NA
3-hydroxybenzoyl-CoA	Hbe NO_3	NA	NA	0.8	4.3	199.3	15.2	0.3	1.5	1.1	0.9
4-oxopimeloyl-CoA_2	Hbe NO_3	NA	NA	NA	NA	67.6	NA	NA	NA	NA	NA
6-hydroxycyclohex-1-enecarbonyl-CoA_1	Hbe NO_3	NA	NA	NA	NA	42.2	NA	NA	NA	NA	NA
3-hydroxybenzoate	Hbe O_2	NA	NA	NA	NA	1542	1954	NA	NA	NA	NA
3-(4-hydroxyphenyl) propanoyl-CoA	Hpp NO_3	NA	NA	NA	NA	NA	NA	128.1	125.8	NA	NA
4-hydroxybenzoyl-CoA_2	Hpp NO_3	1.3	NA	NA	NA	NA	NA	29.3	NA	7.3	NA
3-hydroxy-3-(4-hydroxyphenyl)propanoyl-CoA	Hpp NO_3	NA	NA	4.4	NA	2.9	NA	11.6	NA	6.0	NA
3,4-didehydroadipyl-CoA semialdehyde-3	Hpp O_2	NA	NA	NA	42.0	NA	NA	NA	50.4	NA	NA
4-hydroxybenzoate	Hpp O_2	NA	NA	NA	NA	NA	NA	1073	12297	NA	NA
3-(4-hydroxyphenyl) propanoate	Hpp O_2	NA	NA	NA	NA	NA	NA	NA	4862	NA	NA
4-hydroxybenzoyl-CoA_1	Hpp O_2	NA	NA	NA	NA	1.1	NA	NA	252.0	NA	103.4
phenylglyoxylyl-CoA	Phe NO_3	NA	NA	NA	NA	NA	NA	NA	NA	173.2	16.6
phenylacetate	Phe O_2	NA	NA	NA	NA	NA	NA	NA	NA	NA	855.9
phenylacetyl-CoA	Phe O_2	2.0	0.4	1.2	NA	1.7	0.2	0.8	0.2	45.6	89.4
3-oxo-5,6-dehydrosuberyl-CoA semialdehyde_2	Phe O_2	NA	NA	NA	38.8	NA	NA	NA	4.0	25.6	60.7
3-oxo-5,6-dehydrosuberyl-CoA semialdehyde_1	Phe O_2	NA	NA	NA	NA	NA	NA	NA	NA	7.7	11.5

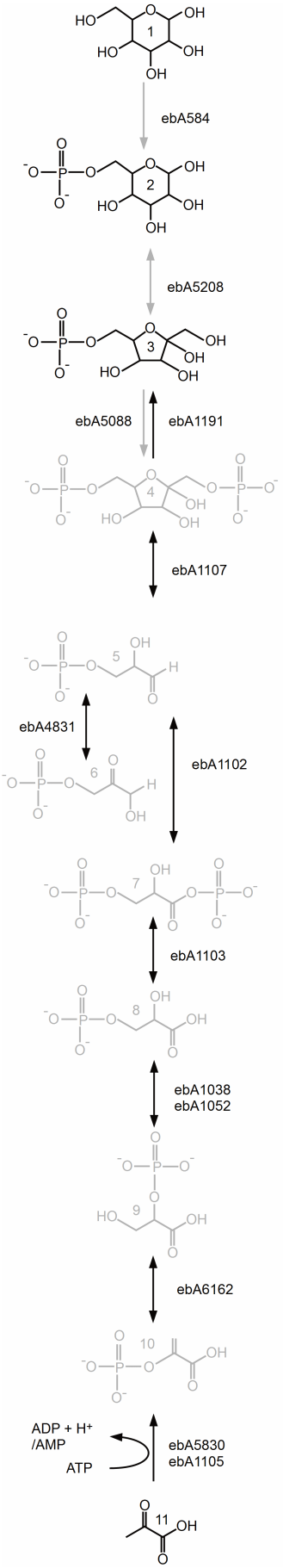

		Ace NO3	Ace O2	Ben NO3	Ben O2	Hbe NO3	Hbe O2	Hpp NO3	Hpp O2	Phe NO3	Phe O2
1,6-anhydro-glucose		283	447	194	739	188	364	224	531	NA	284
(1) glucose		2345	2301	2454	2008	2776	1641	3034	1862	2004	2103
ebA584	T	20	27	23	27	26	35	24	25	19	33
	P	NA	NA	NA	NA	NA	NA	NA	NA	NA	NA
(2) glucose-6-phosphate		9645	930	53256	5	10525	123	10306	4988	744	1284
ebA5208	T	31	34	29	35	33	34	31	33	30	31
	P	NA	NA	NA	NA	NA	NA	NA	NA	NA	NA
(3) fructose-6-phosphate		386	NA	1224	NA	360	26	315	569	43	NA
fructose		296	179	102	175	366	354	322	210	152	130
ebA1191	T	124	100	79	93	78	78	92	82	47	79
	P	396	468	240	499	NA	310	142	105	NA	211
ebA5088	T	41	30	29	30	28	29	28	26	31	38
	P	NA	NA	NA	NA	NA	NA	NA	NA	NA	NA
(4) fructose 1,6-bisphosphate		NA	NA	NA	NA	NA	NA	NA	NA	NA	NA
ebA1107	T	111	83	51	75	66	74	62	70	29	76
	P	451	472	422	556	306	522	222	339	311	494
(5) D-glyceraldehyde 3-phosphate		NA	NA	NA	NA	NA	NA	NA	NA	NA	NA
ebA4831	T	1397	816	1085	611	1259	638	1165	1131	511	853
	P	471	323	284	260	356	458	381	385	317	393
(6) glycerone phosphate		NA	NA	NA	NA	NA	NA	NA	NA	NA	NA
ebA1102	T	304	226	212	207	196	249	225	197	96	147
	P	408	512	335	462	226	357	148	277	NA	313
(7) 1,3-bisphospho-D-glycerate		NA	NA	NA	NA	NA	NA	NA	NA	NA	NA
ebA1103	T	118	90	64	67	76	70	80	56	30	64
	P	525	648	438	473	449	397	253	274	355	500
(8) 3-phospho-D-glycerate		NA	NA	NA	NA	NA	NA	NA	NA	NA	NA
ebA1038	T	10	7	6	7	21	9	27	6	15	13
	P	NA	NA	NA	NA	NA	NA	NA	NA	NA	NA
ebA1052	T	218	219	139	138	142	142	160	171	55	133
	P	511	553	523	534	408	483	489	524	386	478
(9) 2-phospho-D-glycerate		NA	NA	NA	NA	NA	NA	NA	NA	NA	NA
ebA6162	T	638	405	371	349	347	329	445	357	237	337
	P	1421	1351	1262	1289	1193	1162	1229	1236	1194	1294
(10) phosphoenol-pyruvate		NA	NA	NA	NA	NA	NA	NA	NA	NA	NA
ebA5830	T	416	477	286	402	282	416	425	302	168	168
	P	776	1726	865	1522	438	893	675	798	107	602
ebA1105	T	141	80	76	69	115	67	103	70	49	81
	P	277	144	NA	261	NA	113	NA	NA	111	182
(11) pyruvate		499	933	1908	462	1720	1823	694	1085	NA	684

supplement 15: Gluconeogenesis

supplement 16: Annotation of all genes related to respiration

	Annotation EnzymeDetector		Annotation Oldenburg	
locus_tag	**EC**	**recommended name**	**EC**	**PRODUCT**
ebA1196				Cytochrome C1 subunit of cytochrome bc1
ebA1197	1.10.2.2	ubiquinol- cytochrome-c reductase		Cytochrome B subunit of cytochrome bc1
ebA1198	1.10.2.2	ubiquinol- cytochrome-c reductase	1.10.2.2	Iron-sulfur subunit of cytochrome bc1
ebA1215	1.7.1.4	nitrite reductase [NAD(P)H]		Assimilatory nitrite reductase, small subunit
ebA1216	1.7.1.4	nitrite reductase [NAD(P)H]		Assimilatory nitrite reductase, large subunit
ebA156	1.9.3.1	cytochrome-c oxidase		Putative cytochrome c oxidase subunit I
ebA158	1.9.3.1	cytochrome-c oxidase		Chain II protein of putative cytochrome c oxidase
ebA179	1.7.2.5	nitric-oxide reductase	1.7.99.7	Nitric-oxide reductase subunit B
ebA2575				Predicted electron transport subunit of NADH:ferredoxin oxidoreductase
ebA2576				Electron transport complex protein RnfB
ebA2578				Electron transport complex protein rnfD (Nitrogen fixation protein rnfD)
ebA2579				Electron transport complex protein rnfC (Nitrogen fixation protein rnfC)
ebA2581				Electron transport complex protein rnfG (Nitrogen fixation protein rnfG
ebA2585				Electron transport complex protein rnfE (Nitrogen fixation protein rnfE)
ebA2586				Protein rnfH
ebA2880	1.9.3.1	cytochrome-c oxidase		Cytochrome C oxidase subunit transmembrane protein (EC 1.9.3.1),
ebA2882				Cytochrome oxidase, cytochrome c subunit
ebA2883	1.7.2.1	nitrite reductase (NO-forming)		Probable cytochrome c subunit of cbb3 type cytochrome oxidase
ebA2965	1.18.1.1	rubredoxin-NAD+ reductase		Flavorubredoxin reductase [(nitric oxide reductase)reductase]

supplement 16 continued: Annotation of all genes related to respiration

	Annotation EnzymeDetector		Annotation Oldenburg	
locus_tag	EC	recommended name	EC	PRODUCT
ebA2999	3.6.3.14	H+-transporting two-sector ATPase	3.6.1.34	F0-ATP synthase, a subunit
ebA3000	3.6.3.14	H+-transporting two-sector ATPase	3.6.3.14	F0-ATP synthase, c subunit
ebA3002	3.6.3.14	H+-transporting two-sector ATPase	3.6.1.34	F0-ATP synthase, b subunit
ebA3003	3.6.3.14	H+-transporting two-sector ATPase	3.6.3.14	F1-ATP synthase, delta subunit
ebA3004	3.6.3.14	H+-transporting two-sector ATPase	3.6.1.34	F1-ATP synthase, alpha subunit
ebA3006	3.6.3.14	H+-transporting two-sector ATPase	3.6.1.34	F1-ATP synthase, gamma subunit
ebA3007	3.6.3.14	H+-transporting two-sector ATPase	3.6.1.34	F1-ATP synthase, beta subunit
ebA3008	3.6.3.14	H+-transporting two-sector ATPase	3.6.3.14	F1-ATP synthase, epsilon subunit
ebA3665	1.9.3.1	cytochrome-c oxidase	1.9.3.1	probable cytochrome-c oxidase subunit II
ebA3666	1.9.3.1	cytochrome-c oxidase		Cytochrome c oxidase, subunit I (EC 1.9.3.1)
ebA4227	1.9.3.1	cytochrome-c oxidase	1.9.3.1	Cytochrome C oxidase, subunit 2
ebA4228	1.9.3.1	cytochrome-c oxidase	1.9.3.1	Cytochrome C oxidase, subunit 1
ebA4231	1.9.3.1	cytochrome-c oxidase	1.9.3.1	Cytochrome c oxidase, subunit III
ebA4537				Di-heme cytochrome c (class I), probably related to cytochrome c oxidase function
ebA4540				Cytochrome c1, probably related to cytocrome c oxidase function
ebA4542	1.9.3.1	cytochrome-c oxidase	1.9.3.1	Subunit III of cytochrome c oxidase, also similar to C-terminal domain of long variants of subunit I
ebA4544	1.9.3.1	cytochrome-c oxidase	1.9.3.1	Cytochrome c oxidase, subunit I
ebA4547	1.9.3.1	cytochrome-c oxidase	1.9.3.1	Cytochrome c oxidase, subunit II
ebA4638				Cyanide insensitive terminal oxidase
ebA4639				Cyanide insensitive terminal oxidase
ebA4835	1.6.99.5	NADH dehydrogenase (quinone)	1.6.5.3	NADH dehydrogenase I, chain B
ebA4836	1.6.99.5	NADH dehydrogenase (quinone)	1.6.5.3	NADH dehydrogenase I, chain C

supplement 16 continued: Annotation of all genes related to respiration

	Annotation EnzymeDetector		Annotation Oldenburg	
locus_tag	**EC**	**recommended name**	**EC**	**PRODUCT**
ebA4837	1.6.5.3	NADH:ubiquinone reductase (H+-translocating)	1.6.5.3	NADH dehydrogenase I, chain D
ebA4837	1.6.99.5	NADH dehydrogenase (quinone)		
ebA4838	1.6.5.3	NADH:ubiquinone reductase (H+-translocating)	1.6.5.3	NADH dehydrogenase I, chain E
ebA4840	1.6.5.3	NADH:ubiquinone reductase (H+-translocating)	1.6.5.3	NADH dehydrogenase I, chain F
ebA4841	1.6.5.3	NADH:ubiquinone reductase (H+-translocating)	1.6.5.3	NADH dehydrogenase I, chain G
ebA4842	1.6.99.5	NADH dehydrogenase (quinone)	1.6.5.3	NADH dehydrogenase I, chain H
ebA4843	1.6.99.5	NADH dehydrogenase (quinone)	1.6.5.3	NADH dehydrogenase I , chain I
ebA4844	1.6.5.3	NADH:ubiquinone reductase (H+-translocating)	1.6.5.3	NADH dehydrogenase I, chain J
ebA4846	1.6.5.3	NADH:ubiquinone reductase (H+-translocating)	1.6.5.3	NADH dehydrogenase I , chain L
ebA4847	1.6.5.3	NADH:ubiquinone reductase (H+-translocating)	1.6.5.3	NADH dehydrogenase I, chain M
ebA4848	1.6.5.3	NADH:ubiquinone reductase (H+-translocating)	1.6.5.3	NADH dehydrogenase I, chain N
ebA4872				Cytochrome c, class IC
ebA4874				Cytochrome c, class IC
ebA4878				NADH:ubiquinone oxidoreductase, subunit RnfE
ebA4881				Electron transport complex protein
ebA4882				Electron transport complex protein
ebA4883	1.6.99.5	NADH dehydrogenase (quinone)		Putative electron transport complex protein
ebA4884				Electron transport complex protein
ebA4887				NADH:ferredoxin oxidoreductase
ebA5023				Probable cytochrome b561
ebA5131	1.9.3.1	cytochrome-c oxidase	1.9.3.1	Cytochrome-cbb3 oxidase, subunit I
ebA5132	1.9.3.1	cytochrome-c oxidase	1.9.3.1	Cytochrome-cbb3 oxidase, subunit II
ebA5134	1.9.3.1	cytochrome-c oxidase	1.9.3.1	Cytochrome-cbb3 oxidase, subunit III
ebA5197				Cytochrome c family protein
ebA539	1.18.1.1	rubredoxin-NAD+ reductase		Fusion protein of nitric oxide reductase (flavorubredoxin NorV) with its associated reductase (NorW)

supplement 16 continued: Annotation of all genes related to respiration

	Annotation EnzymeDetector		Annotation Oldenburg	
locus_tag	**EC**	**recommended name**	**EC**	**PRODUCT**
ebA6262				Putative cytochrome c-type protein
ebA6272	1.7.2.4	nitrous-oxide reductase	1.7.99.6	Nitrous-oxide reductase
ebA6282	1.7.99.4	nitrate reductase	1.7.99.4	Nitrate reductase, gamma subunit
ebA6285	1.7.99.4	nitrate reductase	1.7.99.4	Nitrate reductase, beta subunit
ebA6286	1.7.99.4	nitrate reductase	1.7.99.4	Nitrate reductase, alpha chain
ebA6329	1.9.3.1	cytochrome-c oxidase		Putative denitrification protein NorE (EC 1.9.3.1)
ebA6958	1.6.99.3	NADH dehydrogenase		Putative NADH dehydrogenase
ebA7148				potential ortholog of Methylophilus methylotrophus cytochrome c"
ebA7150				Diheme cytochrome c
ebA888	1.7.99.1	hydroxylamine reductase		Cytochrome cd1 nitrite reductase precursor,
ebB158				Terminal quinol oxidase membrane protein subunit similar to DoxD of Acidianus spp.
ebB168	1.6.99.5	NADH dehydrogenase (quinone)	1.6.5.3	NADH dehydrogenase I , chain K
ebB214				Putative cytochrome c
ebB6	1.7.2.5	nitric-oxide reductase	1.7.99.7	Nitric-oxide reductase subunit C
ebD11	1.6.5.3	NADH:ubiquinone reductase (H+-translocating)		NADH dehydrogenase I chain A (EC 1.6.5.3)

supplement 17: Transcription of all genes related to aerobic or anaerobic respiration

locus tag	Ace NO3	Ace O2	Ben NO3	Ben O2	Hbe NO3	Hbe O2	Hpp NO3	Hpp O2	Phe NO3	Phe O2
ebA1196	2188	857	1422	937	1587	906	1515	1291	701	1542
ebA1197	950	481	809	427	597	434	690	484	227	522
ebA1198	1468	854	827	523	830	805	873	864	203	856
ebA1215	10	11	10	14	10	17	7	10	14	10
ebA1216	6	5	6	10	6	10	5	7	11	6
ebA156	3	1	3	5	3	6	2	4	9	3
ebA158	2	1	1	3	2	3	1	2	3	2
ebA179	4704	3929	5135	2833	2176	1133	3722	671	2987	2023
ebA2575	1	0	2	4	39	3	2	27	4	1
ebA2576	1	0	1	1	106	1	6	47	3	1
ebA2578	1	0	1	3	53	2	10	35	3	1
ebA2579	1	0	1	2	63	2	5	30	3	1
ebA2581	1	0	1	3	66	2	20	65	5	2
ebA2585	11	9	10	13	247	13	112	284	26	14
ebA2586	7	2	8	15	114	14	53	125	22	6
ebA2880	8	7	8	13	5	10	4	6	12	4
ebA2882	9	12	10	17	7	11	6	8	12	6
ebA2883	3	4	2	6	2	4	0	3	4	1
ebA2965	13	17	16	19	22	20	18	21	16	22
ebA2999	1912	917	1728	526	849	829	1434	870	308	893
ebA3000	10600	3935	5487	2800	3592	3624	7216	4388	1548	4599
ebA3002	2613	1009	1471	893	1084	973	1785	1079	507	1364
ebA3003	2194	867	1092	857	930	864	1402	958	443	1300
ebA3004	3759	1425	2026	1614	1874	1378	2642	1545	1481	2313
ebA3006	3577	1524	2074	1550	1874	1297	2777	1510	1744	2437
ebA3007	2972	1822	1860	1559	1611	1351	2473	1324	1896	2293
ebA3008	6945	5280	4749	3549	4359	3310	5872	3827	5430	6493
ebA3665	203	92	104	149	54	62	92	48	93	89
ebA3666	76	38	39	44	20	32	32	17	40	31
ebA4227	14	5	20	19	45	43	34	40	200	78
ebA4228	4	1	4	8	11	14	6	12	59	37
ebA4231	13	5	10	16	20	28	13	24	81	80
ebA4537	2	0	1	4	1	3	1	2	4	1
ebA4540	2	0	2	4	2	4	1	2	6	1
ebA4542	1	0	1	3	1	3	0	1	3	0
ebA4544	1	0	1	2	1	3	0	1	3	0
ebA4547	1	0	1	2	1	2	0	1	3	1
ebA4638	3	1	2	5	3	5	2	3	7	3
ebA4639	3	1	3	5	3	5	2	4	7	3
ebA4835	2602	1311	1782	813	1871	925	1816	2043	344	1148
ebA4836	1487	702	1143	583	1264	654	1252	1200	238	667
ebA4837	1820	767	1314	740	1532	766	1642	1628	409	943
ebA4838	4670	2697	3960	2079	4049	2837	5030	4964	1267	2950
ebA4840	2212	1216	1503	980	1771	1199	2156	2107	632	1271
ebA4841	882	562	631	431	674	451	888	699	337	521

supplement 17 continued: Transcription of all genes related to aerobic or anaerobic respiration

locus tag	Ace NO3	Ace O2	Ben NO3	Ben O2	Hbe NO3	Hbe O2	Hpp NO3	Hpp O2	Phe NO3	Phe O2
ebA4842	3014	1533	2176	909	2415	973	3093	1165	1157	1181
ebA4843	2906	1701	2107	920	2043	964	2706	1288	1041	1287
ebA4844	1194	739	819	359	795	377	1072	483	391	507
ebA4846	596	410	368	196	352	208	450	232	166	216
ebA4847	974	659	586	353	592	349	771	448	271	392
ebA4848	671	422	438	271	534	255	603	354	271	298
ebA4872	154	215	209	310	227	357	280	327	534	505
ebA4874	99	126	148	204	156	242	190	240	390	353
ebA4878	99	77	108	79	89	69	110	94	101	73
ebA4881	115	78	88	84	82	80	105	97	72	65
ebA4882	53	50	44	46	37	48	52	63	33	36
ebA4883	75	68	48	66	56	81	61	85	37	51
ebA4884	222	232	146	207	176	308	195	274	79	145
ebA4887	96	87	81	101	82	101	91	100	47	72
ebA5023	25	34	129	48	81	70	37	83	33	55
ebA5131	692	350	518	482	601	1293	597	707	430	341
ebA5132	233	159	173	197	218	426	216	318	146	172
ebA5134	984	732	686	695	912	1671	947	1295	561	718
ebA5197	19	24	35	29	22	37	23	30	62	27
ebA539	356	26	165	38	31	31	95	22	47	23
ebA6262	3913	2191	2436	2154	1688	1066	3250	915	1234	1660
ebA6272	3906	1703	2487	1255	1421	1562	2015	851	1203	1199
ebA6282	786	12	1488	22	1125	176	306	26	724	17
ebA6285	1271	22	2483	32	1736	276	482	34	1461	27
ebA6286	753	11	1359	17	951	111	271	14	837	12
ebA6329	23	21	27	32	30	30	26	25	40	31
ebA6958	2	2	2	5	3	5	2	3	6	3
ebA7148	4	2	7	18	4	11	3	11	15	5
ebA7150	4	2	9	18	3	9	4	10	13	7
ebA888	10690	7488	5981	4458	3834	1766	3563	615	2666	2450
ebB158	10	8	9	15	10	14	6	11	24	12
ebB214	11	16	14	12	7	5	7	4	6	3
ebB6	7229	7950	7159	4181	2570	1922	5011	1193	3772	4922
ebD11	1818	1056	1450	508	1337	581	1423	1327	320	866

A)

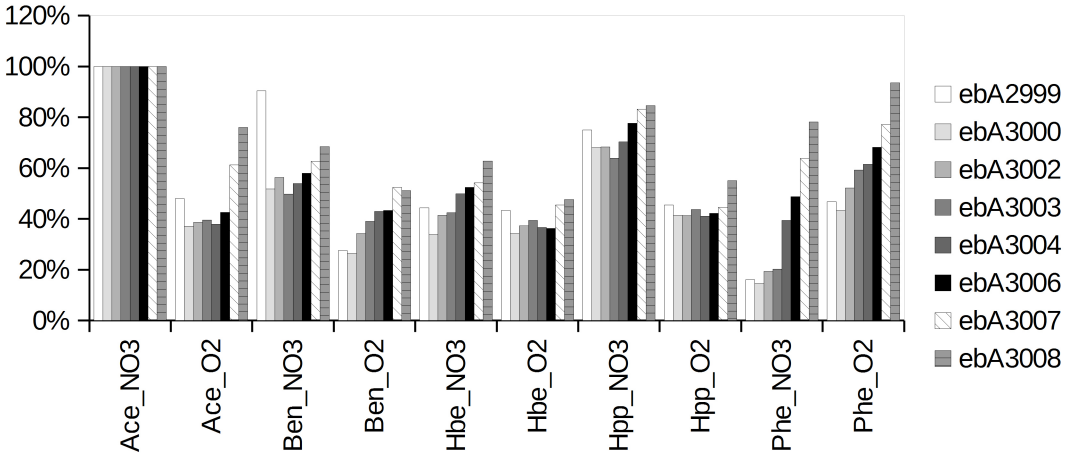

B)

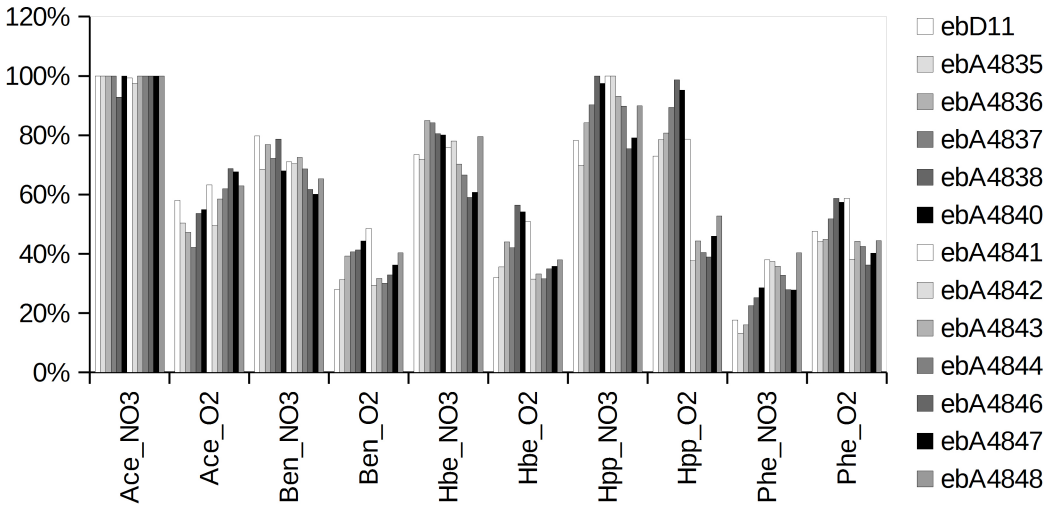

supplement 18: Gene expression of individual subunits of ATP-synthase (A) and NADH dehydrogenase (B)

supplement 19: ATP content in bacterial cells as described in literature and found in this work

Reference	Organism	ATP [mol/cell]
Benett 2009	*E. coli*	1.3E-12
Buckstein 2008	*E. coli*	9.0E-18
Hamilton 1967	*Micrococcus sp.*	9.9E-19
Hamilton 1967	*Pseudomonas sp.* (C6)	2.0E-18
Hamilton 1967	*Pseudomonas sp.* (GU-1)	2.6E-18
Hamilton 1967	*Serratia sp.*	2.8E-18
Hamilton 1967	*Pseudomonas sp.* (GL-7)	3.9E-18
Hamilton 1967	*Vibrio sp.*	7.1E-18
Hamilton 1967	*Chromobacterium marinum*	1.3E-17
Lowry 1971	*E. coli*	1.2E-18
Lowry 1971	*E. coli*	1.3E-18
Lowry 1971	*E. coli*	1.8E-18
Yaginuma 2014	*E. coli*	2.0E-13
	Aromatoleum aromaticum EbN1	
this work	Ace_NO_3	8.5E-19
this work	Ace_O_2	8.9E-19
this work	Ben_NO_3	8.1E-19
this work	Ben_O_2	2.0E-18
this work	Hbe_NO_3	1.2E-18
this work	Hbe_O_2	2.8E-18
this work	HPP_NO_3	8.0E-19
this work	HPP_O_2	1.8E-18
this work	Phe_NO_3	7.5E-19
this work	Phe_O_2	2.0E-18

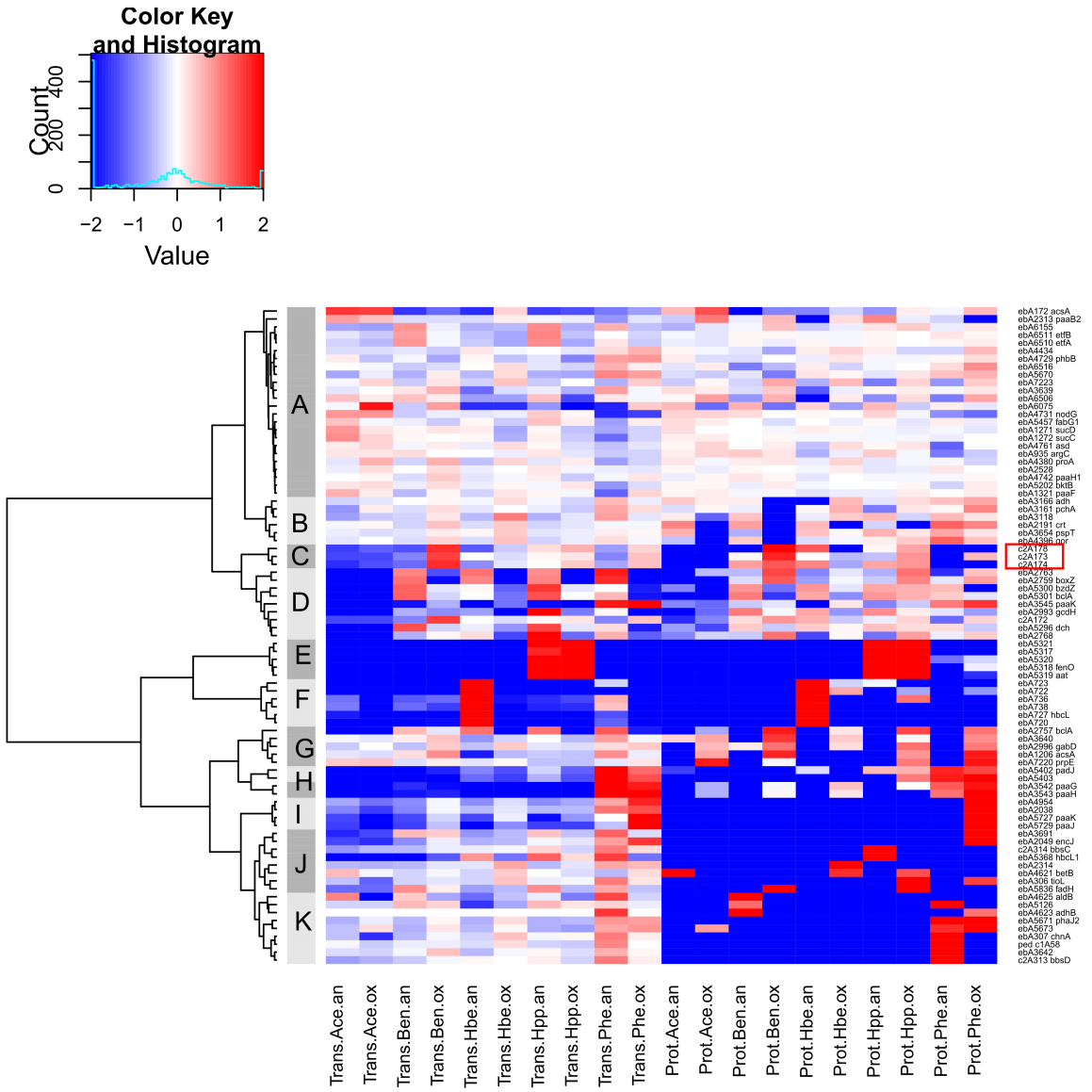

supplement 20: Hierarchical cluster analysis of transcript and protein related to b-oxidation; Analysis of log2 ratios regarding the mean value of transcript or protein, euclidean distances and wards minimum distance clustering

supplement 21: Thiolases not related to specific degradation pathways

Gene	Annotation	EC		Ace NO3	Ace O2	Ben NO3	Ben O2	Hbe NO3	Hbe O2	Hpp NO3	Hpp O2	Phe NO3	Phe O2
ebA5202	Thiolase	2.3.1.9	T	1419	1489	1148	1528	1140	1300	1210	1449	718	1028
			P	1530	1531	1292	1591	1377	1414	1431	1520	1165	1569
c2A172	β-Ketoadipyl CoA thiolase	2.3.1.9	T	22	22	30	163	59	49	62	69	31	80
			P	214	349	796	1158	1001	511	596	854	305	845
ebA3639	Putative acyl-CoA thiolase	2.3.1.16	T	37	44	49	65	19	35	40	28	72	41
			P	501	447	332	526	165	364	420	451	390	460
ebA5673	Hypothetical protein, family DUF35	2.3.1.9	T	60	100	54	96	57	90	56	51	134	145
			P	NA	81	NA	NA	NA	NA	NA	NA	148	242
ebA2049	Putative β-oxoacyl-CoA thiolase	2.3.1.16	T	8	7	12	20	14	15	21	19	37	65
			P	NA	NA	NA	NA	NA	NA	NA	NA	NA	108
ebA2314	Putative acetyl-CoA acyltransferase	2.3.1.16	T	16	15	16	20	20	36	16	20	36	33
			P	NA	NA	NA	NA	NA	110	NA	NA	NA	NA

supplement 22: Dehydrogenases not related to specific degradation pathways

Gene	Annotation	EC		Ace NO3	Ace O2	Ben NO3	Ben O2	Hbe NO3	Hbe O2	Hpp NO3	Hpp O2	Phe NO3	Phe O2
ebA4731	3-hydroxyacyl-CoA dehydrogenase	1.1.1.36	T	2328	2288	996	1163	1123	1211	1728	1364	405	456
			P	764	764	723	612	621	589	764	574	333	267
ebA4729	3-hydroxyacyl-CoA dehydrogenase	1.1.1.36	T	872	591	759	493	856	589	684	410	1365	1433
			P	934	710	705	856	764	958	788	786	887	1018
ebA4742	acyl-CoA dehydrogenase	1.1.1.157	T	604	644	495	796	513	563	656	447	580	705
			P	436	502	528	490	409	478	453	447	458	493
ebA6506	acyl-CoA dehydrogenase	putative	T	212	167	216	168	90	90	212	57	180	150
			P	884	1388	476	1251	189	921	456	1021	414	1298
ebA2528	putative 3-hydroxyacyl-CoA dehydrogenase	putative	T	657	891	717	869	652	723	843	702	653	624
			P	366	321	370	343	325	373	295	319	402	350
c2A173	acyl-CoA dehydrogenase	1.1.1.157	T	22	22	30	163	59	49	62	69	31	80
			P	NA	NA	226	711	219	148	157	384	NA	323

supplement 23: Genes putatively related to stress response: Oxidoreductases, sigma factors, chaperones and other

Annotation	locus tag		Ace NO3	Ace O2	Ben NO3	Ben O2	Hbe NO3	Hbe O2	Hpp NO3	Hpp O2	Phe NO3	Phe O2
Oxidoreductases												
catalase	ebA2102	T	481	1700	445	895	146	64	261	31	206	460
		P	1214	NA	1144	256	870	387	976	126	369	NA
superoxide dismutase (Fe)	ebA5077	T	2913	3364	3807	3531	2173	2984	3004	3358	2393	4373
		P	256	384	264	352	305	297	299	458	368	454
catalase	ebB152	T	6	1	3	8	4	8	3	5	9	3
		P	NA	NA	NA	NA	NA	NA	NA	NA	NA	NA
alkyl hydroperoxide reductase	ebA6469	T	2416	1967	1867	1181	2327	1394	2153	1775	1308	2199
		P	NA	NA	NA	NA	NA	NA	NA	NA	NA	NA
peroxiredoxin	ebA2918	T	137	240	225	471	199	598	234	282	431	395
		P	420	467	670	387	694	703	782	801	810	863
peroxiredoxin	ebA4399	T	938	1686	7538	2494	11990	3234	4193	2641	4019	1995
		P	489	633	550	733	546	666	524	620	588	648
glutathione peroxidase protein	ebA6393	T	160	74	158	122	125	89	196	170	138	90
		P	178	NA	169	NA	NA	101	172	158	238	155
peroxiredoxin	ebA4948	T	81	123	92	98	83	99	83	94	68	103
		P	330	NA	226	208	262	187	377	285	331	219
putative Cytochrome c peroxidase	ebA5105	T	8	6	6	13	6	14	6	8	17	6
		P	NA	NA	NA	NA	NA	NA	NA	NA	NA	NA
rubredoxin-NAD+ reductase	ebA2965	T	13	17	16	19	22	20	18	21	16	22
		P	NA	NA	NA	NA	NA	NA	NA	NA	NA	NA
cytochrome-c peroxidase	ebA3202	T	44	36	53	63	41	62	36	41	97	39
		P	NA	NA	NA	NA	NA	NA	NA	NA	NA	NA
Alternative sigma factors												
RpoS	ebA778	T	192	202	212	205	261	219	272	268	255	262
		P	NA	NA	NA	NA	NA	NA	NA	NA	NA	NA
rpoN1	ebA3393	T	728	969	578	910	583	790	611	515	714	761
		P	NA	197	NA	161	NA	NA	NA	86	NA	114
sigma-32	ebA4241	T	117	223	237	577	174	414	164	298	195	180
		P	NA	NA	NA	NA	NA	NA	NA	NA	NA	NA
RpoD	ebA4365	T	894	653	649	496	670	569	709	699	249	544
		P	NA	529	112	709	NA	299	NA	196	NA	340
sigma24	ebA4517	T	60	37	59	40	35	26	37	37	30	46
		P	NA	NA	NA	NA	NA	NA	NA	NA	NA	NA
RpoE	ebA5463	T	1105	928	842	630	963	728	1053	1251	590	990
		P	NA	NA	NA	NA	NA	NA	NA	NA	NA	NA
sigma factor	ebA6072	T	101	217	84	105	41	19	50	13	23	28
		P	NA	NA	NA	NA	NA	NA	NA	NA	NA	NA
sigma 54	ebA6931	T	4	2	3	7	3	7	3	5	8	5
		P	NA	NA	NA	NA	NA	NA	NA	NA	NA	NA
Chaperones and heat shock proteins												
chaperone bssE	c2A306	T	17	15	22	27	52	39	41	50	83	42
		P	NA	NA	NA	NA	NA	NA	NA	NA	NA	NA
chaperone GroEL	ebA1185	T	1129	3882	2558	6031	1380	2395	1513	1964	1548	2726
		P	2716	2910	2630	3301	2713	2818	2571	2651	2633	2859
putative chaperone norQ	ebA183	T	216	781	239	502	76	80	152	74	137	554
		P	369	128	391	98	262	NA	330	NA	118	NA
Heat shock protein chaperone hslU	ebA2637	T	251	284	194	294	179	246	207	204	219	266
		P	295	295	237	382	165	281	278	343	210	421

supplement 23 continued: Genes putatively related to stress response: Oxidoreductases, sigma factors, chaperones and others

Annotation	locus tag		Ace NO3	Ace O2	Ben NO3	Ben O2	Hbe NO3	Hbe O2	Hpp NO3	Hpp O2	Phe NO3	Phe O2
heat shock protein 20	ebA2730	T	364	718	698	1863	305	1079	184	778	585	870
		P	357	334	371	355	280	404	339	427	488	497
TorD family cytoplasmic chaperone	ebA2939	T	159	67	141	34	298	81	173	107	570	291
		P	NA	NA	NA	NA	NA	NA	NA	NA	155	NA
molecular chaperone DnaK	ebA3469	T	31	24	11	21	14	16	17	17	7	14
		P	NA	NA	NA	NA	NA	NA	NA	NA	NA	NA
molecular chaperone DnaJ	ebA4793	T	249	367	309	361	158	251	163	220	107	235
		P	225	241	163	281	127	233	169	156	120	119
molecular chaperone DnaK	ebA4794	T	1713	2397	3092	3906	1243	1881	1180	2037	1097	1702
		P	2017	2258	1984	2421	1609	2021	1801	1926	1224	1922
heat shock protein GrpE	ebA4795	T	1148	1569	2118	1604	876	1545	920	1611	385	953
		P	576	533	421	463	414	484	560	514	455	387
heat shock protein 90 hptG	ebA4865		1065	990	1618	1580	611	812	640	773	223	578
		P	1318	1625	1072	1735	671	1110	897	1164	404	1116
ethylbenzene dehydrogenase, chaperone ebdD2	ebA5795	T	109	87	158	110	132	163	117	94	301	148
		P	NA	NA	NA	NA	NA	NA	NA	NA	NA	NA
chaperone narJ	ebA6283	T	600	8	1118	15	865	133	209	15	646	10
		P	257	NA	384	NA	238	NA	195	NA	85	NA
chaperone protein HscA	ebA6396	T	248	115	303	235	216	138	332	236	209	149
		P	250	316	406	548	218	NA	467	380	NA	329
co-chaperone HscB	ebA6397	T	794	382	1345	934	886	495	1328	797	880	645
		P	65	NA	86	NA	116	NA	139	87	98	NA
copper chaperone copZ	ebB181	T	218	202	220	198	193	216	204	266	389	291
		P	386	247	383	308	355	432	364	367	472	390
chaperonins cpn10 groeS	ebB35	T	1033	3588	2123	4694	1384	2725	1413	2150	989	2455
		P	225	287	274	277	267	247	278	257	261	290
disulfide bond chaperone	ebA6835	T	58	55	46	80	48	53	53	44	46	50
		P	NA	NA	NA	NA	NA	NA	NA	NA	NA	NA
heat shock protein 90 hptG	ebA4865	T	1065	990	1618	1580	611	812	640	773	223	578
		P	1318	1625	1072	1735	671	1110	897	1164	404	1116
heat shock protein	ebB88		571	1186	1142	2547	532	1572	359	1093	951	1224
		P	156	133	148	151	155	136	181	220	307	223
heat shock protein GrpE	ebA4795		1148	1569	2118	1604	876	1545	920	1611	385	953
		P	576	533	421	463	414	484	560	514	455	387
			Other									
betaine aldehyde dehydrogenase (BADH) oxidoreductase protein betB	ebA4621	T	31	20	17	20	17	29	21	18	15	26
		P	125	NA	NA	NA	NA	97	NA	80	NA	NA
universal stress protein uspA	ebA222	P	NA	NA	117	NA	NA	87	NA	149	118	NA
		T	46	60	68	88	71	70	73	79	131	87
universal stress protein	ebA1926	T	33	29	38	46	48	49	36	41	76	54
		P	NA	NA	NA	NA	NA	NA	NA	NA	148	NA
universal stress protein (Usp)	ebA3574	T	103	115	89	111	103	115	98	87	88	95
		P	NA	NA	NA	NA	93	72	NA	79	115	130
universal stress protein	ebB179	T	326	362	371	319	362	480	353	329	445	302
		P	317	174	287	186	253	215	335	250	428	310
stress-induced morphogen BolA	ebD120	T	513	468	252	318	290	333	297	223	76	260
		P	192	209	171	135	212	175	153	110	181	172

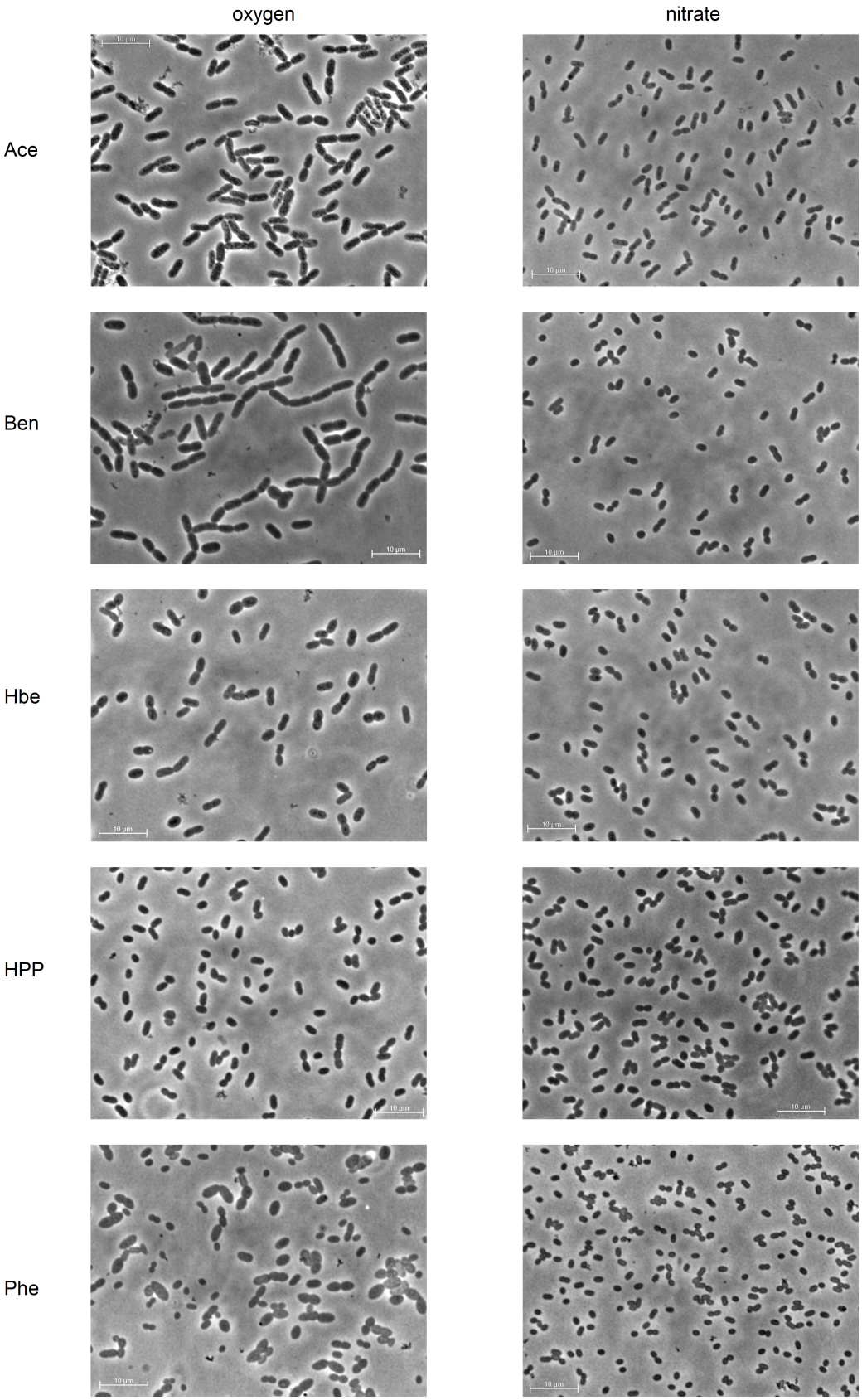

supplement 24: Microscopic images of A. aromaticum cells at 1000x enlargement (Daniele Lange, MPI)

supplement 25: Physiological parameters and calculated rates by Kathleen Trautwein (MPI), Av. indicates the calculated avarage value and AvDev. the corresponding standard deviation

parameter	unit		Ace NO3	Ben NO3	Hbe NO3	HPP NO3	Phe NO3	Ace O2	Ben O2	Hbe O2	HPP O2	Phe O2
ΔTime to OD 0.3	**h**	Av.	15.83	22.13	20.95	21.67	41.25	10.33	13.87	12.83	23.17	25.17
Optical density 660nm	**-**	Av.	0.29	0.3	0.29	0.3	0.3	0.32	0.3	0.3	0.29	0.29
		AvDev.	0.01	0	0	0	0	0	0.01	0	0.01	0
Cellular dry weigth CDW	**g/l**	Av.	0.11	0.09	0.06	0.06	0.1	0.1	0.1	0.11	0.1	0.1
		AvDev.	0	0	0.01	0.01	0.01	0.01	0	0	0	0
Cell count	**cells/l**	Av.	1.93E+011	1.40E+011	1.94E+011	1.42E+011	3.98E+011	6.89E+010	5.56E+010	1.14E+011	1.85E+011	1.84E+011
		AvDev.	5.00E+009	8.91E+009	2.00E+010	5.47E+009	1.22E+010	9.22E+009	6.25E+008	4.38E+009	1.41E+010	1.94E+010
Doubling time tD	**h**	Av.	3.07	3.76	5.06	5.78	7.58	2.10	3.42	2.41	5.12	6.76
growth rate μmax	**1/h**	Av.	0.23	0.18	0.14	0.12	0.09	0.33	0.20	0.29	0.14	0.10
		AvDev.	0.01	0.01	0.01	0.00	0.00	0.00	0.01	0.00	0.00	0.00
Max. biomass production rate	**g CDW/(l*h)**	Av.	0.02	0.01	0.01	0.01	0.01	0.03	0.01	0.02	0.01	0.02
cell weight	**pg/cell**	Av.	0.59	0.65	0.30	0.43	0.26	1.41	1.80	0.93	0.56	0.57
Substrate consumed	**mM**	Av.	5.53	1.64	1.27	1.36	1.15	3.92	1.13	1.52	1.36	0.99
		AvDev.	0.12	0.15	0.01	0.01	0.04	0.01	0.04	0.03	0.15	0.02
Substrate consumed [carbon]	**mM**	Av.	11.06	11.49	8.87	12.47	10.39	7.85	7.9	10.61	16.18	8.95
		AvDev.	0.23	1.05	0.08	0.09	0.36	0.02	0.29	0.19	1.33	0.22
Nitrate consumption	**mM /h**	Av.	0.78	0.81	0.7	0.54	0.56	–	–	–	–	–
		AvDev.	0.02	0.01	0.01	0.02	0.01	–	–	–	–	–
Nitrite formation	**mM /h**	Av.	0.65	0.26	0.29	0.25	0.13	–	–	–	–	–
		AvDev.	0.01	0.02	0.01	0.01	0.01	–	–	–	–	–
Nitrite consumption	**mM /h**	Av.	0.99	0.32	0.36	0.5	0.24	–	–	–	–	–
		AvDev.	0.13	0.01	0.01	0.03	0	–	–	–	–	–
Substrate consumption	**mmol /(g CDW*h)**	Av.	7.58	2.87	3.36	1.74	0.87	11.76	2.2	3.15	2.67	1.12
Substrate consumption [carbor	**mmol /(g CDW*h)**	Av.	15.16	20.11	23.54	15.69	7.84	23.51	15.43	22.05	24.04	10.06
Nitrate consumption	**mmol /(g CDW*h)**	Av.	6.89	8.98	12.04	8.69	5.42	–	–	–	–	–
Nitrite formation	**mmol /(g CDW*h)**	Av.	5.73	2.88	4.99	4.13	1.25	–	–	–	–	–
Nitrite consumption	**mmol /(g CDW*h)**	Av.	8.72	3.53	6.22	8.11	2.33	–	–	–	–	–
Yield per substrate	**mg CDW/mmol**	Av.	20.48	55.1	46.06	45.34	90.18	24.72	88.93	69.85	76.92	104.53
Yield per carbon	**mg CDW/mmol**	Av.	10.24	7.87	6.58	4.94	10.02	12.36	12.7	9.98	6.46	11.61

supplement 26: Phasines and other PHB granule associated proteins

Annotation	locud tag		Ace NO3	Ace O2	Ben NO3	Ben O2	Hbe NO3	Hbe O2	Hpp NO3	Hpp O2	Phe NO3	Phe O2
granule-associated protein phbP	ebA6668	T	2530	1619	1803	1475	2386	2382	1813	1906	1921	1741
		P	804	781	834	762	839	805	825	723	916	839
phasin	ebA6852	T	390	166	210	176	199	177	262	139	142	1035
		P	742	771	579	537	607	712	624	200	NA	528
predicted phasin	ebA1323	T	5025	2650	1815	1328	1393	1874	2826	2924	859	446
		P	1104	1183	1140	1100	1038	1035	1081	1061	541	635
phasin	ebA5033	T	914	1721	1095	2402	793	1613	1108	1178	2062	1710
		P	387	284	342	445	377	354	392	431	305	NA
granule-associated protein-like protein	ebA2771	T	266	690	217	514	208	333	546	719	385	183
		P	575	973	781	985	403	483	358	684	NA	NA
polyhydroxyalkanoate synthesis repressor PhaR	ebA4732	T	1852	2044	1488	3560	1716	2274	2247	1789	1408	1067
		P	449	370	459	373	455	481	490	494	514	330

supplement 27: putative benzoate transport systems, gene expression and cytosolic protein scores

annotation	locus tag		Ace NO3	Ace O2	Ben NO3	Ben O2	Hbe NO3	Hbe O2	Hpp NO3	Hpp O2	Phe NO3	Phe O2
ABC transporter subunit	ebA5303	T	189	182	707	771	516	750	899	522	1165	888
		P	550	285	981	703	981	903	1048	1118	1270	1214
ABC-transporter	ebA5304	T	42	49	152	102	104	111	223	99	129	140
ABC-transporter	ebA5306	T	88	100	395	240	298	201	580	292	366	294
ABC-transporter	ebA5307	T	106	97	401	256	381	212	757	412	454	331
		P	54	NA	284	180	250	221	212	213	341	304
ABC-transporter	ebA5309	T	75	70	274	205	253	159	517	315	312	269
		P	NA	NA	NA	NA	NA	NA	104	159	189	248
benzoate MFS transporter benK	ebA5311	T	42	35	207	228	183	168	434	270	255	208

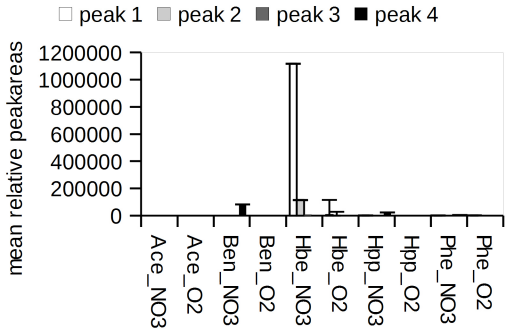

supplement 28: 2-Ketocyclohexane-1-carboxyl-CoA, 5-Methyl-3-oxo-4-hexenoyl-CoA, 6-Hydroxycyclohex-1-enecarbonyl-CoA_1, 6-Hydroxycyclohex-1-enecarbonyl-CoA_2

supplement 29: Operon paa transcription as three mRNA units

locus_tag	mRNA	name	role
ebA3539	A		Conserved hypothetical protein
ebA3540	A	paaY	Putative carbonic anhydrases/acetyltransferase
ebA3541	X	paaZ	3.3.2.12/1.17.1.7
ebA3542	B	paaG	5.3.3.18
ebA3543	B	paaH	1.1.1.35
ebA3544	B	paaI	3.1.2.-
ebA3545	C	paaK	6.2.1.30
ebA3547	C	paaA	1.14.13.149
ebA3548	C	paaB	
ebA3550	C	paaC	1.14.13.149
ebA3551	C	paaD	Putative ring oxidation complex protein 3
ebA3553	C	paaE	probable ring-hydroxylation complex protein 4
ebA3555	C	paaR	probable transcriptional regulator
ebA3554	C		hypothetical protein
ebA3556	C		Putative ABC transporter protein

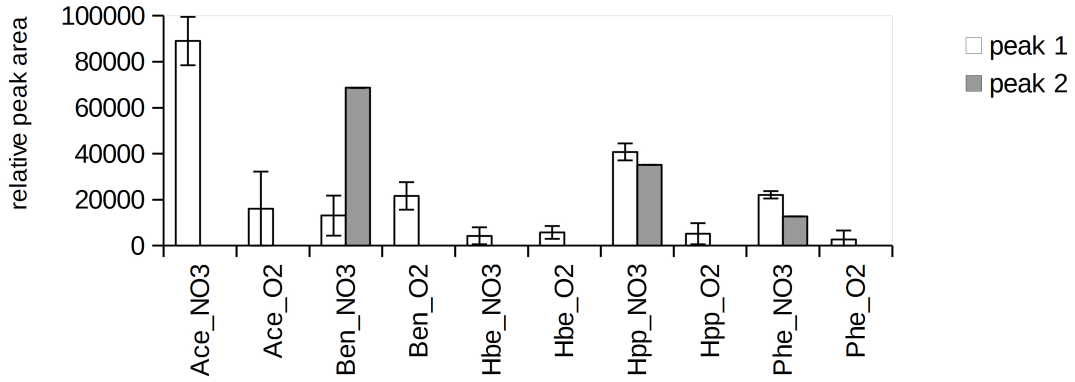

supplement 30: 2-ene-5-oxo-cyclohex-1-carbonyl-CoA and 6-Ketoxycyclohex-1-ene-1-carboxyl-CoA (isomergoup 3)

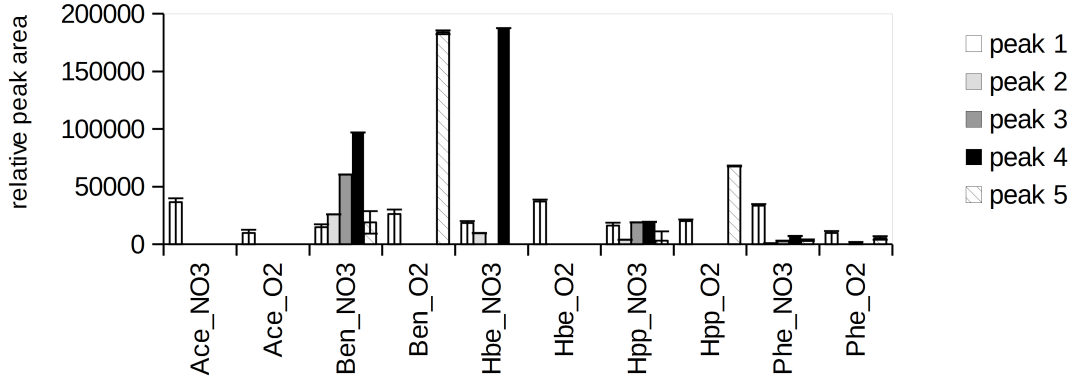

supplement 31: Exact mass signals of 2,3-Didehydro-pimeloyl-CoA_1, 6-Oxo-2-hydroxycyclohexane-1-carboxyl-CoA, 2,3-Didehydro-pimeloyl-CoA_2, 2-hydroxy-5-oxo-cyclohex-1-carbonyl-CoA, 2,3-Didehydro-pimeloyl-CoA_3

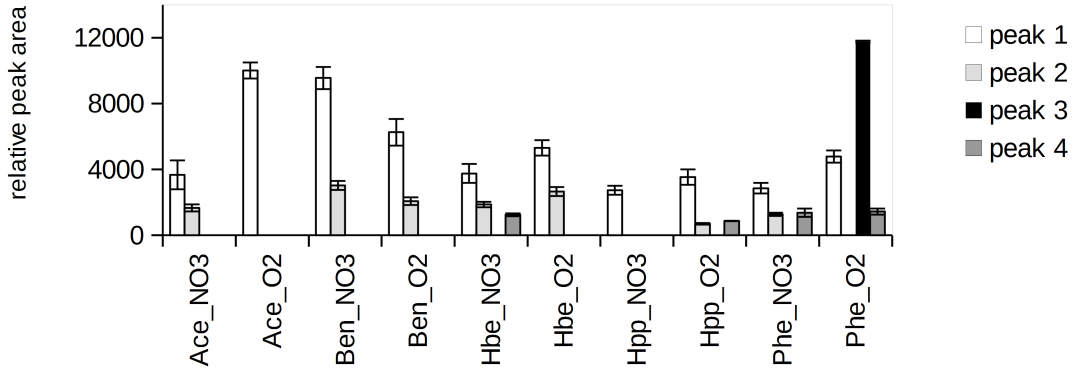

supplement 32: Exact mass signals of 2,3-Dihydro-2,3-dihydroxybenzoyl-CoA, 2,3-Dihydro-2,3-dihydroxybenzoyl-CoA-Isomer, 2,5-dioxo-cyclohex-1-carbonyl-CoA_2, 2,5-dioxo-cyclohex-1-carbonyl-CoA_1

Danksagung

Zur Entstehung dieser Arbeit haben viele Menschen beigetragen, bei denen ich mich an dieser Stelle herzlich bedanken möchte, auch wenn ich nicht alle namentlich nennen kann. Mein ganz besonderer Dank gilt Herrn Prof. Schomburg, dafür dass ich dieses hochinteressante Thema bearbeiten durfte. Besonders möchte ich mich für das entgegengebrachte Vertrauen und die besondere Förderung meiner Weiterbildung in der Methodenentwicklung bedanken. Außerdem bedanke ich mich herzlich bei Herrn Prof. Ralf Rabus, der dieses spannende Kooperationsprojekt erst ermöglicht und mit hochwertigen Diskussionen bereichert hat sowie als Zweitgutachter zur Verfügung stand. Eine herzlicher Dank gilt auch Herrn Prof. Michael Hust für die unkomplizierte Bereitschaft den Vorsitz der Prüfungskommission zu zu übernehmen.

Des weiteren möchte ich mich bei Herrn Dr. Robert Geffers für die Bereitstellung der Transkriptomdaten und bei Herrn Dr. Lars Wöhlbrand für die aufwändige Bereitstellung der Proteomdaten bedanken. Mein ganz besonderer Dank gilt Frau Dr. Kathleen Trautwein für die enge Zusammenarbeit bei der Kultivierung und physiologischen Untersuchungen sowie für die anregenden fachlichen Diskussionen.

Ein großer Dank gilt allen ehemaligen und aktuellen Mitgliedern der Arbeitsgruppe für das gute Arbeitsklima, bereichernde fachliche und private Diskussionen sowie unzähligen kleinen und großen Hilfestellungen. Besonders möchte ich mich bei Frau Dr. Meina Neuman-Schaal für das Korrekturlesen meiner Arbeit sowie zahlreicher Hilfestellungen bei Problemen aller Art bedanken. Mein besonderer Dank geht auch an Sarah Kleist und Nelli Bill für den ausgiebigen fachlichen und persönlichen Austausch im Laufe der Arbeit. Des weiteren möchte ich mich bei Dr. Alexander Riemer für die gute fachliche Zusammenarbeit am Modell und den netten Freizeitausgleich bedanken.

Ein ganz besonderer Dank geht an meine Familie und Freunde für ihre Unterstützung, ihr Vertrauen und ihre Geduld. Ohne euch hätte ich diese Arbeit nicht fertigstellen können. Besonders bei Lars möchte ich mich bedanken für seine ruhige und bedingungslose Unterstützung.